Analysis of the Tectonic and Basin Evolution of the Seychelles Microcontinent during the Mesozoic to Cenozoic, based on seismic and well data.

By

Jean-Luc A. Mondon

Department of Geosciences and AEON-ESSRI, Nelson Mandela Metropolitan University, South Africa.

Submitted in fulfilment of the requirements for the degree of Magister Scientiae in the Faculty of Science of the Nelson Mandela Metropolitan University, Port Elizabeth, South Africa.

October, 2014

Supervisor / Promoter: Prof. M.J. de Wit

(AEON-Africa Earth Observatory Network)

AEON

Earth Stewardship Science Research Institute

Nelson Mandela Metropolitan University

for tomorrow

This is the story of how the microcontinent of the Seychelles "emerged" from the supercontinent of Gondwana

Declaration of own work

I, Jean-Luc A. Mondon, student number 207059606, hereby declare that this thesis: **Analysis of the Tectonic and Basin Evolution of the Seychelles Microcontinent during the Mesozoic to Cenozoic based on seismic and well data**, for Master in Geology, is my own work and that it has not previously been submitted for assessment or completion of any postgraduate qualification to another university or for another qualification.

……..

Jean-Luc Andre Mondon October 2014

Acknowledgments

First and foremost I wish to thank my supervisor Professor Maarten J. de Wit for the introduction to AEON at NMMU, and his support in all aspects for this project, including the start, completion and funding. I also owe a large debt to Callum R. Anderson and Gideon Brunsdon for the many weeks each of them spent assisting me with my project especially during the editing process. I would like to thank Bastien Linol and Safiya Hassan for numerous thoughtful discussions, comments and insights about the sedimentary aspect of this study. I would also like to thank Professor Moctar Doucouré for his help and insights on the seismic aspect of this project. Special thanks go to Jade Greve and Megan de Jager who assisted me in putting the document together. Thanks to PetroSeychelles, for providing the necessary data such as digital well-logs, seismics and unpublished reports which comprises the main database for this project.

Thanks to all my friends from Seychelles and South Africa for their continuous support during the duration I have stayed in South Africa to undergo my academic career path. Lastly I would like to thank my mother, Sheila Mondon, and father, Robert Ah-Weng for their patience, support, and encouragement throughout the course of this project.

Abstract

The Seychelles Microcontinent (SMc) is a fragment of continental lithosphere that experienced multiple phases of rifting and thermal subsidence during its isolation and submergence within the Indian Ocean. Originally part of central Gondwana, along with India and Madagascar, the SMc first emerged during Mesozoic fragmentation of Gondwana (*ca.* 220 – 180 Ma) along a complex rifted margin. Fragmentation involved three major rift phases, viz.: 1) Middle Triassic – Middle Jurassic (Rift I), associated with the "Karoo rifts" and break-up between [India-Madagascar-Seychelles] and East Africa; 2) Middle Jurassic – Early Cretaceous (Rift II), associated with the rifting and break-up of Madagascar from [India-Seychelles]; 3) Late Cretaceous (Rift III), associated with the rifting and final break-away of the SMc from India.

In this study, the tectonic and sedimentary history of the SMc is analysed using 2D seismic reflection datasets and three exploration wells. Seismic to well-log correlations provide a chrono-stratigraphic framework that identifies seven sequences from the Middle Triassic to the Paleogene. This also identified horst and graben structures related to the extensional tectonics and thermal subsidence of this continental fragment. The latter is reflected also in changes of its litho-facies preserved on the SMc, from terrestrial to marine. The oldest sedimentary rocks identified on the SMc are Middle Triassic organic rich claystones (Sequence 7, Rift I), which grade upwards into alternating Upper Triassic sandstones and mudstones (Sequence 6, Rift I) followed by upward coarsening Lower Jurassic mudstones to sandstone units (Sequence 5, Rift I). These sequences are interpreted as lacustrine facies that evolved into fluvial channel migration facies and finally into progradational delta front facies. Sequence 5 is overlain by Middle Jurassic oolitic limestones that grade upwards into organic rich mudstones (Sequence 4, thermal subsidence after Rift I); the latter are interpreted as restricted-marginal marine deposits. Following Sequence 4, separated by a major break-up unconformity (BU), are the Upper Cretaceous open marine deposits comprising limestones, claystones and sandstones, and terminated with basaltic volcanics (*ca.* 66 Ma) prior to the separation of the SMc from India (Sequence 3, Rift III). This is overlain by the post-rift – thermal subsidence sequences comprising open marine claystones and shelf limestones (Sequence 2) followed by a sequence of shelf limestones (Sequence 1) that form the present carbonate platform, the Seychelles Plateau that lies approximately 200 m below the present sea-level.

Backstripping and subsidence analysis quantifies 3 stages of subsidence; Phase A: Slow subsidence (*ca*. 5-20 m/Ma), from the Middle Jurassic to the Upper Cretaceous that terminated during a major marine transgression during ingression of the Tethys Sea between East Africa and [Madagascar-Seychelles-India]. This created marine conditions and the subsequent deposition of Sequences 4 and 3; Phase B: Accelerated subsidence (*ca*. 35-60 m/Ma) recorded throughout the Paleocene to the middle Eocene leading to deeper marine conditions and the subsequent deposition of Sequence 2; and Phase C: Reduced subsidence (*ca*. 10-30 m/Ma) following the interaction between the Carlsberg Ridge and the Reunion hotspot (*ca*. 55 Ma) that possibly introduced a reduction in subsidence and the subsequent deposition of Sequence 1 as the SMc drifted and thermally subsided to its submerged present location, and is now dominated mainly by marine carbonates. The effects of the Madagascar and Seychelles/India separation (*ca*. 84 Ma) are not observed in the subsidence analysis, possibly because it involved transcurrent-rotational movement between the two plates over a short period of time.

Table of contents

List of Figures

List of Tables

List of Acronyms

A: Africa

C: Carbonates

EAO: East African Orogeny

I: India

LIP: Large Igneous Province

M: Madagascar

MSL: Mean Sea-level

OB: Owen Bank – A1

RB: Reith Bank - 1

SB: Sequence boundary

SMc: Seychelles Microcontinent

SP: Seychelles Plateau

WB: Wave Base

SS: Seagull shoals - 1

SC: Siliciclastics and Carbonates

TWT: Two way time

Chapter 1. Introduction

1.1 Background

The Seychelles Archipelago of the Western Indian Ocean, lies south of the equator (1º-12º S, 46º -56º E), and about 1500km off the eastern coast of Africa. The famous granitic islands of Seychelles have been recognised for their geological uniqueness, since it is not common for granites to occur in the middle of an ocean unless they are surrounded by underlying continental crust. The Seychelles granitic islands are indeed now known to be underlain and surrounded by a submerged continental crust referred to as the Seychelles Microcontinent (SMc), also referred to as the Seychelles Plateau (SP) (Figure 1.1).

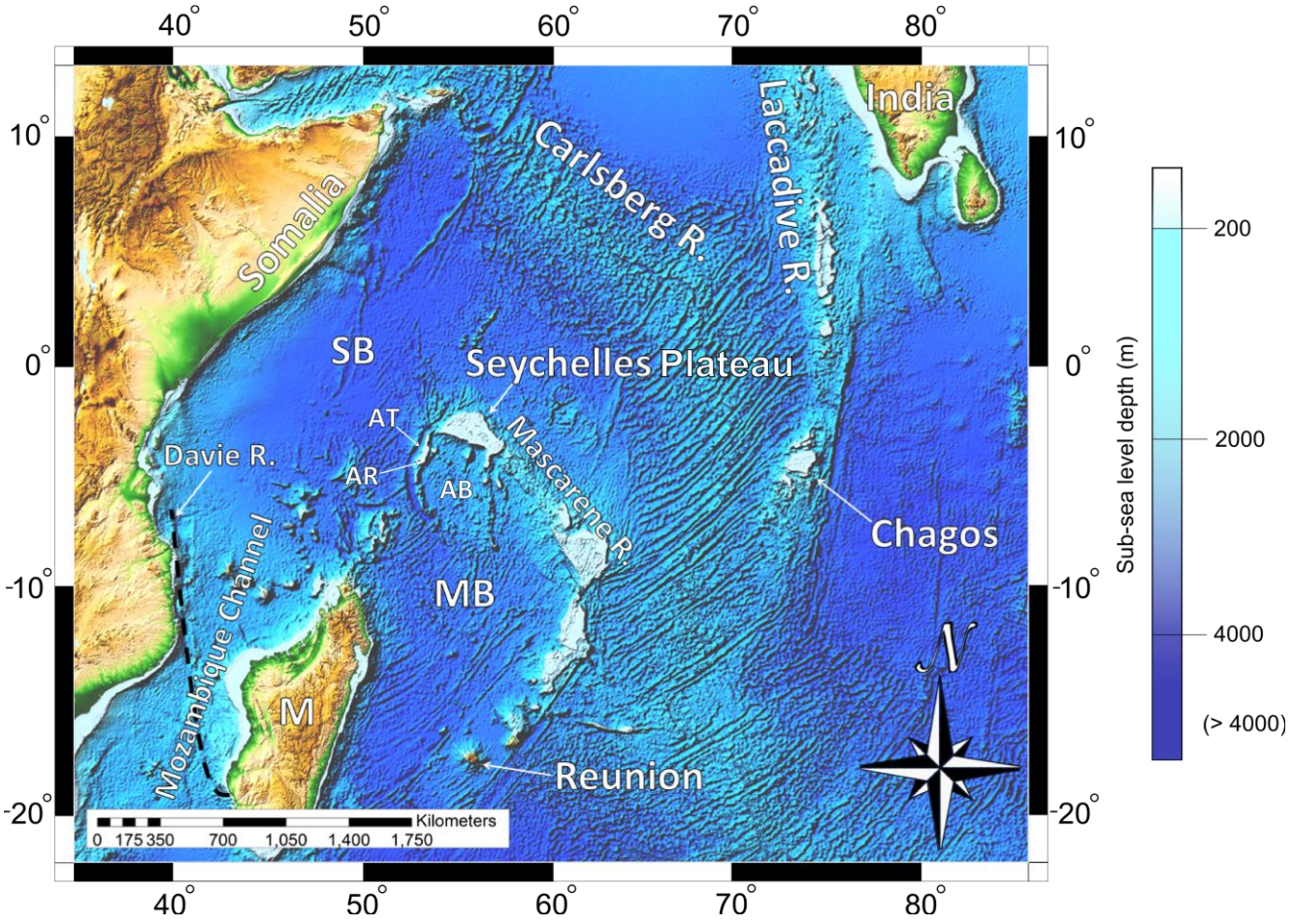

Figure 1.1: Western Indian Ocean indicating the locality of the Seychelles and the general bathymetry of the region. SB = Somali Basin; MB = Mascarene Basin; M = Madagascar, AT = Amirantes Trench, AR = Amirantes Ridge, AB = Amirantes Basin. (Source: Adapted from Amante and Eakins, 2009).

The SMc was part of the central "Gondwana" supercontinent that started to break up during the Triassic - Jurassic (*ca.* 220 -160 Ma). The break-up of Gondwana first led to the formation of various ocean basins such as the Somali and Mascarene basins, as eastern Gondwana separated into individual continental fragments. This ultimately led to the submergence of the SMc (*ca.* 80 – 60 Ma), during the final stages of opening of the Indian Ocean (du Toit, 1937; Baker; 1963, de Wit, 1988; Reeves *et al.*, 2002, Harris and Ashwal, 2002; Torsvik *et al.*, 2013). A detailed tectonic history of the emergence of the Seychelles microcontinent during Gondwana break-up is summarized in Chapter 2.

The Seychelles Archipelago comprises 115 islands that can be sub-divided geologically into two groups: (1) a granitic group (43 islands) and (2) a coralline group (72 islands).

The granitic islands are embedded in the Seychelles Plateau, which is submerged at about 150-200 m below MSL (Figure 1.2). They are mostly steep, rugged and have generally mountainous topography with flat and narrow coastlands that are mostly covered with calcareous and siliceous sands (Figure 1.3). The highest point rises up to 905 m above MSL on the largest and main island of the archipelago, Mahe, which is approximately 27km long and 8 km wide (*ca.* 175 km^2 in area).

The coralline islands are evolved atolls, flat, mostly low-lying and covered by calcareous sands with elevation of less than 6 m above the MSL (Figure 1.4). These coralline islands presumably originated from isolated oceanic seamounts, and most of them lie outside the boundary of the SMc (Figure 1.2) (e.g. Platte and Coetivy Island). Based on the general geometry of the SMc and the carbonate composition of the top of the offshore plateau, it is considered as an isolated shallow carbonate platform, surrounded by deep oceanic crust (>2000 m).

The climate of the archipelago is generally tropical and humid. Most of these islands lie outside the cyclone belt and seldom experience cyclones (Grandcourt, 1995; Joseph *et al.*, 2011).

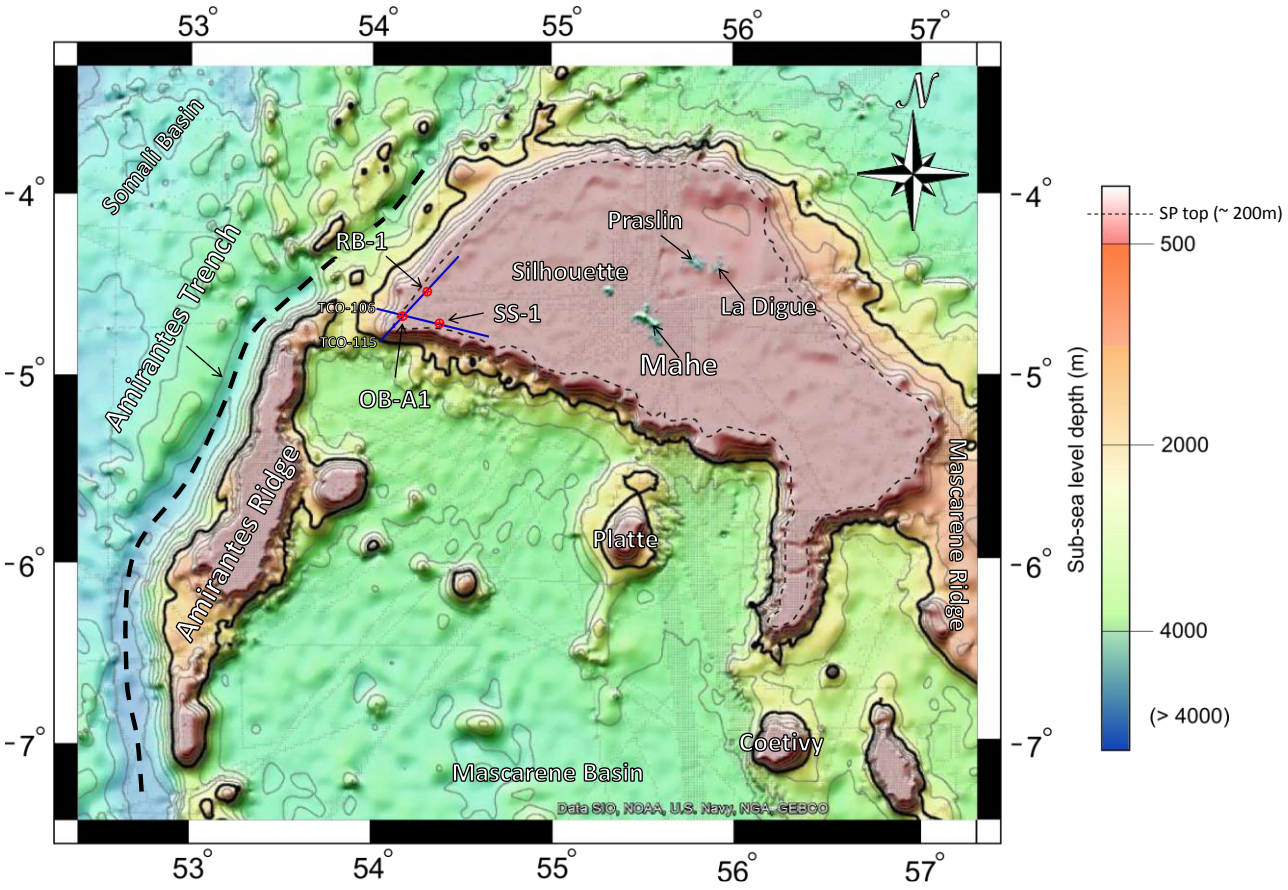

Figure 1.2: Locality and general bathymetry of the study area, including the Seychelles Plateau, the various granitic islands (Mahe, Praslin, La Digue) and coralline islands (e.g. Platte and Coetivy). The position of the wells on the Western shelf shown by the red circles (OB-A1 = Owen Bank – A1; RB-1 = Reith Bank – 1; SS-1 = Seagull Shoals - 1) and the two seismic profiles analysed in this study are shown by the solid blue lines (TCO-106 and TCO-115) (Source: Global Topography for Google Earth and Satellite Geodesy by Becker et al., 2009 and Smith et al., 1997).

Figure 1.3: Granitic islands: (A) Praslin; (B) La Digue; (C)North Island with Silhouette in the background.

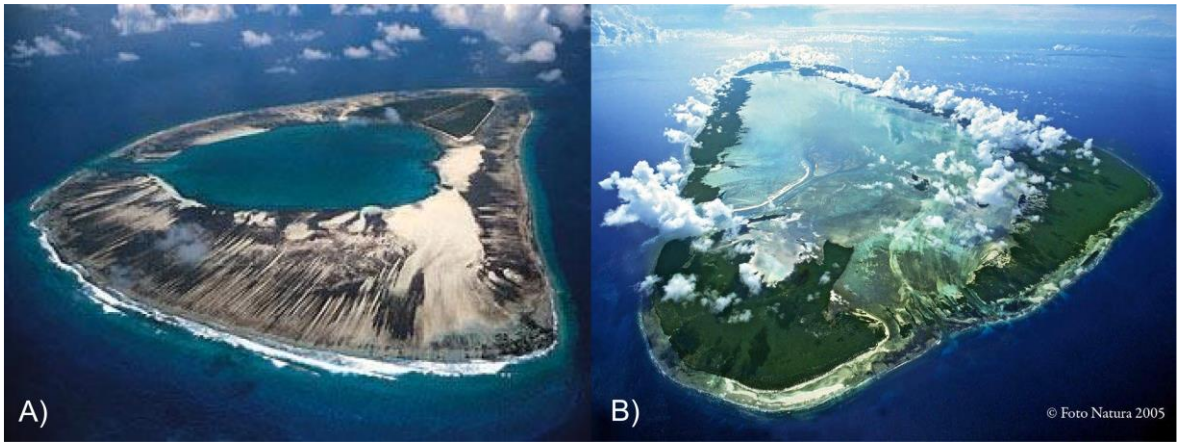

Figure 1.4: Coralline islands: (A) Alphonse Atoll; and (B) Aldabra Atoll.

The present location of the SMc suggests that it has undergone a complex break-up history that involved the repeated fragmentation of parts of eastern Gondwana during the Middle Jurassic to Early Paleogene (*ca.* 180 – 66 Ma). Much of the geologic archives of the rifting history of central Gondwana that relates to the formation of SMc and its history of submergence lies offshore, in the form of a thick cover of sedimentary sequences (*ca.* 1-10 km). Observations from well data indicate that the rifting dates back to the Triassic, during which sedimentation in Central Gondwana was widespread, especially across East and Southern Africa (e.g. Linol *et al.*, *in press*, 2014). Rift related sedimentary sequences are referred to as the Karoo Supergroup (Amoco Seychelles Petroleum Company, 1981a; 1981b; 1981c; Plummer and Belle, 1995; Plummer, 1996; Linol *et al.*, *in press*, 2014). The SMc also records post-rift sequences that are likely part of thermal subsidence phases as the East and West Gondwana separated during the Middle Jurassic onwards until the Seychelles subsequently separated from India and drifted to its present location.

It is postulated that the Seychelles' granitic basement formed part of an Andean type continental arc that evolved during the multiple phase amalgamation of Eastern Gondwana along the East African Orogeny (EAO). This orogeny is associated with continent-continent collision (E-W compression) that occurred around 750-530 Ma. This amalgamation of the associated continental landmasses led to the formation the "Transgondwanan supermountain range" (Figure 1.5), comparable in size and complexity as to the Alpine-Himalayan mountain system (Fritz *et al.*, 2013).

Mozambique, Tanzania, Madagascar and other regions of East African also display planes of weaknesses (megashears) with similar trends as that of the Seychelles Neoproterozoic granites (NW-SE) that resulted from the E-W compression and further exhumation (e.g.

Mahe). These initial sets of planes of weaknesses are thought to have been reactivated during rifting and the break-up of Gondwana (e.g. East African offshore NS rift basins, Morondava Basin of Madagascar) or transcurrent faulting (Figure 1.5) (Baker, 1963; Meert and Lieberman, 2008; Fritz *et al.*, 2013).

Most of the exposed granitic islands (e.g. Mahe, Praslin, La Digue) of the Seychelles form part of crystalline crust with an upper crustal thickness of about 13km. The average total thickness of the continental crust is approximately 33km (depth range to the Moho) (Ashwal *et al.*, 2002; Torsvik *et al.*, 2013).

Similar magmatic rocks to that of the Seychelles granites includes the banded gneiss complex in NW India (Rajasthan) and granite batholiths in central-northern Madagascar, all of which yield similar Neoproterozoic dates to that of the Seychelles' granites (*ca.* 750 Ma). This is consistent with models in which these landmasses were once located in the same realm (Reeves, 2013). Thereafter, approximately 8-10 km of exhumation and erosion exposed these plutonic rocks (e.g. Seychelles granite basement) along a regional peneplain across which younger Karoo-aged sediments accumulated, during the early rifting of Gondwana (Figure 1.6) (Stern, 1994; Hoffman, 1999; Meert, 2001; Torsvik *et al.*, 2001; Tucker *et al.*, 2001; Ashwal *et al.*, 2002; Fritz *et al.*, 2013; Linol *et al.*, *in press*, 2014; Reeves *et al.*, *in press* 2014).

Madagascar comprises extensive sequence of Phanerozoic sedimentary rocks flanking its western coast. These sediments are located within three main basins; Diego, Majunga and Morondava Basins (Figure 1.7). The early sequences of these sedimentary basins and the depositional environments are directly related to the Karoo and Early Jurassic rifting that eventually led to the break-up of Gondwana and the separation of Madagascar.

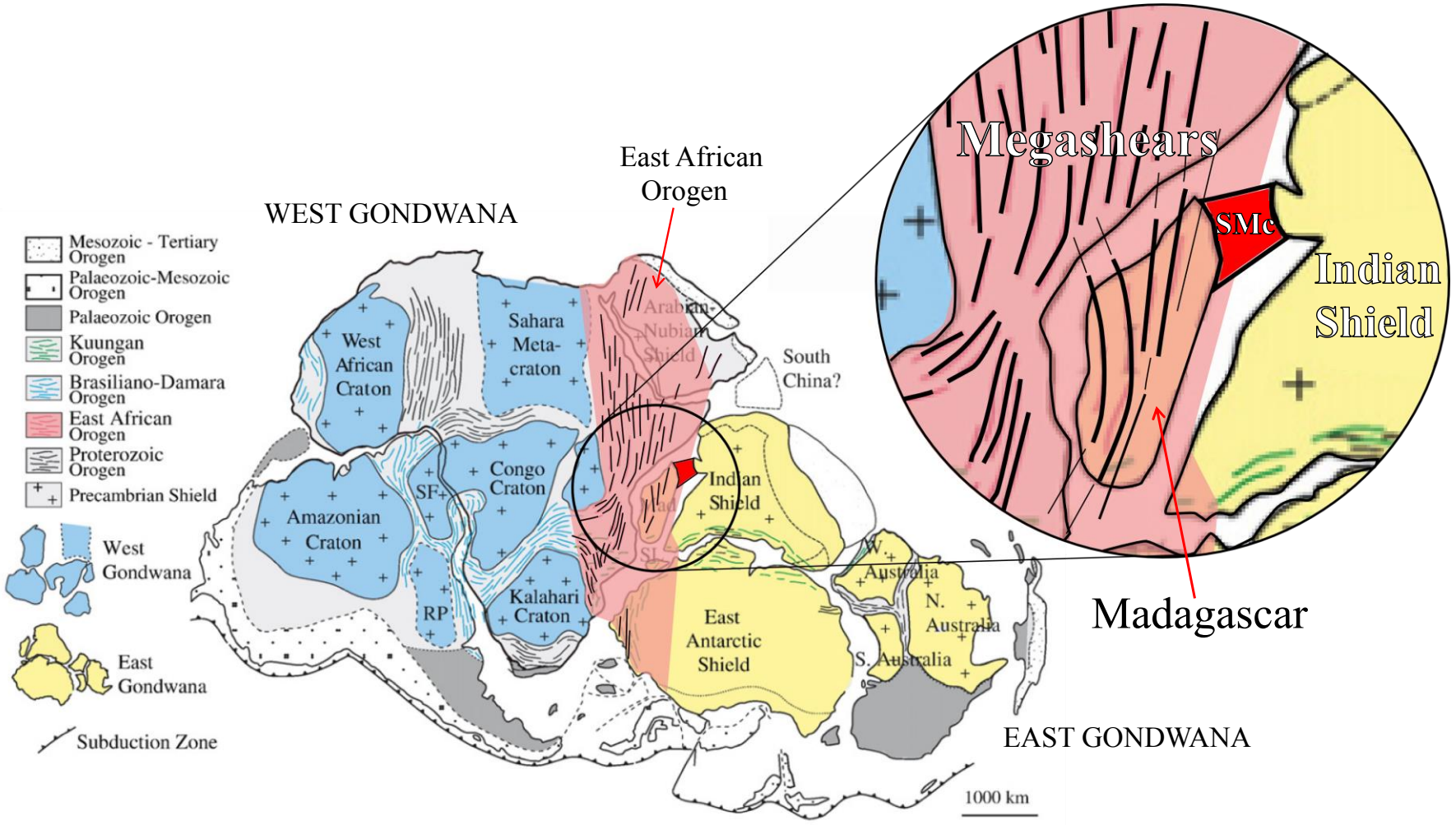

Figure 1.5: The Gondwana supercontinent (ca. 550 Ma). West Gondwana cratons are shaded pale blue and East Gondwana cratons are shaded yellow. The various Neoproterozoic orogenic belts occur around those main cratons during the amalgamation of Gondwana supercontinent. Those associated with the final amalgamation of the supercontinent are the East African orogen (light red), the Brasiliano–Damara orogen (blue), the Kuungan orogen (green) and SMc in red (Source: Modified from Meert and Lieberman, 2008 and Fritz et al., 2013)

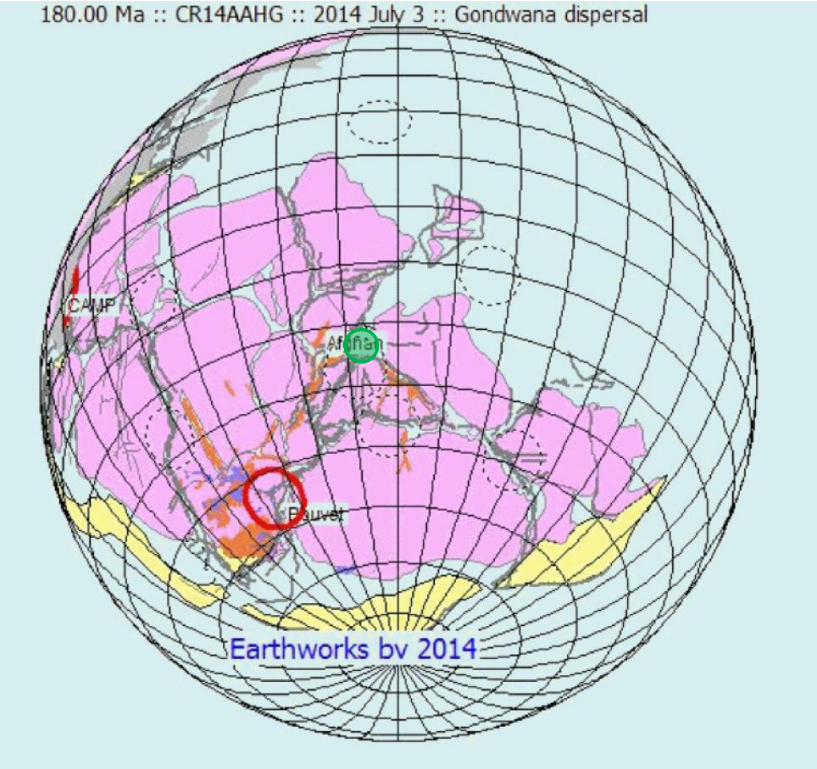

Figure 1.6: Gondwana reconstruction (ca. 180 Ma). Notice the various continental shields in pink, and the Karoo rifts in pale brown across south central Gondwana. The "outbreak" of the Bouvet plume is circled red and the position of the Seychelles circled green (Source: C. Reeves, www.reeves.nl/gondwana).

Seismic interpretation and borehole data from Morondava Basin shows an initial phase of extensional block faulting and rifting associated with the Karoo strata (Triassic). These sediments are mainly deposited in fluvio-lacustrine environments following the end of the Dwyka glaciation period in the late Permian. These pre-rift sediments were clearly deposited prior to the development of the Gondwana breakup rift because they were not influenced in the Late Liassic phase of extensional faulting. (Geiger, 2004). Over lying the rifted sediments are wedge-shaped sedimentary bodies (syn-rift) that occur within a series of late Early Jurassic half-grabens (the Andafia Formation). The half grabens were formed from the previous extensional faulting event (N-S and NNE-SSW striking faults, see Figure 1.5) as the fault-blocks became rotated. As a result, the floor of these basins were tilted westwards during tectonism and the sediments deposited in it exhibit a westward dip in their bedding planes, leaving the basement rocks outcropping on the eastern side of this continental fragment of Madagascar (Figure 1.7). These sediments, predominantly of shallow marine mudstones, possibly lagoonal settings, were deposited when extensional faulting ceased and followed by prolonged period of thermal subsidence (passive margin).

Madagascar was never fully submerged like the SMc, the sedimentary rock record was influenced mainly by fluvial environment such as west-facing fan delta fronts, alluvial fans, braided streams, lakes and swamps. Thereafter the rifting from the Karoo and early Jurassic, an extensive erosional surface developed above the syn-rift sediments, which is considered to be the breakup unconformity. Thereafter, prolonged thermal subsidence following the Bouvet magmatism event permitted the deposition of the Paleogene marine carbonates and other continental sequences (Sakaraha and Bemaraha formations) on the western coast (Figure 1.7) (Rakotosolofo, 1999; Rakotosolofo *et al.*, 1999; Schandelmeier *et al.*, 2004, Geiger, 2004). The SMc has similar shear orientations, but may have a thicker or higher basement on the eastern shelf, similar to Madagascar since they were once connected.

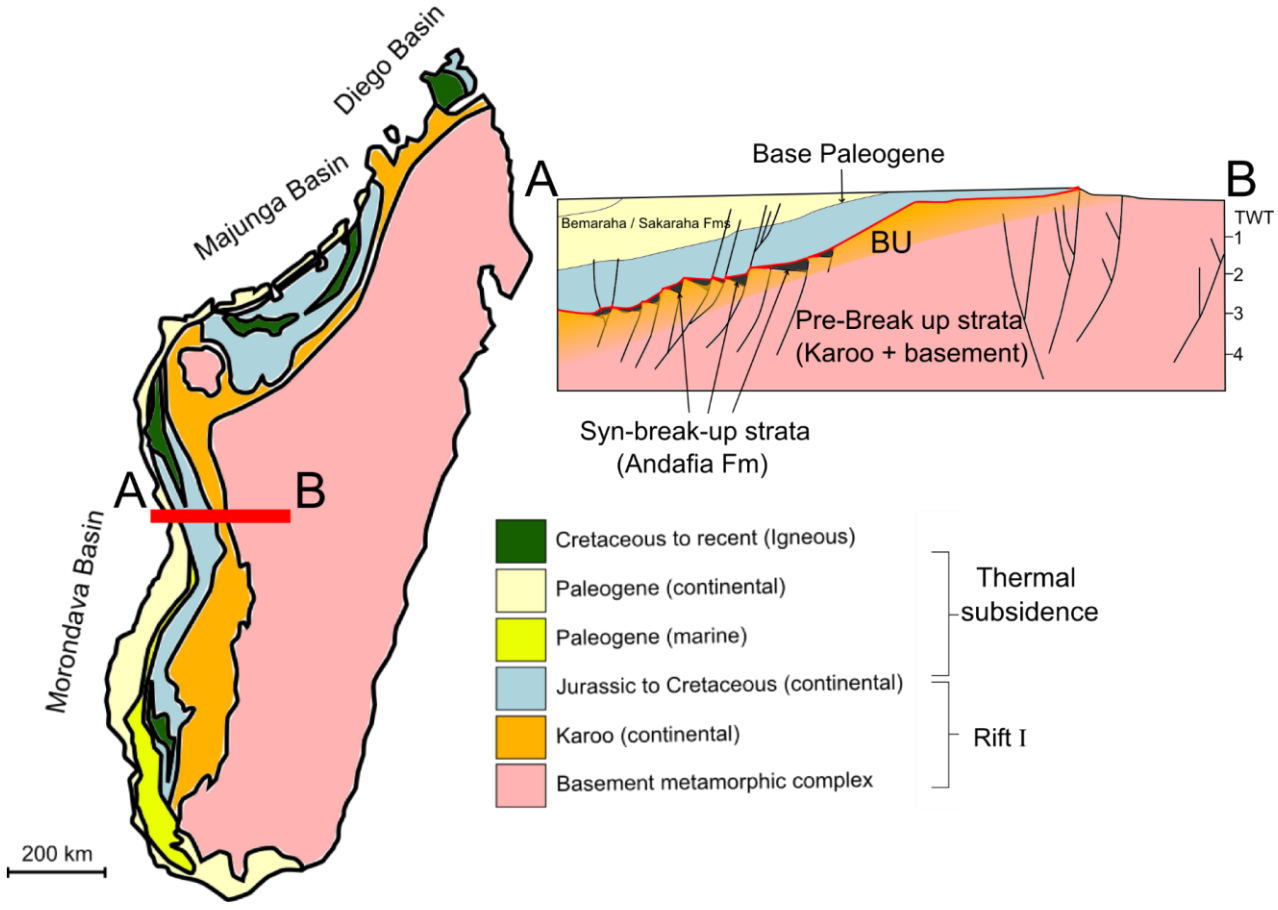

Figure 1.7: Simplified geological map of Madagascar, showing the various basins (Source: Modified from Geiger, 2004; Schandelmeier et al., 2004).

Du Toit (1937) first suggested that the Seychelles, being the only granitic island archipelago in the middle of the western Indian Ocean, continental crust was thought to be the most probable origin of these granitic islands. Subsequently, oil companies started to

gain interest in the region, and petroleum exploration activities increased substantially over the past few decades since the 1960s. As a result, a significant number of seismic surveys have been completed off the SMc since the 1970s, and geophysical data has verified the existence of the submerged continental crust in the Seychelles. In addition, seismic responses also indicated direct hydrocarbon indicators (DHIs) occur within the SMc. These DHIs include bright or flat spots, phase changes and gas chimneys at different locations that have been further correlated with well shows, gas sniffer anomalies and sea surface UV fluorescence anomalies (Plummer, 1994).

Seismic exploration activities commenced in the 1960s around the Mascarene Ridge and by 1973 attention was drawn to the hydrocarbon potential of the Seychelles when a regional seismic survey was completed by Bhurma Oil Company in the Indian Ocean (Wolden and Belle, 1992). This seismic survey included reflection profiles that display deep conformable sedimentary packages, as well as rotated fault blocks within the SMc (Khanna and Pillay, 1988; Plummer *et al.*, 1998).

From 1977 – 1986, 14237 km of seismic data was acquired across the SMc (7585 km of which were deep water survey) and 27911 km of aeromagnetic coverage was also acquired within the Seychelles territory. This was completed by Mobil, whose earlier survey started off the eastern coast of Kenya to Southern India; approximately 1900 km of this survey includes areas around the SMc, the Amirantes Ridge and other banks around the Seychelles. This survey also revealed gentle dipping reflectors and thick sedimentary successions, which further indicated the continental nature of the SMc. From 1987-1996, a total of 8442 km of seismic lines were shot by Enterprise Oil Exploration, 3370 km of which were deep water surveys, and over 5000 km of UV fluorescence and gravity data was also acquired (Seychelles National Oil Company, 1999). A summary of the seismic exploration surveys across the SMc is given in Table 1.1 (Seychelles National Oil Company, 1999).

Table 1.1: Summary of the seismic exploration surveys across the SMc (Seychelles National Oil Company, 1999)

	Seismic reflection survey	**Aeromagnetic and UV fluorescence survey**
1977-1986, By EXON Mobil	7585m	27911m
1987-1996, By Enterprise Oil	3370m	5000m

In the early 1980s, three wells were drilled by Amoco Seychelles Petroleum Company on the western shelf of the microcontinent; the Owen Bank-A1, the Reith Bank-1 and Seagull Shoal-1 well. All wells intersected thick successions of Cenozoic and Mesozoic strata, which proved the sedimentary origin of the cover and the underlying continental crust of the SMc (Amoco Seychelles Petroleum Company, 1981a, 1981b, 1981c). Seismic interpretation studies along various lines from the SMc have revealed a number of distinct listric faults that form part of rotated fault block systems. Such features are related to the extensional tectonics that the SMc has experienced during Gondwana break-up and subsequent expansion of the Indian Ocean, as the SMc broke off from Africa, Madagascar and India (Plummer and Belle, 1995; Plummer *et al.*, 1998). Several different types of sedimentary sequences have been revealed, via seismic interpretation, which include: rift continental clastics sequences and post-rift subsidence sequences with some volcanics, marine clastics and shelf carbonates sequences (Figure 1.8) (Plummer and Belle, 1995).

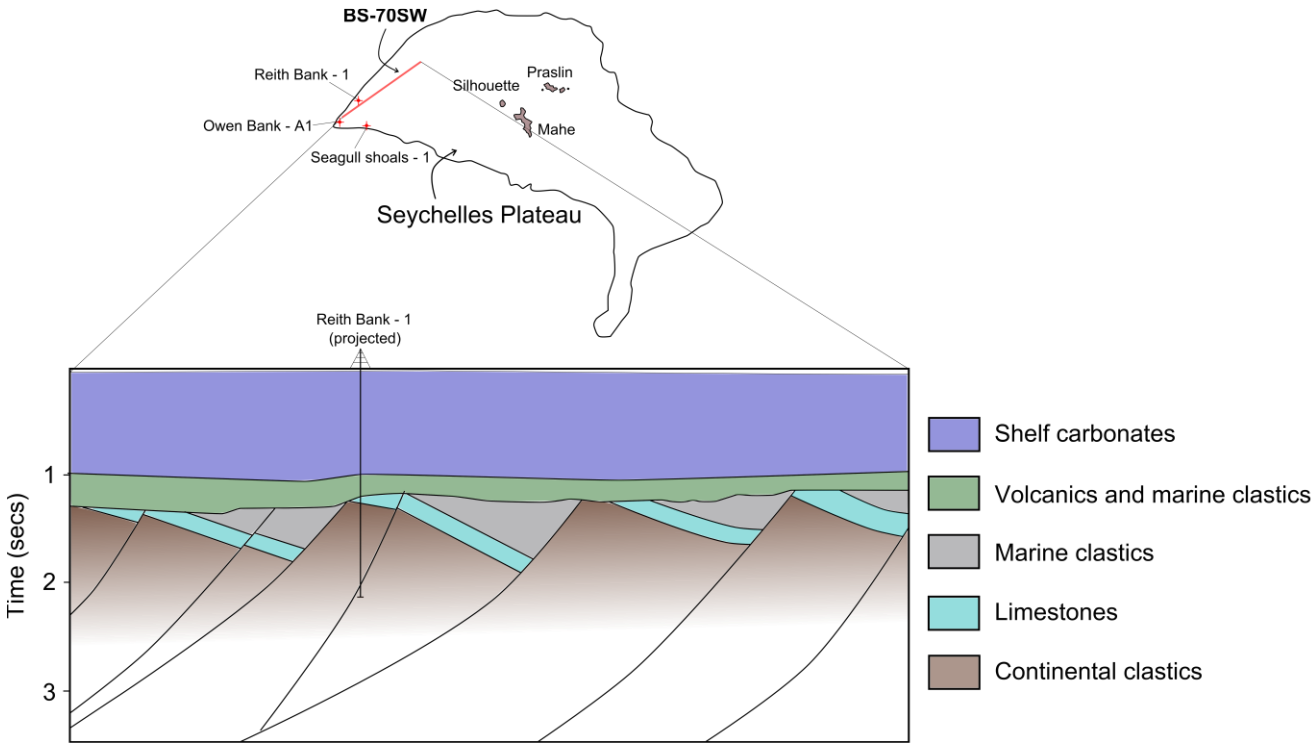

Figure 1.8; Seismic line BS-70SW projected through Reith Bank-1 on the western shelf showing tilted fault blocks of Early Jurassic and older continental clastics, and Middle to Late Jurassic marine limestones and clastics beneath a significant mid-Cretaceous unconformity (Source: Modified after Plummer and Belle, 1995)

The SMc is therefore surrounded almost entirely by rifted margins as it broke off from various continents almost on every side at different times (Figure 1.9). It is for this reason

that Oil companies have recently been interested as well. Similar to rifted margins across the eastern flank of Africa such as Tanzania and Mozambique offshore has yield exploration aspects in the last decades as several petroleum traps have been identified along those passive margins.

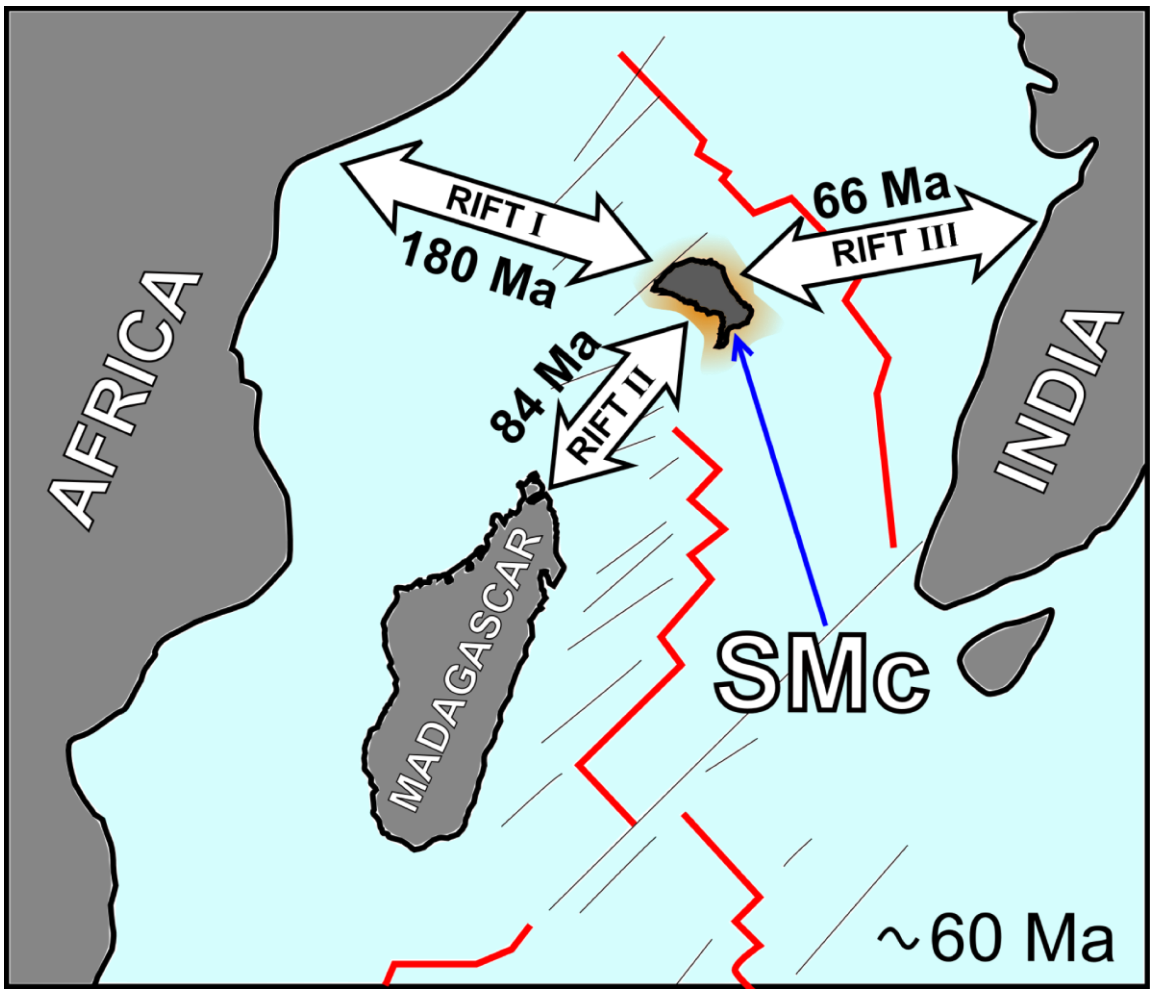

Figure 1.9: Various rifting events (I, II, III) that led to the fragmentation of East Gondwana and ultimately the break-up of the SMc from Africa (ca. 180 Ma), Madagascar (ca. 84 Ma) and India (ca. 66 Ma). (Source: Modified after Reeves, 2013.)

Rift-related basins and passive margins such as the SMc have stratigraphic successions that can be divided simply into mechanical rift sequences and post-rift thermal subsidence sequences. Rift sequences are recognized by their overall geometry of rotated fault blocks separated by extensional listric faults. Major unconformities generally separate the rift and thermal subsidence sequences. Such unconformities are known as break-up unconformities (BU) (Figure 1.10) (Franke, 2013). Prominent seismic reflectors arise as a consequence of episodes of non-deposition, and/or erosion following tectonic events such

as rifting, subsidence and/or eustatic sea-level changes. These unconformities are classified as sequence boundaries in a seismic context (*c.f.* Vail *et al.*, 1977) and are generally assigned a minimum age based on the age of their overlying sediments, or various absolute dating methods. These unconformities, also collectively referred to as seismic unit boundaries, are recognized by clinoform terminations such as toplaps, offlaps and downlaps, as analysed for the SMc in this project.

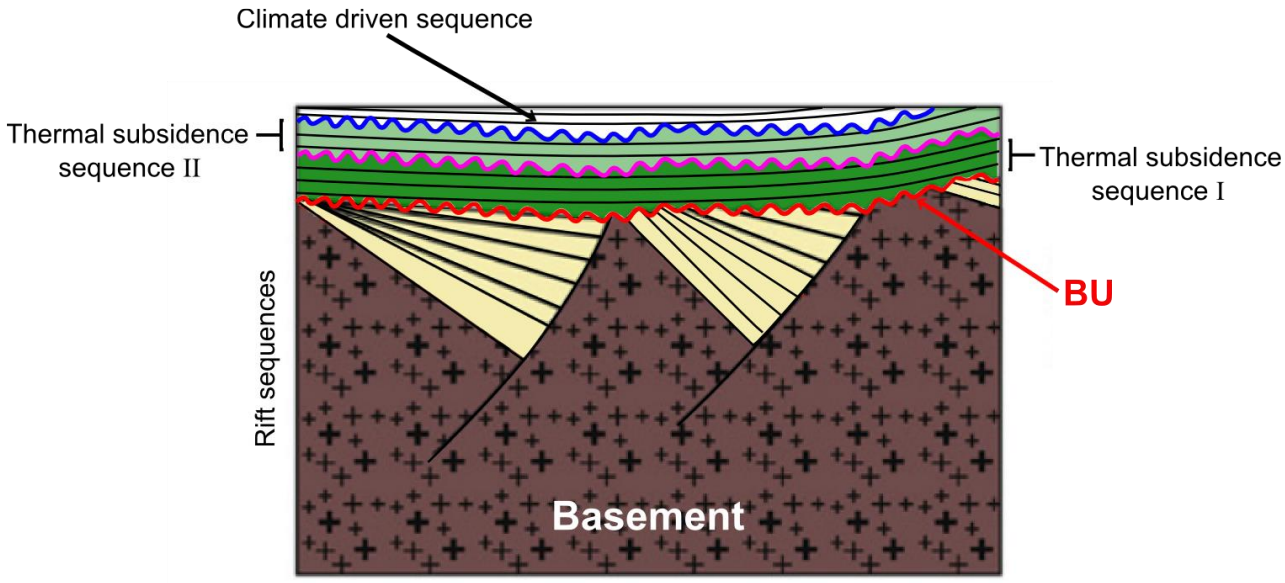

Figure 1.10: Schematic cross section diagram illustrating rift sedimentation (yellow), and a break-up unconformity (BU = red). Notice; Rift sedimentary infill typically shows wedge shaped reflector packages. BU truncates the wedge-shaped rift sediments, and are generally overlain by 1st order thermal subsidence sequences (green and pale green). Further changes, such as those related to climatic changes (2nd order) are separated by sequence boundaries (red, purple and blue lines) especially after subsidence when the climatic factors have more influence on the nature of transgressions and regressions (Source: modified from Franke, 2013).

Sequence Stratigraphy

Sloss (1949) introduced the term "sequence" as an "unconformity bounded unit" and in his scheme a sequence represents a period of relative high sea-level (or base-level) highs (MFS = maximum flooding surface), and that bounding unconformities represent sea-level lows (MRS = maximum regression surface). Sequences display stratal onlap onto the basement or unconformities as a response to increasing accommodation space for deposition of sediments during the next transgression phase or sea-level rise (Figure 1.10). Periods of non-deposition or erosion are characterised by truncation surfaces and toplaps (Sloss,

1963; Vail *et al.*, 1977; Vail *et al.*, 1991; Emery and Myers, 1996; Vincent *et al.*, 1998; Keighley *et al.*, 2003a; Keighley *et al.*, 2003b; Catuneanu *et al.*, 2009). Such sequence characteristics will be explored in the seismic section of this project.

Van Loon (2000) summarized three main types of sequences as: unconformity bound; litho-facies related; and sea-level bound sequences.

1) Unconformity bound sequences are geologic packages of ranks higher than Groups or Supergroups.

2) Lithofacies related sequences are geologic packages that record successions of related facies originating in specific palaeo-environments.

3) Sea-level bound sequences represent bounding surfaces of sequences that can be correlated laterally and originate from the same sea-level cycle.

Sequence boundaries are primarily identified through seismic stratigraphic interpretation and further correlation with the bio-stratigraphy and well-logs. Thereafter, the wells are correlated based on the identified regional major unconformities or sequence boundaries (Embry and Johannessen, 1992; Van Loon, 2000; Catuneanu *et al.*, 2009; Catuneanu *et al.*, 2011). Sequences are directly related to the accommodation space created for sedimentary sequences to be deposited, and are influenced by various processes: climate (e.g. glaciation), tectonics (spreading rates; hotspot activity and orogeny) and sediment supply and loading (Figure 1.11) (Miller *et al.*, 2001). Different processes induce different magnitudes and rates of sea-level change. Five orders of sea-level cycles have thus been identified (e.g. 1^{st} to 5^{th} order cycles; Vail *et al.*, 1977).

Climate driven eustatic cycles involve the cyclicity of temperature variations of the earth's atmosphere that eventually leads to global warming and global cooling. A global rise in temperature leads to glacial retreat and melting of the ice caps to the ocean, and further ocean water expansion, all of which ultimately lead to eustatic rise in sea-level and transgression onto the continental landmasses at a fairly high rate (>10 $km.yr^{-1}$) (Miller *et al.*, 2011). Global drop in temperature leads to water retention over the continental landmasses and at the poles through glacial formation and further ocean contraction ultimately causing eustatic drop in the sea-level (Miller *et al.*, 2011; Rowley 2013). The change in the eustatic sea-level here ranges to over 300 m. Climatic changes cause short term variations in eustatic sea level (10^3-10^6 year scale), unlike tectonic processes which

cause long term changes (10^7-10^8 year scale) such as ridge volume (related to spreading rates) and orogeny (e.g. continental collision; continental break-up) (Figure 1.11). According to Zachos *et al.*, (2001), the higher frequency change in climate is generated by periodic oscillations in the Earth's orbital characteristics such as eccentricity, obliquity and precession that affect the distribution of incident solar ray energy onto the Earth's surface.

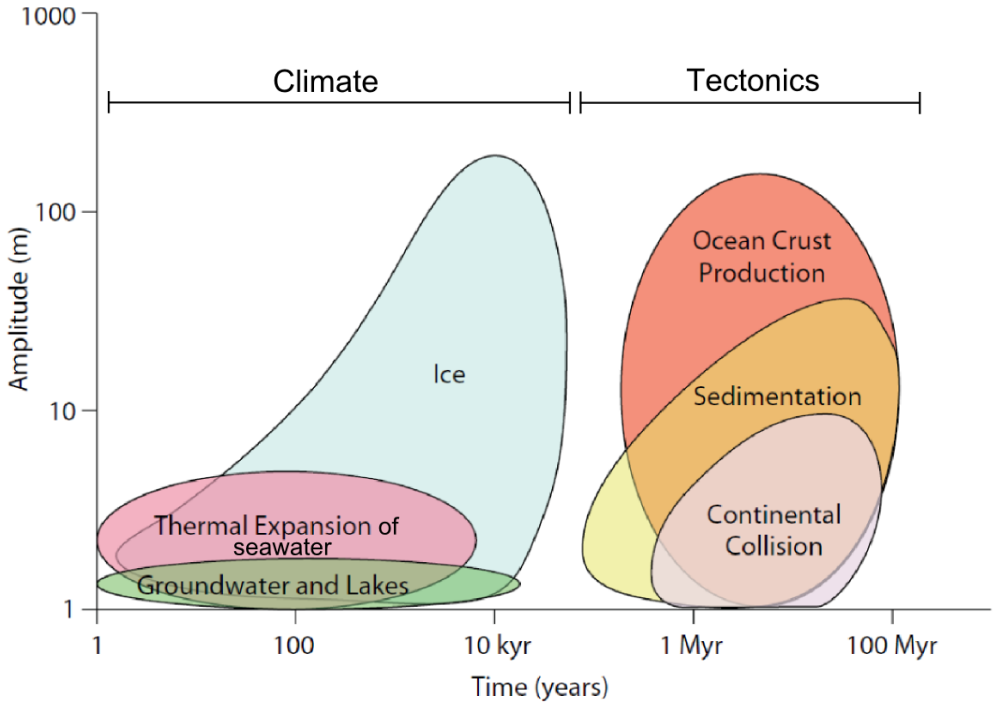

Figure 1.11: Mechanisms for sea-level change, with their range of amplitude and time (Source: Taken from Miller et al., 2001)

Pitman (1978) suggested that volumetric changes of mid ocean ridge systems also lead to eustatic fluctuations in the sea-level during the spreading evolution. This is because ocean ridges are basically thermal bulges that are capable of displacing sea water depending on their spreading rates (Figure 1.12). In a particular experiment, Pitman (1978) initially calculated the rates of spreading for fast and slow mid-ocean ridges through a 70 Myr period. He concluded that a constant spreading rate displaced seawater to the deep ocean basins from the shallow seas of the continental shelves. This is because such ridges showed a decrease in ridge volume over time. On the other hand, a ridge with a slow initial spreading rate (e.g. 2 cm/y) that eventually increases to a faster rate (e.g. 6 cm/y) displaced water across the continental shelves forming shallow seas. This is because the increase in the spreading rate of the mid-ocean ridge caused an increase in the ridge volume, which in turn causes the displacement of seawater from the deep ocean basins onto the continental shelves. Pitman (1978) concluded that during rapid rates of seafloor spreading, there will

be a landward shift of the shoreline (transgression), a eustatic rise in sea-level, whereas during slow rates of seafloor spreading there will be a seaward shift of the shoreline (regression), a eustatic fall in the sea-level (Figure 1.12).

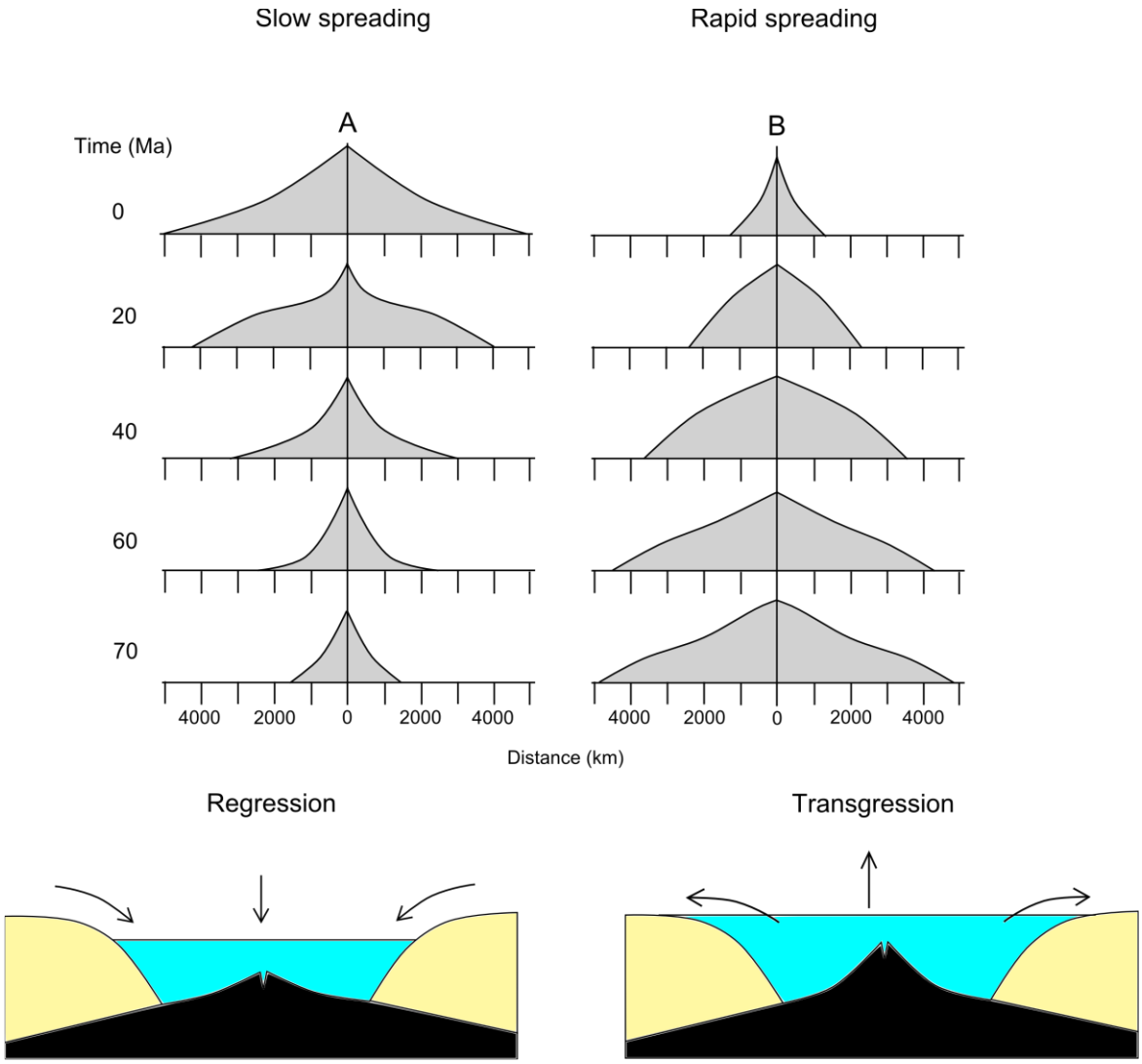

Figure 1.12: Curves illustrating; (A) Slow spreading rates of ridges that cause decreased ridge volume and ultimately sea-level drop and regression, seaward shift in shoreline, and; (B) Fast spreading rates of ridges that cause increased ridge volume and ultimately sea-level rise and transgression, landward shift in shoreline (Source: Modified after Pitman, 1978)

A model initially proposed by McKenzie (1978), explains that within a vertical column of continental lithosphere there will be symmetric stretching during an extensional rifting event. The instantaneous initial mechanical stretching is associated with subsidence that ultimately leads to a rift phase, resulting in rapid sedimentary infill, also referred to as rift sequences as the sea-level protrudes into the rift basin. This McKenzie model explains that subsidence is directly related to isostatic compensation causing asthenospheric mantle

upwelling and intrusion into the lithosphere, which in turn causes a higher temperature gradient. This thermal anomaly which lies beneath the stretched lithosphere eventually begins to cool through thermal conduction and contract. This increase in mantle density as lithospheric stretching ceases and cools, causes a subsequent episode of subsidence called thermal subsidence. This second subsidence occurs exponentially, as the lithosphere attains its original thermal state but at a much slower rate than the rapid initial subsidence in the process of maintaining isostatic equilibrium which leads to a further rise in local sea-level of the region (Figure 1.13) (McKenzie, 1978; Cochran, 1983; Cloetingh and Kooi, 1989).

Well-logs, also referred to as wireline logs, provide primary data used in basin analysis and is central to this study. Well-logs essentially records specific lithological characteristics against depth of the rock formations traversed by a measuring probe down the well, acquiring in situ measurements of the physical properties of the rock sequence. There are various types of well-logs, each recording a different rock property (e.g. Serra, 1984). Well-logs are correlated with seismic cross sections for higher resolution stratigraphy. Well-cuttings or well-chips are retrieved as the principal source of subsurface sampling since it is less expensive than coring; however it is also less efficient and less accurate. The reason for this is that well cuttings can experience mixing and general contamination by the drilling fluid (e.g. mud) during retrieval to the surface. Nevertheless, from cuttings, reconstruction of a lithological sequence in terms of thickness and composition can only be trusted if used hand in hand with related information such as wirelogs or seismic data (Serra, 1984).

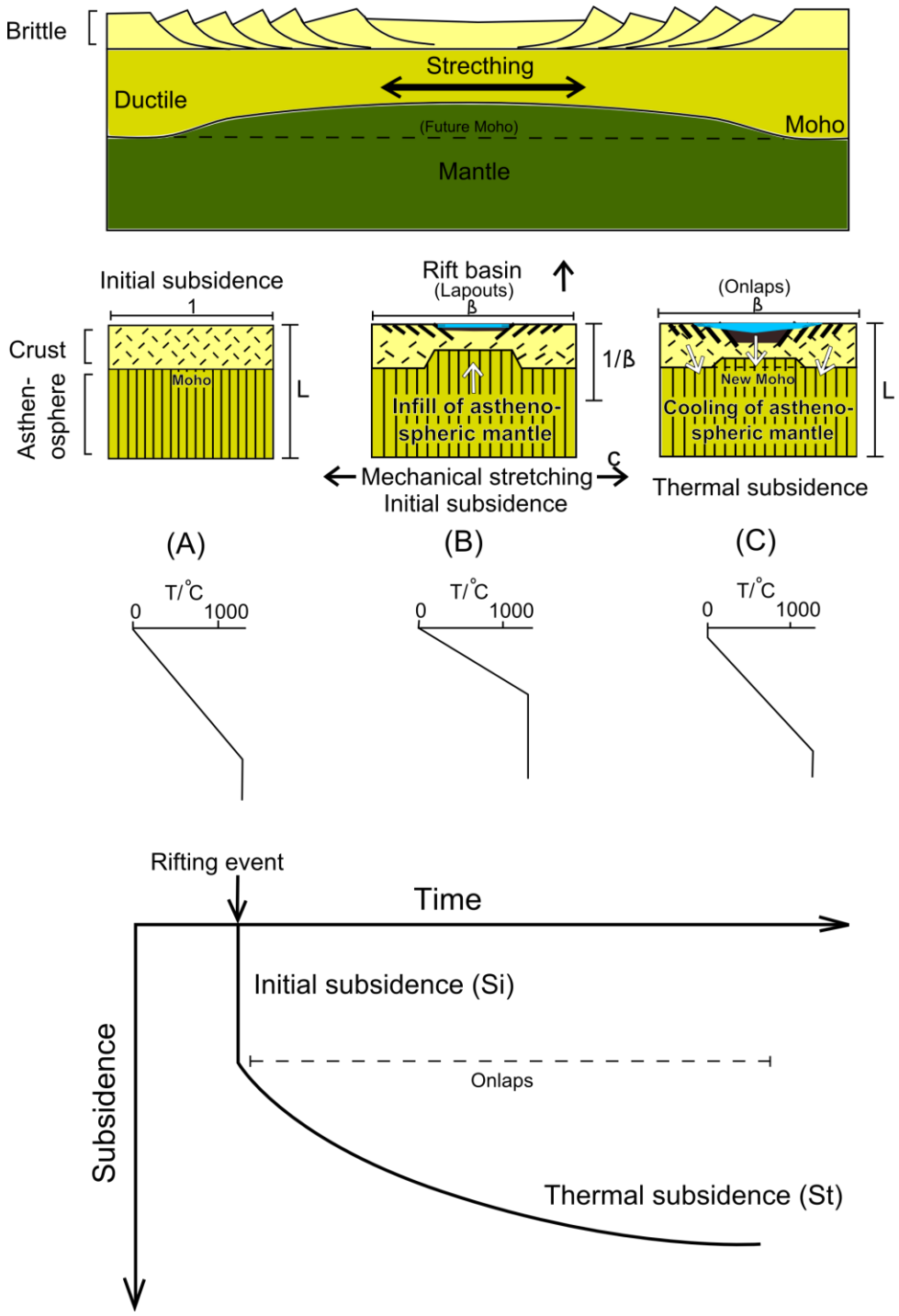

Figure 1.13: Mechanical stretching model of McKenzie (1978), showing initial stretching that leads to thermal subsidence. Notice: (A) T=0; (B) Instantaneous extension 1 to β, and crustal thinning to 1/ β (β = extension factor), resulting in higher temperature gradients; and (C) Thermal subsidence when rifting ceases (Source: Modified from Cochran, 1983).

1.2 Thesis objectives and outline

This project aims to improve the existing geological knowledge of the origin and evolution of the SMc by describing the Phanerozoic sedimentary geology of the Seychelles and analysing for the influence of various tectonic episodes on the sedimentation. This is achieved through interpreting the offshore geological and geophysical data. A CD-ROM of the dataset is attached at the end of this thesis document, this includes paleontology, stratigraphy, well-logs and seismic reflection data. The dataset used in this thesis have been collected mainly from the past unpublished in-house reports, produced in particular, by the oil companies (e.g. Exxon, Enterprise Oil, Amoco Seychelles Petroleum Company). Bio-stratigraphy is used as the main age-control, since no reliable radiometric dating has been completed on the rock chips from the wells along the western shelf of SMc. Seismic data from the study area (Figure 1.2) is also analysed, interpreted and integrated into a sequence stratigraphic framework. From this extensive data set a sequence stratigraphic framework is constructed and is presented together with the reconstructed palaeo-environmental interpretations of the western shelf in this project. From this a tectonic evolution of the SMc is derived.

Chapter 2 of this thesis presents a detailed review of the tectonic setting and evolution of the Seychelles during the break-up of eastern Gondwana, based on literature research. This helps to determine the age of the main stratigraphic events during the break-up regime that can be recognized in the stratigraphy of the SMc, such as disconformities as observed in the available data. Chapter 3 outlines the geology of the Seychelles and the surrounding region, which provides an overview of the main, previous geologic work that has been conducted in the Seychelles. Chapter 4 describes the data sets and methodology used in this project, which includes seismic stratigraphic analysis, bio-stratigraphy, litho-stratigraphy from well-logs, sedimentary facies analysis, depositional environment analysis and finally backstripping method applied to the main stratigraphic units identified, and the subsidence analysis of SMc. Chapter 5 presents the detailed results from the seismic, bio-stratigraphy, litho-stratigraphy and the facies analysis which further includes the stacking patterns, facies associations and sequence analysis and correlation. Chapter 5 also summarizes the subsidence history of the SMc in relation to the overall break-up regime that the SMc experienced within the Gondwana framework, followed by the results analysis and discussions. Lastly, Chapter 6 summarizes and concludes this thesis by presenting the main findings and interpretations.

Chapter 2. Tectonic evolution of the Seychelles Microcontinent

Gondwana was intact between the end of the Neoproterozoic (*ca.* 550 Ma) until Early Jurassic (*ca.* 160 Ma) (Figure 2.1). The SMc formed a central part of the Gondwana Supercontinent within that time period; NE of Madagascar and SW of India in a reconstructed Gondwana (Figure 2.1). The current position of the SMc suggests that this continental fragment has been subjected to a complex tectonic history since the break-up of Gondwana (de Wit, 1988; de Wit and Ransome, 1992; Suwa *et al.*, 1994; Reeves and de Wit, 2000; Reeves *et al.*, 2002, Reeves, 2013).

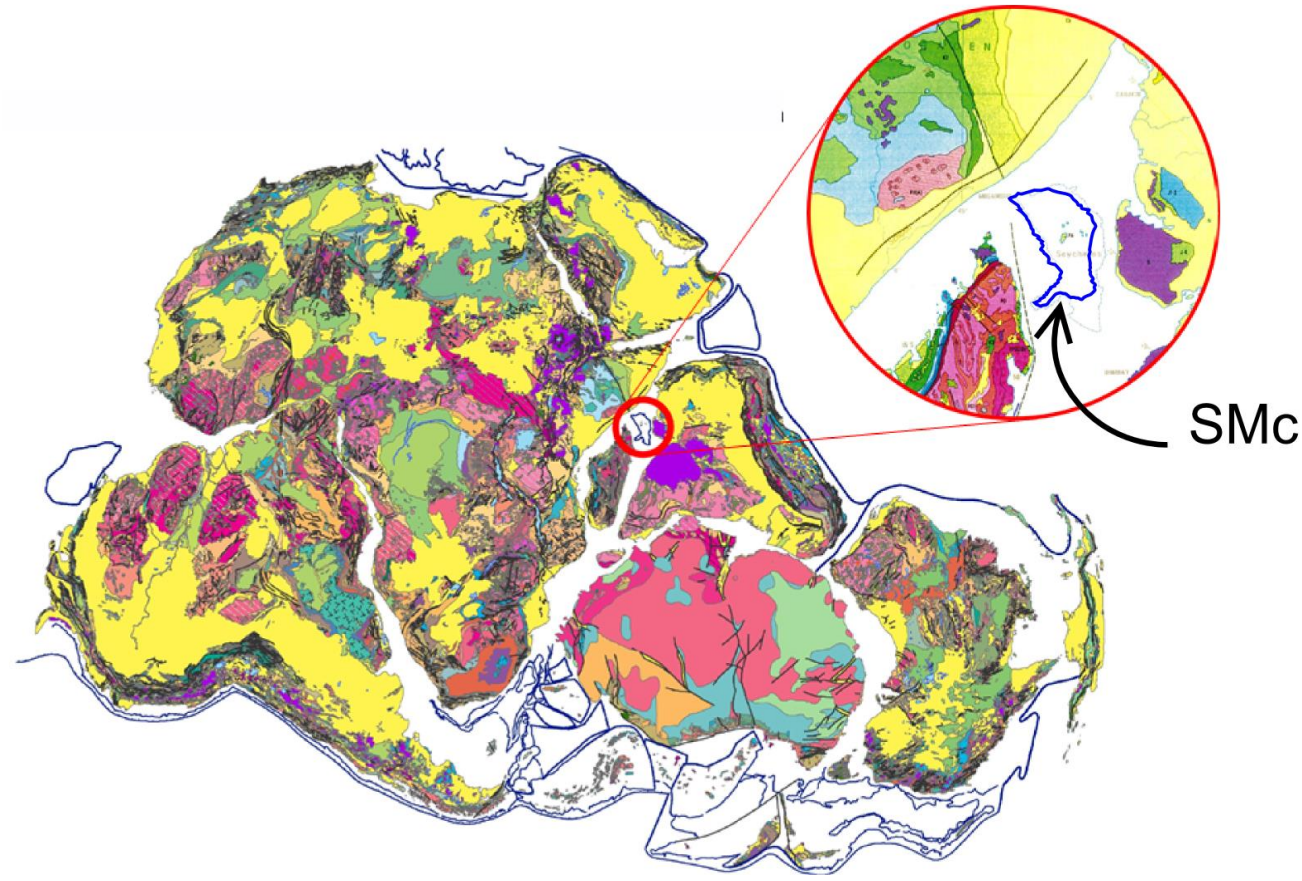

Figure 2.1: Geological map of Gondwana (updated by Gondwana GIS database), highlighting the Seychelles microcontinent in the red circle during Carboniferous-early Jurassic at around 150 Ma (Source: de Wit et al., 1988)

2.1 Amalgamation of East and West Gondwana

The amalgamation of Gondwana is thought to have taken place in the Early Neoproterozoic and lasted into the early Palaeozoic (*ca.* 850 - 500 Ma) (de Wit *et al.* 1988). This phase involved the collision and "collage" of the individual shields that originated from the break-up of Rodinia (e.g. Kalahari shield, Congo shield, Amazonian shield), which subsequently amalgamated to form Gondwana (*ca*, 1300–900 Ma). This ultimately caused the closing of the Mozambique Ocean and formed a series of linear orogenic belts around the individual shields in the late-Neoproterozoic. This event is also referred to as the "Pan African orogeny" (Figure 2.2) (Powell and Pisarevsky, 2002; Fritz, 2013; Satish and Kumar, 2013). As a result this caused the Seychelles' granite emplacement (*ca.* 750 Ma) which is derived from metamorphism and partial melting of Pre-Cambrian crust during the compression tectonics associated with the amalgamation of Eastern Gondwana (Tucker *et al.*, 2001; Torsvik *et al.*, 2001; Ashwal *et al.*, 2002; Li *et al.*, 2008) (See Chapter 3 for details).

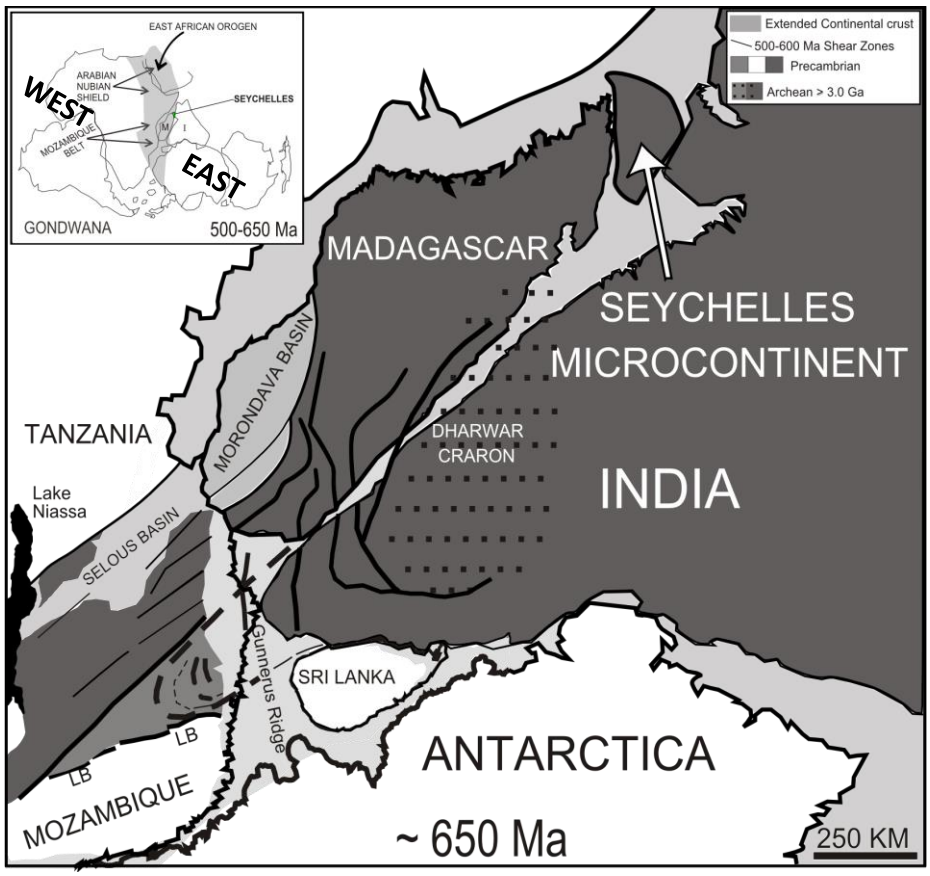

Figure 2.2: Tight reconstruction of Gondwana fragments juxtapositions against East Africa at 650 Ma within the East African Orogen (top left). The fit of the SMc and Madagascar is derived using piercing points of dated shear zones (solid black lines) projected to the continental margins (Source: Modified from de Wit, 2003).

2.2 East – West Gondwana separation and the proto-Somali Basin

The earliest rifting across central Gondwana took place in the Late Palaeozoic sometime around 350-250 Ma, forming a series of elongated grabens and failed rift basins that initiated the deposition of the Karoo sediments around south-central Africa, in what are known as the Karoo rifts. This rifting event eventually led to the break-up of Gondwana which was initiated by the reactivation of the early inland failed rifts (Daly *et al.*, 1989; Trouw and de Wit, 1999; Catuneanu *et al.*, 2005; Linol, 2013; Linol *et al*., *in press*, 2014). These rifts accumulated mainly non marine Carboniferous to Early Jurassic sediments, although there was a marine incursion recorded in the southern Karoo by the end of the Carboniferous (Wopfner and Kreuser, 1986; Catuneanu *et al.*, 2005; Johnson *et al.*, 2006, Reeves *et al*., 2014).

The origin of the onset of the Karoo rifts is unclear, though it is speculated to have been formed during the formation of the southern Gondwanide from which the Cape Fold Belt (CFB) formed part of (*ca.* 250 Ma). The earlier accepted theory was that such regional rifting that led to the Gondwanide Orogeny was formed in a compressional back-arc setting related to flat slab subduction along the southern margin of Gondwana (Lock, 1980). A dextral strike-slip component also formed due to oblique subduction in the process, and this is visible throughout the CFB (Trouw and de Wit, 1999).

In contrast, Lindeque *et al.*, (2011) proposed that the CFB may have originated from an arc-continent collision during subduction to the south, which inland gave rise to a Jura-type fold belt. More recently, it was proposed that the CFB formed due to a sinistral strike-slip orogen linked to oblique reactivation of the southern Namaqua suture and the northern boundary of the CFB created the South African Karoo foreland basin (Lindeque *et al.*, 2011; Tankard *et al.*, 2012).

A second phase of rifting occurred during Late Triassic to Middle Jurassic time at approximately 200 – 180 Ma. This phase is thought to have been linked to mantle processes, for example the very large Central Atlantic Magmatic Province (CAMP) associated with the initial break-up of Pangea (*ca.* 200 Ma) (Knight *et al.*, 2004; Blackburn *et al.*, 2013). Subsequently, the Bouvet mantle plume erupted forming the Drakensberg basalts associated with the formation of the Karoo and the Ferrar LIP (*ca.* 180 Ma) (Encarnacion *et al.*, 1996; Riley and Knight, 2001; Reeves, 2013; Reeves *et al*., 2014). This occurred as a result of the extension and opening of East and West Gondwana which propagated a rift system flanking

the East coast of Africa (NE - SW). This led to the development of a major passive margin and formation of today's east African coast, a part of which the SMc occupied (Reeves, 2014). Further rifting eventually resulted in the break-up of East and West Gondwana and the opening of the proto Indian Ocean, Somali Basin and Mozambique Basin (*ca.* 175 Ma) followed by seafloor Spreading and oceanic crust formation (*ca.* 160 Ma) (Torsvik, 1998; Jokat *et al.*, 2009; Reeves, 2013; Reeves *et al.*, 2014). The extensional regime between the East and West Gondwana was accommodated also by dextral strike-slip/transcurrent fault systems between East and West Gondwana, along the Davie Fracture Zone between Mozambique and Madagascar, and along the Owen Fracture Zone between Somali and Seychelles (Reeves and de Wit, 2000; Reeves *et al.*, 2014). This break-up event is represented by the oldest recognized seafloor anomaly in the Somali Basin (M22) of 156 Ma (Figure 2.3) (Reeves *et al.*, *in press* 2014; Mukhopadhyay *et al.*, 2012).

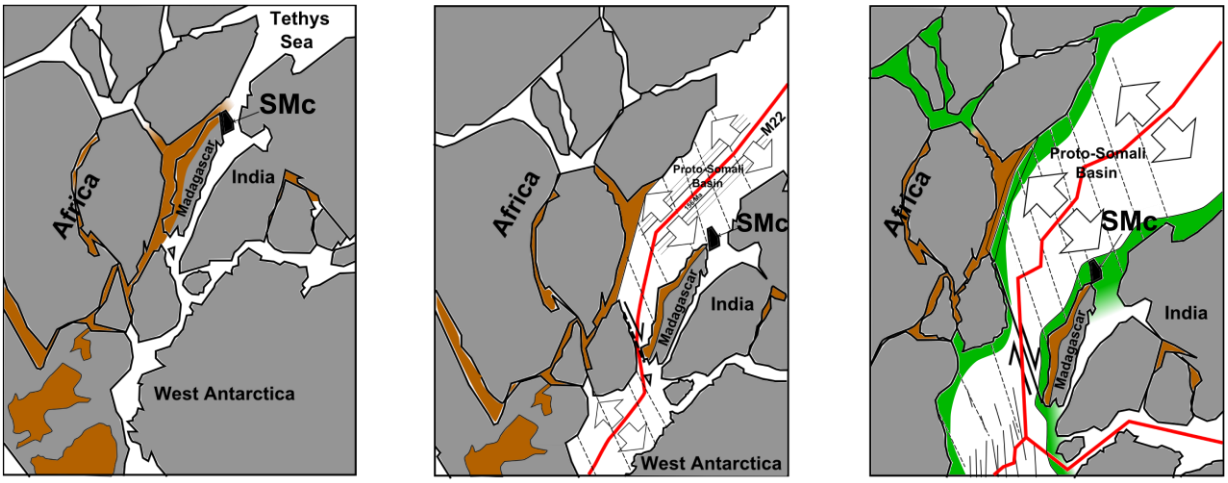

Figure 2.3: Three stages (180-140-100 Ma) of the separation of East and West Gondwana, shown by the Precambrian fragments (grey). Karoo aged sediments are shown in brown and Cretaceous sediments shown in green. Notice: SMc is indicated in black (Source: Modified after Reeves, 2013).

2.3 East Gondwana break-up and the opening of the modern Indian Ocean

Rifting continued along the western margin of East Gondwana after the Middle Jurassic. This phase is marked by a marine transgression phase at around 180 Ma after the proto Somali ocean basin started to form and the Tethys Sea protruded southwards into Gondwana. According to Reeves *et al*. (2014), it is postulated that this rifting phase was a continuation of the Carboniferous – Triassic rifting event which lasted until around 160 Ma when there East and West Gondwana separated completely. This produced shallow restricted – marginal marine conditions along the eastern coast of West Gondwana and along the western coast of East Gondwana including the future western shelf of the SMc. This led to the period marked by the development a regional oolitic marker, as observed in the wells of the western shelf of the SMc (see Chapter 5.3 and Chapter 5.4 for details).

Initially the ocean growth was confined to the proto Somali basin (*ca.* 175 Ma) and migrated southwards along the East Africa as rifting proceeded to cause total separation of East and West Gondwana (*ca.* 160 Ma). Australia/Antarctica separated from Madagascar/India/Seychelles sometime in the Early Cretaceous, which correspond to the M9 magnetic anomaly (*ca.* 133 Ma), related to the Kerguelen mantle plume that erupted at around 136 Ma and ultimately formed the Kerguelen Ocean (Storey, 1995; Gibbons *et al.*, 2013: Reeves, 2013; Reeves *et al*., 2014). Further rifting occurred as a consequence of a major strike slip movement between Madagascar and India/Seychelles, and this lasted until the Early Cretaceous (pre-88 Ma) when Madagascar eventually separated from greater India/SMc at around 84 Ma as they drifted over the Marion mantle plume which erupted at around 88 Ma (Gibbons *et al.*, 2013; Reeves, 2013; Torsvik *et al.*, 2013; Reeves *et al*., 2014). As a result the Mascarene Basin was formed and drifting started when the Mascarene spreading ridge formed and the Indian plate moved anti-clockwise as it drifted northwards. At the same time the Amirantes Ridge also formed. It has been speculated that it was formed as a result of the anti-clockwise rotation of the Indian plate (Coffin and Rabinowitz, 1992; Torsvik, 1998, Mukhopadhyay *et al*., 2012; Gibbons *et al.*, 2013; Reeves *et al*., 2014), which induced seafloor spreading south of the western shelf, and partial subduction flanking the western margin of the SMc to form the Amirantes Ridge - Trench Complex (*ca.* 82 Ma) (Figure 2.4-Figure 2.5) (Fisher *et al.*, 1968; Suwa *et al.*, 1994; Plummer and Belle, 1995; Plummer, 1996; Eagles and Hoang, 2013) (see Section 3.6).

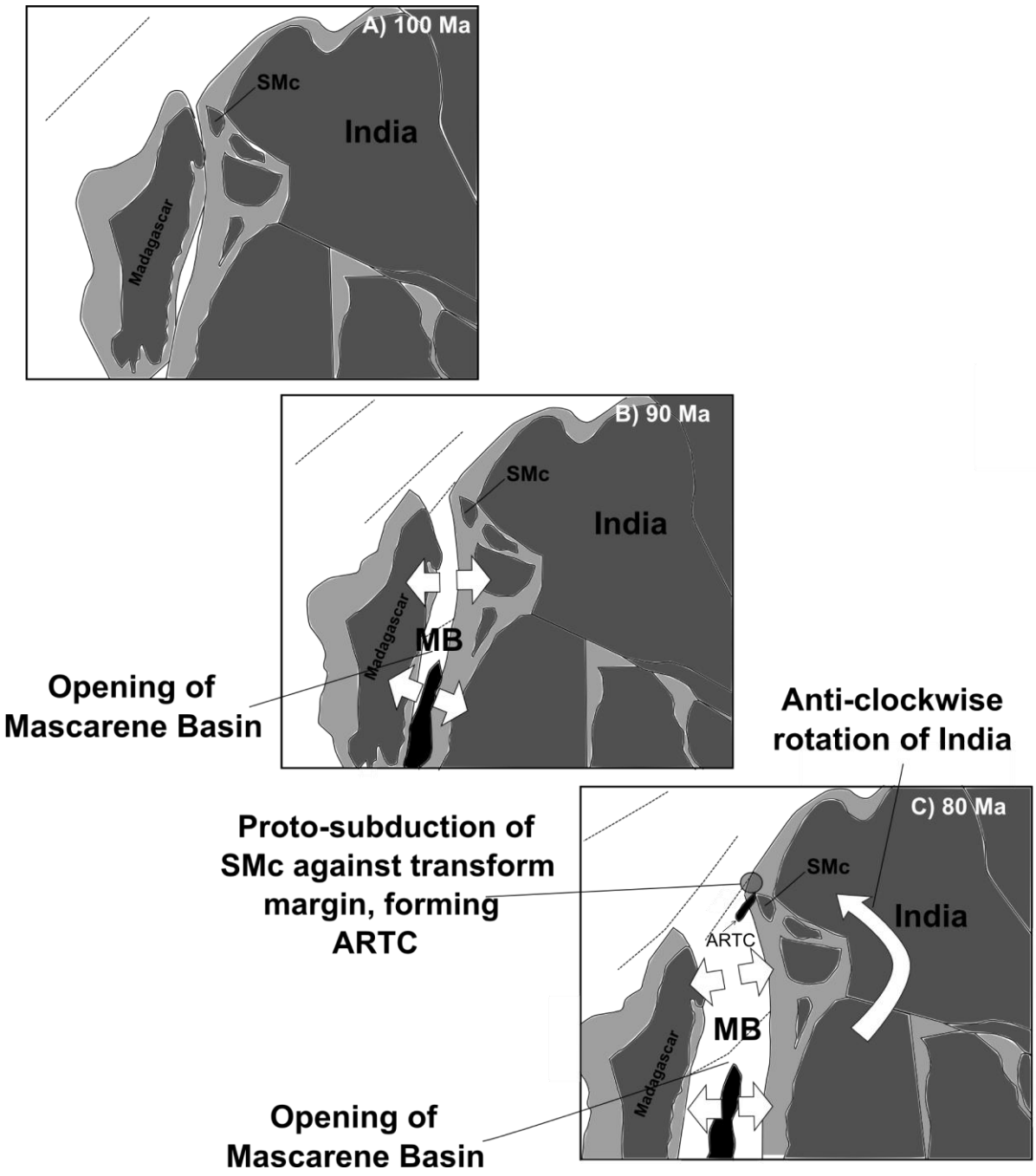

Figure 2.4: Three stages (100-90-80 Ma) of the separation of Madagascar from Seychelles/India, showing the opening of the Mascarene Basin and the formation of the Amirantes Ridge-Trench Complex (ARTC) following the anti-clockwise rotation of India Seychelles. The Precambrian fragments shown in grey, the extended continental crust is shown in pale grey and new oceanic crust is shown in black. Notice: SMc/India rotated at a significant rate from 90-80 Ma. SMc is indicated in black. (Source: Modified after Reeves et al., in press 2014).

After breaking off from Madagascar, the Indian plate (India/SMc) moved rapidly northwards (*ca.* 116 km/Myr) over the Reunion hotspot which ultimately initiated further rifting and the eventual break-up between the SMc from India which led to the eruption of

the Reunion plume forming the Deccan LIP and ultimately the Carlsberg Ridge (*ca.* 66 Ma) (Ganerod *et al.*, 2011). Shortly after this eruption, the SMc drifted away from India at around 63 Ma (Figure 2.5). This ultimately formed the Silhouette and North Islands that comprise of younger granite complexes cut by young basaltic dykes (*ca.* 63-66 Ma) as the SMc drifted over the Reunion hotspot (Baker, 1963; Stephens, 1996; Torsvik, 1998; Ashwal *et al.*, 2002; Schlüter, 2008; Ganerod *et al*., 2011) (see Section 3.4).

During the Early Paleogene, as India and SMc further drifted away from each other, the Mascarene Spreading centre stopped and relocated to the North of the SMc as the Central Indian Ridge linked up with the Carlsberg Ridge to accommodate for this spreading. This was probably imposed by a vigorous plume (Torsvik *et al.*, 2013). This caused the Seychelles to re-join the African plate and further drift southwards to its present location (Figure 2.5) (Coffin and Rabinowitz, 1992; Plummer and Belle, 1995; Plummer *et al.*, 1999; Ganerod *et al*., 2011; Reeves, 2013; Torsvik *et al.*, 2013). The Indian plate eventually collided with the Eurasian plate forming the Himalayan-Tibet Alpine orogeny at approximately 50 Ma (Figure 2.5) (Searle *et al*., 1987; Yin and Harrison, 2000; Hodges, 2000).

Paleogene sedimentation, dominated by open marine reef and shelf carbonates covered the whole of the SMc (>500 m thick) as clastic sediments became rare because the lack of substantial eroding source of nearby landmasses to provide the clastic input at the time. At the end of this long history of break-up and drift regime, the SMc and Indian plate drifted to their current positions.

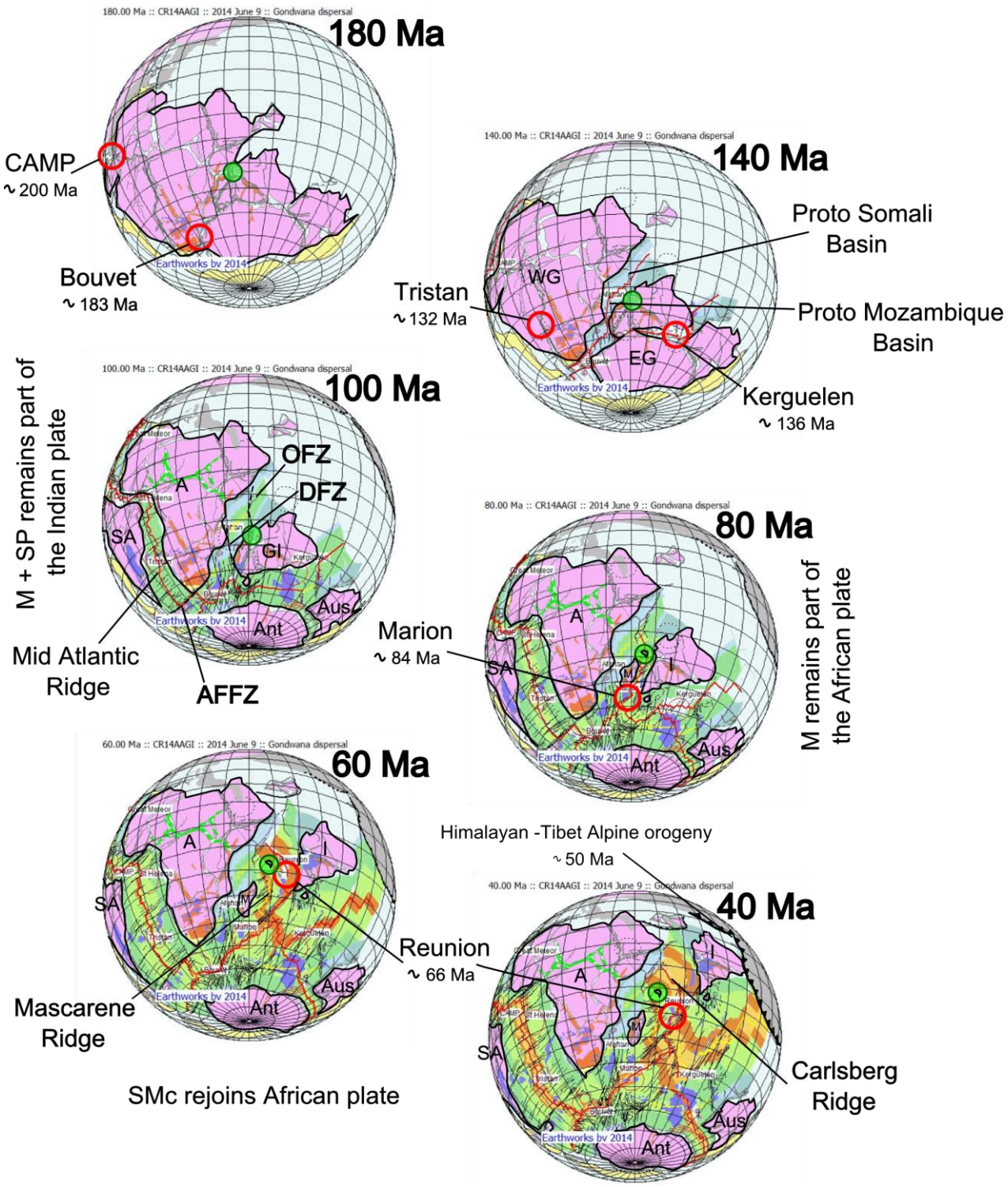

Figure 2.5: Sequences of Gondwana break-up highlighting the Indian Ocean, shown at ca.180 Ma, 140 Ma, 100, 80 Ma, 60 Ma and 40 Ma. The red circles indicate the position of the various hotspots and the green circle indicates the successive positions of SMc. WG=West Gondwana; EG=East Gondwana; A=Africa; SA=South America; M=Madagascar; GI= Greater India (India+Madagascar+Seychelles); I= India; Ant=Antarctica; Aus=Australia; OFZ= Owen Fracture Zone; DFZ= Davie Fracture Zone; AFFZ= Agulhas-Falkland Fracture Zone (Source: C. Reeves, www.reeves.nl/gondwana)

As a result of the break up regime (Figure 2.5 and Table 2.1), the sedimentary facies changed from continental to restricted marine and to open marine depositional environments.

Table 2.1: Summary of the main tectonic events that eventually led to the amalgamation and the separation of East and West Gondwana in a Seychelles Framework

Tectonic events	**Igneous activities (Ma)**	**Time period**	**Age of tectonic events and the onset of seafloor spreading (Ma)**
Pan African Orogeny / Amalgamation of Gondwana	Alkali granites (~750 -755)	Late Proterozoic – Early Cambrian	~850-530 (e.g. Fritz *et al*., 2013)
Separation of Pangea	CAMP LIP (~200)	Rhaetian	~200 (e.g. Knight *et al*., 2004; Blackburn *et al*., 2013)
Separation of East and West Gondwana	Karoo-Ferrar LIP from Bouvet plume outbreak (~ 183)	Toarcian	~165 (e.g. Torsvik *et al*., 1998)
Separation of Australia/Antarctica from Madagascar/India/Seychelles	Kerguelen basalts (~136)	Valanginian	~130 (e.g. Storey, 1995)
Separation of Madagascar from Seychelles/India	Late Cretaceous basalts from Marion plume outbreak (~88)	Coniacian	~84 (e.g. Torsvik *et al*, 1998, de Wit, 2003)
Separation of Seychelles from India	Deccan basalts from Reunion plume outbreak (~66)	Maastrichtian to Danian	~63 (e.g. Torsvik *et al*., 2001; Ashwal *et al*., 2002; Reeves *et al*., 2002; 2013; 2014)

Chapter 3. Regional geology of the Seychelles

3.1 The granite basement of Seychelles

The surface geology of the Seychelles comprises mainly of granite and coralline islands. The granites form part of a Neoproterozoic continental basement (*ca.* 750 Ma) (e.g. Mahe and Praslin group), and the younger granites originate from the volcanic complexes (*ca.* 65 Ma; Silhouette and North island only) (Figure 3.1).

The uniqueness of the Seychelles granites was long recognized by du Toit (1937) who suggested that these granites were probably part of a submerged continental crust. The granites' origin was only confirmed in the early 1960s when they were extensively studied by Baker (1963), who mapped all the main granitic islands, and also realised the absence of sedimentary rocks at the exposed surface of the Seychelles. This therefore led to the idea that these granites must have originated from an underlying source, which is the current submerged continental crust, the SMc. According to Baker (1963), these Neoproterozoic granites of the Seychelles are unmetamorphosed granitoids and alkali granites, comprising phenocrysts of microclines with microperthites, irregular aggregates of clear and smokey quartz, sparse aggregates of fibrous amphiboles, with common accessories such as biotite, sphene and apatite.

More recent geochemical and petrologic studies, including isotopic analysis, have further separated the Seychelles' granites into: the "grey Mahe type granites" ($_{Nd}$ = +2.85 ± 0.17, I_{Sr} = 0.7031 ± 0.17); and the "pink to grey Praslin type granites" (E_{Nd} = +0.8 to –3.8, I_{Sr} = 0.707–0.726). The latter also contain a much higher LILE (Large-Ion Lithophile Elements) content (Rb>180 ppm, U >4.2 ppm, Th >20 ppm, Pb>30 ppm) (Ashwal *et al.*, 2002). According to Ashwal *et al.* (2002), this difference is probably derived from a mixed source of juvenile mantle components and siliciclastic contaminants possibly as old as Archean (Figure 3.1). High precision U – Pb zircon dating on 14 granitoids from seven granitic islands yielded dates between 748.4 ± 1.2 Ma and 808.8 ± 1.9 Ma, and define a dominant period of igneous activity between 748 – 755 Ma (Tucker *et al.*, 2001). These dates represent the crystallization ages of the granitic intrusion of the Seychelles. These dates correlate closely to chemically similar volcanic and plutonic rocks of north-eastern Madagascar and north-western India, which likely originated, therefore, within the same tectono-magmatic province during the amalgamation of Gondwana (*ca.* 850-530 Ma) (e.g. Tucker *et al.*, 2001; Ashwal *et al.*, 2002; de Wit, 2003).

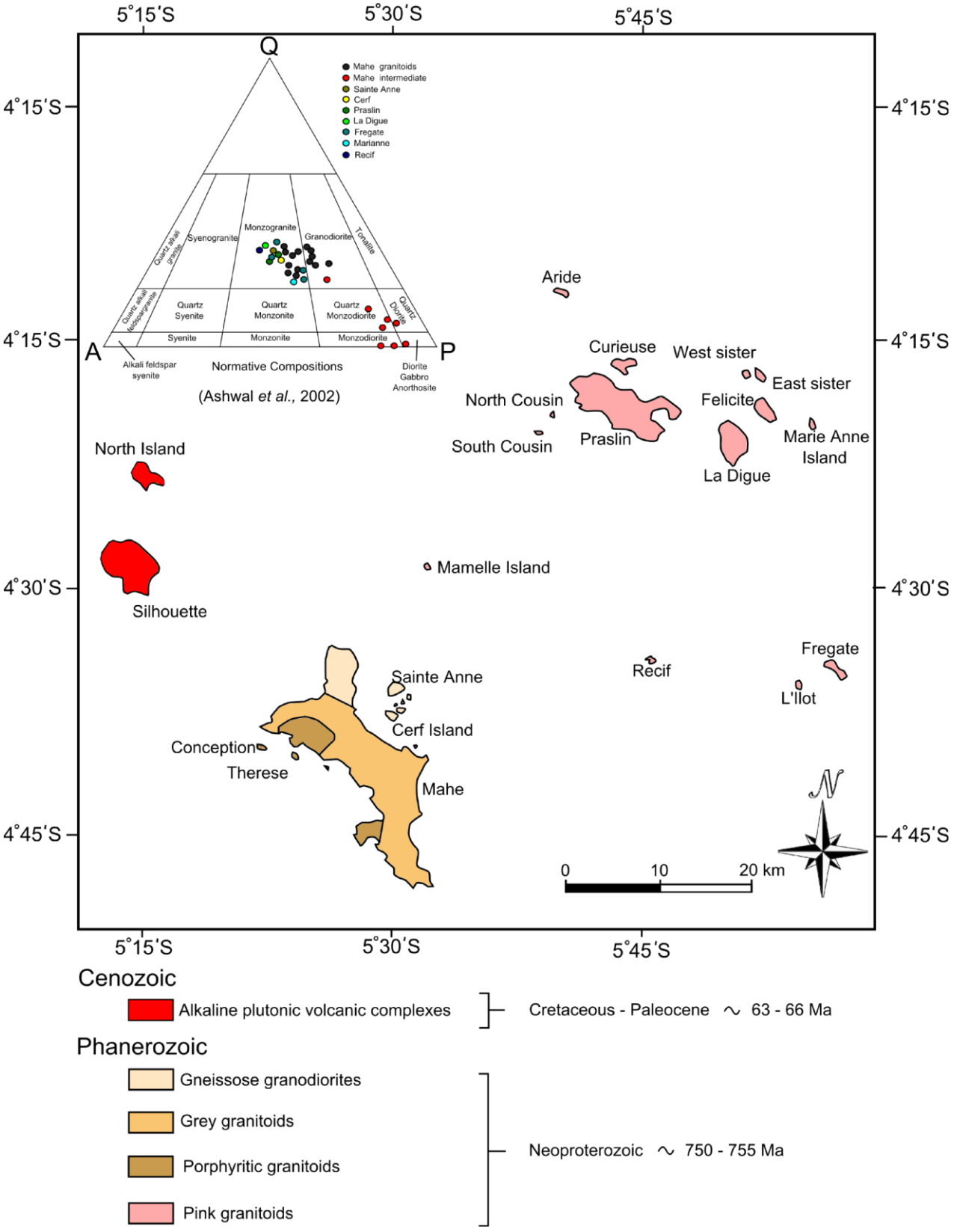

Figure 3.1: Map illustrating the general geology of the main granitic islands, of the Seychelles archipelago indicating the distribution of the different granites and the petrology of the older granitoids (QAP) (Source: Modified from Baker, 1963; Ashwal et al., 2002)

Baker (1963) also identified basaltic and dolerite dykes (olivine tholeiites) that cut across the main granitic islands of the Seychelles (Figure 3.2). Subsequent high precision U – Pb zircon dating of the main dolerite dikes on Mahe also produced dates of approximately 750 Ma (Torsvik *et al.*, 2001). These dolerite intrusion dates are therefore coeval with the main Mahe group granite intrusions. Paleomagnetic analysis of these dykes places Seychelles 600 km away from North-West India at 750 Ma and close to North-East of Madagascar (Torsvik *et al.*, 2001; Ashwal *et al.*, 2002), prior to the collision during the amalgamation of Gondwana.

Figure 3.2: Dolerite dike (outlined by dashed red line) cutting through granitoid at CCCL Quarry, Petite Paris, Mahe, Seychelles (photograph courtesy of M.J. de Wit).

3.2 Geophysical analysis and petroleum potential

A stratigraphic interpretation of the SMc based on gravity and seismic analyses by Perlmuter *et al.*, (1995), suggests thick sedimentary layers exist across the entire southern shelf of the SMc. A major gravity low was interpreted as being related to palaeo-rift deposits. Through further analyses and observations of paleogeographic reconstructions, seismic lines, and well data, it was concluded that the syn-rift section of that specific region represented a Triassic to Jurassic interval of lacustrine deposition, possibly followed by a Jurassic marine transgression (Perlmuter *et al.*, 1995). Generally, the analyses made on the SMc indicated that the stratigraphy varied all the way from the Late Triassic through the Middle Jurassic, with the most reservoir-prone units being deposited at both highstand and lowstand sequences. During the Middle Jurassic, marine lowstand deposits were assessed to have the

greatest reservoir potential, and in the Early Jurassic time, transgressive systems were assessed to have the most hydrocarbon potential (Perlmuter *et al.*, 1995).

3.3 Sediment cover of the granite basement

A primary palaeo-environmental study that was done on core and cuttings from the wells of the western shelf of the Seychelles was based on bio-stratigraphy conducted by Robertson Research International Limited in the early 1980s. As a result, several species of benthic- and planktonic foraminifera and various types of palynormorphs were identified, and the age determinations was based on the published ranges of the identified species (e.g. Amoco Seychelles Petroleum Company, 1981a; 1981b; 1981c)

The foraminiferal fossils identified are mainly Cenozoic in age and their availability indicates brackish and marine environments such as estuaries, intertidal zones, shelves, platforms, reefs, continental shelf and slopes and deep oceanic marine basins. The foraminiferal fossils from most wells include benthic and few planktonic foraminifera. Benthic foraminifera live at and within the basin floor's substrate, whereas planktonic foraminifera live in the upper part of the water column of the open oceans hence indicating deeper – open marine environments. Benthic foraminifera exist in near-coastal, lagoonal, inner and outer shelf, and upper and lower slope and basinal environments. Milionid types mainly occur in shallow coastal regions up to only 50 m in depth, and rotaliinid types occur in both shallow and deeper waters at about 50 m to several thousand meters in depth in outer shelf environments and are also common along the slopes of shelves (Amoco Seychelles Petroleum Company, 1981a; 1981b; 1981c; Rameil *et al.*, 2000). Planktonic foraminifera are absent or rare in shallow-marine environments as they exist within deep water. The majority of planktonic species of foraminifera occur in the upper part of the water column within the upper 50 m to 100 m near the surface (photic zone). They do not occur below 200 m depth as they prefer to live within the photic zone, and the thinner walled species occur in the top parts as they are more light dependant (Figure 3.3) (Amoco Seychelles Petroleum Company, 1981a; 1981b; 1981c; Rameil *et al.*, 2000).

Palynomorph species are also identified, including dinocysts, acritarchs spores and pollen. They are generally older than most of the foraminiferal species identified. Most of the palynomorphs are Mesozoic and lower Cenozoic in age. The presence of the palynomorphs indicates the relation between marine and terrestrial environments. According to Rameil *et al.*, (2000), the palynormorphs provide very useful information on high-resolution sequence

stratigraphy and palaeo-environmental interpretation of shallow-marine and deep marine carbonate rocks. This is because palyno-facies or palynomorphs are linked to the distance of the shoreline, therefore a rapid flooding, transgression or marine flooding will cause a significant change in the composition of the palyno-facies assemblages (Figure 3.3) (Rameil *et al,*. 2000).

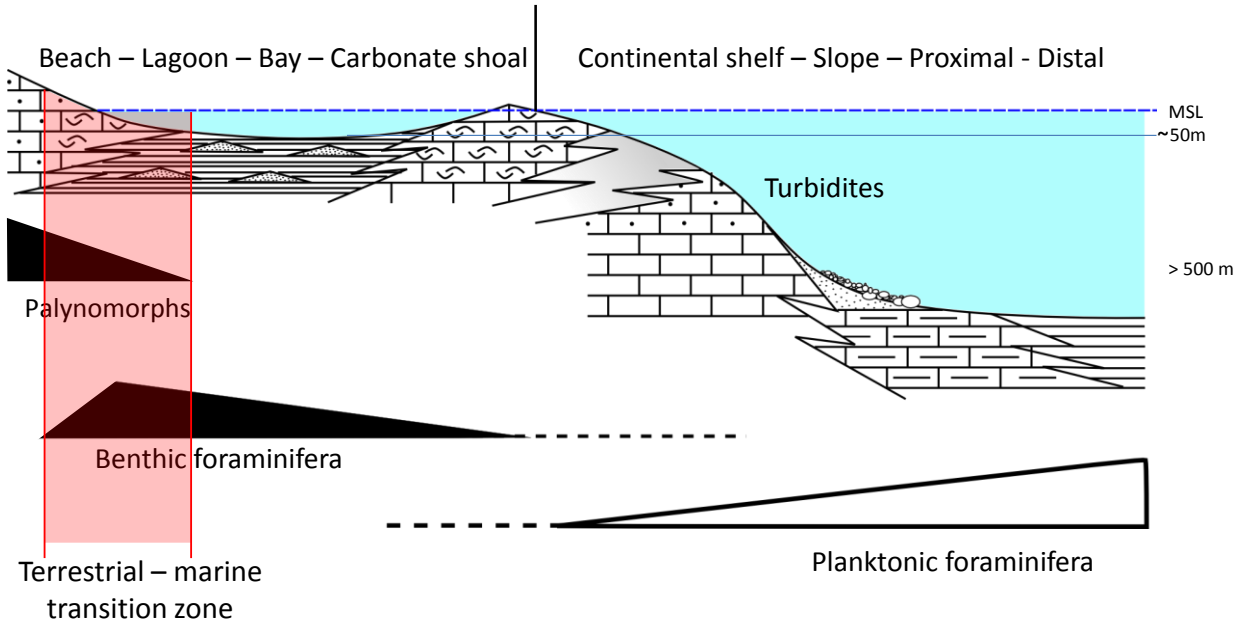

Figure 3.3: General distribution of the main foraminiferal groups from the coast to distal environments (Source: Modified after Rameil et al., 2000).

3.4 Deccan volcanism

Silhouette and North Island are known to be the youngest complexes (*ca.* 65 Ma) compared to the Neoproterozoic granites (*ca.* 750 Ma) amongst the islands of the Seychelles Archipelago (Stephens, 1996). These two islands are located north-west of the main island of Mahe (Figure 3.1) and comprise mainly of syenites, alkaline granites and trachytic tuffs. The volcanic tuffs yielded K/Ar dates in the range of 34 - 63 Ma, suggesting that Silhouette is probably an extinct volcano with a central microgranite core, surrounded by syenites and ultimately volcanic breccia and volcanic sheets linked to the Reunion hotspot and the Deccan basalts. Subsequently, more precise age dating of the rocks of Silhouette using Rb-Sr Isochrons yielded a more precise age of 63.2 ± 1.0 Ma, close to the age of the Deccan eruption (*ca.* 66 Ma), the most likely break-up time of Seychelles from India (Stephens, 1996).

3.5 Offshore stratigraphy of the Seychelles Plateau

Several stratigraphic studies have been conducted on the offshore sedimentary record of the SMc, especially during the drilling phase in the 1980s by Amoco Seychelles Petroleum Company. Most of the relevant studies have been summarized and used as data throughout this thesis focussing primarily on integrating the bio-stratigraphy, litho-stratigraphy, sedimentary with seismic data. The overall stratigraphy of the western shelf of SMc resembles a typical passive margin. The oldest and deepest rocks encountered by the wells drilled on the western shelf of the SMc are equivalent to the Karoo Supergroup rocks which are presumed to have initially formed as a result of a major deglaciation event that occurred in the mid Permian. As a result, these ultimately initiated continental fluvial processes that lasted until the Early Jurassic as Gondwana drifted away from the polar region (Catuneanu *et al.*, 2005). This deglaciation event caused large volumes of sediments to be deposited via continental fluvial processes across south central Gondwana which included the east African realm around Mozambique, Tanzania, Madagascar, north western Antarctica and the Seychelles. These sediments are known as the early Karoo sediments (Figure 3.5 -Figure 3.4) (Amoco Seychelles Petroleum Company, 1981b; Veevers *et al.*, 1994; Catuneanu *et al.*, 2005; Linol, 2013; Linol *et al.*, *in press*, 2014).

As previously mentioned (Chapter 2), the Karoo rifting event (*ca.* 350 - 250 Ma) which started in Devonian - Carboniferous period caused the formation of a number of basins across south central Gondwana in the form of elongated grabens, half grabens and failed rifts which acted as sinks for the Karoo age sediments during and after deglaciation (Wopfner and Kreuser, 1986; Catuneanu *et al.*, 2005; Johnson *et al.*, 2006). This rifting event eventually terminated with the eruption of extensive Middle Jurassic flood basalts at approximately 183 Ma (e.g. the Drakensberg Group) of the Karoo LIP. This is related to the thermal induced extensional rifting and thermal subsidence from around 180 Ma due to the Bouvet plume magmatism during the initial opening of the proto Indian Ocean and the eventual onset of seafloor spreading and separation of the East and West Gondwana (Duncan *et al.*, 1997; Riley and Knight, 2001; Johnson *et al.*, 2006). As a result, successive basins accumulated sediments from the late Jurassic, Cretaceous and the Cenozoic successions after the East – West Gondwana break-up (Figure 3.4) (Coffin and Rabinowitz, 1992; Plummer *et al.*, 1998; Torsvik *et al.*, 2001; Tucker *et al.*, 2001; Ashwal *et al.*, 2002; Ishwar-Kumar *et al.*, 2013).

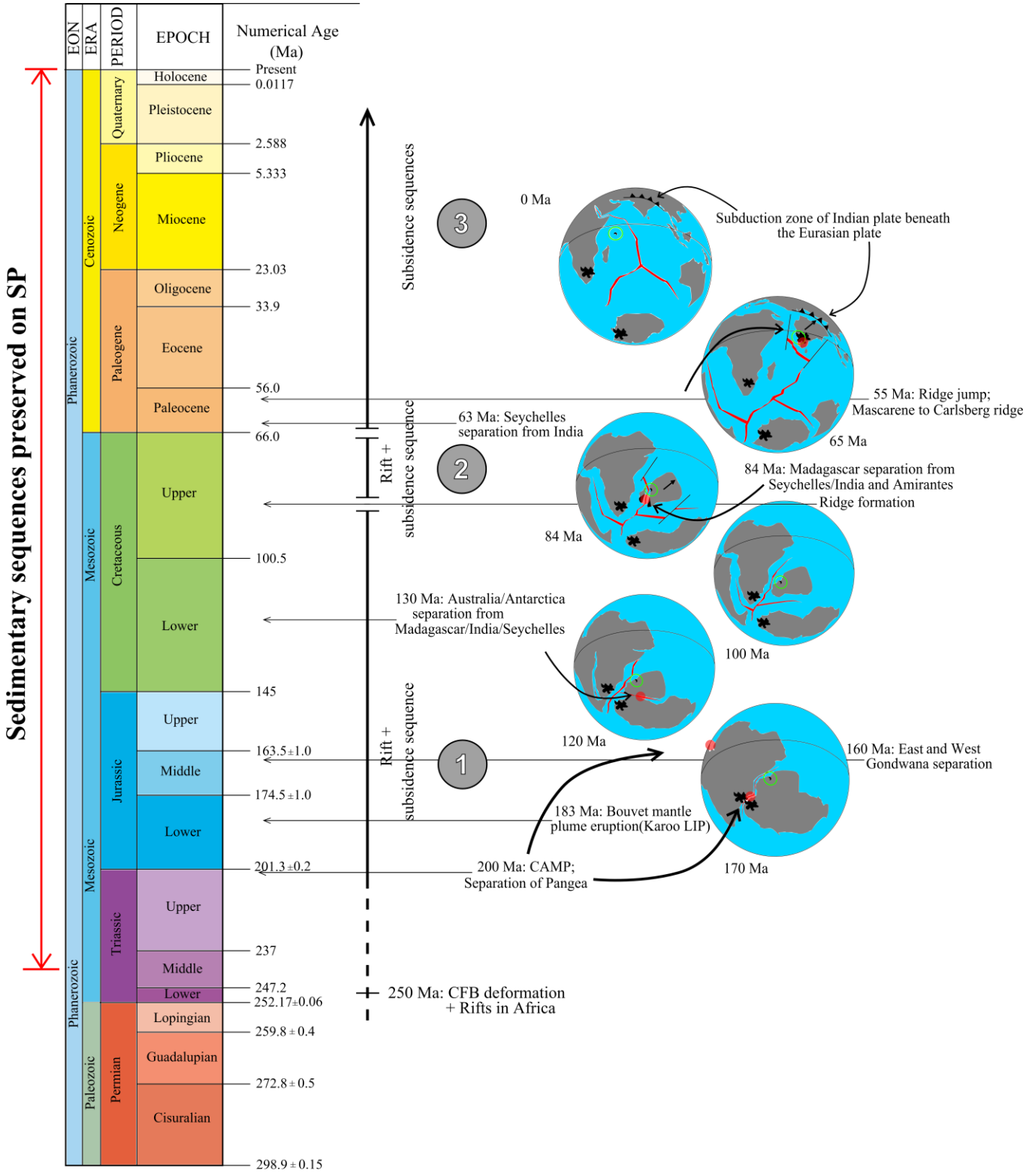

Figure 3.4: Summary of the tectonic events that led to the break-up of Gondwana and the subsequent position of the SMc in the Gondwana break-up framework. Refer to Chapter 2 for detailed history of the break up regime recorded by the Seychelles stratigraphy. (Source: Walker et al., 2013 and www.reeves.nl/gondwana)

(i) Early Mesozoic to Middle Mesozoic rift sequences

The Middle Triassic – Early Jurassic sequences occur extensively across the western margin of the SMc and are referred to as the "Karoo equivalent Supergroup" (Amoco Seychelles Petroleum Company, 1981b; Plummer, 1998b). These sequences comprise predominantly of fluvial sandstones that display planar cross bedding fining upwards trends and conglomeratic base; and lacustrine claystones and siltstones that are extensively observed in the Reith Bank- 1. Marking the end of the latter sequence is a Middle Jurassic unconformity. The wells of the western shelf of the SMc did not penetrate through the base of this sequence, hence no glacial sediments were recorded, nor was any basement granite intercepted (Figure 3.5) (Amoco Seychelles Petroleum Company, 1981b; Walton and Khanna, 1992). These Mesozoic sequences appear to be very similar and most probably equivalent to the Adigrat Sandstone (Upper Triassic – Lower Jurassic) of Ethiopia (Purcell, 1981) based on the history of deposition which also consist of cross-bedded and conglomeratic sandstones, interbedded by siltstones, dolomites and marls (Figure 3.5).

(ii) Middle Mesozoic to Late Mesozoic rift and thermal subsidence sequences

The Middle Jurassic to Cretaceous period represents a time when there were abundant marine incursions into central Gondwana, as recorded by the deposition of calcareous clastics and carbonates onto the continental shelves including the Seychelles Microcontinent (*ca.* 200 – 140 Ma) (Linol *et al*., *in press*, 2014). This is likely the first recorded thermal subsidence phase in the Seychelles offshore sedimentary record (Figure 3.5) (Amoco Seychelles Petroleum Company, 1981a, 1981b, 1981c).

The first thermal subsidence sequence is observed on the western shelf of the SMc as Middle Jurassic to the Lower Cretaceous (*ca.* 200 – 140 Ma) marine siltstones, claystones and minor sandstones. This thermal subsidence phase together with the previous rifting led to this transgressive sequence which generally grades up from thin oolitic limestone marker bed at the base with sands to thick mudstones. This sequence is probably associated with a marine incursion to introduce the marine conditions, hence related to the formation of the proto Somali Basin when the Tethys Sea progressed southwards along the major rift basins during the Middle Jurassic following the extensional rifting associated to the East – West Gondwana separation. This oolitic limestone marker can be observed in all three wells of the western shelf (Figure 3.5) (Walton and Khanna, 1992). These areas were of very low energy which provided appropriate sheltered environment for both benthic and neritic organisms, but more importantly provided good accommodation space for the deposition of

fine grained sediments such as claystones, siltstones and limestone, similar to for example Ogaden Basin of Ethiopia (Purcell, 1981), offshore Mandawa and Ruhu Basins, Tanzania (Kapilima, 2002) and the Morondava basin, Madagascar (Rakotosolofo, *et al.*, 1999).

The abundance of some large miospores (e.g. *Calliala sporites spp.*) indicates proximity to shelf, which suggests the probable time period these sediments were deposited, as the Somali Basin was opening, and provided the requisite coastal environment. Furthermore, through the Early Jurassic to Middle Cretaceous (*ca.* 200 – 100 Ma), the succession becomes more marine, as evidenced by the increase in the availability of benthic foraminifera (e.g. *Lenticulina sp.* and *Haplophragmoides sp.*) and microplankton, although very rare, which occur at lower depths (e.g. *Adnatasphaeridium filamentosum, Gonyaula-cysta jurassica, Sentusidinium sp.* and *Palaeoperidinium paeminosum*) (Figure 3.5) (Plummer *et al.*, 1998).

The Early Jurassic sections throughout the three wells are dominated by the abundance of spores and pollen (e.g. *Exes-ipollenites tumulus, Classopollis cf. meyeriana, C. classoides, Callialasporites spp., and C. dampieri*). Microplanktons are very rare in these sections (e.g. *Pareodinia spp., Sentusidinium spp. and Acanthomorph acritachs*). From the Late Jurassic onwards, spores and pollen do occur but are very rare as well (e.g. *Classopollis classoides*) and bisaccates in the Early Cretaceous (e.g. *Contignisporites fornicatus and Cicatricosisporites spp.*). The latter microfossil assemblage indicates the evolution in the depositional environment from shallow restricted marine to shallow near-shore, and then to a progressively open marine environment. This suggests a change from the rift to thermal subsidence deposition (Plummer *et al.*, 1998). Furthermore, mature liptinitic coaly claystone source rock bearing oil prone Type II kerogen has been found in the early Middle Jurassic section of the Seagull Shoals. This source rock was deposited in a deltaic-coastal plain during the later stages of the rifting that led to the early split between the East and West Gondwana (Oxfordian - Kimmeridgian). Source rock from Owen Bank - A1 has indicates an oil prone marginal marine lower portion from a deltaic upper portion which is probably gas prone (Figure 3.5) (Plummer *et al.*, 1998).

Based on the history of deposition, the above mentioned sequences are most probably equivalent to the Hamalei Formation (Liassic – Lower Oxfordian), Aurandab Formation (Upper Oxfordian – Lower Kimmeridgian), Garbaharre Formation (Upper Kimmeridgian) and the Main Gypsum Formation (Neocomian) of the Ogaden Basin Ethipoia-Somalia. The Hamalei Formation comprises thick carbonates that include limestones, oolitic limestones

(Bajocian), dolomite, and anhydrite. The overlying Uarandab Formation comprises mainly intercalations of fissile claystones and marls with oolites. The overlying Gabredarre Formation compises oolitic marly limestones intercalated at the top with evaporites and claystones. The overlying Gypsum Formation comprises dolomitic limestone followed by a thick gypsum succession (Figure 3.5) (Purcell, 1981). The latter was formed as a result of the Tethys Sea episodically flooding the rift basins from the Late Triassic to Early Jurassic and mixed with the continental derived siliciclastics (Purcell, 1981). By the Bajocian renewed subsidence further caused the sea to protrude further inland: and this is when the Seychelles first became exposed to the shallow marine environment recorded as the oolitic limestones seen in all three wells of the Western shelf.

(iii) Late Mesozoic to Cenozoic Sequences

The Late Mesozoic (Cenomanian - Maastrichtian) sedimentary successions preserved in the SMc comprises limestone, calcareous claystones and thin beds of volcanic ash interrupted by thick volcanic strata (*ca.* 62-75 Ma) of welded tuffs and ash, basaltic lava, dacite and andesite layers (Table 3.1) (Late Cretaceous). The carbonates and calcareous deposits at the start of this sequence formed initially as part of marine shelf carbonates, lime mud/calcareous claystones with minor clastics. The dacite and andesite layers are probably derived a partial subduction that occurred as Madagascar broke off from India/SMc (*ca.* 80 Ma) which resulted in the formation of the Amirantes Ridge (see Section 3.6). The basaltic lava from this sequence is most probably due to the Deccan volcanic eruption prior to the separation of Seychelles from India, and which ultimately terminates with an Upper Cretaceous unconformity (*ca.* 65 Ma) (Figure 3.5) (Amoco Seychelles Petroleum Company, 1981a, 1981b, 1981c; Khanna and Pillay, 1992). Absolute ages have been obtained from the wells of the SMc using sidewall core samples collected mainly from the volcanic rocks which are predominantly basalts with welded tuffs (Table 3.1).

Table 3.1: Absolute ages acquired through K/Ar dating method (Amoco Seychelles Petroleum Company; 1981a; 1981b; 1981)

Well	Depth of sidewall samples (m)	K/Ar age (Ma)
Owen Bank – A1	1506	74.7 ±1.3
Reith Bank - 1	1644	~62
	1762	~66.1 ±1.3
Seagull Shoals - 1	N/A	N/A

Based on the history of deposition, the Cretaceous sequences are most probably equivalent to the shallow marine sequences of the Ogaden Basin of Ethiopia-Somalia: Mustahil Formation (Albian - Aptian); Ferfer Gypsum (Albian - Aptian); and the Bellet Uen Formation (Turonian - Cenomanian). The Mustahill Formation comprises calcareous claystone at base that grade upwards into limestones (dolomitic in some places). The Ferfer Gypsum comprises mainly limestone at base which eventually grades into evaporites at the top. The Bellet Uen Formation comprises marls and dolomitic limestones with few intertercallations of claystones, marls and sandstones (Purcell, 1981) (Figure 3.5). By the Albian – Aptian times, a second major transgressive cycle was experienced across nearly the whole of the east Africa and the horn of Africa (Purcell, 1981).

The remainder of the stratigraphy of the SMc comprises post-rift Paleogene marine clastics (Paleocene – Middle Eocene) of calcareous claystones, with interbeds of calcareous sandstones and dolomitic limestones. This is probably equivalent to the Jesoma Sandstone (Paleocene) from the Ogadem Basin of Ethiopia, which is composed of mainly of shallow marine calcareous sandstone. From the Middle Eocene to recent, the general lithology changes to pure limestone. This is also seen in the Taleh Formation and KarKar Formation (Middle to Upper Eocene) of Ethiopia which comprises limestones, marls and evaporates with minor interbeds of calcareous claystones and sandstones (Figure 3.5) (Purcell, 1981). In general, these latter carbonate rich sequences possibly represent another subsidence phase following the separation of the SMc from India and the subsequent formation of the Carlsberg Ridge (*ca.* 66 Ma). The limestones may represent the carbonate platform deposition that accumulated as the SMc drifted to its present location, and its origin is most likely due to the calcification of the numerous amounts of foraminiferal tests that died as a result of the increased acidity of the ocean following the massive volcanic eruptions during the Cretaceous (e.g. Keller *et al.*, 2009). After this time the SMc became an entirely isolated single continental fragment. Following the break-away from India, the SMc submerged and accumulated the thick carbonates (Figure 3.5) (Walton and Khanna, 1992; Torsvik *et al*, 1998; Torsvik *et al.*, 2001; de Wit, 2003; Ashwal *et al.*, 2002; Reeves *et al.*, 2002; Reeves *et al.*, *in press* 2014). More details of facies analysis of the mentioned sequences of the SMc are provided in Section 5.4.

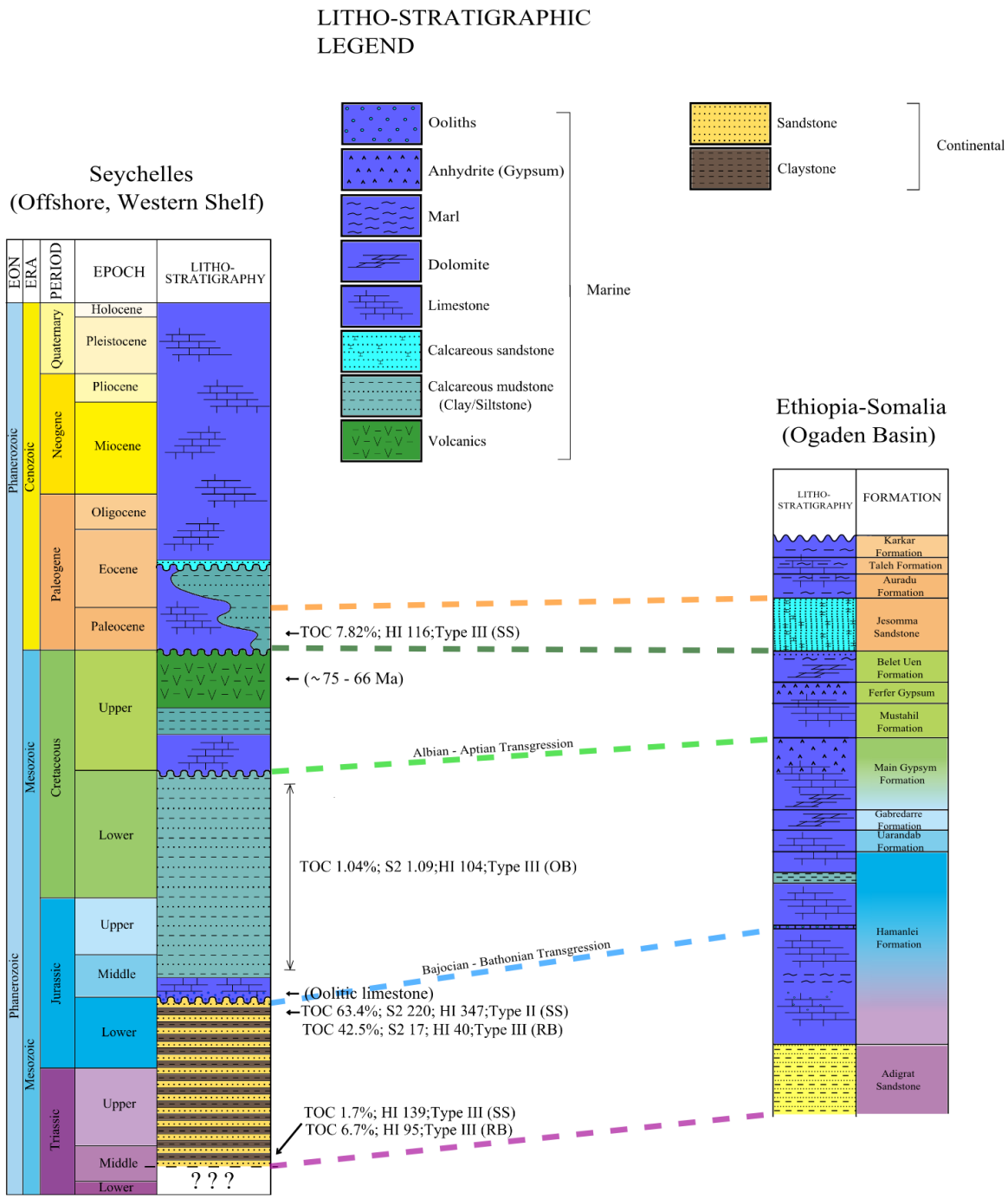

Figure 3.5: General stratigraphic correlation between the SMc and Ogaden Basin of Ethiopia-Somalia, which includes the pre-break-up-rift siliciclastic sequences (Triassic to Jurassic), overlain by the carbonate syn-rift sequences (Jurassic to Cenozoic), major unconformities, and potential source rock horizons of SMc (OB: Owen Bank – A1, RB: Reith Bank - 1; SS: Seagull Shoals - 1) (Source: Modified after Plummer et al., 1999; Purcell, 1981)

The general structure and lithology of the sedimentary basin to which the SMc once belonged includes Mesozoic and Cenozoic sediments that are dominated by extensional horst and graben structures of the bottom, which are then overlain by conformable thermal subsidence sequences. These exhibit a transition from continental siliciclastics to marine sediments within the rift, syn-rift and post-rift sequences (Plummer and Belle, 1995, Plummer *et al*., 1998). This is similar to the geology of offshore Mozambique. Apart from a series of metamorphic terranes, a great proportion of Mozambique's geology comprises of high grade Archaean - Neoproterozoic crystalline basement extension of the Zimbabwe Craton subsequently intruded by large volumes of granitic rocks. The Carboniferous - Upper Jurassic rifting led to numerous intra-cratonic Karoo basins (e.g. Zambezi Depression), which followed by post-Karoo continental deposits and volcanics, and further Meso-Cenozoic continental and marine deposits with a thick Pliocene to Quaternary cover offshore (Figure 3.6). Offshore Mozambique, is also a unique bathymetric feature known as the Beira High (BH). This structure is approximately 280 km long and 100 km wide, parallel to the Zambezi Delta. This structure lies beneath the Mesozoic and Cenozoic sedimentary sequences and its origin is enigmatic. Conflicting opinions of the BH's origin varies from either magmatic (oceanic), continental or sedimentary with an overprint by compressional forces (Mahanjane *et al.,* 2012). The stratigraphy and structure of Rovuma basin, across the Zambezi Delta (Mozambique), is delineated by the Karoo sequence within the rotated fault blocks of the basement and post-Karoo rock sequence of increasing clay contents and ultimately marine carbonates as the syn-rift and post-rift phases (Figure 3.6) (Mahanjane, 2012; Salazar *et al.,* 2013; Sacramento *et al.,* 2014).

The basement to the Middle Jurassic section comprises thick terrigenous – carbonate sedimentary sequences within the rotated fault blocks. The Upper Jurassic section are characterised by the red-beds syn-rift deposits. The Lower Cretaceous section comprises shaly glauconitic marine sandstones, which then changes to the Upper Cretaceous carbonates comprising of mainly marine shelf build-ups and minor siliciclastics. The latter sequences all show thinning over the Beira high. These are then followed by the post rift – thermal subsidence sequences. These include the Paleocene section that comprises shelf and carbonate build-up deposits together with siliciclastics with drapes. Thereafter, the Eocene – Miocene section comprises calcarenitic and calcilutitic formations indicating shelf slope or fore reef setting with prograding clinoforms. Finally the Tertiary – Quaternary section displays the prograding Zambezi Delta front that comprise of mainly turbidite deposits, with the presence of slides and slumps (Figure 3.6) (Salazar *et al.,* 2013).

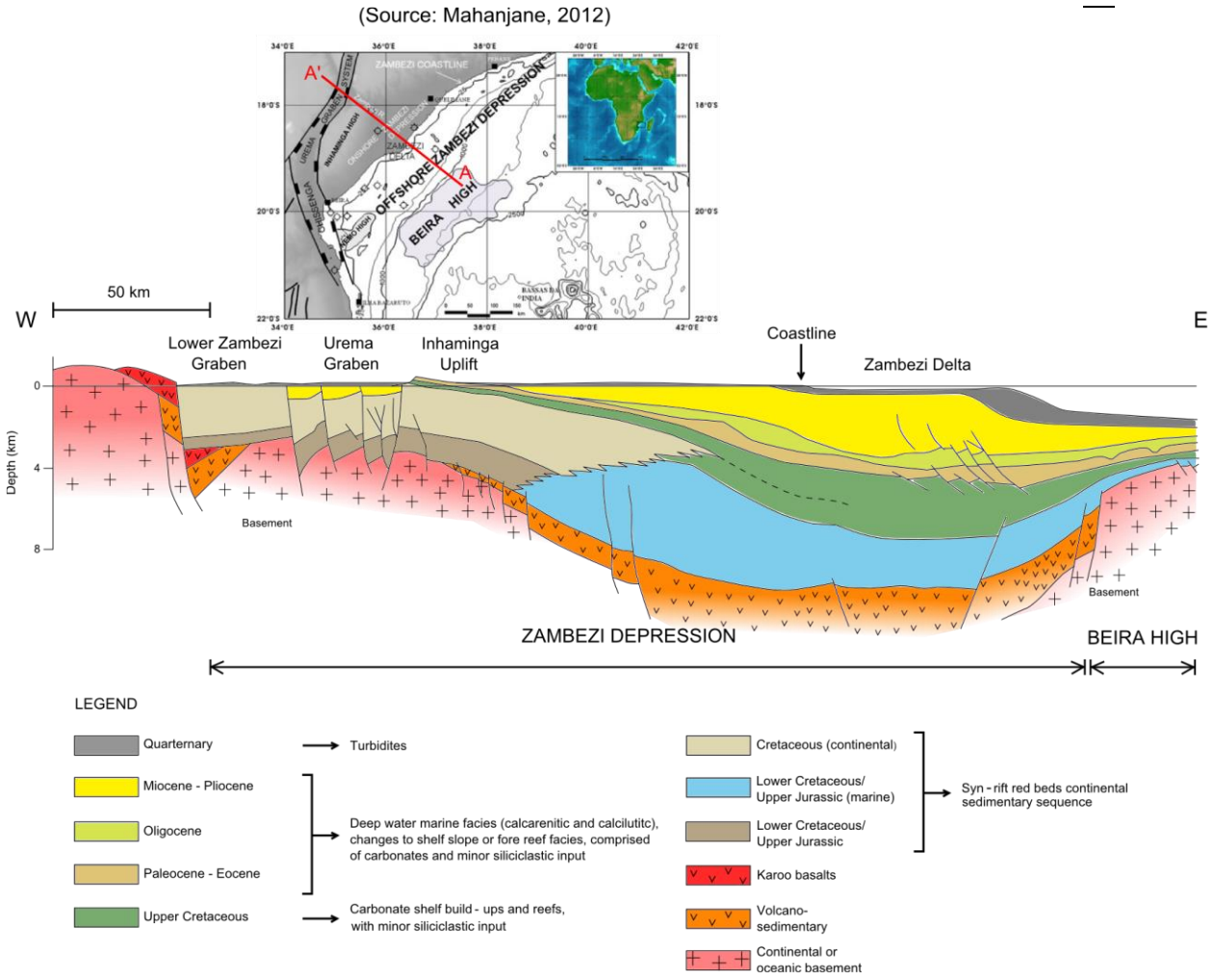

Figure 3.6: Cross section through the passive margin of onshore and offshore Mozambique across the Zambezi river mouth. Notice the prominent rotated fault blocks in the basement comprising of thick sedimentary sequences, and the fault planes are mostly aligned in a NE-SW direction (Source: Sacramento et al., 2014).

3.6 Amirantes Ridge and Trench Complex

South-west of the SMc is a curved bathymetric feature, approximately 550km long, known as the Amirantes Ridge. Running parallel to the western margin of the SMc is the Amirante trench (Figure 3.7). This ridge and trench system was formed during the Late Cretaceous (Miles, 1982; Plummer, 1996; Mukhopadhyay *et al*., 2012). There has been much debate in the literature about its origin, with mechanisms ranging from subduction (Miles, 1982; Suwa, 1994; Mukhopadhyay *et al*., 2012), to transpressional strike slip fault (Plummer, 1996), to a bolide impact (Hartnady, 1986).

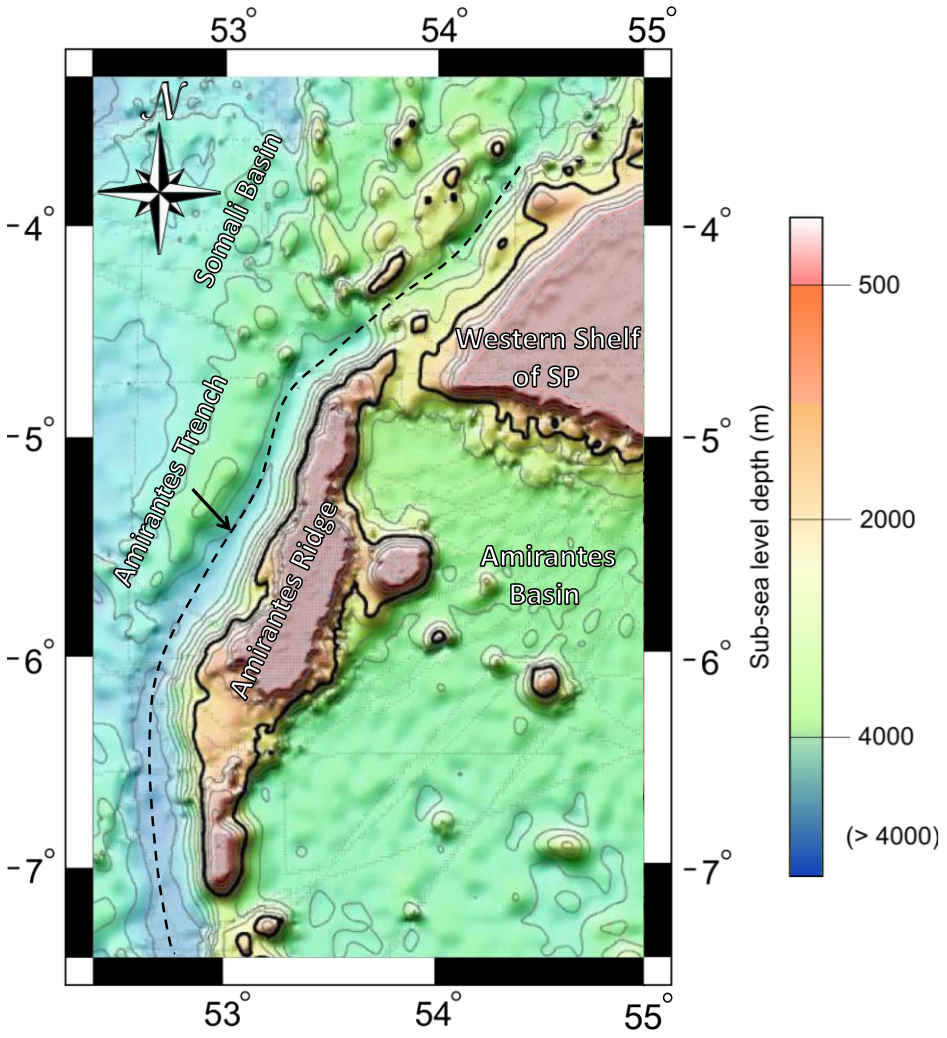

Figure 3.7: Locality and general bathymetry of the Amirantes Ridge - Trench Complex (ARTC), including the western part of the Seychelles Plateau, (Source: Global Topography for Google Earth and Satelite Geodesy by Becker et al., 2009; and Smith et al., 1997)

Hartnady (1986), states that an extra-terrestrial impact happened some 65 Ma that caused the extinction of the dinosaurs and many more organisms (K-Pg Boundary) could be the very same one that collided in the Indian Ocean which ultimately formed the Amirante Basin and Ridge. This theory is referred to as the "Shiva crater". The likely hood of this being correct is very low for no existing offshore geophysical survey has come across any evidence. According to Plummer (1996) the Amirante Ridge was formed when a major transform fault was formed as a result of the separation between Madagascar and Seychelles-India. This fault generally strikes N-S and was sinistral in nature. In addition, as the two plates experienced a counter clockwise rotation, whereby India/SMc moved faster in relation to Madagascar and seafloor spreading occurred as a result of the opening

between the two plates south of SMc forming the Mascarene Basin (Plummer, 1996). Fisher *et al.* (1967) explains that oceanic tholeiitic basalts were dredged from depths between 2500-3000 m from each flank of the Amirante ridge and they yielded dates of approximately 82 Ma. This supports sea floor spreading occurred around that time when Madagascar separated from India/SMc. In the northern part of this system along the western margin of the Seychelles Plateau, a compressional zone led to the formation of the Amirante Ridge - Trench Complex (Miles, 1982; Plummer, 1996).

According to Mukhopadhyay *et al*., (2012), a compressional zone could have also been formed due to the formation of the Carlberg Ridge about 65 Ma, which their "pushed" the Seychelles microcontinent southwards. Based on the orientation of the plates, this allowed the western plate of the sinistral transform to experience a compression between the plates; hence partial subduction was experienced between the two. This ultimately formed an island arc feature, the Amirante ridge. Unlike previous similar theories, Mukhopadhyay *et al*., (2012) further explained his theory in three phases; (i) Madagascar separated from India (89-85 Ma) following eruption of the Marion plume. Seafloor spreading occurred along northern Mascarene Ridge. (ii) Very slow and limited spreading along northern Mascarene Ridge continued until eruption of the Reunion plume erupted (*ca.* 66-65 Ma) (Mukhopadhyay *et al*., 2012). Reunion plume activity then affected the plume circulation beneath Mascarene Ridge, which eventually resulted in abandonment of spreading along this centre. The increased pressure from the active plume beneath the abandoned Mascarene ridge caused a ridge jump to eventually form the Carlsberg spreading Ridge and causing the Mascarene to be inacticve (Campanile *et al*., 2007; Mukhopadhyay *et al*., 2012). (iii) Spreading of the Carlsberg Ridge eventually forced India to move north and at the same time displacing Seychelles south (Purushotham, 2002; Campanile *et al*., 2007; Mukhopadhyay *et al*., 2012). This increase in compression of the crust between the Seychelles and Madagascar was compensated as the western limb of the initial sinistral transform thrusted below the eastern limb. This subduction lasted for a short period of time as compression was released when the opening of Central Indian Ridge started and the spreading rate along the Carlsberg Ridge was reduced (Purushotham, 2002; Campanile *et al*., 2007; Mukhopadhyay *et al*., 2012).

Chapter 4. Materials and Methodology

The datasets that have been made available for this project by the Seychelles Petroleum Company (SEYPEC) comprise: seismic data (SEGY); well-log data (gamma and DT check-shot); and core and well cutting descriptions. "Transgressive and regressive" cycles from the well data of the study area are identified based on the model designed by Johnson and Murphy (1989) and Embry and Johannessen (1992), in which regional unconformities are identified from the major changes recorded in the well-logs, facies succession and seismic data. The following methods have been used to analyse the data.

4.1 Seismic stratigraphy

Two seismic profiles (TCO-106 and TCO-115) are used specifically to analyse the structure and the major unconformities between rift and post-rift sequences of the study area. This is because these seismic lines are the only ones of good robust quality that are linked to the wells of the study site. These seismic data were normal stacked, acquired by Schlumberger in the early 1980s, contracted by Amoco who, at the time, held acreage on the Western shelf of the Seychelles (Figure 4.1).

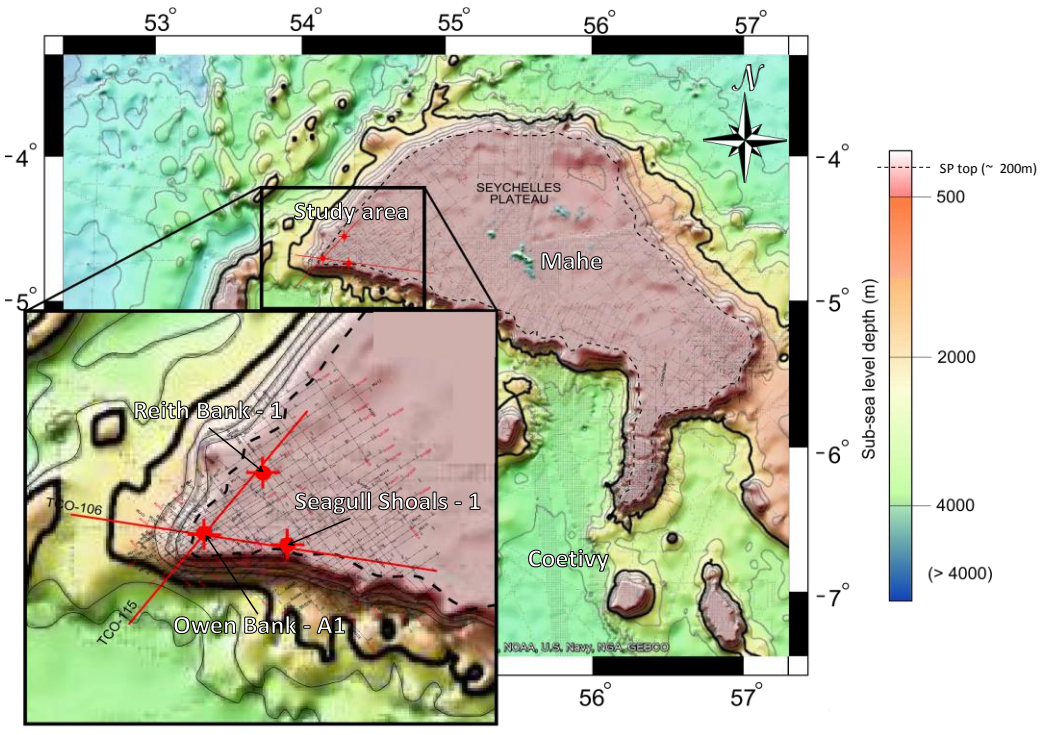

Figure 4.1: Bathymetrical map, illustrating the study area and the general seismic reflection coverage across SP (fine solid black lines). The location of the seismic reflection data used are highlighted in solid red lines (TCO-106 and TCO-115) and the wells as red circles (Owen Bank – A1, Reith Bank – 1 and Seagull Shoals - 1) (Source: Global Topography for Google Earth and Satelite Geodesy by Becker et al., 2009 and Smith et al., 1997)

The seismic profiles are analysed for different clinoform terminations and other stratal geometries to enable assigning different boundaries/surfaces, which are in turn correlated laterally. Following Emery and Myers (1996), there are five main stratal or clinoform terminations used in this study to identify sequence stratigraphic surfaces or boundaries; three occur above the surface/boundary (offlap, onlap and downlap), and two occur below a surface/boundary (truncation and toplap). Offlaps also define specific stratal stacking patterns or clinoform terminations that indicate forced regressions from a subaerial unconformity, hence a stratigraphic surface or boundary. Downlaps on the other hand indicate an increase in accommodation due to transgression across a stratigraphic boundary or surface (Figure 4.2).

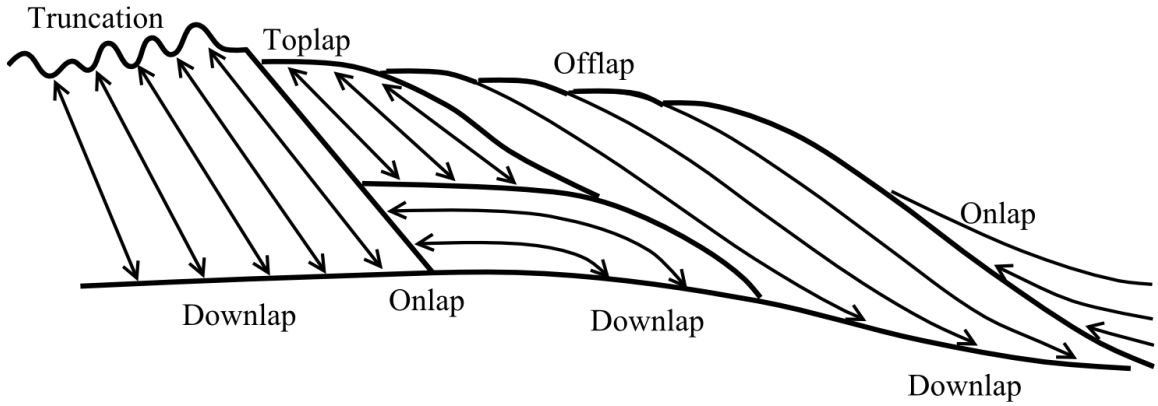

Figure 4.2: The various clinoform terminations used in seismic stratigraphy, illustrating top and bottom boundary (Source: Taken from Emery and Myers, 1996)

Seismic interpretation is conducted in this study using the seismic software "OpendTect 4.40j" (developed by dGB Beheer B.V.) on a Windows 7 platform. The well data of the respective wells that each seismic line cut across are used for the lithological and depth control calibration of the seismic profiles, and to correlate the bio-stratigraphic markers from the well data to the seismic data. This has been made possible by the seismic-to-well-log correlation plug-in available in OpendTect 4.40j that integrates the seismic data to the well-logs along with the bio-stratigraphic markers to provide a chrono-stratigraphic framework for the interpreted horizons, as well as the seismic stratigraphy, and finally a sequence stratigraphy.

Dip steering median filter is applied to each seismic line to improve the quality of the data for higher and better resolution, which eventually improves the accuracy of the structural and stratigraphic interpretation (Figure 4.3).

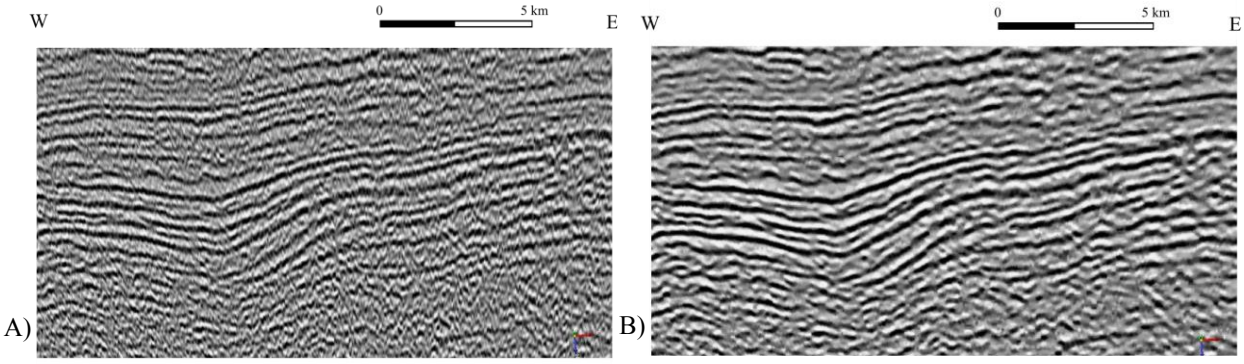

Figure 4.3: Random section of seismic profile TCO-115 indicating the contrast between (A) non-steered and (B) steered median filtered. Notice how less chaotic and less noisy B is compared to A.

4.2 Biostratigraphy

The well chip and core samples were examined initially by Robertson Research International Limited for micro- and macro-fossils at 3-10 m intervals. Their bio-stratigraphic charts were not available and therefore had to be re-constructed from the final geological reports (Amoco Seychelles Petroleum Company, 1981a, 1981b, 1981c). For all three wells it was reported that the data is discontinuous in some parts, especially Seagull shoals – 1. Nevertheless, the various species availability are plotted against depth for each well, and boundaries of zones are identified where species become extant or where they become extinct.

4.3 Litho-stratigraphy

The litho-stratigraphy is constructed primarily on the description of various lithologies from the core and well cutting reports (Table 4.1). The interpreted thickness of the various lithological units is done by using the integration of the logs, cuttings and core descriptions. The coarsening – and fining- upward trends in the litho-stratigraphic units are interpreted from the gamma ray logs, which are reported in the stratigraphic sections as well.

Table 4.1: Core and well cutting depths examined here.

Well	**Conventional cores (m)**	**Sidewall cores (m)**	**Well cuttings (m)**
Owen Bank – A1	4085-4096	216-1523 (29 samples)	100-4080
Reith Bank - 1	3179-3186, 3879-3888	427-3888 (367 samples)	1360-3898
Seagull Shoals -1	2735-2745	360-2668 (61 samples)	100-2745

The sidewall core data is used in this project mainly to confirm the lithology at specific depths and act as a baseline for the wire-log interpretations. Consideration of both sidewall core data and gamma log data together increases the robustness of estimations of lithological boundaries. Qualitative base level curves for each well are drawn from the rock record respectively as to aid in the identification of the depositional environments and maximum flooding surfaces (MFS) and further correlation.

Both gamma and DT-Check shot logs are also used to identify boundaries that separate different packages or sedimentary sequences when there is a major change or discontinuity in the readings (e.g. Serra, 1984). The purpose of constructing these stratigraphic sections is to classify the various facies based on the cuttings, core descriptions and the various successions. In addition, this permits the identification and lateral correlations of the various bounding surfaces of sequences from the different wells in association with the changes in lithological facies, bio-stratigraphic records and depositional environment.

4.4 Facies analysis and stacking patterns

The various facies are identified as homogeneous lithological packages with uniform characteristics, which are compared, grouped and correlated throughout the three wells using the reconstructed litho-stratigraphic sections which includes the various criteria (lithology, texture, sedimentary structures ect). In turn, homogeneous successions of facies are identified along with their top and bottom bounding surfaces which make up individual sequences based on Walter's law (e.g. Walker, 1992). These bounding surfaces identified in this project are in the form of non-depositional surfaces, referred to as maximum regression surfaces (MRS) and/or erosional surfaces (hiatus). Following a MRS is a maximum flooding surface (MFS) that corresponds to the time of maximum accommodation space, and because a MFS is of regional extent, this surface can also be used for correlation (Johnson and Murphy, 1989; Embry and Johannessen, 1992).

Observed vertical changes in the facies are linked to variations in the depositional environment especially along a proximal – distal profile, at which 1st – 2nd order depositional sequences are in turn correlated between the three wells. This is because each bed within each respective sequence is linked genetically to another successive bed of the same identified sequence from another well that has developed from the same cycle of base level change. Sequence formations depend on a positive accommodation (Transgression = T) followed by a negative accommodation (Regression = R) as a non-deposition or sub

aerial unconformity is formed at the top of the cycle (T-R cycles). This is identified by analysing the stacking pattern along with the well-logs following Vail *et al.* (1991).

In order to further understand the lateral and vertical trends of deposits in sedimentary basins in terms of eustasy, correlation of spatial data is necessary (e.g. well-logs or borehole lithological logs). This is achieved by: 1) matching of marker bed horizons with distinctive log responses, and 2) matching of distinct geophysical log patterns (e.g. fining- or coarsening-upward trends). This is further enhanced when associated with detailed biostratigraphy and sequence stratigraphy (Diessel, 2007).

The identified bounding surfaces (MRS) or unconformities are integrated with the bio-stratigraphy to test if there is any correlation with any age boundary to prioritize the MRS or major unconformity recognized through the logs and seismic data (Serra, 1984).

4.5 Method of backstripping and subsidence analysis

The submergence of SMc and the sediment accumulation along its margins is due to subsidence that resulted from continental thinning during rifting and extensional tectonics and drifting of the SMc away from Africa, India and Madagascar (e.g. Plummer and Belle, 1995), as described in previous chapters. In this study, the stratigraphic data of the three main wells are used to calculate the subsidence of SMc's basement during the mid-Mesozoic to Cenozoic (*ca.* 180 – 0 Ma), from the first episode of break-up between East and West Gondwana to the final separation and drifting of the SMc. This calculation follows the standard method of backstripping and decompaction (e.g. Allen and Allen, 2005), and is performed in this study to test the evolution of the SMc related to the various tectonic events, its subsidence, its submergence and its eventual isolation.

Subsidence analysis of wells based on the decompaction of sedimentary units is a standard method for investigating offshore sedimentary basins (Leeder, 1999; Miall, 1999; Allen and Allen, 2005). This is done by constructing plots showing the sediment accumulation rate versus time. The total subsidence of a basin comprises variations of the accommodation taking into account the global change in sea-level (eustatism) (Figure 4.4). The accommodation is estimated by the sum of the water depth (palaeo-bathymetry) which is acquired from the sedimentological and biological data, and the decompacted stratigraphic thickness which is calculated using the empirical formula relative to the composition of each stratigraphic unit (Figure 4.4) (Allen and Allen, 2005). The general method of backstripping is explained on the following pages.

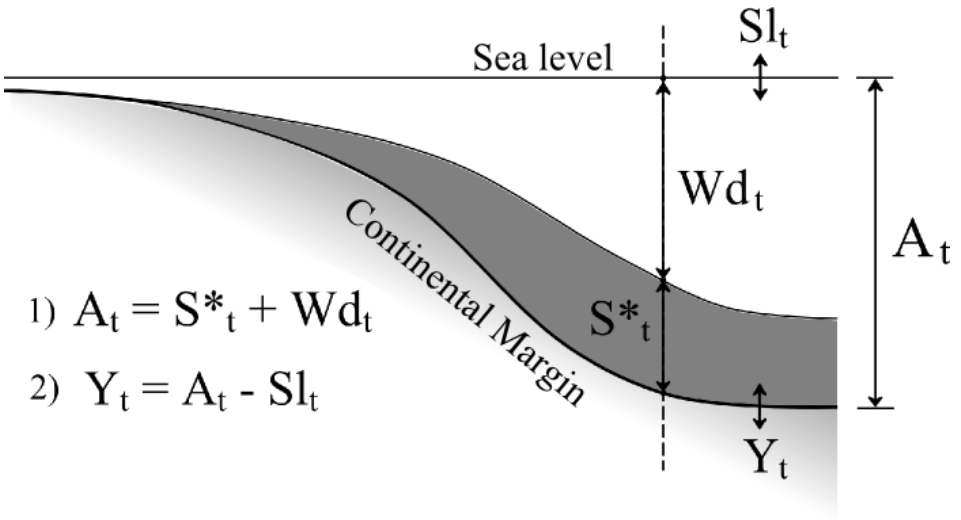

Figure 4.4: Schematic cross section through a basin margin illustrating the calculation method of the total subsidence. Where: A_t = accommodation, S^*_t = thickness of the decompacted deposits, Wd_t = bathymetry, Y_t = Total basement subsidence, Sl_t = absolute eustatism at the deposition time (t).

Backstripping is basically a numerical method that is used to decompact the stratigraphic units or sequences. It also accounts for the sediments and water load at each episode of deposition to calculate the tectonic subsidence (e.g. Hölzel, 2008). It quantifies the total subsidence of the basin basement by correcting for sediment compaction at the respective depths and times of deposition of each stratigraphic unit (e.g. Vail *et al.*, 1991).

When new material is deposited within a basin, previously deposited sequences become buried, compacted, as they are subjected to a fluid expulsion and an increase in both pressure and temperature which changes their physical properties (e.g. density, porosity, compaction etc.). These properties vary among different lithologies and are approximated by Allen and Allen (2005), as summarized in

Table 4.2, for the chosen lithologies used in this study.

Table 4.2: Physical properties of different lithologies used in the backstripping method (Taken from Allen and Allen, 2005)

Lithology	**Surface porosity**	**Porosity-depth coefficient (km-1)**	**Sediment grain density (kgm-3)**
Claystone	0.63	0.51	2720
Sandstone	0.49	0.27	2650
Chalk / limestone	0.56	0.71	2710

The total subsidence is divided into two parts, one caused by the tectonism and the other by the sediment and water load. The overall backstripping procedure removes this effect of sediment and water loading and compaction from the total basement subsidence, hence allowing the quantification of tectonic subsidence (e.g. McKenzie, 1978; Cochran, 1983; Vail *et al.*, 1991). This is here performed using the software "CoSub" (Dauteuil *et al.*, *in press*, 2014), which is improved from the standard 1D Airy backstripping method (Allen and Allen, 2005).

For each litho-stratigraphic unit, the following physical parameters are calculated according to their proportions of silt and clay (C) compared to sand (total silt and clay thickness/total thickness of silt, clay and sand); or silt and clay compared to limestone (total silt and clay thickness/total thickness of silt, clay and limestone) depending on which is more dominant between sand and limestone. The outcome from the well backstripping method provides a record of the basin's Meso-Cenozoic subsidence history.

As previously mentioned the calculation is based on the reduction of porosity of the lithologies (compaction) with depth as pressure is applied from successive deposited sediments onto the underlying sediments which then exhibit an exponential porosity–depth relationship, as indicated by the formulae below (e.g. Hölzel, 2008).

$$\varphi = \varphi_0 e^{-cy}$$

(where φ is the porosity at any given depth y, φ_0 is the initial porosity and c is a lithology-dependent coefficient that describes the rate at which the exponential decrease in porosity takes place with depth)

The various lithological properties that are accounted for in this backstripping method are listed below:

Compaction:	(C x 0. 51 + (100-C) x 0. 27)/100
Porosity:	(C x 0.63 + (100-C) x 0.49)/100
Density:	(C x 2750 + (100-C) x 2650)/100

For simplicity, the igneous lithologies, such as dacite, andesite and basalt, have been assigned to sand in this computation for backstripping because their physical rock properties are difficult estimate. Other input data required for this computation are as follows:

1). Age of the unit tops (Ma): Numerical ages of each unit top are determined from the bio-stratigraphy using the recent geological time scale of Walker *et al*., (2013).

2). Depth of unit base and top below the present day MSL (km): Determined from the well-logs.

3). Eustatic sea-level (km): Estimated from the Meso-Cenozoic sea-level curve devised by Miller *et al*., (2011). This sea-level curve is the most recent, based also on new oxygen isotope data and is derived from backstripping of New Jersey sites, which yields lower amplitudes long-term sea level range of 100–200 m versus older curves (e.g. 250 m from Haq *et al*., 1987).

4). Palaeo-bathymetry (km): Taken foraminiferal species (benthic and planktonic) that has been previously identified by Robertson Research International Limited (Amoco Seychelles Petroleum Company, 1981a, 1981b, 1981c) and various other criteria, for example sedimentological characteristics such as ooliths ect (see Section 5.6.1).

Chapter 5. Results and Discussions

5.1 Seismic stratigraphy

The two seismic reflection profiles TCO-106 and TCO-115 are approximately 100 km and 80 km, respectively. A maximum two-way travel time (TWT) of 8 and 6 seconds were obtained for seismic line TCO-115 and TCO-106, respectively, with CDPs at 25m spacing and sampling rates of 2 ms to obtain the available seismic lines. Well-log to seismic correlation of each seismic line is presented in Figure 5.1-Figure 5.2.

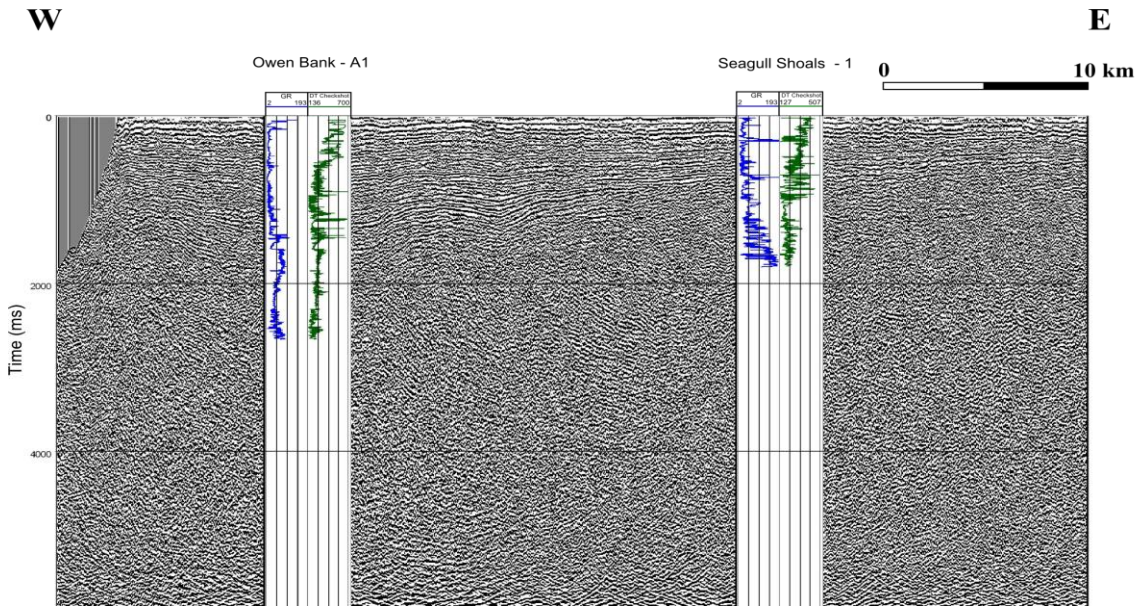

Figure 5.1: Well correlation of Owen Bank – A1 and Seagull Shoals – 1 with seismic profile TCO-106, based on well coefficients of 0.483926 and 0.392682 respectively.

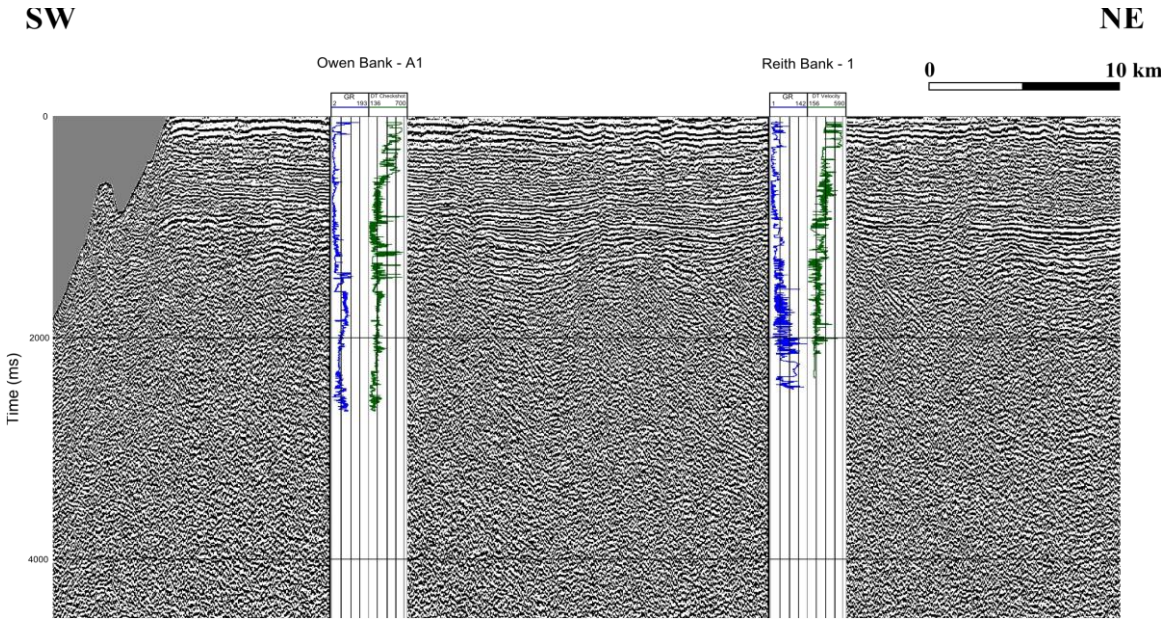

Figure 5.2: Well correlation of Owen Bank – A1 and Reith Bank – 1 with seismic profile TCO-115, based on well coefficients of 0.37394 and 0.512662 respectively.

5.1.1 Seismic reflection profile: TCO-106

Reflection profile TCO-106 and a summary of the interpretation is presented below. Detailed interpretations are produced in Appendix A.1 showing the various observed clinorform terminations identified and the interpretations used to identify the different surfaces observed (solid red lines) according to literature (Figure 5.3). The identified surfaces are in turn uncomformities and are traced and correlated in OpendTect, as a result a geological interpretation profile of the seismic profile TCO-106 is summarized below (Figure 5.), where the interpreted features from Appendix A.1 were used to pick these unconformities, ultimately representing sequence boundaries.

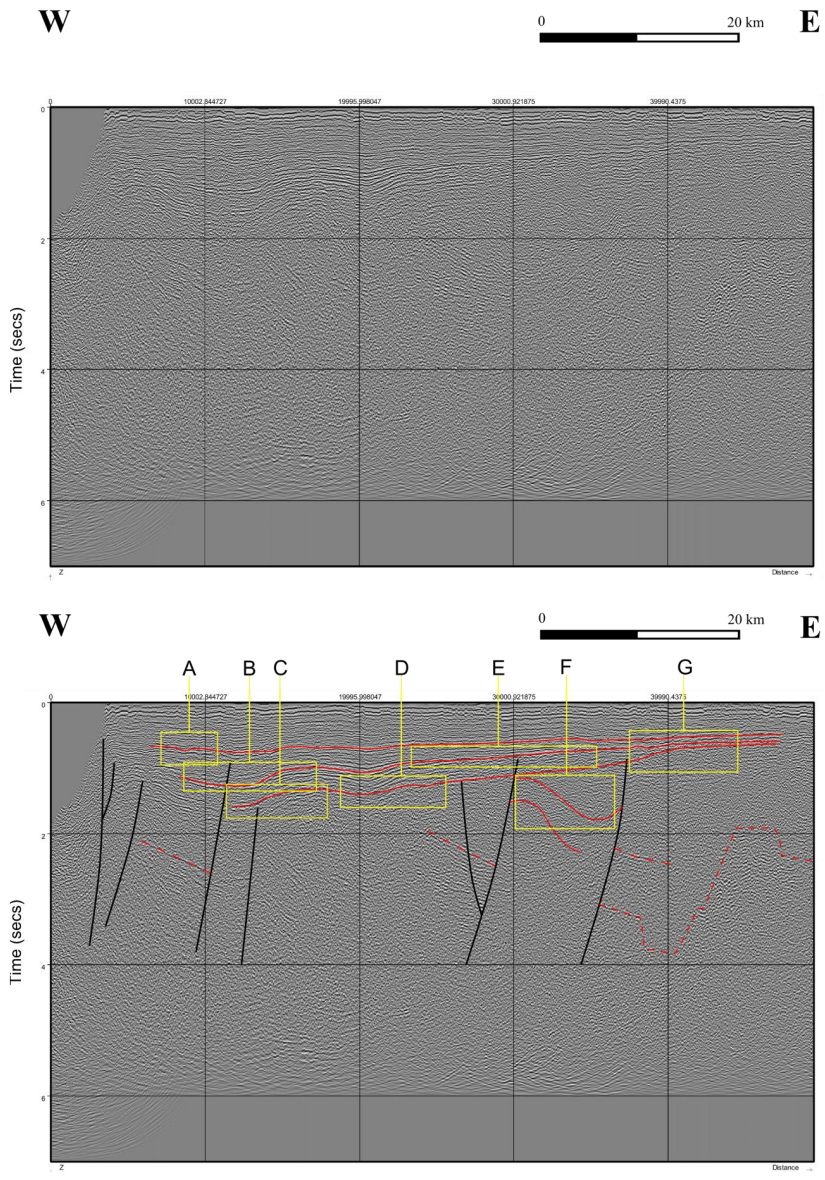

Figure 5.3: Seismic profile TCO-106 indicating the positions (yellow boxes) of the clinorform terminations (A-G) used to identify the various horizons or boundary surfaces (see Appendix A.1). The red lines represent identified seismic bounding surfaces / unconformities (sequence boundaries). Interpreted faults shown in black. Notice the west dipping faults and the horsts and graben structures.

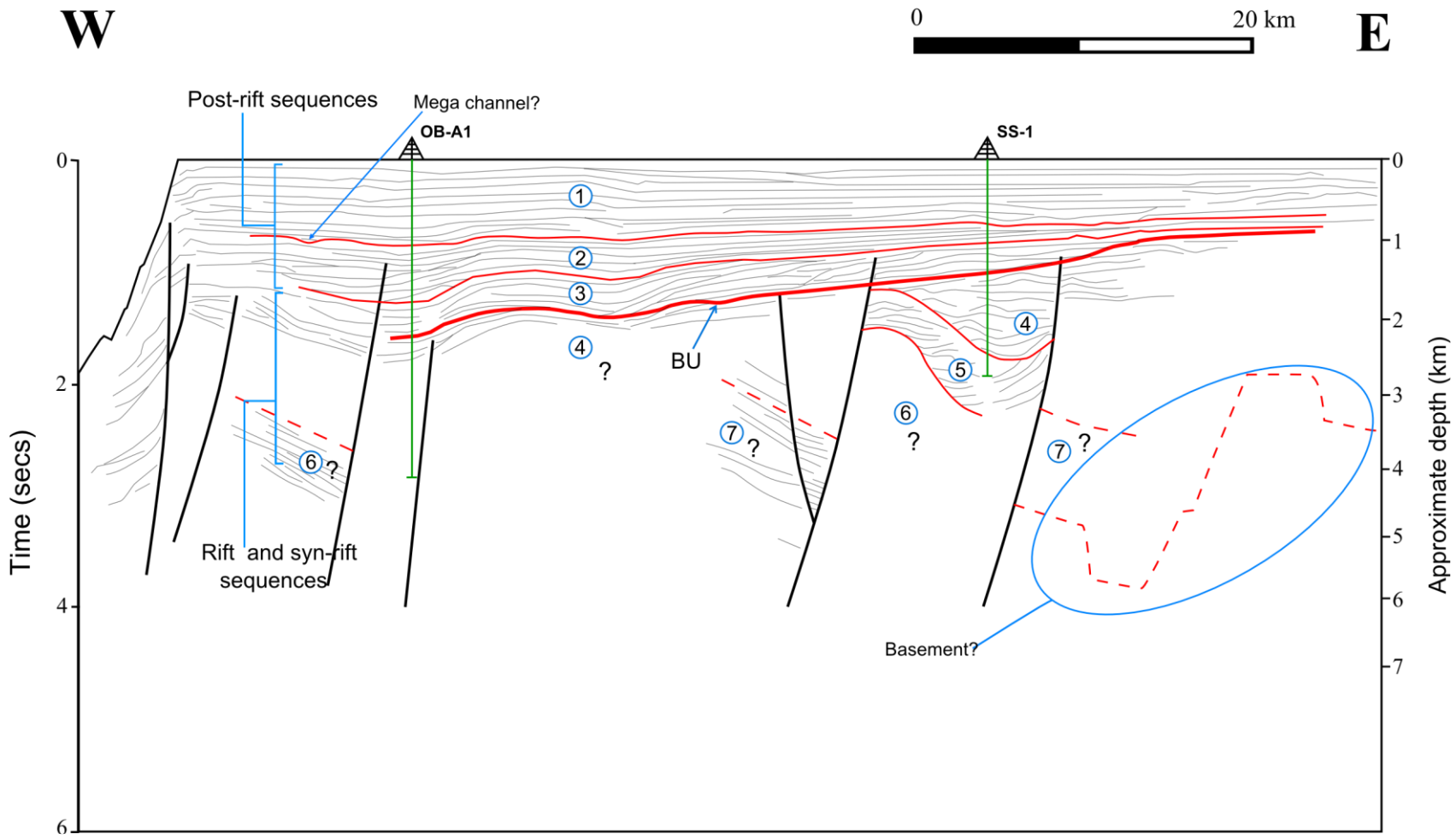

Figure 5.4: Geological interpretation of the seismic reflection profile TCO-106, with the identified major unconformities/sequence boundaries bounding the seismic units (1-7) indicated by the red horizons , notice the rotated fault blocks below the break-up unconformity (BU) and the general horst and graben structures and the lowermost un-interpretable seismic event indicated by the red dashed lines(basement?).

5.1.2 Seismic reflection profile: TCO-115

Reflection profile TCO-115 and a summary of the interpretation is presented below. Detailed interpretations are given in Appendix A.2 showing the various observed clinorform terminations identified and the interpretations used to identify the different surfaces observed (solid red lines) according to literature (Figure 5.5). The identified surfaces are in turn uncomformities and are traced and correlated in OpendTect, as a result a geological interpretation profile of the seismic profile TCO-115 is summarized below (Figure 5.), where the interpreted features from Appendix A.2 were used to pick these unconformities, ultimately representing sequence boundaries.

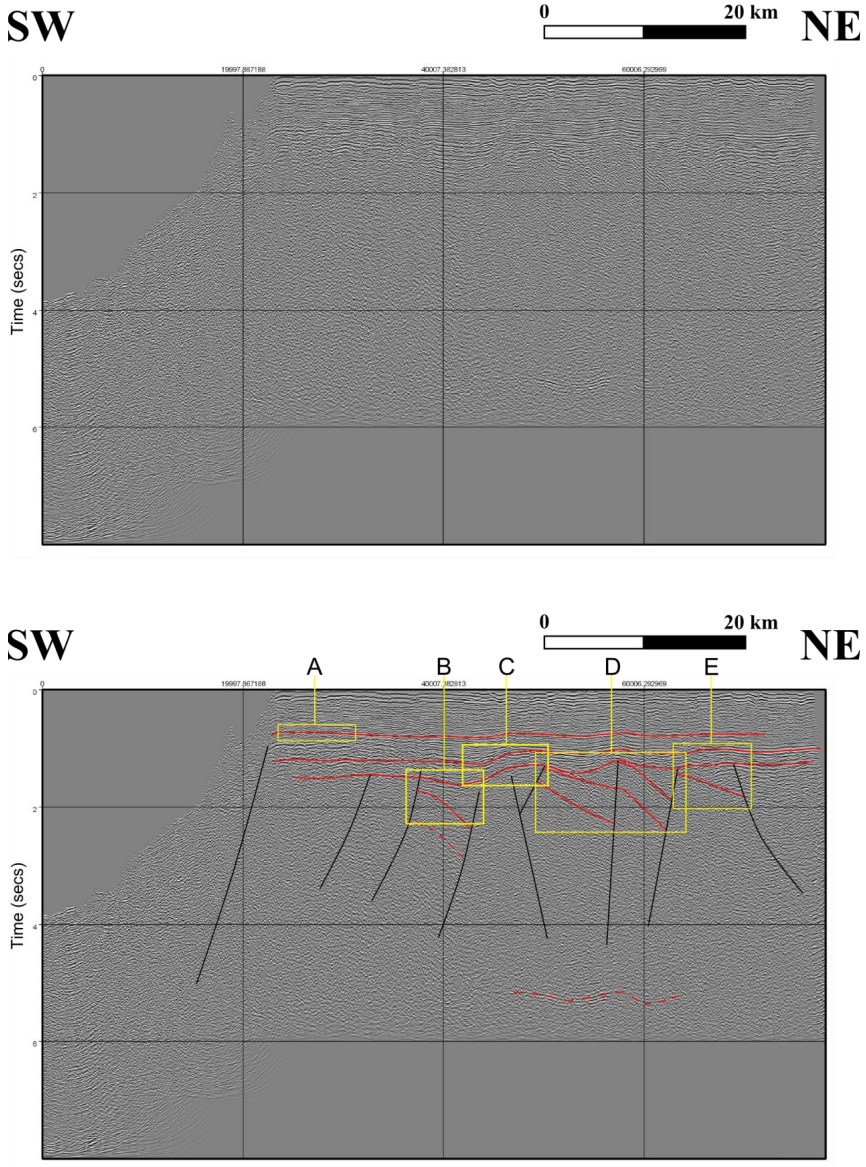

Figure 5.5: Seismic profile TCO-116 indicating the positions (yellow boxes) of the clinorform terminations (A-E) used to identify the various horizons or boundary surfaces (see Appendix A.2). The red lines represent identified seismic bounding surfaces / unconformities (sequence boundaries). Interpreted faults shown in black. Notice the south-west dipping faults and the horsts and graben structure.

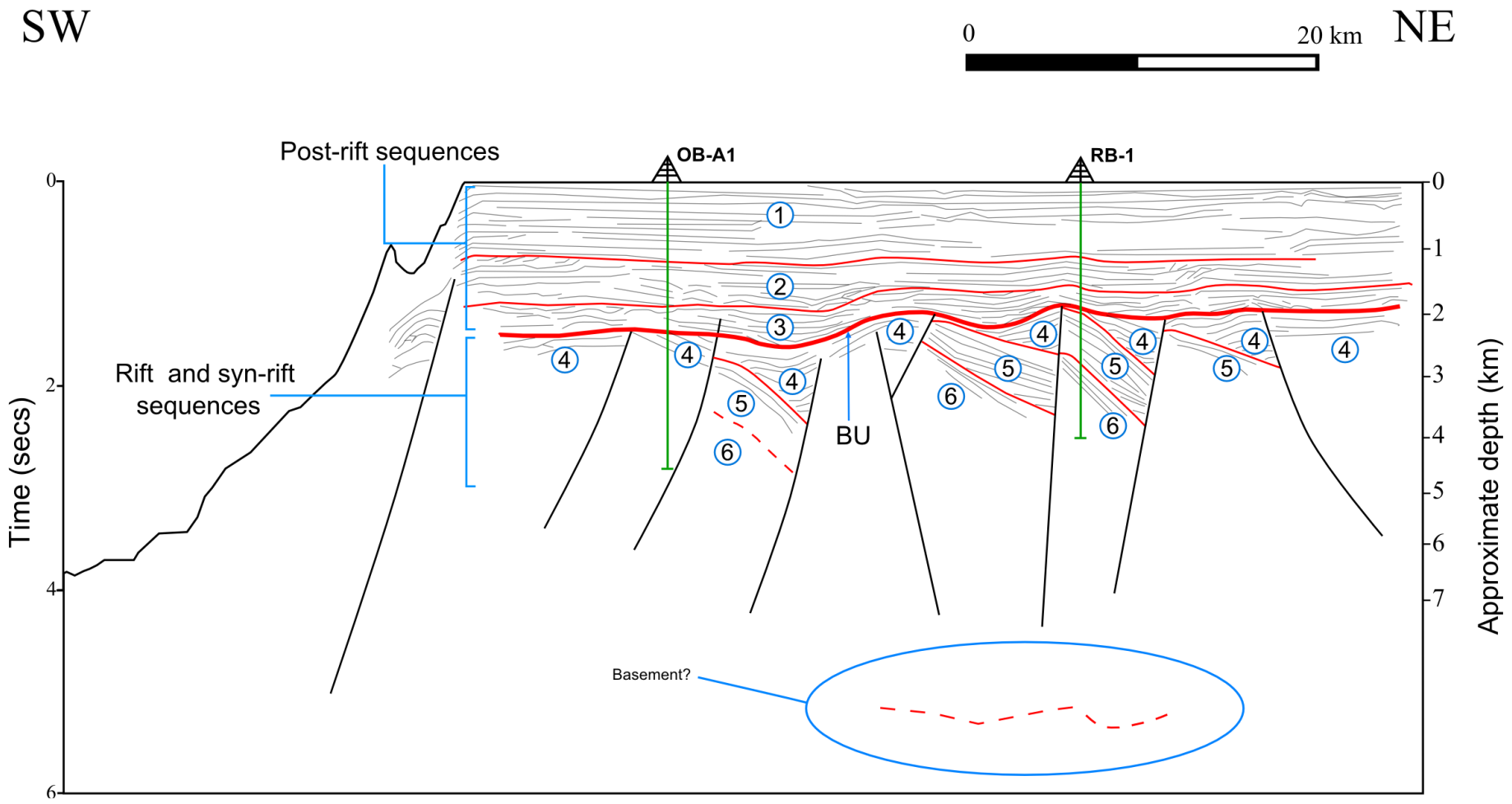

Figure 5.6: Geological interpretation of the seismic reflection profile TCO-115, with the identified major unconformities/sequence boundaries indicated by the red horizons, notice the rotated fault blocks and the general horst and graben structure and the lowermost un-interpretable seismic event indicated by the red dashed lines(basement?)

A 3D correlation model is generated from OpendTect 4.40j and the bounding surfaces of each identified seismic unit are shown on each seismic line, where each of their geometries are visible (Figure 5.7).

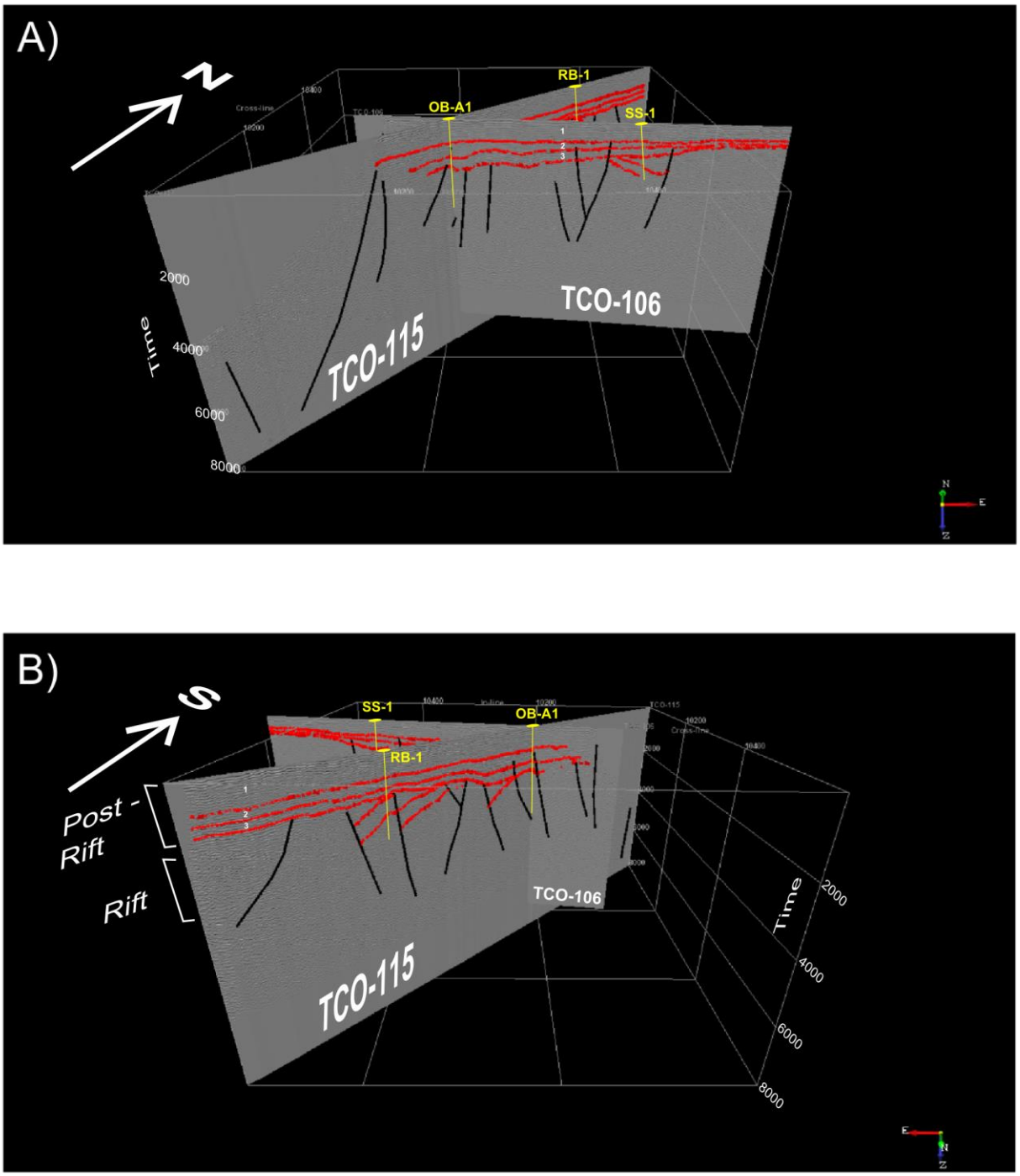

Figure 5.7: 3D correlation of seismic units (sequences) identified on seismic lines: TCO-106 and TCO-115, viewed in the OpendTect 4.40j interface. Views are: A) from south to north; and B) from north to south. Notice 1-3 conformable units possibly post rift thermal subsidence sequences, and underlying are the block faulted rift and syn-rift sequences

5.2 Bio-stratigraphy

The data is discontinuous in some parts of the wells, especially Seagull shoals – 1, due to the cavernous lithologies such as carbonates which may have caused low sample recovery. Nevertheless, biozone boundaries have been identified (Amoco Seychelles Petroleum Company, 1981a, 1981b, 1981c), and, bio-stratigraphic charts are reconstructed in this study for each well; these are presented in Figure 5.8-Figure 5.10.

Generally, the oldest age interpretation amongst the three wells is from Middle Triassic rock strata penetrated by Reith Bank – 1. The oldest rocks penetrated by Owen Bank – A1 and Seagull shoals – 1 are Lower Jurassic. The youngest sediments encountered is Pleistocene in Owen Bank – A1. The other two wells reached ages no younger than Oligocene. The Middle Jurassic to Lower Cretaceous section is most extensive and complete in the Owen Bank – A1 (Figure 5.8-Figure 5.10). All three wells show a general increase in the abundance of marine foraminifera upwards. This increase in the presence of foraminiferal species mainly starts in the Middle Jurassic which indicates a gradual change in the depositional environment from continental to marine with time. This is also supported by the gradual increase abundance of the palynomorphs with depth, which is consistent with an increase in proximity to land before the appearance of foraminifera. It seems that a mixed marine - terrestrial environment started around the Middle Jurassic. This probably represents a sequence boundary. A totally barren zone also exists at the Upper Cretaceous. This part of the sequence is rich also in volcanic material, and perhaps very few species survived during this time (*Omphalocuclus macroporus* and *Siderolites spp.*). This therefore suggests that the volcanic debris was deposited in a marine environment (Figure 5.8-). Another barren zone is seen to occur in the lower Reith Bank – 1 section, interpreted as Upper Triassic and possibly linked to an unknown mass extinction period or a section of zero recovery (Figure 5.10) (Amoco Seychelles Petroleum Company, 1981b).

5.2.1 Owen Bank – A1

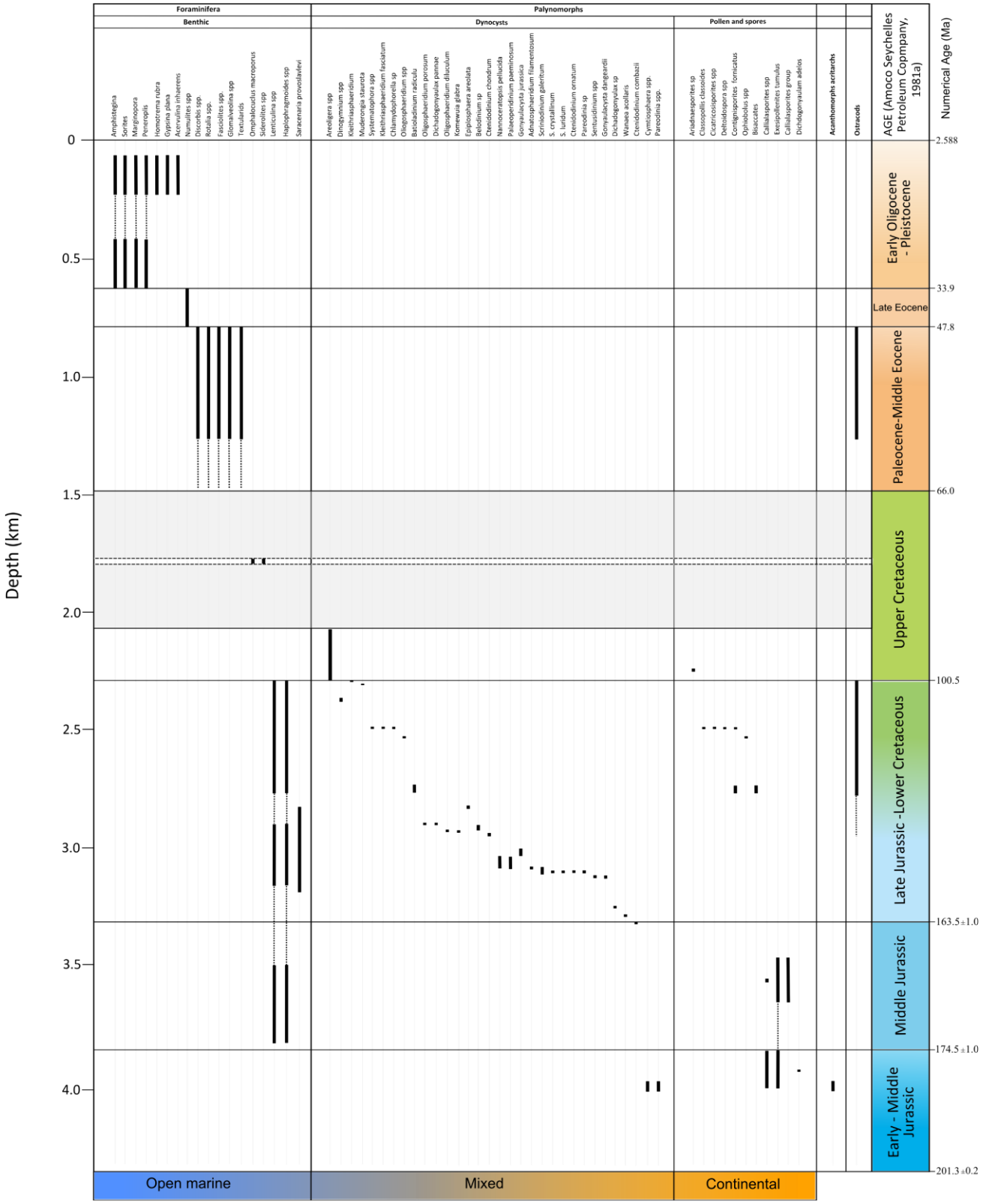

Figure 5.8: Biostratigraphy of the Owen Bank – A1 well of the western shelf of the SMc. Compiled from the paleontological and palynological data of Amoco Seychelles Petroleum Company (1981a)

5.2.2 *Reith Bank - 1*

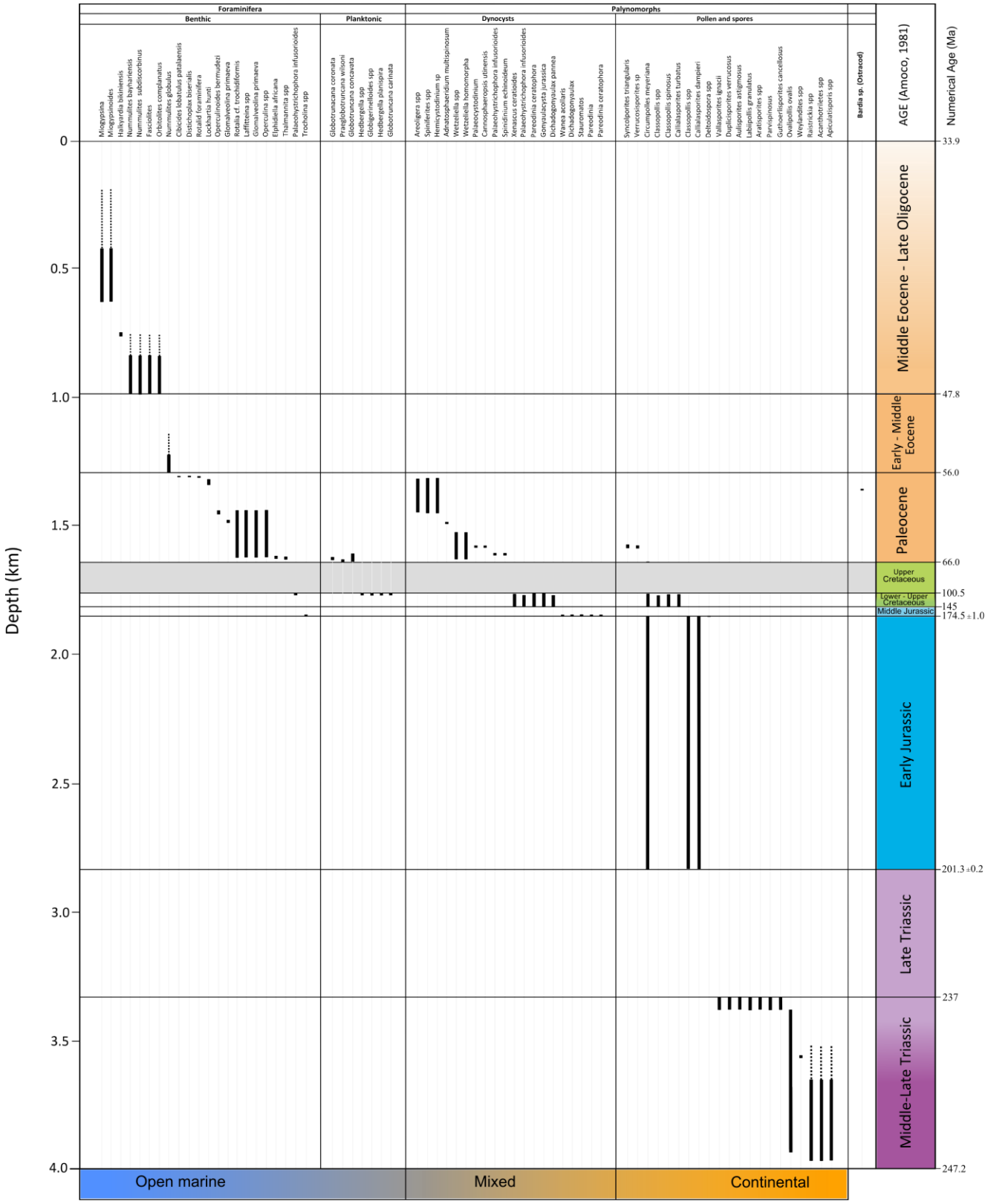

Figure 5.9: Biostratigraphy of the Reith Bank – 1 well of the western shelf of the SMc. Compiled from the paleontological and palynological data of Amoco Seychelles Petroleum Company (1981b)

5.2.3 Seagull Shoals - 1

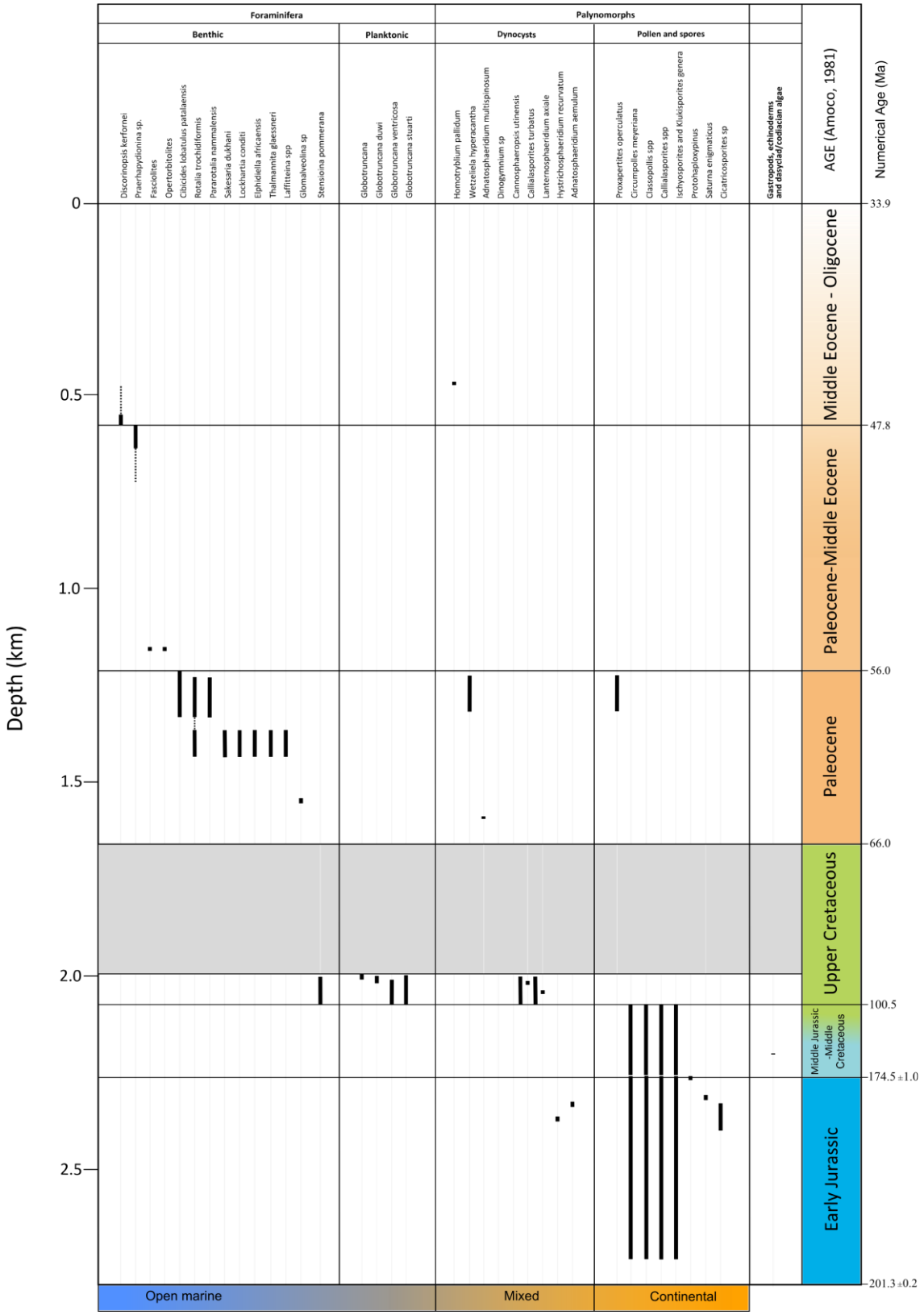

Figure 5.10: Biostratigraphy of the Seagull Shoals well of the western shelf of the SMc. Compiled from the paleontological and palynological data of Amoco Seychelles Petroleum Company (1981c)

5.3 Litho-stratigraphy and facies analysis

As mentioned in the previous section, the cutting data is discontinuous at some depths, mainly due to low sample recovery. However sufficient distance was covered down the three main wells to reconstruct the litho-stratigraphy and for facies analysis. The core data covered small intervals in each well on the western shelf as the drilling company only sampled conventially when they saw indications of hydrocarbon from the well cuttings (e.g. dark coaly claystones or black claystones). The well-logs on the other hand, covered most depths of the wells (Figure 5.11, Figure 5.12 and Figure 5.13).

The general low gamma readings from the top sections reflect the carbonate nature of the upper lithologies of each well, which includes limestones, calcareous sandstones and dolomites and probably lime mud. Further down, each well exhibited fluctuating levels of high and low gamma readings. This originates mainly from alternating lithologies that include fine grained siliciclastics such as claystones, siltstones and volcanics (recognized by high radioactive contents) and sandstones and limestones (recognized by low radioactive contents) of continental origins. The litho-stratigraphy of each well is reconstructed based on the combination of core and cutting data, and the identified lithological boundaries are based on the gamma readings (Figure 5.11-Figure 5.13).

This section also describes detailed sedimentary structures and characteristics of the identified facies of the Triassic to Cretaceous and Cenozoic successions of the wells from the western shelf of the SMc. Identified litho-facies of each well allows vertical facies analysis to be performed to identify the processes of deposition. The identified litho-facies of each well is presented and summarized in Figure 5.11-Figure 5.13).

5.3.1 *Owen Bank – A1*

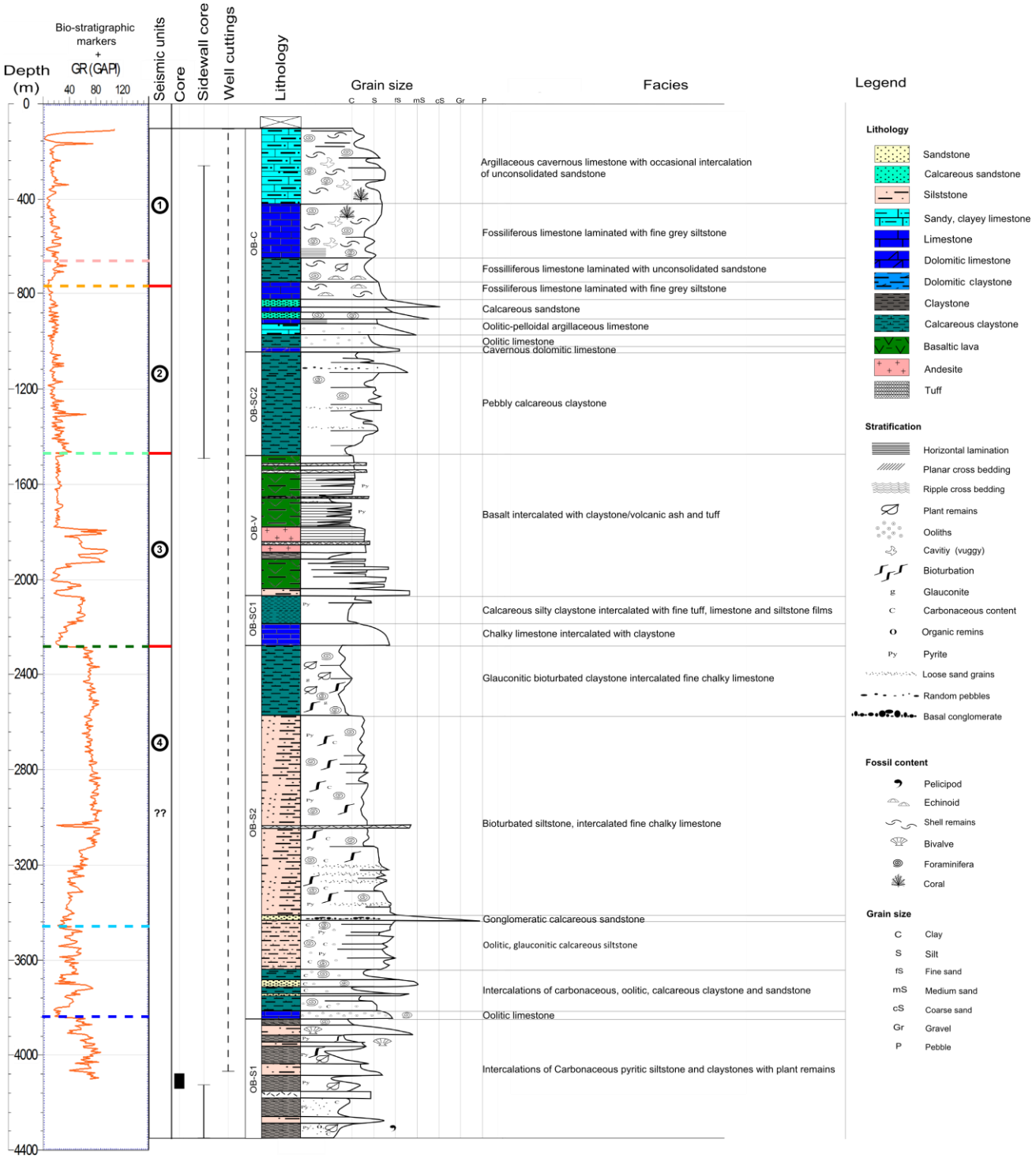

Figure 5.11: Interpreted litho-stratigraphy and facies successions of Owen Bank – A1 of the western shelf of SMc, using the well data (logs, core and cutting descriptions), integrated with the seismic units (1-4) and bio-stratigraphic markers (Solid red line = seismic boundary, Pink marker = Upper Eocene; Orange marker horizon = Middle Eocene; Lime green marker horizon = K-Pg; Green marker horizon =Upper Cretaceous; Light blue marker horizon = Middle Jurassic; Dark blue marker horizon = Early Jurassic)

5.3.2 *Reith Bank – 1*

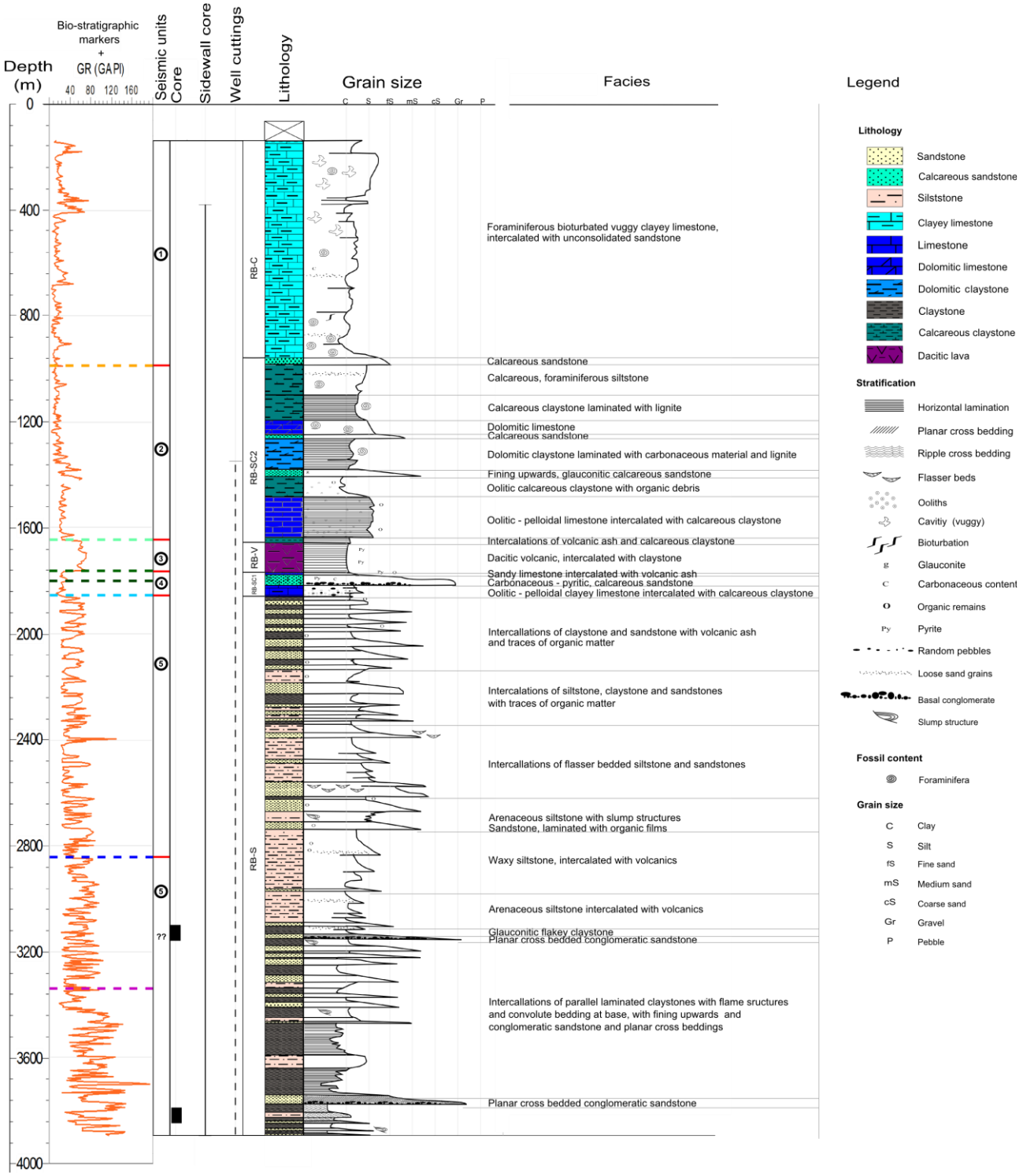

Figure 5.12: Interpreted litho-stratigraphy and facies successions of Reith Bank – 1 of the western shelf of SMc, using the well data (logs, core and cutting descriptions), integrated with the seismic units(1-5) and bio-stratigraphic markers (Solid red line = seismic boundary, Pink marker = Upper Eocene; Orange marker horizon = Middle Eocene; Lime green marker horizon = K-Pg; Green marker horizon =Upper Cretaceous; Light blue marker horizon = Middle Jurassic; Dark blue marker horizon = Early Jurassic)

5.3.3 Seagull Shoals – 1

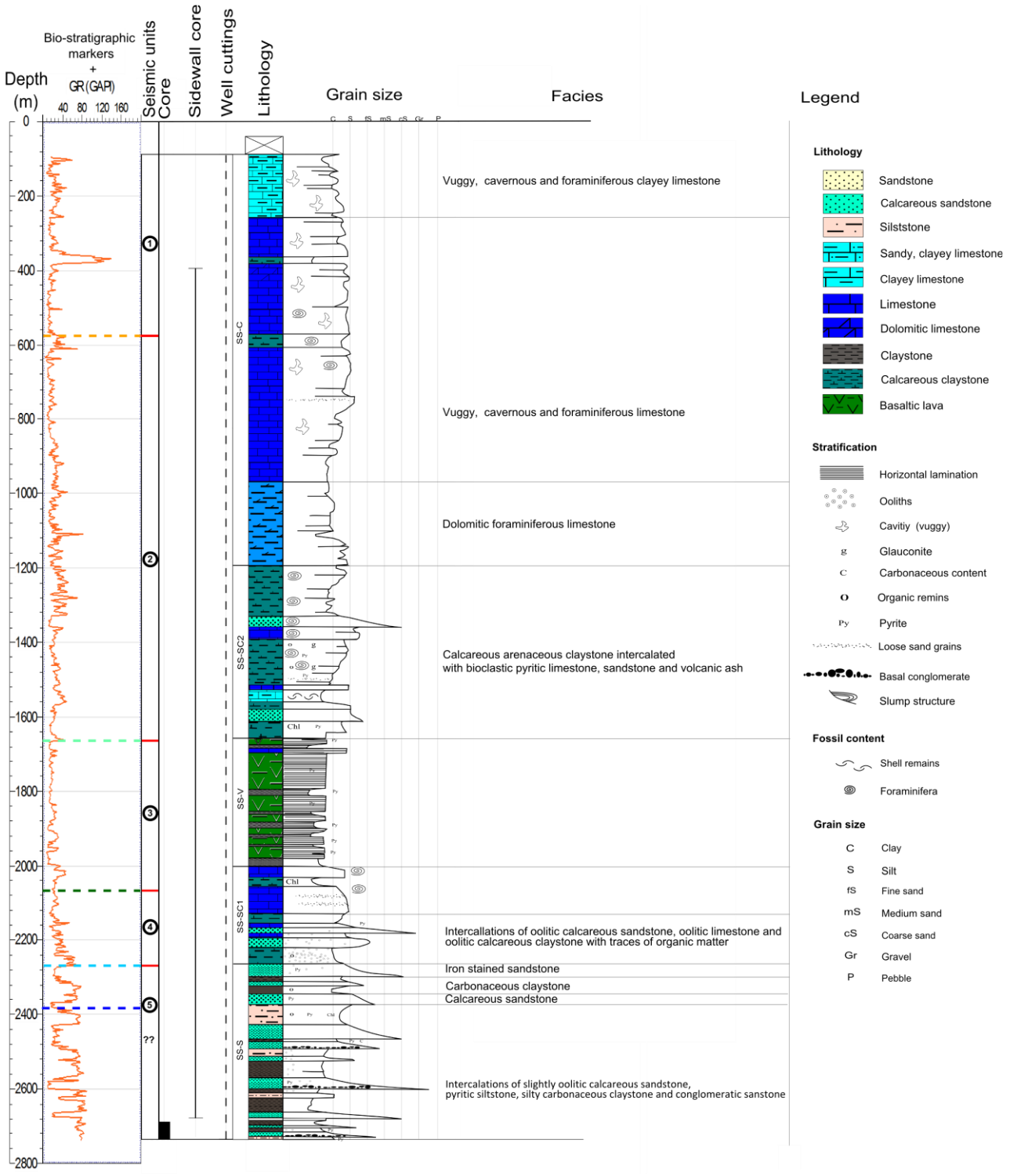

Figure 5.13: Interpreted litho-stratigraphy and facies successions of Seagull Shoals - 1 of the western shelf of SMc, using the well data (logs, core and cutting descriptions), integrated with the seismic (1-5) units and bio-stratigraphic markers (Solid red line = seismic boundary, Pink marker = Upper Eocene; Orange marker horizon = Middle Eocene; Lime green marker horizon = K-Pg; Green marker horizon =Upper Cretaceous; Light blue marker horizon = Middle Jurassic; Dark blue marker horizon = Early Jurassic)

5.4 Facies association and depositional environment interpretation

The successions of facies examined and defined from the previous section are integrated into three depositional systems: 1) Shelf – shallow marine; 2) Shallow restricted – marginal marine; and 3) Fluvial, lacustrine - deltaic deposits.

5.4.1 Shelf – shallow marine

5.4.1.1 Owen Bank – A1

From *ca.* 2280 m to 115 m depth of Owen Bank – A1 section, the general facies successions are interpreted as shelf – shallow marine environment. From the bottom it comprises massive limestone that grades upwards into calcareous claystone commonly interbedded by volcanic ash. This succession abruptly changes to vesicular basalt intercalated with claystone, welded tuff, volcanic ash and some andesites (dated as 74.7 ±1.3 Ma). This volcanic succession is in turn overlain by pebbly calcareous claystone which is then intercalated at the top by oolitic limestones and thick calcareous sandstone. This then changes to thick clayey limestone beds which become increasingly vuggy and cavernous at the top (Figure 5.14A).

The latter succession is interpreted as shallow marine to marine platform conditions (carbonate platform). The vuggy and cavernous nature of the limestones suggests a drop in the MSL which caused the carbonates to become subjected to dissolution and karstification (e.g. Lüdmann, 2013). The lack of clastic sediments indicates that the area was in clear open marine conditions, possibly inner to outer shelf environment (Figure 5.14A) (e.g. Jones and Desrochers, 1992; Fournier *et al.*, 2004; Wilson *et al.*, 2012; Lüdmann, 2013). The basalt layer probably represents continental break up due to the availability of the basaltic lava, possibly from the Upper Cretaceous basalts during or after the Madagascar separation from India/SMc (*ca*. 82 Ma) or prior to the SMc separation from India (Deccan basaltic traps, *ca.* 65 Ma).

5.4.1.2 Reith Bank - 1

From *ca.* 1778 m to 115 m depth of Reith Bank – 1 section, the general facies succession is interpreted as shelf – shallow marine environment. From the bottom it comprises crystalline dacite interbedded with calcareous claystone, volcanic ash, devitrified glass and welded tuffs (dated as 66.1 ±1.3 Ma). This volcanic succession is abruptly overlain by coarsenning up mixed carbonate – minor siliciclastic succession of predominantly calcareous claystone with occasional traces of carbonaceous material, calcareous sandstones, and oolitic limestone at the very base. Dense ooliths gradually decreases upwards. This then changes

to thick vuggy limestone successions, which is clayey at the top, with abundant benthonic foraminifera and possible remnants of bioturbation.

The latter succession indicates probable rise in the MSL as the ooliths becomes less dense and eventually disappear upwards from the base, implying deeper marine conditions. The general increase in the abundance of foraminifera and thicker limestone beds represents the onset of carbonate platform sedimentation. Furthermore, the lack of clastic sediments indicates that the area was in clear open marine conditions (Figure 5.14C) (e.g. Jones and Desrochers, 1992; Fournier *et al.*, 2004; Wilson *et al.*, 2012; Lüdmann, 2013). The dacite layer suggests violent explosive eruptions which most probably originated from a subduction process that led to the possible formation of the Amirantes Arc (e.g. Lajoie and Stix, 1992; Suwa et al., 1994).

5.4.1.3 Seagull Shoals - 1

From *ca.* 2130 m to 100 m depth of Seagull Shoals – 1 section, the general facies succession is interpreted as shelf – shallow marine environment. From the bottom it comprises massive limestone interbedded with calcareous claystone and fine layers of volcanic ash. This abruptly changes to a layer of volcanics which is predominantly in the form of amygdaloidal basaltic lava, interbedded with welded tuff and calcareous claystones. The volcanic succession is then abruptly overlain by a mixed carbonate - siliciclastic succession of predominantly calcareous silty claystone, with traces of pyrite, interbedded with thinner beds of limestone, with abundant foraminifera, shell fragments, and fine layers of volcanic ash at the base. These then changes to thick vuggy, cavernous limestone, interbedded with fine layers of calcareous sandstone, dolomite and siltstone (Figure 5.14B).

The latter succession possibly represents the onset of a carbonate platform in a shallow open marine condition, and the lack of clastic sediments indicates that the area was in open marine conditions (Figure 5.14B) (e.g. Jones and Desrochers, 1992; Fournier *et al.*, 2004; Wilson *et al.*, 2012; Lüdmann, 2013). The basalt layer, which has not been dated, most likely represents a continental break-up due to the availability of the basaltic lava similar to Owen Bank - A1 (e.g. Deccan basaltic traps).

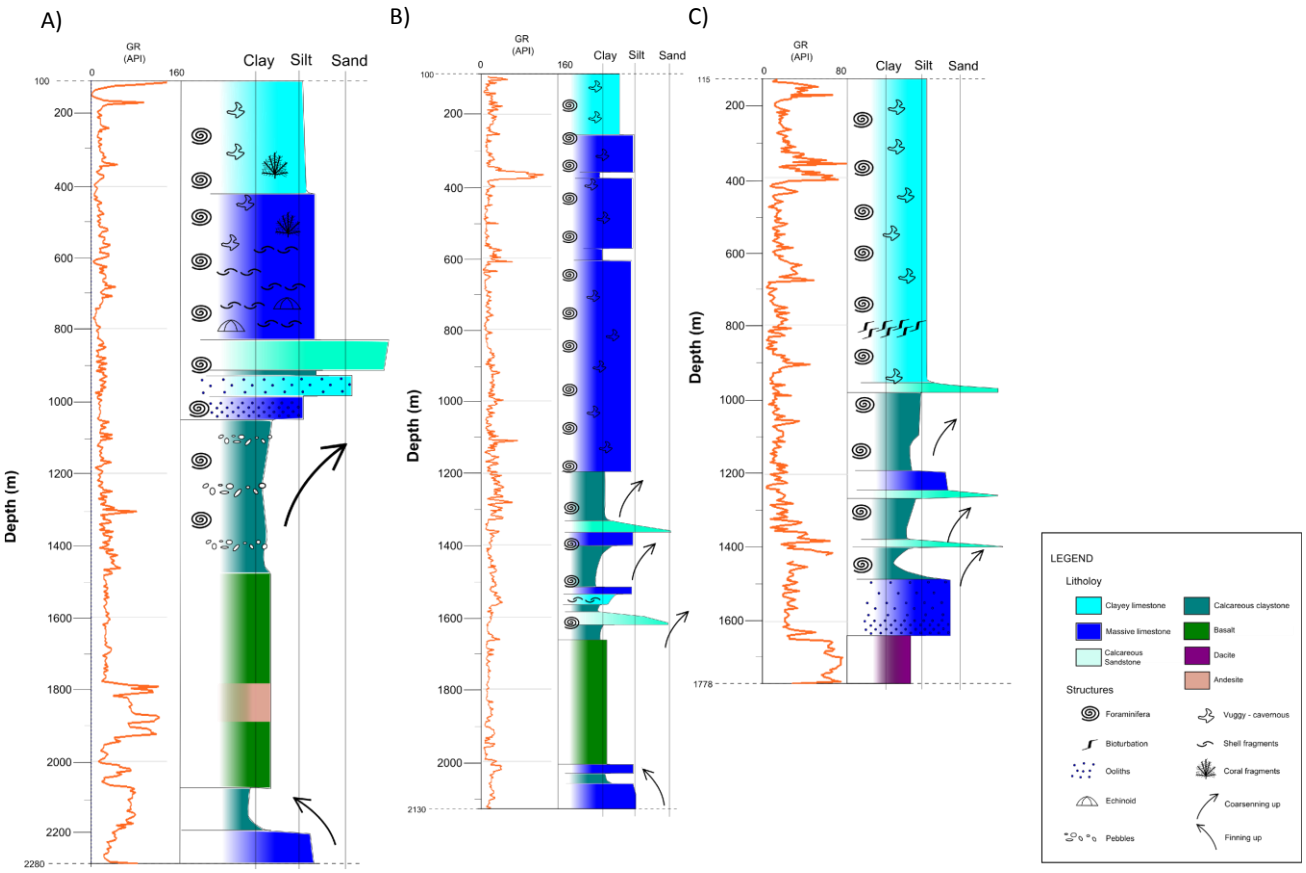

Figure 5.14: Shelf – shallow marine facies of the Upper section of: A) Owen Bank – A1; B) Seagull Shoals – 1; and C) Reith Bank – 1, integrated with the gamma ray logs. Notice there is no apparent trend in the gamma ray logs at the top carbonates. Shallow restricted – marginal marine

5.4.1.4 Owen Bank – A1

From *ca.* 3850 m to 2280m depth of Owen Bank – A1 section, the general facies succession has been interpreted as a shallow restricted – marginal marine environment. From the bottom it comprises extensive fining upwards trends in the lithologies, which generally starts with a distinct dense oolitic limestone grading up into calcareous claystones then to sandstone and further siltstone and finally claystone. In addition, there is evidence of bioturbation over hundreds of metres thick siltstone and glauconite in the top-most layer of claystone. There are abundant benthic foraminiferal remains and traces of pyrite and also dark coaly laminae. Generally, these lithologies are interbedded with thin layers of limestone and sandstones (Figure 5.15A).

The latter succession indicates a major marine trangressive phase in probably a marginal - restricted shallow marine environment (e.g. lagoonal- estuarine origin). The presence of coaly laminae indicate the anoxic condition of the palaeo-environment and the sandstone

interbeds indicates the proximity to shore and general fluctuation in the MSL (Figure 5.15A) (e.g. Rameil *et al.*, 2000; Phillips, 2003; Yubo *et al.*, 2011). Furthermore the presence of glauconite in the thick uppermost claystone layer suggests that the deposition of the sediments is still within the shallow marine environment but getting deeper (e.g. Porrenga, 1967; Compton and Wiltshire, 2009).

5.4.1.5 Reith Bank - 1

From *ca.* 1858 to 1778 m depth of Reith Bank – 1 section, the general facies succession is interpreted as shallow restricted – marginal marine. It is much thinner than that for Owen Bank – A1. It comprises dense oolitic limestone at the base that grades into a thick layer of oolitic calcareous sandstone with basal conglomerate at around *ca.* 1818 m depth. The top of this conglomeratic calcareous sandstone is marked by a thin layer of limestone also containing traces of organic matter and interbeds of very fine films of volcanic ash (Figure 5.15C).

The latter section indicates a general coarsening up in the succession, due either to higher energy environment or a possible drop in the MSL that ultimately formed possible shallow marine sheet sandstones or barrier beaches or carbonates coarsening upward cycles into the limestones. The general succession indicates an initial marine trangressive phase interrupted by an unconformity, possibly due to sudden change in the energy environment, for example increase in discharge to deposit the conglomeratic sandstones. This suggests a marginal - restricted shallow marine environment (Figure 5.15C) (e.g. lagoonal- estuarine origin) (e.g. Phillips, 2003; Yubo *et al.*, 2011).

5.4.1.6 Seagull Shoals – 1

From *ca.* 2259 to 2130 m depth of Seagull Shoals – 1 section, the general facies succession is interpreted as shallow restricted – marginal marine. It is much thinner than that for Owen Bank – A1, and it is composed initially of a dense oolitic calcareous claystone from the base as well, which eventually changes to a series of oolitic calcareous sandstone and limestones as well. There is a coarsening up in the succession, as well, from claystone into sandstone (Figure 5.15B).

The latter succession suggests an initial marine trangressive phase, as is indicated by initial thick dense ooliths in the claystone that gradually decreases upwards. The general coarsening upwards trend in this section is possibly due to shallow marine sheet sandstones or barrier beaches or carbonates coarsening upward cycles into the limestones, similar to the

section of Reith Bank – 1 illustrated in the previous section. This indicates a marginal to restricted shallow marine environment (e.g. lagoonal- estuarine origin) (Figure 5.15B) (e.g. Cant, 1992; Phillips, 2003; Yubo *et al.*, 2011).

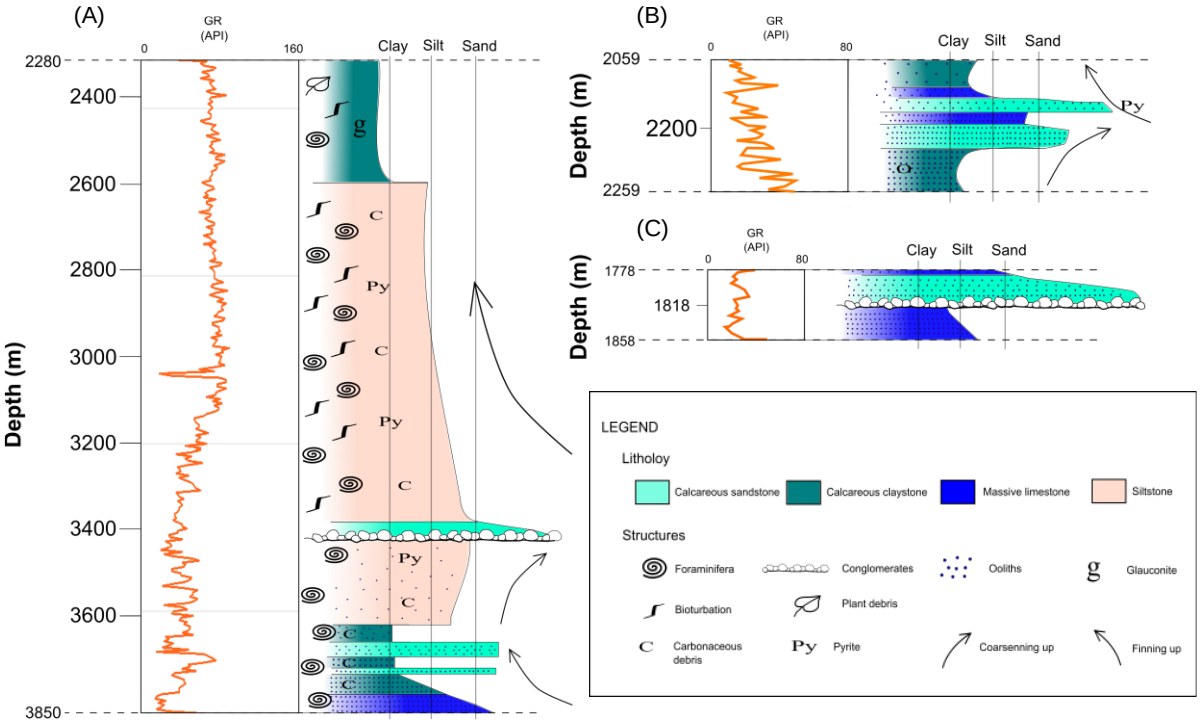

Figure 5.15: Shallow restricted – marginal facies of the Middle section of: A) Owen Bank – A1; B) Seagull Shoals – 1; and C) Reith Bank – 1, integrated with the gamma ray logs. Notice: the gradual increase in the gamma ray reading indicates the transgressive phase in the Owen Bank – A1 section.

5.4.2 Fluvial – overbank/lacustrine – deltaic

5.4.2.1 Owen Bank – A1

From *ca.* 4374 to 3850 m depth of Owen Bank – A1 section, the general facies succession is interpreted as fluvial – lacustrine – deltaic environment. From the base, this section comprises predominantly of medium - dark grey non-calcareous claystones with traces of pyrite, dark carbonaceous material, and contains evidence of bioturbarion, gastropods, plants and unidentified organic debris. These claystones are interbedded with medium grey siltstones and becomes slightly oolitic at the top. Coarsening upwards cycles are also visible towards the top of this section. Furthermore, with the exception of the top of this section, plant and other organic debris is evident and there is an absence of foraminifera. There is also 20 m thick aplite layer at around 4150 m deep, which is probably a dyke/sill (Figure 5.16).

The alternating siltstones and thick claystones from this section indicate that these units probably originated initially from active fluvial channel migration with lacustrine intervals that eventually grades into a deltaic system (marine incursion) as it gets calcareous and oolitic at the top with some foraminiferal remains. The latter is further supported by the availability of foraminifera at the top. The coarsening upwards cycles is possibly due to the prograding delta front depositional system (Figure 5.16) (e.g. Coleman and Gagliano, 1964; Nijman and Puigdefabregas, 1978; Bhattacharya and Walker, 1992; Roberts, 1997; Pirmez *et al.*, 1998; Dalrymple and Choi, 2007; Higgs, 2012).

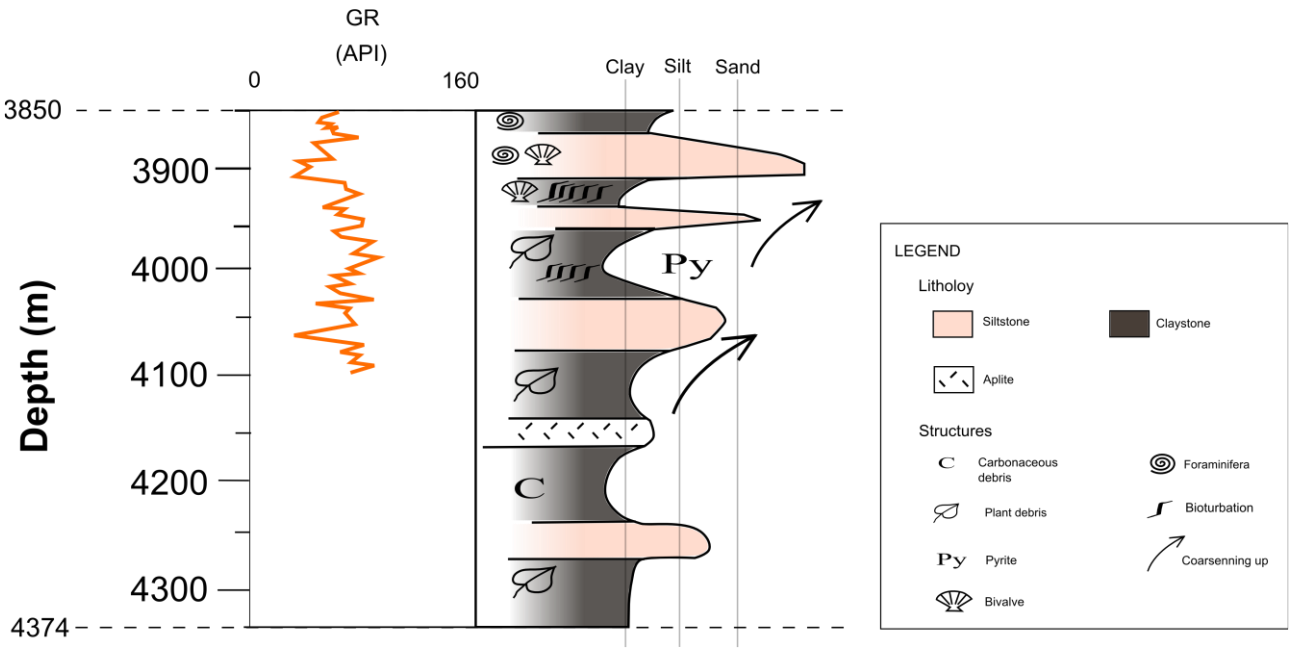

Figure 5.16: Fluvial/lacustrine - deltaic facies association of the bottom part of Owen Bank – A1. Notice: the two black arrows indicating the gradual drop in the gamma ray reading indicates two possible coarsening upwards cycles of facies.

5.4.2.2 Reith Bank – 1

From *ca.* 3898 to 1858 m depth of Reith Bank – 1 section, the general facies succession is interpreted as fluvial–lacustrine environment. From the base, this section comprises of medium - dark grey non-calcareous claystones with traces of pyrite, dark carbonaceous plants material and unidentified organic debris intercalated by non-calcareous sandstones or conglomeratic sandstones. These then changes upwards to highly alternating sandstone and mudstone facies within which there are repeated fining upwards cycles from sandstone to siltstone or claystone, and furthermore there are flaser beds and also slump structures in some sandstone layers (Figure 5.17).

The thick basal organic rich claystone strata indicates anoxic low energy condition, characteristic of lacustrine environment, followed by the more alternating lithologies (sandstones and mudstones), suggests an active fluvial environment and possibly lacustrine/overbank deposits evidenced by the thick claystone units (e.g. Nijman and Puigdefabregas, 1978; Phillips, 2003; Labrequel *et al.*, 2011). The fining upwards of sandstones into siltstone or claystones and the availability of clay lenses (flaser) are characteristics of pointbar deposits. The clay lenses are formed when clay sediments are deposited in the troughs of ripples on the pointbar bank when the river flow is reduced significantly, allowing the clay size deposits to be deposited as suspended load. In general, the lithological changes are consistent with the gamma logs seen as alternating high and low gamma readings and fining upward trends (Figure 5.17) (e.g. Dalrymple, 1992; Phillips, 2003; Labrequel *et al.*, 2011).

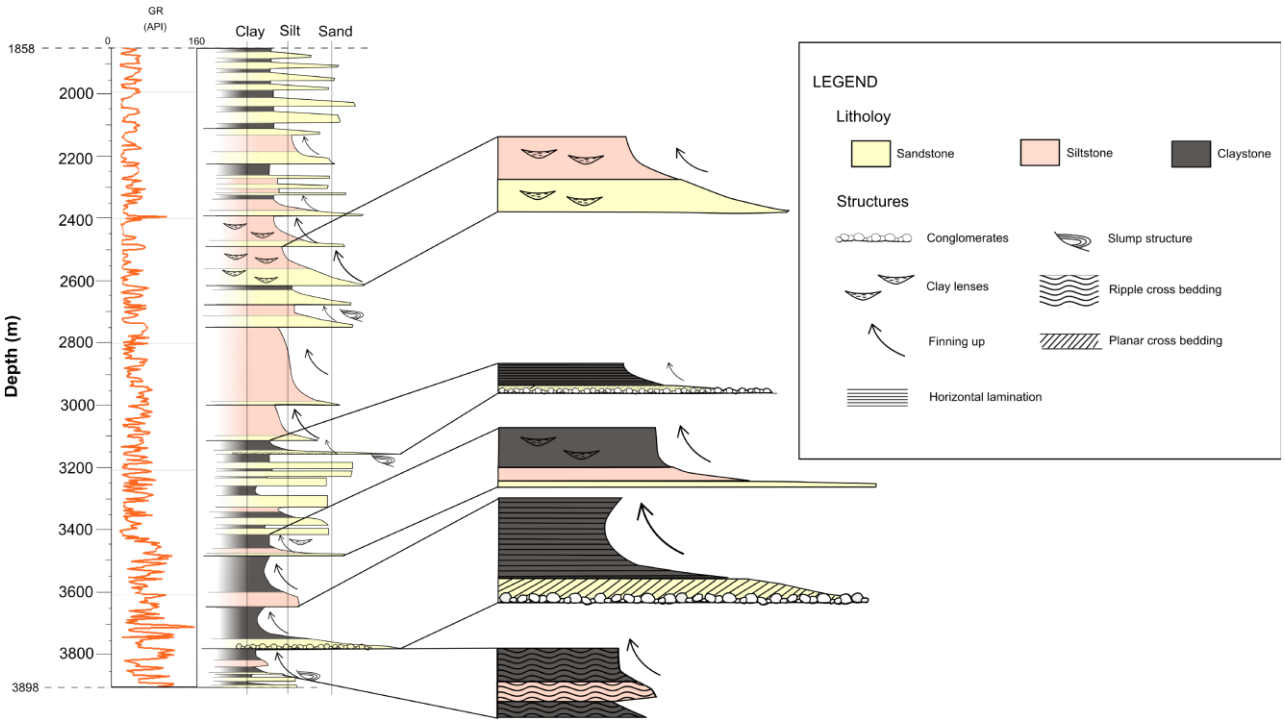

Figure 5.17: Fluvial - lacustrine association of the bottom part of Reith Bank – 1. Notice: the level of fluctuation in the Gamma ray log that coincide with the sand/clay content alternations.

5.4.2.3 Seagull Shoals - 1

From *ca.* 2745 to 2259 m depth of Seagull Shoals – 1 section, the general facies succession is interpreted as a fluvial – deltaic environment. From the base this section comprises of calcareous claystone that grades up into calcareous sandstone with basal conglomerates.

There are three visible major coarsening upwards cycles from claystone to siltstone and to oolitic - conglomeratic sandstone (Figure 5.18).

The alternating lithologies from this section indicates that these units probably originated initially from fluvial system that grades into a marine setting as it gets calcareous and oolitic at the top of each coarsening upwards cycle. The latter is further supported by the presence of benthic foraminifera. The coarsening upwards cycles are possibly due to the prograding delta front depositional system which is further evidenced by the gamma ray response (Figure 5.18) (e.g. Coleman and Gagliano, 1964; Nijman and Puigdefabregas, 1978; Bhattacharya and Walker, 1992; Roberts, 1997; Pirmez *et al.*, 1998; Dalrymple and Choi, 2007; Higgs, 2012). The calcareous conglomeratic sandstone might also indicate a shore-face environment (Figure 5.18) (e.g. Roberts, 1997; Pirmez *et al.*, 1998; Dalrymple and Choi, 2007; Higgs, 2012).

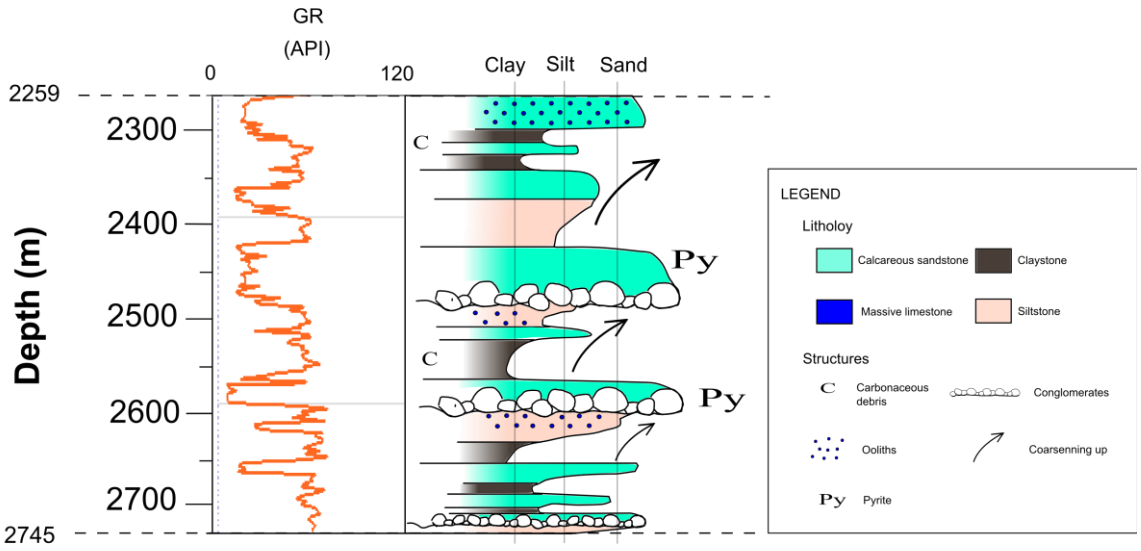

Figure 5.18: Fluvial - deltaic facies association of the bottom part of Seagull Shoals – 1. Notice: the three arrows indicate the gradual drop in the gamma ray reading which indicates three possible coarsening upwards cycles.

5.5 Seismics, litho- and bio-stratigraphic correlation

The seismic lines along with the identified and traced horizons/surfaces are correlated with the well-logs and the bio-stratigraphic markers (see details in Chapter 5.2) in OpendTect. The seismic profiles TCO-106 and TCO-115, with bio-stratigraphic and litho-facies correlations are presented in Figure 5.19 and Figure 5.20. The lowest interpretable stratal reflectors are approximately 2-2.5 seconds (TWT) deep (*ca.* 3-4 km). Below this the seismic data becomes very chaotic and interpretation increasingly uncertain. This is due to the significant variation of the P-wave velocities of the seismic source as it travelled through

the thick vuggy – cavernous carbonate successions of the carbonate platform and the basal volcanic successions; increasing the impedance of the seismic signal. Furthermore, the seismic signals experience attenuation they travel deeper through the lower successive rocks causing more noise (e.g. Wyllie *et al.*, 1962; Toksöz *et al.*, 1976; Mavko and Nur, 1979; Dutta *et al.*, 2008; Adam *et al.*, 2009). This eventually causes poor seismic signal to noise ratio, which is in turn generally causing low correlation coefficients between the wells and the seismic data. With the seismic-to-well-log correlations and the integration of bio-stratigraphic well tops, the rift and post-rift seismic sequences and their bounding surfaces were identified and mapped. The identified seismic bounding surfaces correlate well with the well tops at shallower depths (< 1.5 seconds). Deeper down the seismic profiles (1.5- 3 seconds), the well tops correlated poorly to those of the seismic profiles. Nevertheless, there are seven major sequences that have been identified in this study (Figure 5.19 and Figure 5.20). Furthermore, as a result of seismic stratigraphic interpretation and tectono-stratigraphic analysis, the break-up unconformity (dark green marker horizon = K-Pg boundary *ca.* 66 Ma) was identified and mapped throughout the two seismic lines as well. The rift sequences (Triassic - early Cretaceous) beneath the break-up unconformity, seems to have been deposited in graben and half-graben systems indicated by the wedge shaped packages. Overlying the rift sequences are the Upper Cretaceous – Paleogene sequences which comprises post-rift sequences, predominantly basal marine claystones and overlying shelf carbonates which were deposited during the drift-phase and thickened above the graben and half-graben systems (Figure 5.19 and Figure 5.20).

The shelf carbonate and marine clastic sequences seem to be fairly conformable, implying little impact from any tectonism, since these accumulated during and after the last break up event. This infers that these sequences might be part of the final drift phases (post rift). Below this, the phase of active rifting formed complicated faulting that appears to have formed angular unconformities (rift onset unconformities). This has clearly changed the pattern of depositional environments, as the wedged shaped seismic units accumulated coarse fluvial and fine marine sediments that are seen in the failed rift basins or half grabens (syn-rift sediments). Such tectonism has caused the sediments below the break-up unconformity to be of variable thickness, for example the thinning of the Cretaceous volcanics and marine clastics beneath the Cenozoic sequences. Extensional rifting is evident due to the availability of the observed faults, horst and graben structures. It is observed that the rotated fault blocks below the Upper Cretaceous are structurally higher in

Reith Bank – 1 and Seagull Shoals – 1, resulting in a great proportion of the Lower Cretaceous sequence being eroded during faulting. A deep seismic event/marker detected by the high reflection properties amongst the lower chaotic section at depths of around 2-4 seconds from seismic profile TCO-106 and 5 seconds from seismic profile TCO-115. This is possibly the top of the basement granite (see Chapter 5.1). Notice clinoforms from Sequences 1-3 bounded by three top-most identified sequence boundaries display sigmoidal patterns sub-parallel to the topsets and oblique prograding patterns show toplap terminations at the top which indicate aggradation during progradation due to the increase in accommodation from marine transgression (e.g. Serra, 1984; Catuneanu et al., 2009).

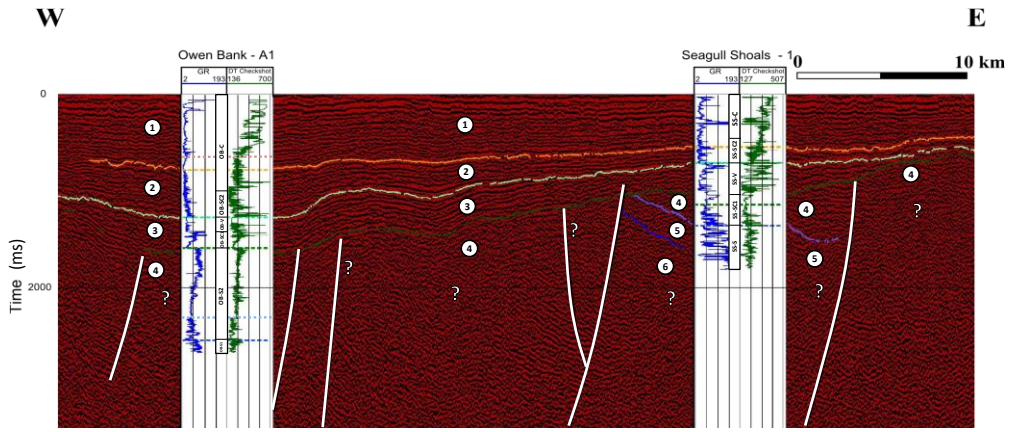

Figure 5.19: Seismic and well-log correlation of TCO-106 (Pink marker=Upper Eocene; Orange marker horizon=Middle Eocene=SB1; Lime green marker horizon=K-Pg=SB2; Dark green marker horizon=Upper Cretaceous=SB3; Light blue marker horizon=Middle Jurassic=SB5; Dark blue marker horizon=Early Jurassic=SB6).

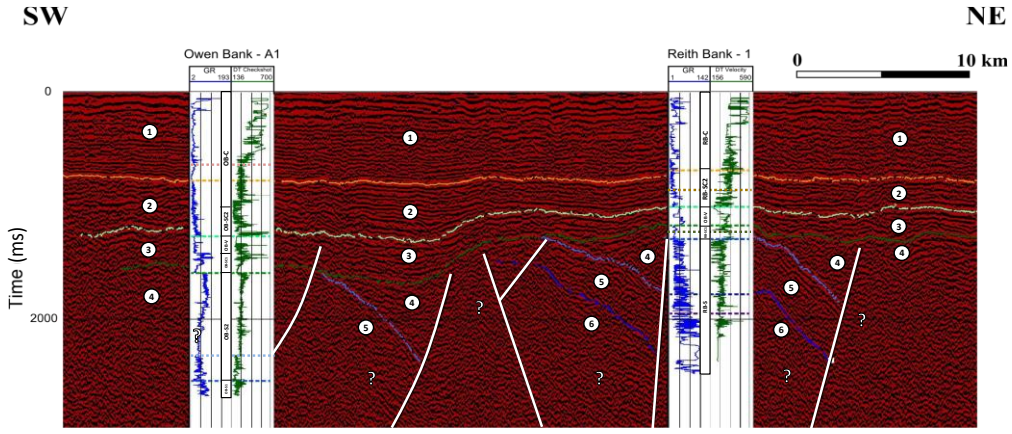

Figure 5.20: Seismic and well-log correlation of TCO-115 (Pink marker=Upper Eocene; Orange marker horizon=Middle Eocene = SB1; Lime green marker horizon=K-Pg=SB2; Dark green marker=Lower Cretaceous=SB3; Light blue marker horizon=Middle Jurassic=SB5; Dark blue marker horizon=Early Jurassic=SB6; Purple marker horizon=Upper Triassic).

5.6 Data computation and results of backstripping

There are three main episodes of subsidence identified from the backstripping method: Episodes A, B and C (Figure 5.21 and Figure 5.27). The last phase of subsidence (Episode C) does not seem to level off as it approaches 0 Ma.

5.6.1 Calculated SMc palaeo-bathymetry

At present the SMc's surface (SP) is 200 m below MSL. Relative to this present-day MSL, the calculated palaeo-bathymetry from the Middle Jurassic to present ranges between 10 m and 50 m. The Middle Jurassic to Lower Cretaceous shallow marine to near shore/restricted marginal sequences comprise distinct oolitic limestones at base which gradually change upwards to calcareous siltstones and claystones. The presence of ooliths and benthic foraminifera, and glauconite at the top of this section suggest that the palaeo-bathymetry is approximately 10 – 30 m, from bottom to top (Figure 5.21 and Figure 5.27). The Upper Cretaceous shallow marine - shelf deposits comprise volcanic and igneous strata, overlying limestones, calcareous claystones and sandstones, with some evidence of planktonic foraminifera, which suggest an increase in depth, therefore the estimated palaeo-bathymetry is approximately 30 - 50 m (Figure 5.21 and Figure 5.27). The Paleocene to middle Eocene shallow marine shelf deposits comprises calcareous claystones and dolomitic limestones, with also some evidence of planktonic foraminifera and glauconite approximates at 50 m depths. Above the latter sequence, the middle Eocene to Pleistocene section comprise almost entirely of shelf carbonates with evidence of benthic foraminifera and coral reef with minor ooliths, hence the estimated palaeo-bathymetry is approximately 20 m (Figure 5.21 and Figure 5.27).

5.6.2 Subsidence episode A

The first episode of subsidence starts at around 174 Ma with the onset of a shallow marine incursion into inland Gondwana and terminates at about 66 Ma. This Middle Jurassic – Upper Cretaceous subsidence has a magnitude of 2750 m (Owen Bank-A1), 315 m (Reith Bank-1) and 520 m (Seagull Shoals-1), with average rates of subsidence of 20 m/Ma, 5 m/Ma and 5 m/Ma, respectively (Phase A) (Figure 5.21). These sediments correlate with the Middle Jurassic (Aalenian-Bajocian) and Upper Jurassic (Albian–Cenomanian) transgression and ultimately the deposition of Sequences 4 and 3, respectively. These sequences were deposited as a consequence of transgression as subsidence followed the separation of the East and West Gondwana that caused the Tethys Sea to protrude inland and corresponds to a sea-level rise of 120 m magnitude (see Figure 5.27).

5.6.3 Subsidence episode B

The second episode starts at around 66 Ma with an increased rate of subsidence compared to the previous phase A, and terminates at about 48 Ma. This Paleocene to middle Eocene subsidence (Phase B) has a magnitude of 550 m (Owen Bank-A1), 875 m (Reith Bank-1) and 1080 m (Seagull Shoals-1), with average rates of subsidence of 35 m/Ma, 50 m/Ma and 60 m/Ma, respectively (Figure 5.21). These sediments correspond to the deposition of Sequence 2, which initially started with the onset of the separation of SMc from India. Carbonates (limestone) and minor siliciclastics (mudstones and minor sandstones) were deposited. The most probable reason for this is that the SMc was still in close proximity to India that was still supplying some degree of siliciclastic sediments during the separation of the SMc from India. The separation of the SMc from India caused a transgression from the Paleocene to the middle Eocene until the SMc was completely disconnected and fully submerged from the Indian plate upon the formation of the Carlsberg Ridge. This transgression period corresponds to a sea-level rise of 25 m magnitude (see Figure 5.27).

5.6.4 Subsidence episode C

The third episode of subsidence starts at around 48 Ma, during a reduced rate of subsidence. This middle Eocene to Pleistocene subsidence (Phase C) has a magnitude of 430 m (Owen Bank-A1), 670 m (Reith Bank-1) and 310 m (Seagull Shoals-1), with average rates of subsidence of 10 m/Ma, 30 m/Ma and 15 m/Ma, respectively (Figure 5.21). This episode corresponds to the deposition of Sequence 1, which comprises almost entirely of limestones and some minor calcareous sandstones. The most probable reasons for this reduced rate of subsidence is possibly due to an increased ridge effect from the nearby Carlsberg Ridge or due to the Reunion hotspot directly interacting with the Carlsberg Ridge when they coincided at *ca*. 55 Ma (see Figure 5.27).

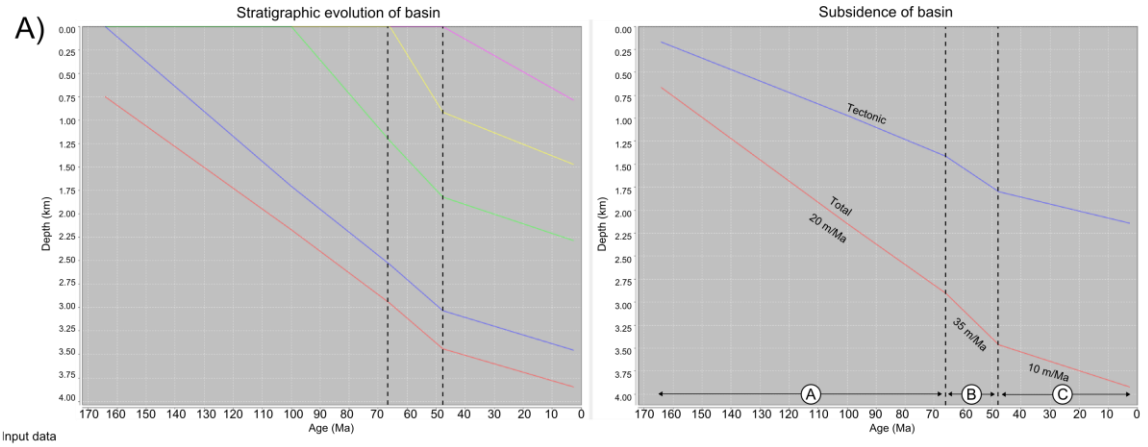

Input data

Units	Clay (%)	Age (Ma)	Depth of unit base (km)	Depth of unit top (km)	Compaction coefficient (km-1)	Surface Porosity (%)	Density (kg/m3)	Paleobathymetry (km)	Eustatic sea level (km)	Sea water density (kg/m3)
4ii	84	164	3.844	3.452	0.542	0.6412	2718.4	0.01	0.1	1030
4i	98	84	3.452	2.288	0.5052	0.6272	2718.6	0.03	0.05	1030
3	22	66	2.288	1.475	0.666	0.6846	2712.2	0.02	0.075	1030
2	70	48	1.475	0.789	0.57	0.651	2717	0.1	0.075	1030
1	15	2.6	0.789	0	0.68	0.6895	2711.5	0.05	-0.025	1030

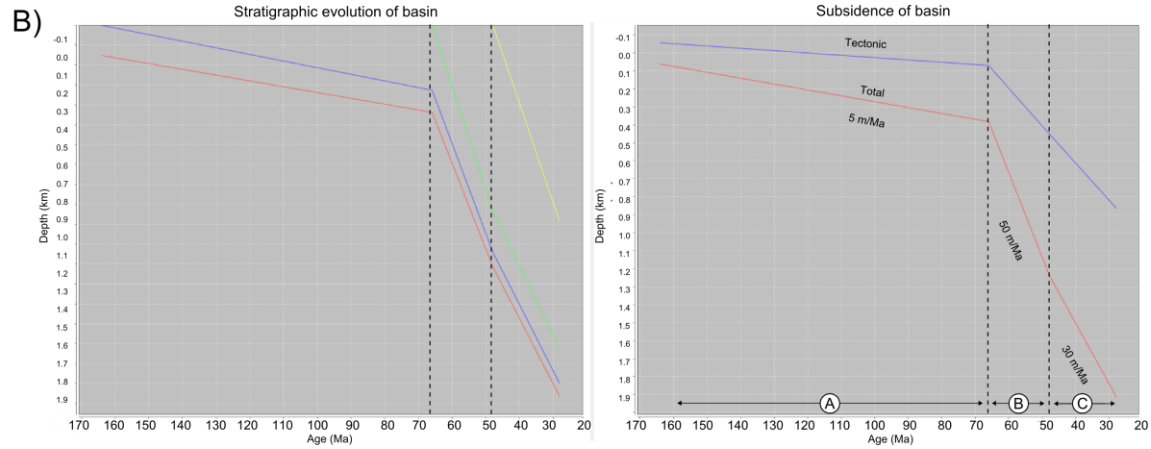

Input data

Units	Clay (%)	Age (Ma)	Depth of unit base (km)	Depth of unit top (km)	Compaction coefficient (km-1)	Surface Porosity (%)	Density (kg/m3)	Paleobathymetry (km)	Eustatic sea level (km)	Sea water density (kg/m3)
4ii	0	164	1.861	1.797	0.71	0.7	2710	0.01	0.1	1030
3	61	66	1.797	1.624	0.588	0.6573	2716.1	0.02	0.075	1030
2	7	48	1.624	0.983	0.696	0.6951	2710.7	0.1	0.075	1030
1	0	28	0.983	0	0.71	0.7	2710	0.05	0	1030

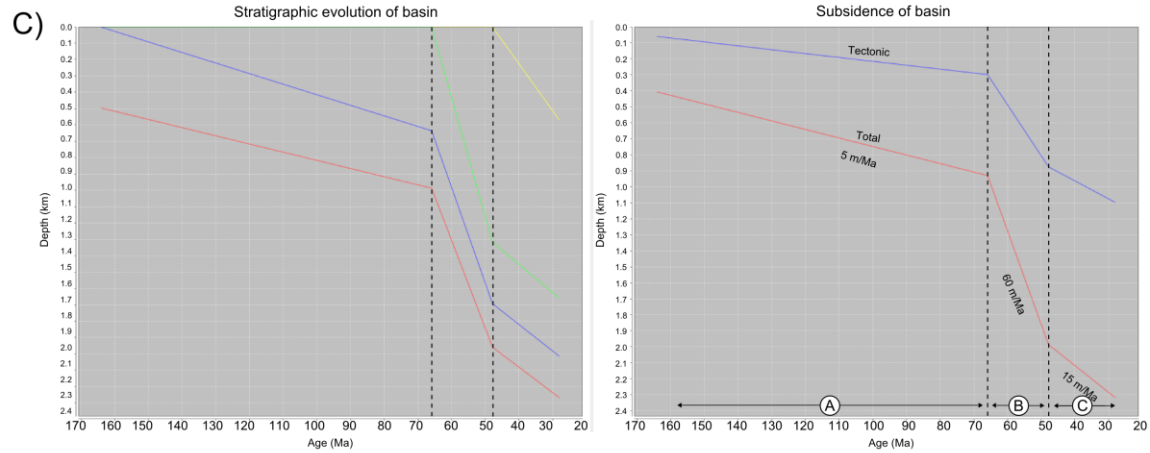

Input data

Units	Clay (%)	Age (Ma)	Depth of unit base (km)	Depth of unit top (km)	Compaction coefficient (km-1)	Surface Porosity (%)	Density (kg/m3)	Paleobathymetry (km)	Eustatic sea level (km)	Sea water density (kg/m3)
4ii	35	164	2.266	2.013	0.64	0.6755	2713.5	0.01	0.1	1030
3	29	66	2.013	1.658	0.652	0.6797	2712.9	0.02	0.075	1030
2	54	48	1.658	0.566	0.602	0.6622	2715.4	0.1	0.075	1030
1	3	28	0.566	0	0.704	0.6979	2710.3	0.05	0	1030

Figure 5.21: Data input and computation for stratigraphic evolution, total and tectonic subsidence from the stratigraphic data of: (A) Owen Bank – A1; (B) Reith Bank – 1; (C) Seagull Shoals – 1 (Generated from CoSub).

The Middle Jurassic onlapping surface (oolitic marker bed) is located below 1500 in all three wells (see Chapter 5.7.2), yet the sea eustatic seal level have not fluctuated more than over 300 m. This confirms that from the Middle Jurassic to recent, the eustatic sea-level rise from deglaciation or any climatic factor was not the main contributing factor that caused the total submergence of the SMc, but rather that the total subsidence was related to thermal contraction of the surrounding Indian Ocean lithosphere into which the SMc became embedded.

5.7 Final analysis and discussions

5.7.1 Depositional system interpretations

The lithological interpretations are relatively similar to those made by previous studies conducted in the Seychelles (e.g. Khanna and Pillay, 1988; Plummer and Belle, 1995, Plummer *et al*., 1998). The base of all three wells in this study comprises almost entirely of claystones that are interpreted as Middle Triassic to Lower Jurassic lacustrine sequences. This gradually changes upwards into highly alternating Lower Jurassic siliciclastics (mudstones and sandstones) which are interpreted as fluvial deposits (fluvial channel migration). The latter then abruptly changes to a Middle Jurassic – Lower Cretaceous sequence which comprises calcareous lithologies; mainly calcareous mudstones, minor sandstones and oolitic limestones which are interpreted as shallow marine deposits at the very base. The next overlying sequence, Upper Cretaceous, comprises of mainly carbonates (limestones) and calcareous claystones, which are then overlain (>500m thick) volcanic deposits (*ca.* 62 -74.7 Ma). The latter sequence is further overlain by Paleocene open marine deposits, predominantly calcareous claystones which gradually changes to almost entirely to a Middle Eocene to recent (Oligocene - Pleistocene) limestone sequence, up to almost the present seafloor. These are interpreted as open marine (carbonate platform). The criteria for the detailed interpretation of the mentioned lithologies as discussed below:

5.7.1.1 Fluvial – overbank/lacustrine – deltaic (Middle Triassic –Early Jurassic)

The fluvial facies in this study forms part of the rift sequences, and they comprise alternations of mainly non-calcareous sandstone, siltstones and claystones (e.g. Nijman and Puigdefabregas, 1978), including minor truncations due to river channel migration within the palaeo-flood plain (e.g. Phillips, 2003). This is a reasonable interpretation for the extensive lower Reith Bank section. River channel migration or meandering likely caused the deposition of alternating sandy fluvial sediments, and subsequent fine mudstone sediments as suspended load when river discharge wanes (e.g. Cant, 1992; Miall, 1992),

evidenced by the highly alternating gamma readings. The dark laminated Middle Triassic claystones also contain of flame structures, convolute bedding, fining upwards conglomeratic sandstones with planar cross beddings, and plant remains. The latter are characteristic of pointbar deposits (Nijman and Puigdefabregas, 1978; Cant, 1992; Miall, 1992; Phillips, 2003). This sequence then changes to more siltstones in the Upper Triassic section and then to more alternating sandstone and claystone in the Lower Jurassic that display fining upward trends in the lithologies. The general increase in the proportion of sands suggests an increase in the energy of the depositional environment and that these sediments are terrestrial in origin (Figure 5.22) (e.g. Nijman and Puigdefabregas, 1978; Cant, 1992; Miall, 1992; Phillips, 2003). This is consistent with the gamma logs as alternating high and low gamma readings and fining upward trends (e.g. Stewart, 1983; Walker, 1984; Cant, 1992). The nature of these sediments' stacking pattern indicates they were probably deposited in active fluvial environment (fluvial channel migration) with possible lacustrine intervals. This is supported by the presence of plant remains and various microspores or pollen species observed through the bio-stratigraphic record, which existed since the Triassic up to the Middle Jurassic boundary (e.g. *Vallasporites ignacii, Aulisporites astigmosus, Aratisporites spp., Duplicisporites verrucosus, Labiipollis granulatus, Parvispinosus sp.*).

Finally, the fluvial system divulged into the ocean via a deltaic system. Deltaic sedimentary stacking patterns display coarsening upwards cycles which are observed in the silt-claystone to sand and is further evidenced by the gamma ray response (Coleman and Gagliano 1964; Walker, 1984; Shepard, 2011). These are best observed from the lower sections of the Owen Bank – A1 and Seagull Shoals – 1 (late Upper Jurassic). For example, in the case of Owen Bank – A1, the alternating clastics (fluvial) display bivalves, foraminiferal remains and two coarsening upward cycles. This is observed in the stacking pattern and gamma ray log towards the top of the sequence. This therefore indicates a marine influence or incursion at the top of this sequence which suggests a change in environment from fluvial to possibly deltaic (Figure 5.22) (e.g. Miall, 1980; Tucker, 2003).

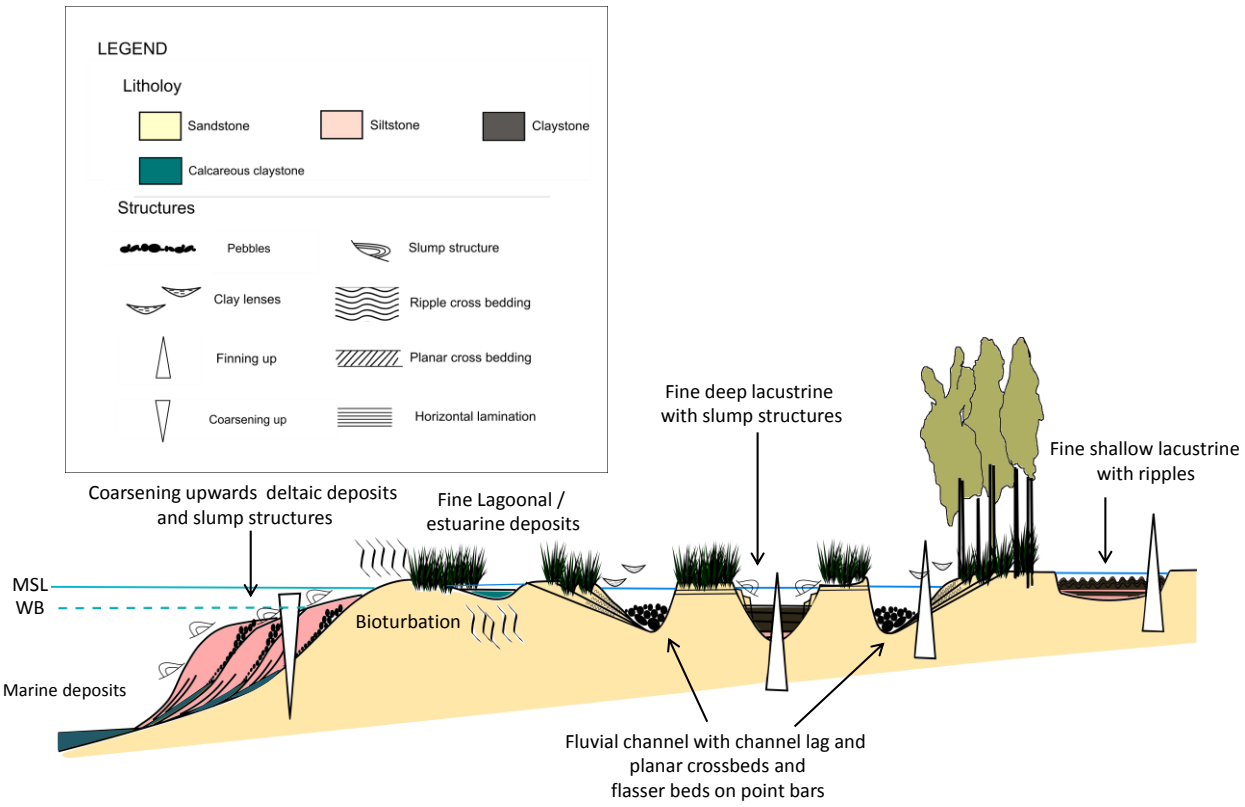

Figure 5.22: Schematic diagram of the interpretation of the paleo-depositional environment illustrating the Fluvial - lacustrine - deltaic facies succession of the three wells of the western shelf of SMc.

Similarly, in the case of Seagull Shoals – 1, the Lower Jurassic sequence is composed of three major coarsening upward cycles, which consist of thick carbonaceous calcareous claystones to sandstone with conglomerate (possibly mouth bars) interbeds and ooliths close to the top. This therefore suggests a coastal marine influence, which is probably deltaic in origin prograding into a marine environment (Figure 5.22). This is further supported by the coarsening upward trends, also seen in the gamma ray logs (e.g. Miall, 1980, Walker, 1984; Tucker, 2003; Higgs *et al*., 2012).

5.7.1.2 Shallow restricted – marginal marine (Middle to Late Jurassic)

The interpreted restricted – marginal marine facies successions comprise calcareous sands, probably lagoonal or estuarine fine deposits. The diagnostic evidence in these sediments for such sheltered depositional includes dense ooliths at base, abundant benthic foraminifera, bioturbation, and abundant of calcareous mudstone deposits with episodic sandstones (Figure 5.23) (e.g. Phillips, 2003; Yubo *et al.*, 2011). These are observed throughout the 3 wells of the study site, but it is most extensively seen in the Owen Bank-A1, because for the other two wells these sequences are thinner (<200m) compared to the

Owen Bank – A1 (>1000m), possibly erosion due to uplifting (tectonism), which is indicated by the seismics as the rotated fault blocks, which caused this sequence to be structurally higher than that of the Owen Bank- A1.

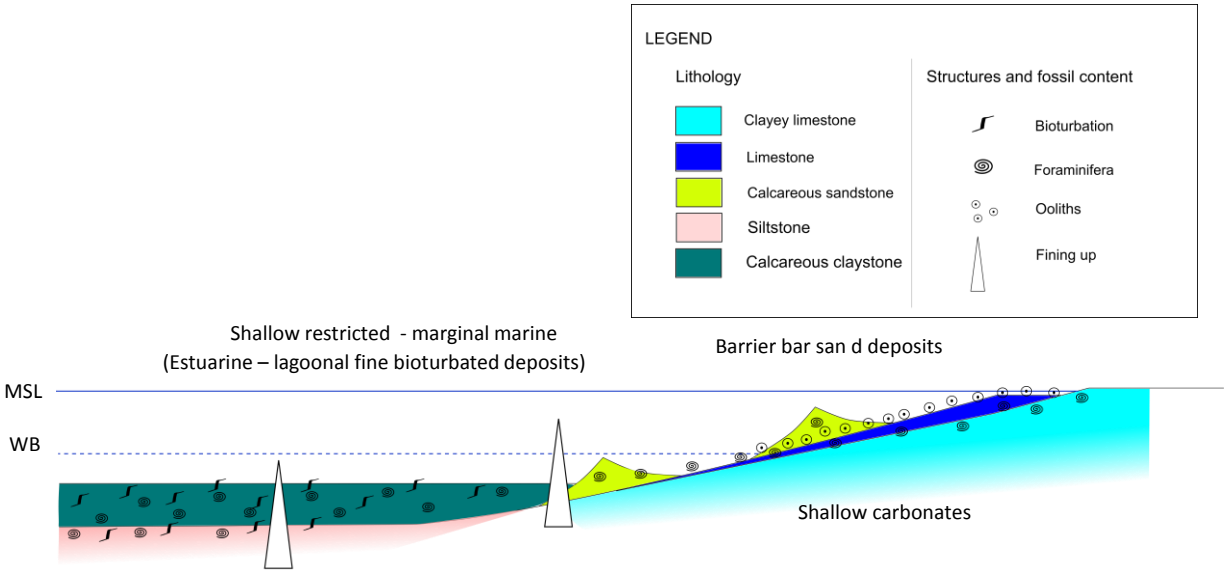

Figure 5.23: Schematic diagram of the interpretation of the palaeo-depositional environment illustrating the restricted – marginal marine facies succession of the three wells of the western shelf of SMc.

This section indicates moderate - low energy sheltered environments and fining upward trends of the successions but also show coarsening upward trends indicating possible barrier bar sands (Yubo *et al*., 2011; Higgs *et al*., 2012). Multiple species of benthic foraminifera exist and the absence of planktonic foraminifera indicates the shallow nature of the depositional environment (Phillips, 2003). The base of this section is marked by the Middle Jurassic unconformity which probably marks the onlap phase as the transgression was initiated. This agrees well with the gamma ray log response shown in the Owen Bank – A1, observed as a gradual increase. The overall increase in the benthic foraminiferal species (e.g. *Lenticulina spp., Haplophragmoides spp., Trocholina spp.*) and dinocysts (e.g. *Areoligera spp., Dinogymnium sp.*) shown in the bio-stratigraphy supports this, as well as dense ooliths at the base, which gradually disappear upwards indicating an increase in water depth.

The general abundance of the terrestrially derived palynomorphs in these sections indicate close proximity to shoreline, hence a marginal marine setting. Furthermore the general increase in abundance of the dinocysts also suggests a deepening in the depositional

environment. This evidence is indicative of a general marine transgression and probable change from restricted - marginal marine (Rameil *et al*., 2000; Phillips, 2003; Yubo *et al*., 2011). The eventual appearance of glauconite at the top of this section suggests a possible shift to inner shelf conditions (e.g. Compton et al., 2009) at the Lower – Upper Cretaceous unconformity. This further supports the transgressive nature of this identified depositional system as it is also shown in the general increase of the gamma readings.

The interpreted shallow marine conditions in these sections of the Middle Jurassic boundary probably originate from the Tethys Sea that intruded into Gondwana (e.g. Higgs *et al*., 2012). This occurred around the time rifting proceeded during the break-up of East and West Gondwana along East Africa (*ca.* 220 -160 Ma) which initiated this marine transgression. This transgressive phase is also recorded in the neighbouring countries such as Ethiopia, Somali, Tanzania, Madagascar and Mozambique (Rakotosolofo *et al*., 1999; Kapilima, 2003). Furthermore, there are equivalent oolitic limestones and evaporates in the main Karoo Basin which form part of the Lower Pindiro evaporates and also in the other Karoo basins of East Africa such as the Kambe Formation (Kapilima, 2003). Similar observations have been made from the Middle Jurassic restricted marginal marine sequence from the Ruvu – Tanga sub-basins of Tanzania (Kapilima, 2003).

5.7.1.3 Shelf – shallow marine (Cretaceous - Paleogene)

The interpreted shelf – shallow marine facies successions comprise carbonate platform limestone and calcareous sands, and marine claystone deposits (Figure 5.24). The diagnostic evidence for the carbonate platform deposits is the high abundance of benthic foraminifera and ostracods, coral and shell fragments, ooliths, calcareous sandstones and thick limestone successions (Jones and Desrochers, 1992; Fournier *et al.*, 2004; Wilson *et al.*, 2012).

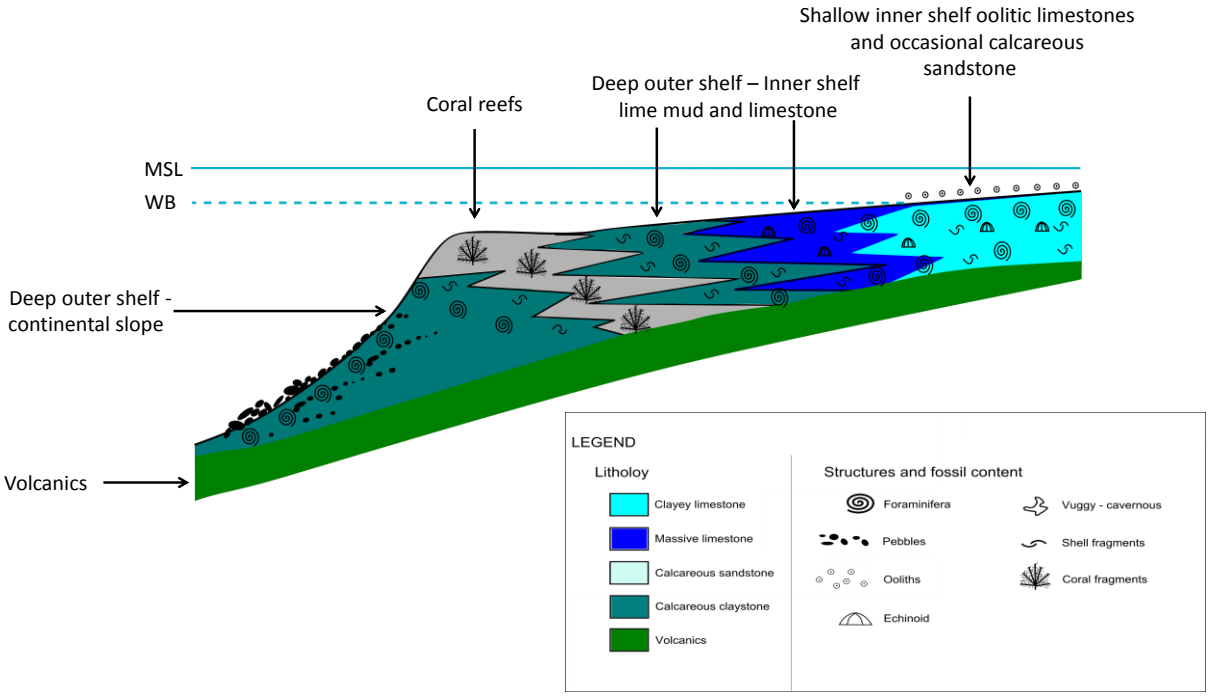

Figure 5.24: Schematic diagram of the interpretation of the palaeo-depositional environment illustrating the Shelf – shallow marine facies succession of the three wells along the western shelf of SMc.

The section starts with Upper Cretaceous massive limestone, followed by a layer of calcareous claystone which gradually grades up into a fairly thick layer of volcanic deposits and igneous layers (>500m). These volcanics are mainly in the form of amygdaloidal-vesicular basaltic lava (Owen Bank – A1 and Seagull Shoals - 1) and crystalline dacite (Reith Bank - 1). The volcanic components of Owen Bank – A1 and Seagull Shoals - 1 also include welded tuffs, volcanic ash and devitrified glass. This mixed volcanic succession originated from sub-aerial volcanic eruptions probably originated from continental separation as indicated by the presence of basaltic lava, or a proto-subduction process along the Amirantes Ridge because of the presence of andesites within the basalts and in the case of Reith Bank -1 as indicated by the presence of dacite. Based on the absolute ages (74.7 ±1.3 Ma, ~62 Ma, ~66.1 ±1.3 Ma) of those volcanics (tuffs) and igneous strata, it can be deduced that these dates fall within the range of the separation of Madagascar from India/Seychelles (*ca.* 82 Ma) and the separation of Seychelles from India (*ca.* 66 Ma) with the eruption of the Deccan trap basaltic lavas that originated from the peak eruption of the Reunion hot-spot at around 65 Ma (Torsvik, 1998; Ashwal *et al.*, 2002; Ganerod *et al.*, 2011; Reeves, 2013; Reeves *et al.*, *in press* 2014).

The bulk of the volcanic sequence from Reith Bank – 1 is crystalline dacite / dacitic lava that indicate violent explosive eruptions which most probably originated from a partial (oceanic – continental) subduction process (e.g. Lajoie and Stix, 1992; Suwa *et al.*, 1994). The andesite intrusions from the base of the volcanic sequence of Owen Bank – A1 also supports a possible partial subduction along the western margin of SMc (Miles, 1982). This in turn probably originated from the anticlockwise rotation when Seychelles and Greater India broke off from Madagascar (*ca.* 84 Ma) (e.g. Fisher *et al.*, 1968; Coffin and Rabinowitz, 1992; Suwa *et al.*, 1994; Plummer and Belle, 1995; Plummer, 1996; Torsvik, 1998, Mukhopadhyay *et al*., 2012; Reeves *et al*., *in press* 2014). This drift phase was accommodated by the transform opening of the Mascarene Basin that further led to ocean spreading. Simultaneously, this led to a partial subduction along the western margin of the SMc (Miles, 1982; Suwa *et al.*, 1994), which ultimately formed a volcanic arc complex (*ca.* 82 Ma), the Amirantes Ridge. The Mascarene spreading centre became extinct when there was a ridge jump as the Deccan eruption initiated the Seychelles/India break-up and the eventual formation of the Carlsberg spreading ridge (*ca.* 66 Ma) (e.g. Coffin and Rabinowitz, 1992; Coffin and Rabinowitz, 1992; Plummer and Belle, 1995; Plummer *et al.*, 1999; Ganerod *et al*., 2011) (see Chapter 2).

Lying unconformably over the volcanic succession is a Paleocene – Middle Eocene sedimentary sequence composed of predominantly calcareous claystones with minor sandstones, and massive limestones at the top, which are occasionally dolomitic. These facies were possibly deposited in a deeper marine environment due to the abundance of the calcareous claystone, most probably beyond the shelf slope or around the shelf slope margin, possibly during the period of high subsidence. These contain planktonic foraminiferal species from Reith Bank – 1 and Seagull Shoals – 1 (e.g. *Globotrunacana coronate, Praeglobotruncana wilsoni, Globotruncana concavata, Hedbergella spp, Globigerinelloides spp*.) which suggest inner to outer shelf environment (e.g. Jones and Desrochers, 1992; Rameil *et al*., 2000). The succession then changes to predominantly limestones which then become vuggy-cavernous at the top. This represents a carbonate platform installation which possibly became sub-aerially exposed at some stage causing dissolution and karstification of the shelf carbonates (e.g. Lüdmann, 2013). There is a high concentration of shell fragments, benthic foraminiferal remains and limestone at the top part of the carbonate platform shelf, along with the occasional bioclastic sandstone layers. This represents a restricted platform interior – open marine shelf, rimmed with marginal sands as

well (e.g. Jones and Desrochers, 1992). This is supported by the occurrence of poorly consolidated calcareous sandstones. Coral fragments represent organic build-ups prior to the shelf slope which is typical of a carbonate platform (e.g. Jones and Desrochers, 1992). Occasional ooids indicates the shallow nature the platform during deposition or drop in MSL. The gamma reading is generally low in these successions and has no apparent trend which is a characteristic nature of carbonate shelf and reef deposits (e.g. Sierra, 1984; Cant, 1992). There are a few random spikes in the gamma reading which probably originate from the occurrence of marine claystones or lime mud. Based on the interpretations it is clear that there is a definite change in facies from continental (fluvial - lacustrine) to marine (shallow – open marine) origin, and there is also a zone of transition between both environments (shallow restricted - marginal marine).

5.7.2 Sequence analysis and regional sequence correlation

Here, a detailed correlation of the seven main stratigraphic sequences is presented, where bounding surfaces have been identified and correlated laterally throughout the three main wells of the study area (Figure 5.25). This local correlation profile (approximately 40 km long) illustrates well the Mesozoic to Cenozoic sequences of the western SMc. In general, the unconformities are modelled as sequence boundaries as well as seismic marker horizons, which have been identified through the well-log correlation. The seismic analyses shows there to be a major rift phase during the Triassic to the Early Jurassic, and a syn-rift phase from the Middle Jurassic to Early Cretaceous. The conformability and thickening of the Late Cretaceous – Paleogene seismic sequences suggest that following the rift phases was a drift phase, with possibly thermal subsidence as the SMc drifted to its current location. This drift phase proceeded until the Seychelles fragment reached the present day isolation (Figure 5.26). The seismic interpretations show that the Mesozoic and Cenozoic sediments of the SMc are dominated by extensional horst and graben structures below the BU, which is below 1.5-2 seconds. These are then overlain by conformable thermal subsidence sequences. These also exhibit a transition from continental siliciclastics to marine sediments within the rift and post-rift sequences (e.g. Plummer and Belle, 1995, Plummer et al., 1998). This is comparable to offshore Madagascar, across the Morondava Basin, also delineated by sequences within rotated fault blocks of the basement and to ultimately marine mudstones and carbonates as the syn-rift and post-rift phases (e.g. Geiger, 2004).

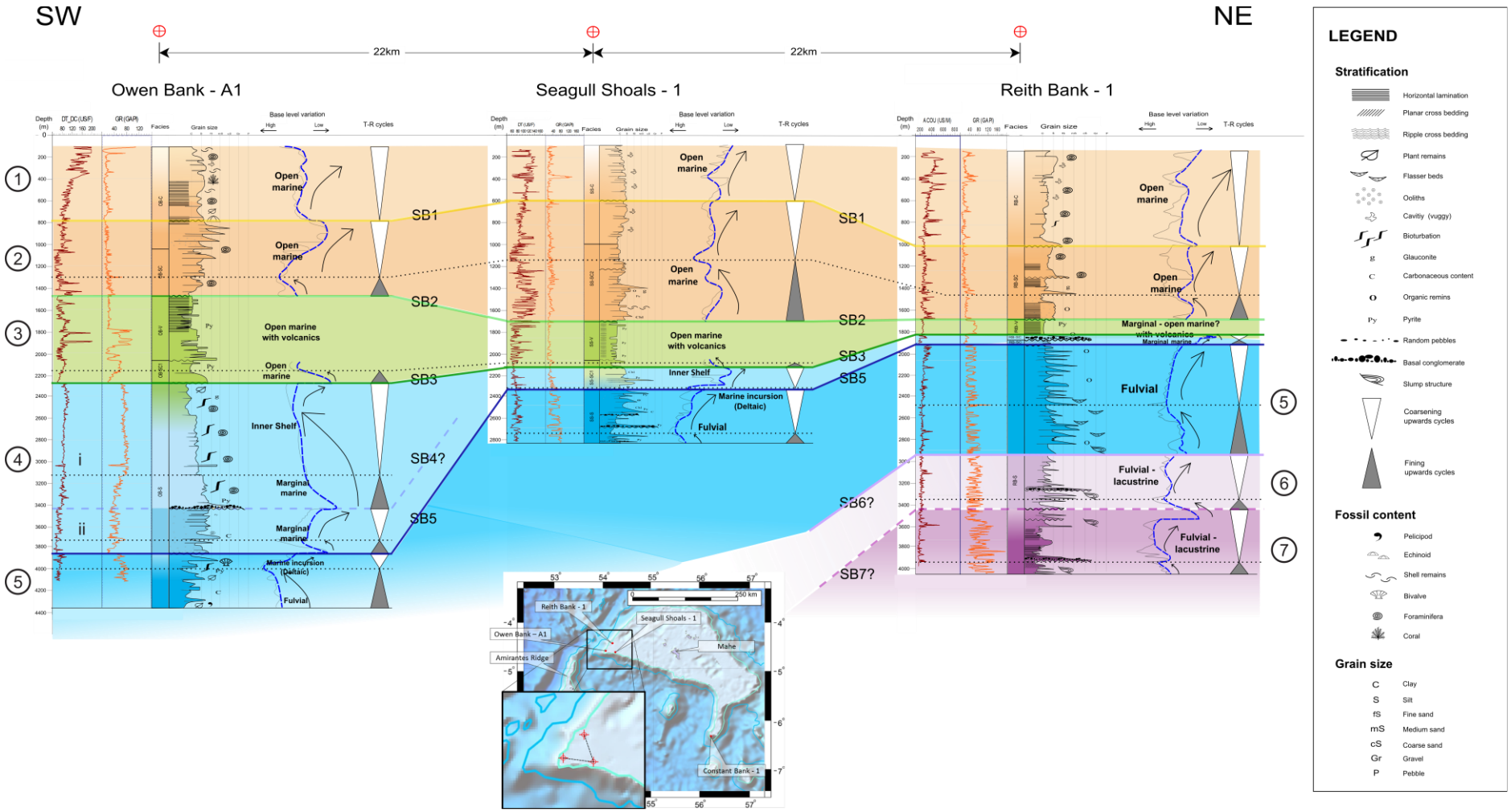

Figure 5.25: Regional sequence-correlation of the Mesozoic and Cenozoic successions of the Owen Bank – A1, Reith Bank – 1 and Seagull Shoals sections of the various sequences (1-7) identified through seismics, bio-stratigraphy and well-logs. The dotted black lines are the MFS that has also been identified within each sequence and used for correlation.

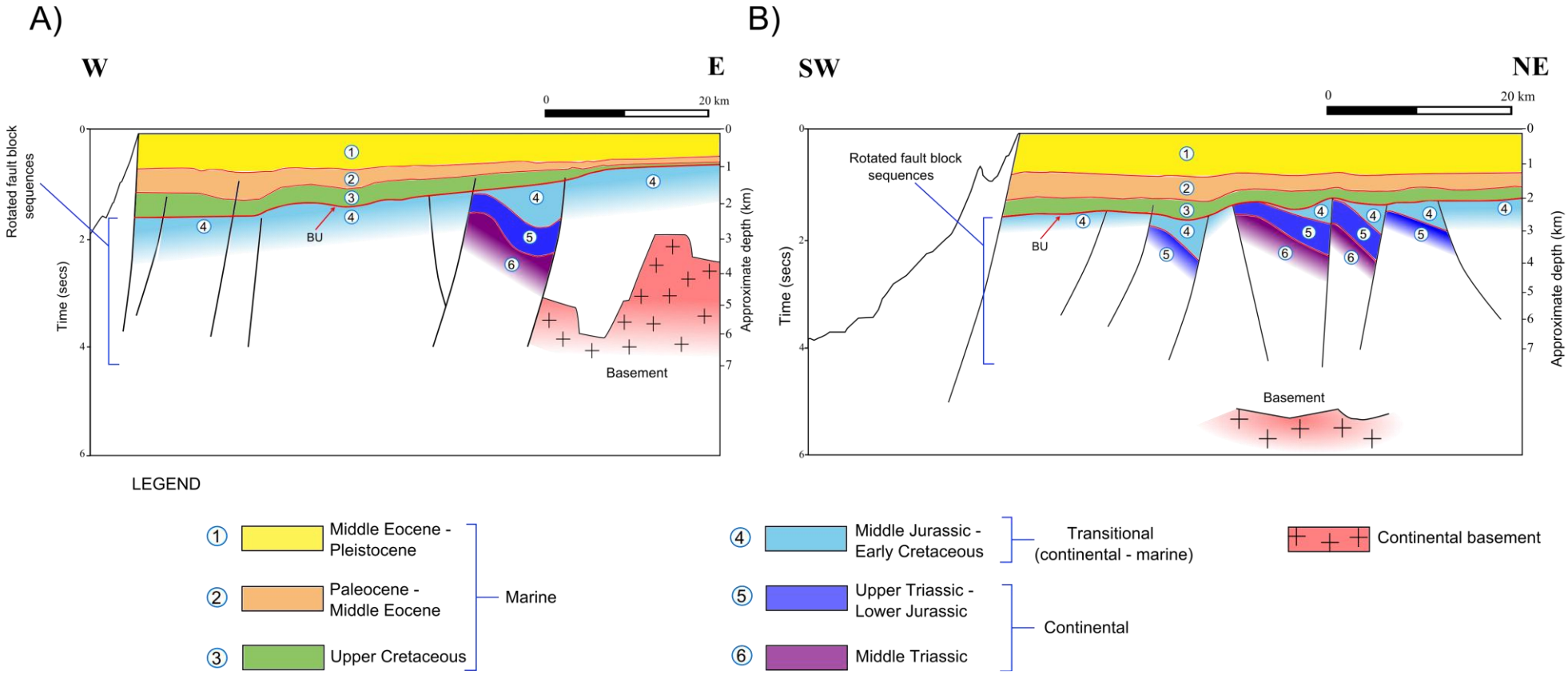

Figure 5.26: Geological interpretations of seismic line A) TCO-106 and B) TCO-115, and the various identified sequences through the correlation of the various identified uncomformities / seismic boundaries which has been correlated with the litho- and bio-stratigraphy. Notice the horst and graben structures which ultimately form part of the rotated fault block also include the rotated continental rift Sequences 5 -6, representing East and West Gondwana break-up (180 Ma). Sequence 4 forms part of the syn-rift phase and represent the transitional facies from continental to marine and the drift phase between East and West Gondwana. Sequences 3 -1 are strictly marine, whereby Sequence 3 represents both rifting and break-up of the SMc from first Madagascar (84 Ma) and second from India (65 Ma). Sequences 2 -1 represents the final drift phases of SMc to its present isolated location.

5.7.3 Subsidence history of the Seychelles Microcontinent

The main identified sequences correspond to three episodes of subsidence that occurred during; Middle Jurassic – Late Cretaceous – Middle Eocene – recent (Figure 5.27). Subsidence episode 1: Starts in the Bajocian, where a major unconformity coincides with the break-up of East and West Gondwana (*ca.* 160 Ma; Torsvik, 1998; Jokat *et al.,* 2009; Reeves, 2013; Reeves et al., 2014). This resulted in a thermal subsidence with average subsidence rate of 5-20 m/Ma. This further resulted in a major transgression across the East African passive margin (Figure 5.27). A subsidence rate of 5-20m/Ma is considered as extremely low which compares to the rate of large intracratonic basins, such as the Paleozoic Russian platform or the Ordovician North Gondwana; Subsidence episode 2: The overall subsidence accelerated from 5-20 m/Ma to 35-60 m/Ma at the end of the Cretaceous (K-Pg boundary) when a major unconformity coincides with the break-up of SMc from India (*ca.* 66 Ma; Torsvik, 1998; Jokat *et al.*, 2009; Reeves, 2013; Reeves et al., 2014). This compares to a mature passive margin with subsidence rates between 50 and 120 m/Ma. This lasted for about 20 Ma from the Paleocene to the Middle Eocene (Figure 5.27); Subsidence episode 3: The rate of subsidence reduced to about 10-30 m/Ma (*ca.* 48 Ma) possibly as a consequence of the ridge effect introduced by the formation of the Carlsberg Ridge around the Lutetian or the interaction of the Reunion plume when it was beneath the Carlsberg Ridge (*ca.* 55 Ma) upon the final opening stages of the Indian Ocean or the Himalayan-Tibet Alpine Orogeny (*ca.* 50 Ma) (Coffin and Rabinowitz, 1992; Plummer and Belle, 1995; Plummer et al., 1999; Ganerod, 2011; Reeves, 2013; Reeves et al., 2014) (Figure 5.27).

Throughout the subsidence history of SMc (Figure 5.27) it is observed that the subsidence from the Owen Bank – A1 is generally greater. A probable reason for this is that this well has always been located more offshore than the other two wells, which includes more water depth, more accommodation space, and ultimately more sediments hence more subsidence (Figure 5.28).

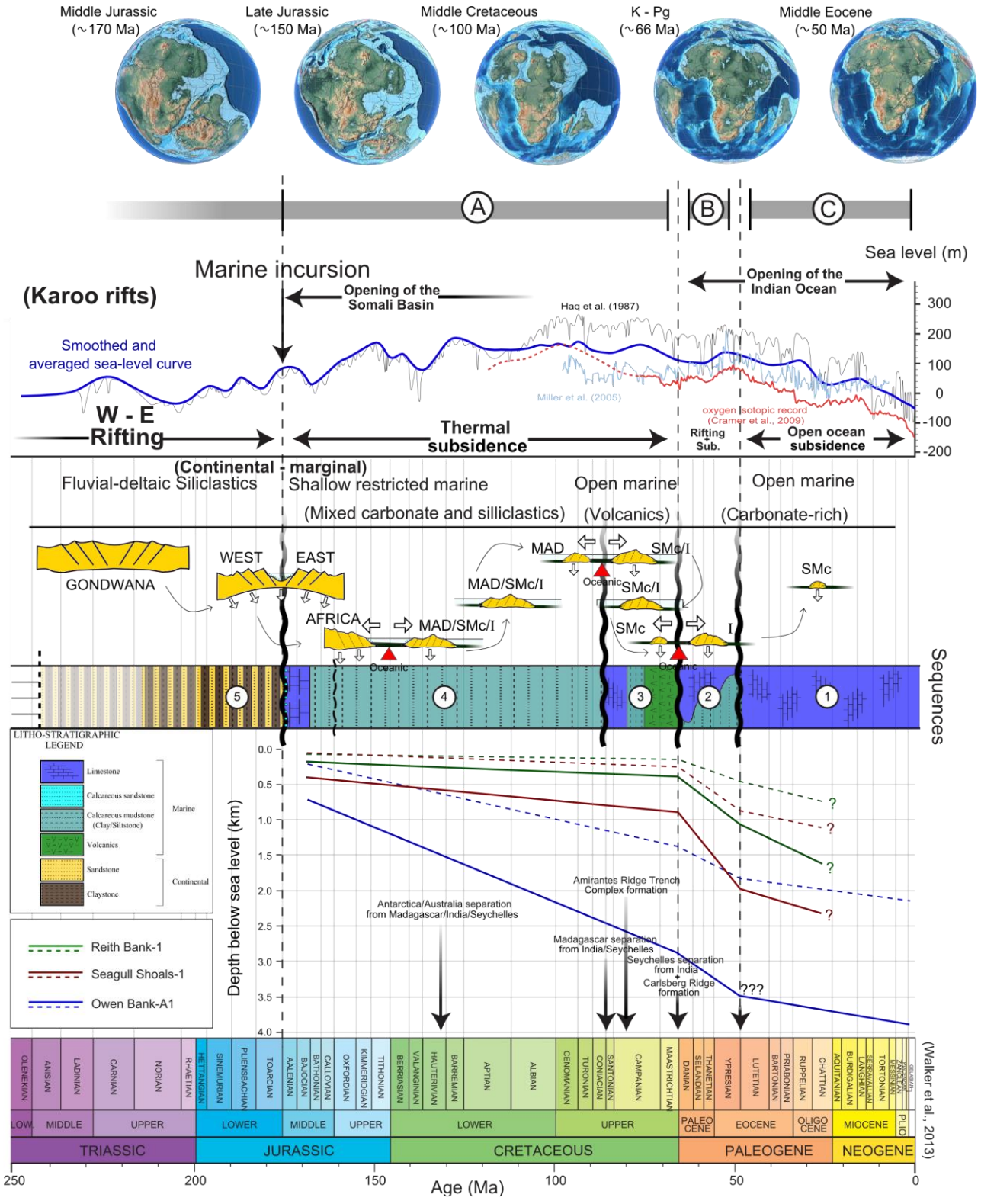

Figure 5.27: Total subsidence (solid) and tectonic subsidence (dashed) curves for the Owen Bank – A1 (blue), Reith bank – 1 (red) and Seagull Shoals - 1 (green) section. The curves show three main episodes of subsidence; A, B and C. Notice the increased rate in subsidence from episode A to B and the reduction to episode C in all three curves. Notice the effect of the separation Madagascar from India/SMc is not recorded.

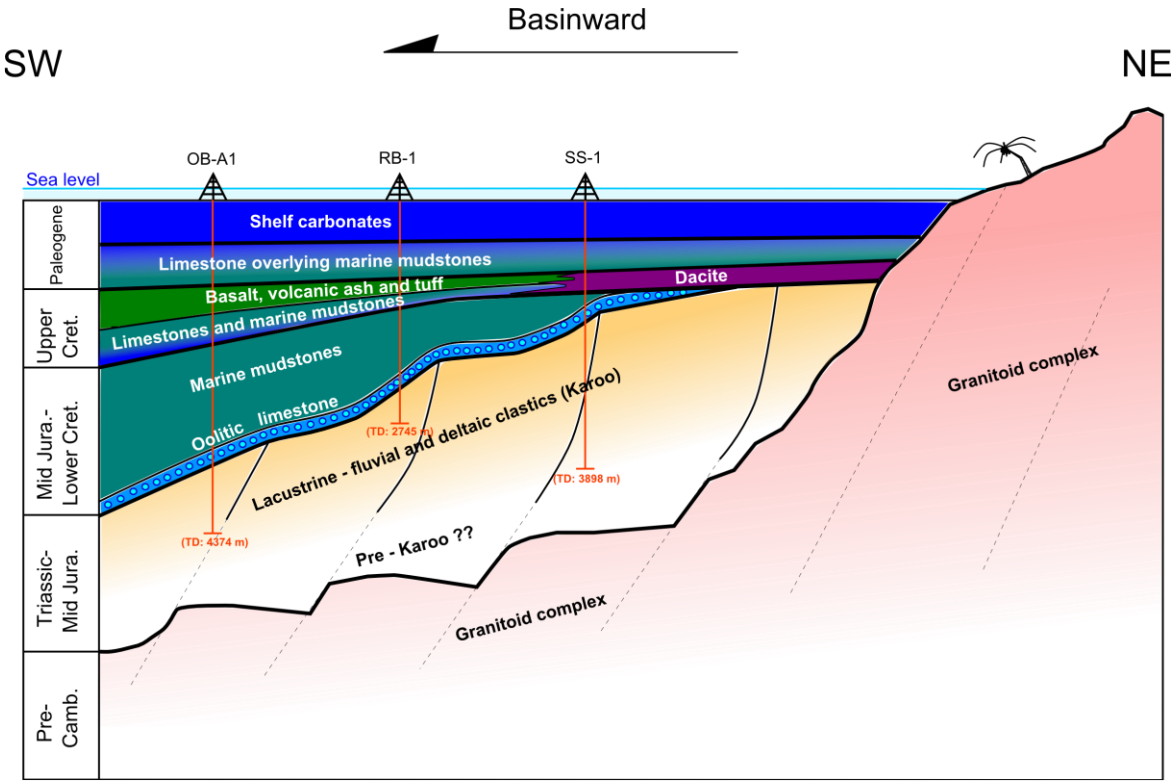

Figure 5.28: Schematic general offshore stratigraphy through the projected wells (OB-A1: Owen Bank – A1; RB-1: Reith Bank – 1; SS-1: Seagull Shoals - 1) illustrating today's western margin of the SMc.

Since the break-up of Gondwana, the evolution of SMc is therefore divided into two stages: 1) Post-rift thermal subsidence that involved thermal contraction of the lithosphere by heat conduction followed by the slow subsidence without faulting after the break-up of East and West Gondwana following the eruption of the Karoo LIP (Subsidence episode A); 2) Syn-rift followed by post-rift thermal subsidence (Subsidence episode B and C) which involved stretching of continental lithosphere (associated with block faulting), crustal thinning, accelerated subsidence, upwelling of asthenosphere and an enhanced temperature gradient (e.g. Deccan LIP) as SMc broke off from India followed by slow subsidence due to lithospheric thickening and the influence of the Carlsberg Ridge.

Chapter 6. Conclusions

The evolution of SMc has been interpreted through the analysis of sedimentary records and the seismic sequences, and its history of extensional tectonics was analysed through interpretation of the seismic profiles and the well-log correlations.

Prior to the East African Orogeny, Neoproterozoic granites now exposed in the Seychelles (e.g. Mahe, Praslin and La Digue) were emplaced along the flank of East Africa (*ca.* 755-750 Ma) during the formation of Gondwana. Shortly after, significant uplift and exhumation of these Neoproterozoic granites occurred as the SMc became part of a Central Gondwana peneplanation surface. From the middle Palaeozoic onwards, rifting episodes led to the eventual break up of Gondwana, into East and West Gondwana, and the episodic opening of the Indian Ocean as further fragmentation of Eastern Gondwana took place. Fragmentation involved three major rift phases, *viz.*: 1) Middle Triassic – Middle Jurassic (Rift I), associated with the "Karoo rifts" and break-up between [India-Madagascar-Seychelles] and East Africa, followed by thermal subsidence after the eruption of the Bouvet plume; 2) Middle Jurassic – Early Cretaceous (Rift II), associated with the drifting of [India-Madagascar-Seychelles] and the rifting of Madagascar from [India-Seychelles]; 3) Late Cretaceous (Rift III), associated with the rifting and final break-away of the SMc from India, followed by thermal subsidence after the eruption of the Reunion hotspot. Thereafter, the SMc experienced its final submergence during the cooling of the surrounding oceanic lithosphere, as it "drifted" to its current position in the western Indian Ocean, as a "lone ranger continental micro-fragment" that was once part of Gondwana.

The various rift margins provided significant accommodation space to accumulate thick Triassic (*ca.* 1500 m), Jurassic (*ca.* 100 – 1500 m), Cretaceous (*ca.* 100 – 800 m) and Cenozoic (*ca.* 1700) sequences. In the SMc, identification of the seven major sequences was determined by correlating the well data, logs and the seismic data, whose bounding surfaces were identified from the seismic data analysis. Although the seismic data is increasingly chaotic with depth due to the low seismic signal to noise ratio, seismic bounding surfaces were identified and correlated with those from the seismic profile at shallower depths (< 1.5 seconds). In the deeper parts of the seismic profiles (1.5- 3 seconds), because of increasing attenuation with depth, the sequence boundaries do not correlate with the well-logs and bio-markers. Thus, the lower bounding surfaces were estimated only by correlating the bio-markers with the well-logs.

The main BU identified, referred as SB3, correlates with the Lower Cretaceous bio-marker. This BU probably formed as a consequence of the separation of Madagascar from India/Seychelles (*ca*. 84 Ma). It is clear though that the sequences below the Paleogene sequences are those that have been affected most by the rift tectonism (Sequences 4 - 7), with distinct rotated fault blocks as identified on the seismic profiles. It is observed that the rotated fault blocks below the Upper Cretaceous are structurally higher in Reith Bank – 1 and Seagull Shoals – 1 than in the Owen Bank – A1. This is consistent with the interpretation that the Lower Cretaceous sequence was eroded from the Reith Bank – 1 and Seagull Shoals – 1 sections, possibly during uplift as a result of rifting. A deep seismic reflector is also detected at depths of around 3-4 seconds from seismic profile TCO-106, and at 5 seconds on seismic profile TCO-115. These reflectors possibly represent the top of the basement granite.

The rift sequences from Triassic to Early Jurassic comprise predominantly of continental sediments. These strata are probably equivalent to the Karoo rocks of the East Africa and Madagascar margins. The oldest sedimentary rocks identified on the SMc are Middle Triassic organic rich claystones (Sequence 7, Rift I), which grade upwards into alternating Upper Triassic sandstones and mudstones (Sequence 6, Rift I), followed by upward coarsening Lower Jurassic mudstones to sandstone units (Sequence 5, Rift I). These sequences are interpreted as lacustrine facies that evolved into fluvial channel migration facies, and finally into progradational delta front facies. These continental sequences are capped by a regional unconformity (SB4) and are in turn overlain by a Middle Jurassic to Lower Cretaceous marine to near shore/restricted marginal sequence starting with an oolitic limestone horizon seen in all three wells. This sequence comprises calcareous siltstones and claystones, with limestones and minor calcareous sandstones (Sequence 4) that represents a thermal subsidence sequence after Rift I. This sequence is part of the syn-rift deposition, capped by the BU (SB3). Overlying this BU are Upper Cretaceous strata, including a combination volcanic rocks. From Owen Bank – A1 and Seagull Shoals – 1, these strata comprise tuff and ash beds, and basaltic lava that overlie the Upper Cretaceous marine strata. In the Reith Bank – 1, a dacite layer, possibly a sill, was identified (Sequence 3, Rift II and III). The marine strata underlying the volcanic layer are predominantly limestones, calcareous claystones and sandstones. Lying unconformably over the volcanic layer are post-rift – thermal subsidence sequences that are separated by another regional unconformity (SB2) that is linked to the rifting of the SMc from India. This sequence

comprises predominantly of Paleocene marine claystones. Above these claystones are mainly limestones of Paleocene to middle Eocene (Sequence 2) which are then separated by a final unconformity (SB1) above which are almost entirely shelf limestones of middle Eocene to recent age exist (Sequence 1).

The seismic interpretation from this study shows that the three top-most sequences thin towards the eastern shelf-edge of SMc (basin edge), similar to sequences observed along the Madagascar margin and over the Beira High of Mozambique. This implies that before Gondwana break-up (*ca.* 180 Ma), the Diego Basin extended as far as the western shelf of SMc, where the Karoo sediments were also deposited across the SMc (Figure 6.1). It is therefore proposed in this study that most of the eastern SMc comprises predominantly granite basement, which is now overlain only by thin Cenozoic carbonates because unlike Madagascar, the SMc eventually became submerged. Most of the other Neoproterozoic granitic islands are situated on the north-central part of SP, consistent with the down throw of the basement on the western shelf, similar to Madagascar, forming a palaeo-rifted margin alongside a terrestrial margin in the Karoo rifts (Figure 6.1).

Backstripping and subsidence analysis quantifies the 3 stages of subsidence following the break-up of East and West Gondwana; Phase A: Slow subsidence (*ca.* 5-20 m/Ma), after rift Sequence 5, from the Middle Jurassic to the Upper Cretaceous that terminated during a major marine transgression during ingression of the Tethys Sea between East Africa and [Madagascar-Seychelles-India]. This created marine conditions and the subsequent deposition of Sequences 4 and 3. Phase B: Accelerated subsidence (*ca.* 35-60 m/Ma) recorded throughout the Paleocene to the middle Eocene leading to deeper marine conditions and the subsequent deposition of Sequence 2. Phase C: Reduced subsidence (*ca.* 10-30 m/Ma) following the interaction between the Reunion plume and the Carlsberg Ridge (*ca.* 55 Ma). This possibly introduced a reduction in the rate of subsidence and the subsequent deposition of Sequence 1 as the SMc drifted and thermally subsided to its submerged present location, and that is now dominated mainly by marine carbonates.

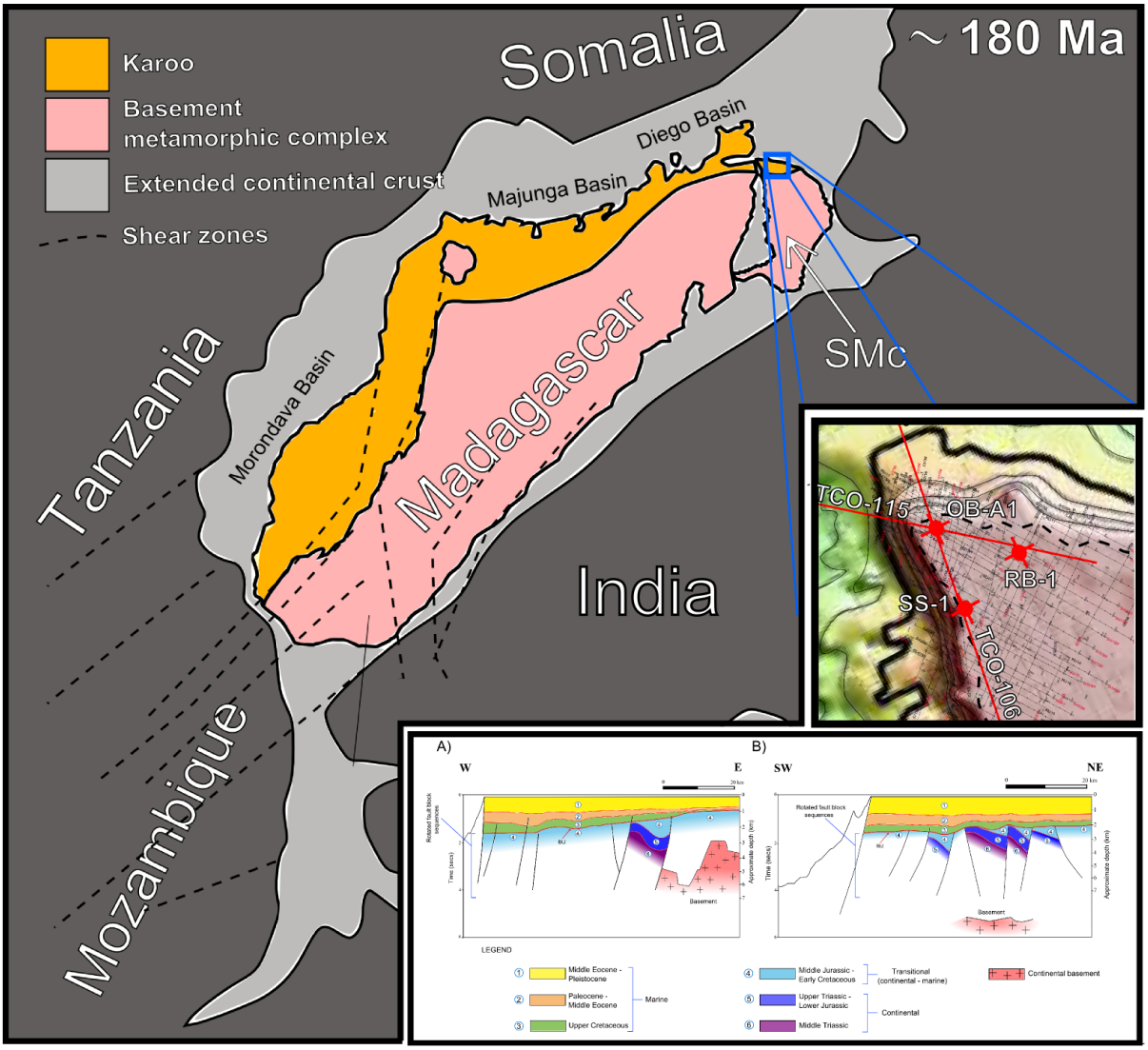

Figure 6.1: Central Gondwana reconstruction at ca. 180 Ma, highlighting the palaeo-position of Madagascar and the SMc. Notice the extension of the Diego Basin into SMc indicating where the Karoo sediments were deposited. The wells of the study site area shown by the red circles: OB-A1 = Owen Bank – A1; RB-1 = Reith Bank – 1; SS-1 = Seagull Shoals – 1. The two seismic profiles analysed in this study are shown by the solid red lines (A: TCO-106 and B: TCO-115) (Source: Modified from Reeves, 2013 and; the Global Topography for Google Earth and Satelite Geodesy by Becker et al., 2009 and Smith et al., 1997).

The effects of the Madagascar and Seychelles/India separation are not observed in the subsidence analysis, possibly because it involved transcurrent-rotational movement between the two plates over a short period of time. It is possible that the counter clockwise rotation of India/Seychelles was relatively faster than that of Madagascar upon separation. This probably resulted in the formation of a proto-subduction zone along the western margin of SMc, hence the origin of the Amirantes Trench and Ridge Complex in the form of a volcanic arc. This is interpreted as a Mascarene post-rift phase that ended with the rifting between

the Seychelles and India, and the subsequent eruption of the Reunion plume and the formation of the Carlsberg Ridge. This rifting episode is well observed through the subsidence analysis as an acceleration in the subsidence rate. Shortly after this the Mascarene spreading ridge became extinct and experienced a ridge jump to accommodate the formation of the Carlsberg Ridge. Subsidence was likely reduced at that time because of the interaction between the Carlsberg Ridge and the Reunion plume. As the Seychelles drifted away from India it became totally submerged due to accelerated thermal subsidence as it converted from a continental shelf to a stand-alone bank surrounded by oceanic lithosphere. Thereafter the SMc accumulated mostly carbonates with only few marine clastics when it was closer to India as seen in the Paleocene – Middle Eocene sequence. The overall tectonic subsidence provided accommodation space that allowed the accumulation of over 500 m of shallow-water platform carbonates during most of the Paleogene.

The data presented in this thesis on the Seychelles has improved the understanding of the history of the opening of the Proto-Indian Ocean along the eastern margin of Africa. It may be confirmed that SMc was part of an extensional basin which was connected with the Somali Basin and thereby to the coast of East Africa, as it relates well to seismic sections of coastal Mozambique and the subsurface lithology of Madagascar and Ethiopia. The tectonic history is clearly reflected in changes of the litho-facies preserved on the SMc, from terrestrial to marine sedimentary sequences, typical of the sedimentary changes along other passive margins and rift basins flanking the Indian Ocean that emerged during the break-up of Gondwana, for example offshore Madagascar, Mozambique, Tanzania, Somalia and Ethiopia. In the process, the SMc experienced significant subsidence that was interrupted by rifting episodes of Madagascar from SMc/India and the SMc from India. These rift phases affected the rates of thermal subsidence, but eventually caused the SMc to become fully submerged.

References

Adam, L., Batzle, M., Lewallen, K. T., and van Wijk, K. 2009. Seismic wave attenuation in carbonates. *Journal of Geophysical Research*, 114, p.1-14.

Allen, P.A., and Allen, J.R., 2005. *Basin Analysis: Principles and applications*. Second edition. Wiley-Blackwell, 560pp.

Amante, C. and B.W. Eakins, 2009. ETOPO1 1 Arc-Minute Global Relief Model: Procedures, Data Sources and Analysis. NOAA Technical Memorandum NESDIS NGDC-24. *National Geophysical Data Center, NOAA*. doi:10.7289/V5C8276M.

Amoco Seychelles Petroleum Company. 1981a. Owen Bank - No.A1 Well: Final Geological Report, Seychelles Western Shelf. *Unpublished Report*, 15pp.

Amoco Seychelles Petroleum Company. 1981b. Reith Bank - No.1 Well: Final Geological Report, Seychelles Western Shelf. *Unpublished Report*, 24pp.

Amoco Seychelles Petroleum Company. 1981c. Seagull Shoals - No.1 Well: Final Geological Report, Seychelles Western Shelf. *Unpublished Report*, 20pp.

Ashwal, L.D., Demaiffe, D. and Torsvik, T. H. 2002. Petrogenesis of Neoproterozoic Granitoids and Related Rocks from the Seychelles: the Case for an Andean-type Arc Origin. *Journal of Petrology*, 43(1), p.45-83.

Baker, B.H. 1963. Geology and Mineral resources of the Seychelles Archipelago. *Geological Survey of Kenya Memoir*, 3, 140pp.

Becker, J.J., Sandwell, D.T., Smith, W.H.F., Braud, J., Binder, B., Depner, J., Fabre, D., Factor, J., Ingalls, S., Kim, S-H., Ladner, R., Marks, K., Nelson, S., Pharaoh, A., Trimmer, R., Von Rosenberg, J., Wallace, G., and Weatherall, P. 2009. Global Bathymetry and Elevation Data at 30 Arc Seconds Resolution: SRTM30_PLUS, *Marine Geodesy*, 32:4, 355-371, DOI:10.1080/01490410903297766

Bhattacharya, J.P., and Walker, R.G. 1992. Deltas. In:Walker, R.G., and James, N.P. (Eds.), *Facies Modes: Response to Sea-level change*. Geological Association of Canada, p.157-177.

Blackburn, T.J., Olsen, P.E., Bowring, S.A., McLean, N.M., Kent, D.V., Puffer, J., McHone, G., Rasbury, T. and Et-Touhami, M.. 2013. Zircon U-Pb

Geochronology Links the End-Triassic Extinction with the Central Atlantic Magmatic Province. *Science*, 340, p.941–945.

Brown, L.F. and Fisher, W.L. 1977. Seismic-stratigraphic interpretation of depositional systems: examples from the Brazilian rift and pull-apart basins. In: *Seismic Stratigraphy - Applications to Hydrocarbon Exploration*. C.E. Payton (ed.). American Association of Petroleum Geologists, Memoir, 26, p.213-248.

Campanile, D., Nambiar, C.G., Bishop, P., Widdowson, M. and Brown, R. (2007) Sedimentation record in the Konkan-Kerala Basin: implications for the evolution of the Western Ghats and the Western Indian passive margin. *Basin Research*, 20(1), p.3-22.

Cant, D.J. 1992. Subsurface facies analysis. In: Walker R.G. and. James N.P (Eds.), *Facies Models, Response to Sea-level Changes*. Geological Association Canada, p.27-45.

Catuneanu, O., Wopfner, H., Eriksson, P.G., Cairncross, B., Rubidge, B.S., Smith, R.M.H., Hancox, P.J., 2005. The Karoo basins of south-central Afri*ca. Journal of African Earth Sciences*, 43, p.211–253.

Catuneanu, O., Abreu, V., Bhattacharya, J.P., Blum, M.D., Dalrymple, R.W., Eriksson, P.G., Fielding, C.R., Fisher, W.L., Galloway, W.E., Gibling, M.R., Giles, K.A., Holbrook, J.M., Jordan, R., Kendall, C.G. St.C., Macurda, B., Martinsen, O.J., Miall, A.D., Neal, J.E., Nummedal, D., Pomar, L., Posamentier, H.W., Pratt, B.R., Sarg, J.F., Shanley, K.W., Steel, R.J., Strasser, A., Tucker, M.E., Winker, C., 2009. Towards the standardization of sequence stratigraphy. *Earth-Science Reviews*, 92, p.1–33.

Catuneanu, O., Galloway, W.E., Kendall, C.G.C., Miall, A.D., Posamentier, H.W., Strasser, A. and Tucker, M.E. 2011. *Sequence Stratigraphy: Methodology and Nomenclature. Newsletters on Stratigraphy*, 44(3), p.173–245.

Chang-Seng, D. and Guillande, R. 2008. *Disaster risk profile of the Republic of Seychelles*. United Nation Development Programme. 131pp.

Cloetingh, S. and Kooi, H. 1989. Tectonics and sea-level changes: a reappraisal in J. Collinson (Ed.), *Correlation in Hydrocarbon Exploration*, Graham and Trotman, London, p.3-11.

Cochran, J.R. 1983. Effects of finite rifting times on the development of sedimentary basins, *Earth and Planetary Science Letters*, 66, p.289-302.

Coffin, M.F. and Rainowitz, P.D. 1992. The Mesozoic East African and Madagascan continental Margins: Stratigraphy and Tectonics. In: Watkins, J., Zhiqiang, F. and McMillen, K.J., (Eds.), *Geology and Geophysics of Continental Margins, American Association of Petroleum Geologists Memoir*, 53, p.207-246.

Coleman, J.M. and Gagliano, S.M. 1964. *Cyclic sedimentation in the Mississippi River deltaic plain*. Gulf Coast Association of Geological Societies Transactions, 14, p.67-80.

Compton, J.S. and Wiltshire, J.G. 2009. Terrigenous sediment export from the western margin of South Africa on glacial to interglacial cycles. *Marine Geology*, 266, p.212–222.

Damuth, J.E. and Johnson, D.A., 1989. Morphology, sediments and structure of the Amirante trench, western Indian Ocean: implications for trench origin. Marine and Petroleum Geology, vol. 6, pp. 232-242.Dalrymple, R.W. 1992. Tidal depositional systems. In: Walker, R.G., and James, N.P. (Eds.), *Facies Models: Response to sea-level change*. Ontario: Geological Association of Canada, p.195-218.

Dalrymple, R.W., and Choi, K. 2007. Morphologic and facies trends through the fluvial–marine transition in tide-dominated depositional systems: A schematic framework for environmental and sequence-stratigraphic interpretation. *Earth-Science Reviews*, 81(3–4), p.135–174.

Dauteuil, O., Robin, C., Guillocheau, F., Linol, B., Calvez, G., and Moreau, F. 2014. Basin Subsidence Quatification: Impacts of Backstripping and Geological Constraints. *Basin Research, in press.*

de Wit, M.J., Jeffery, M., Berg, H, and Nicolayson, L.O., 1988. Geological Map of sectors of Gondwana reconstructed to their position ~150 Ma (with explanatory notes), scale 1:1.000.000. *Tulsa: American Association of Petroleum Geologist.*

de Wit, M.J., and Ransome, I.G.D., 1992. Regional inversion tectonics along the southern margin of Gondwana. In: de Wit, M.J., Ransome, I.G.D., (Eds.), *Inversion tectonics of the Cape Fold Belt, Karoo and Cretaceous Basins of Southern Africa.* Rotterdam: A.A. Balkema, p.15-20.

de Wit, M.J. 2003. Madagascar: Heads it's a Continent, Tails it's an Island. *Annual Review of Earth and Planetary Sciences*, 31, p.213-248.

Douglas, J.C. 1992. Subsurface Facies Analysis. In: Walker, R.G. and James N.P., (Eds.) *Facies Models: Response to sea-level change*, Geological Association of Canada, p.27-45.

Du Toit, A.L. 1937. *Our Wandering Continents*. Oliver and Boyd , U.K., London.

Dutta, T., Mukerji T. and Mavko, G. 2008. How Does Carbonate Cementation In Sandstones Affect Seismic Response? *Society of Exploration Geophysicists Annual Meeting*, 9-14 November, Las Vegas, Nevada.

Eagles, G.and Hoang, H.H. 2013. Cretaceous to present kinematics of the Indian, African and Seychelles plates. *Geophysical Journal International*. p.1-14

Emery, D. and Myers, K.J. 1996. *Sequence Stratigraphy*, Blackwell Science, Oxford, 297pp.

Enterprise Oil. 1995. *Geological Completion Report: Constant Bank – 1*. Unpublished Report, p.1-22.

Fournier, F., Montaggioni, L., and Borgomano, J. 2004. Paleoenvironments and high-frequency cyclicity from Cenozoic South-East Asian shallow-water carbonates: a case study from the Oligo-Miocene buildups of Malampaya (Offshore Palawan, Philippines). *Marine and Petroleum Geology*, 21, p.1–21.

Fisher, L.F., Engel, C.G. and Hilde, T.W.C. 1968. Basalts dredged from the Amirantes Ridge, Western Indian Ocean. *Deep Sea Research*, 15, p.521-534.

Franke, D. 2013. Rifting, lithosphere breakup and volcanism: Comparison of magma-poor and volcanic rifted margins. *Marine and Petroleum Geology* , 43, p.63-87.

Ganerod, M., Torsvik, T.H., Van Hinsbergen, D.J.J, Gaina, C., Corfu, F., Werner, S., Owen-Smith, T.M., Ashwal, L.D., Webb, S.J. and Hendriks, B.W.H. 2011. Palaeoposition of the Seychelles microcontinent in relation to the Deccan Traps and the Plume Generation Zone in Late Cretaceous –Early Palaeogene time. *Geological Society, London, special Publications*, 357, p.229-252.

Geiger, M. 2004. Sedimentary and Stratal Paterrsn in the Jurassic Successions of Western Madagascar: Facies, Stratigraphy, and Architecture of Gondwana Break-up and Sequences. *PhD thesis*, University of Bremen, 145p.

Gibbons, A.D., Whittaker, J.M. and Müller, R.D. (2013). The breakup of East Gondwana: Assimilating constraints from Cretaceous ocean basins around India into a best-fit tectonic model. *Journal of Geophysical Resources: Solid Earth*, 118, p.1–15.

Grandcourt, E.M. 1995. *Coastal Profile of Beau Vallon, Technical Report*. Seychelles Fishing Authority. 66pp.

Haq, B.U., Hardenbol, J., and Vail. P.R. 1987. Chronology of fluctuating sea levels since the Triassic (250 million years ago to present). *Science,* 235, p.1156–1167.

Harris, C. and Ashwal, L. D. (2002). O and H isotope composition of granites and related rocks from the Seychelles. *Contributions to Mineralogy and Petrology*. 143, p.366–376

Hartnady, C.J.H. 1986. Amirante Basin, western Indian Ocean: Possible impact site of the Cretaceous/Paleogene extinction bolide? *Geology*, 14, p.423-426.

Higgs, K.E., King, P.R., Raine, J.I., Sykes, R., Browne, G.H., Crouch, E.M., and Baur, J.R. 2012. Sequence stratigraphy and controls on reservoir sandstone distribution in an Eocene marginal marine-coastal plain fairway, Taranaki Basin, New Zealand. *Marine and Petroleum Geology,* 32(1), p.110–137.

Hodges, K.V. 2000. Tectonics of the Himalaya and southern Tibet from two perspectives. *Geological Society of America Bulletin*, 112 (3), p.324-350.

Hoffman, P.F., (1999).The break-up of Rodinia, Birth of Gondwana, True Polar Wander and the Snowball Earth. *Journal of African Earth Sciences*, 17, p.17–33.

Hölzel, M., Faber, R., and Wagreich, M. 2008. DeCompactionTool: Software for subsidence analysis including statistical error quantification. *Computers and Geosciences*, 34(11), p.1454–1460.

Ishwar-Kumar, C., Windley, B.F., Horie, K., Kato, T., Hokada, T., Itaya, T., Yagi, K., Gouzu, C. and Sajeev, K. 2013. A Rodinian suture in western India: New

insights on India-Madagascar correlations. *Precambrian Research*, 236, p.227–251.

Joseph, P.R., Samson, P.J. and Mondon, J.A. (2011). *Compilation of Iinformation in view of Developing a Geological Risk Map of the Islands of Mahe, Praslin and La Digue.* United Nation Development Programme, SLM Project. Unpublished Report, 257pp.

Kapilima, S. 2002. Tectonic and sedimentary evolution of the coastal basin of Tanzania during the Mesozoic times. *Tanzanian Journal of Sciences*, 29 (1), p.1-16.

Keeley, M.L. and Light, M.P.R. 1993. Basin evolution and prospectivity of the Argentine continental margin. *Journal of Petroleum Geology*, 16(4), p.451-464.

Keighley, D.G., Flint, S., Howell, J., and Moscariello, A. 2003. Sequence stratigraphy in lacustrine basins: a model for part of the Green River Formation, southwest Uinta Basin, Utah, USA. *Journal of Sedimentary Research*, 73, p.987– 1006.

Keller, G., Sahni, A., and Bajpai, S. 2009. Deccan volcanism, the KT mass extinction and dinosaurs. *Journal of Bioscience*, 34, p.709–728.

Khanna, K.K. and Pillay, G.E. 1988. Geology and Petroleum Prospects of Seychelles. *7th Offshore South East Asia Conference. Singapore, 2-5 February*, p.114-124.

Knight, K.B., Nomda, S., Renne, P.R., Marzoli, A., Bertrand, H. and Youbi, N. 2004. The Central Magmatic Province at the Trissic – Jurassic boundary: paleomagnetic and 40Ar/39Ar evidence from Morocco for brief, episodic volcanism. *Earth and Planetary Science Letters*, 228, p.143-160.

Johnson, M.R., van Vuuren, C.J., Visser, J.N.J., Cole, D.I., Wickens, H. de V., Christie, A.D.M., Roberts, D.L. and Brandl, G. (2006) Sedimentary Rocks of the Karoo Supergroup, In: Johnson, M. R., Anhaeusser, C. R. and Thomas, R. J., (Eds.), *The Geology of South Africa*, p.461-499.

Jokat, W., Leinweber, L., Kopsch, K. and Watkeys, M.K. 2009. Fresh Geoscientific Data from the Natal Valley and Mozambique Ridge. *11th SAGA Biennial Technical Meeting and Exhibition, Swaziland*, p.541-542.

Labrecque, P.A., Jensen, J.L., and Hubbard, S.M. 2011, Cyclicity in Lower Cretaceous point bar deposits with implications for reservoir characterization, Athabasca Oil Sands, Alberta, Canada. *Sedimentary Geology*, 242, p.18-33.

Lajoie, J. and Stix, J. 1992. Volcaniclastic rocks, In: Walker, R.G. and James N.P. (Eds), *Facies Models: Response to sea-level change*, University of Montreal, Department of Geology, Quebec, p.101-118.

Li, Z.X., Bogdanova, S.V., Collins, A.S., Davidson, A., De Waele, B., Ernst, R.E., Fitzsimons, I.C.W., Fuck, R.A., Gladkochub, D.P., Jacobs, J., Karlstrom, K.E., Lul, S., Natapovm, L.M., Pease, V., Pisarevsky, S.A., Thrane, K., and Vernikovsky V. 2008. Assembly, configuration, and break-up history of Rodinia: A synthesis. *Precambrian Research*, 160, p.179–210.

Lindeque, A., de Wit, M.J., Ryberg, T., Weber, M., and Chevallier, L. 2011. Deep crustal profile across the southern Karoo Basin and Beattie magnetic anomaly, South Africa: An integrated interpretation with tectonic implications. *South African Journal of Geology*. p.114:265.

Linol, B. 2013. Sedimentology and sequence stratigraphy of the Congo and Kalahari Basins of south-central Africa and their evolution during the formation and break-up of West Gondwana. *PhD thesis*, Nelson Mandela Metropolitan University, 375p.

Linol, B., de Wit, M.J., Barton, E., Guillocheau, F., de Wit, M.J.C, and Colin. J.P. 2014 a. Chapter 7: Paleogeography and tectono-stratigraphy of Carboniferous-Permian and Triassic „Karoo-like" sequences of the Congo Basin. In: de Wit, M.J.,Guillocheau, F., and de Wit, M.J.C. (Eds.), *The Geology and Resource Potential of the Congo Basin*, Springer-Verlag, *In press*.

Lock, B.E. 1980. Flat-plate subduction and the Cape Fold Belt of South Afri*ca. Geology*, 8, p.35-39.

Lüdmann, T., Kalvelagea, C., Betzler, C., Fürstenau J., and Hübscher, C. 2013. The Maldives, a giant isolated carbonate platform dominated by bottom currents. *Marine and Petroleum Geology*, 43, p.326-340.

Mahanjane, E.S. 2012. A geotectonic history of the northern Mozambique Basin including the Beira High – A contribution for the understanding of its development. *Marine and Petroleum Geology*. 6(1), p.1–12.

Mart, Y., 1988. The tectonic setting of the Seychelles, Mascarene and Amirante Plateaus in the Western Equatorial Indian Ocean. *Marine Geology*, 79, p.261-274.

McKenzie, D. 1978. Some remarks on the development of sedimentary basins. *Earth Planetary Science Letters*, 40, p.25-32.

Mavko, G. and Nur, A. 1979. Wave attenuation in partially saturated rocks. *Geophysics*, 44, p.161–178.

Meert, J.G. 2001. Growing Gondwana and rethinking Rodinia, *Gondwana Research*, 4(3), p.278-288.

Meert, J.G. and Lieberman, B.S. 2008. The Neoproterozoic assembly of Gondwana and its relationship to the Ediacaran–Cambrian radiation. *Gondwana Research*, 14, p.5–21.

Miall, A.D. 1980. Cyclicity and the Facies Model Concept in Fluvial Deposits. *Bulletin of Canadian Petroleum Geology*, 28 (1), p.59-80.

Miall, A.D. 1992. Alluvial Deposits. In: Walker, R.G., and James, N.P. (Eds.), *Facies Models: response to sea-level change.* Ontario: Geological Association of Canada, p.119-155.

Miles, P.R. 1982, Gravity models of the Amirante Arc, western Indian Ocean. *Earth and Planetary Science Letters*, 61, p.127-135.

Miller, K.G., Mountain, G.S., Wright, J.D., and Browning, J.V. 2011. A 180-million-year record of sea-level and ice volume variations from continental margin and deep-sea isotopic records. *Oceanography*, 24(2), p.40–53.

Mukhopadhyay, R., Karisiddaiah, S.M., and Ghosh, A.K. 2012. Geodynamics of the Amirante Ridge and Trench Complex, Western Indian Ocean. *International Geology Review*, 54(1), p81-92.

Mutti, E., 1992. *Turbidite Sandstones*. AGIP, Istituto de geologia, Università di Parma, special Publication, 275pp.

Nijman, W. and Puigdefabregas, C., 1978. Coarse-grained point bar structure in a molasse-type fluvial system, Eocene Castisent Sandstone Formation, South Pyrenean Basin. In: A.D. Miall (Ed.), *Fluvial Sedimentology. Canadian Society of Petroleum Geologists, Memoir*, 5, p.487-510.

Perlmutter, M.A., Brennan, P.A., Hook, S.C. Dempster, K. and Pasta, D. 1995. Global cyclostratigraphic analysis of the Seychelles Southern Shelf for potential reservoir, seal and source rocks. *Sedimentary Geology*, 96(1), p.93-118.

Phillips, R.L. 2003. Depositional environments and processes in Upper Cretaceous nonmarine and marine sediments, Ocean Point dinosaur locality, North Slope, Alaska. *Cretaceous Research*, 24. p.499–523.

Pirmez, R.A., Pratson, L.F., and Steckler, M.S. 1998. Clinoform development by advection-diffussion of suspended sediment: Modelling and comparison to natural systems. *Journal of Geophysical Research*, 103, p.24141-24157.

Pitman, W.C., III. 1978. Relationship between eustasy and stratigraphic sequences of passive margins. *Geological Society of America Bulletin*, 89, p. 389–1403.

Plummer, P.S. and Belle, E.R. 1995. Mesozoic Tectono-stratigraphic evolution of Seychelles Microcontinent. *Sedimentary Geology*, 96 (1-2), p.73-91.

Plummer, P.S. 1998. Seychelles Geology and the Shiva Crater Theory. *Phelsuma*, 6, p.9-19.

Plummer, P.S., Joseph, P.R. and Samson, P.J. 1998. Depositional environments and oil potential of Jurassic/Cretaceous source rocks within the Seychelles microcontinent. *Marine and Petroleum Geology*, 15, p.385 -402.

Porrenga, D.H., 1967. Glauconite and chamosite as depth indicators in the marine environment. *Marine Geology*, 5, p.495–501.

Powell, C.McA. and Pisarevsky, S.A. 2002. Late Assembly of East Gondwana. *Geology*, 30, p.3-6.

Purcell, P.G. 1981. Phanerozoic Sedimentary History and Petroleum Potential. In: Chewaka, S. and de Wit M.J. (Eds.), *Plate Tectonics and Metallogenesis: Some Guides to Ethiopian Mineral Deposits, Bulletin,* 2, p.97-114.

Purushotham, A.K. 2002. Geophysical Constraints on Structure and Tectonics of theEastern Arabian Sea and the adjoining West Coats of India with special reference to the Kerala Basin. *PHd Thesis*, Cochin University of Science and Technology, 108pp.

Rakotosolofo, N.A., Torsvik T.H., Ashwal L.D., Eide E.A., de Wit M.J. 1999. The Karoo Supergroup revisited and Madagascar-Africa fits. *Journal of African Earth Science*, 29, p.135–51.

Rakotosolofo, N.A. 1999). Geology, Carbon Isotope Stratigraphy and Palaeomagnetism of the Karoo Sequences of the Southern Morondava Basin, SW Madagascar. *MSc Thesis, Rand Afrikaans University*, 162pp.

Reeves, C.V. and de Wit M.J. 2000. Making ends meet in Gondwana: retracing the transforms of the Indian Ocean and reconnecting continental shear zones. *Terra Nova*, 12, p.272-280.

Reeves, C.V., Sahu, B.K and de Wit. M.J. 2002. A re-examination of the paleo-position of Africa's eastern neighbours in Gondwana. *Journal of African Earth Sciences*, 34, p.101–108.

Reeves, C.V. 2013. The position of Madagascar within Gondwana and its movements during Gondwana dispersal. *Journal of African Earth Sciences, In press Accepted manuscript*.

Reeves, C.V., Teasdale, J., and Mahanjane, E.S. 2014. A global view of East Coast of Africa: Is it really a transform margin? *In press Accepted manuscript*.

Riley, T.R. and Knight, K.B. 2001. Age of pre-break-up Gondwana magmatism. *Antarctic Science*, 13(2), p.99–110.

Roberts, H.H., 1997, Dynamic changes of the Holocene Mississippi River delta plain: the delta cycle. *Journal of Coastal Research*, 13, p.605-627.

Sacramento, A., Basilio, M., Ncucule, L., and Anjos, L. 2014. Rovuma – Uma estrategia sustenavel de Crescimento para Mocabique no upstream. *2º Congresso Nacional de Geologia (CoGeo02) e 12º Congresso de Geoquimica dos Paises de Lingua Portuguesa (12CGPLP), 6 a 12 de Setembro de2014, Maputo, Mocambique*.

Salazar, M.U., Baker, D., Francis, M., Kornphil, D., and West, T. 2013. Frontier exploration offshore the Zambezi Delta, Mozambique, *First Break*, 31, p. 135-144.

Schlüter, T. 2008. *Geological Atlas of Africa: With Notes on Stratigraphy, Tectonics, Economic Geology, Geohazards, Geosites and Geoscientific Education of Each Country*. 2nd ed, Springer, 307pp.

Schandelmeier, H., Bremer F. and Holl, H. G. (2004). Kinematic evolution of the Morondava rift basin of SW Madagascar—from wrench tectonics to normal extension. *Journal of African Earth Sciences*, 38(4), p. 321-330.

Searle, M.P., Windley, B.F., Coward, M.P., Cooper, D.J.W., Rex, A.J., Rex, D., Tingdong, L., Xuchang, X., Jan, M.Q., Thakur, V.C., and Kumar, S. 1897. The closing of the Tethys and the tectonics of the Himalaya. *Geological Society of America Bulletin*, 98, p.678-701.

Seychelles National Oil Company. 1999. *Geonotes Report*. Unpublished Report

Serra, Q. 1984. *Fundamentals of well-log interpretation. The Acquisition of Logging Data*, Elsevier Science Publishers B.V, Amsterdam. 107pp.

Schandelmeier, H.; Bremer, F.; and Holl, H.-G. 2004. Kinematic evolution of the Morondava rift basin of SW Madagascar: from wrench tectonics to normal extension. *Journal of African Earth Science*, 38, p.321–330.

Shepard, F.P. 2011. Criteria in modern sediments useful in recognizing ancient sedimentary environments. In: van Straaten, L.M.J.U. (Ed), *Deltaic and shallow marine deposits*, Elsevier – Publisher, p.1-25

Sloss, L.L. 1963. Sequences in the interior of North Americ*a. Geological Society of America Bulletin*, 74, p.93-114.

Smith, W.H.F., and Sandwell, D.T. 1997. Global Sea Floor Topography from Satellite Altimetry and Ship Depth Soundings. *Science*, 277, p.1956-1962.

Stern, R.J. 1994. Arc Assembly and Continental Collision in the Neoproterozoiz East African orogen: Implications for the consolidation of Gondwanaland. *Annual Review of Earth and Planetary Science*, 22, p.319-351.

Stewart, D.J., 1983. Possible suspended-load channel deposits from the Wealden Group (Lower Cretaceous) of southern England. In: Collinson, J.D. and Lewin, J. (Eds.), *Modern and Ancient Fluvial Systems*. International Association of Sedimentologists Special Publication, 6, p.369-384.

Storey, B.C. 1995. The role of mantle plumes in continental breakup: case histories from Gondwanaland, *Nature*, 377, p.301–308.

Suwa, K., Tokieda, K. and Hoshino, M. 1994. Palaeomagnetic and petrological reconstruction of the Seychelles. *Precambrian Research*, 69, p.281-292.

Tankard, A, Welsink, H., Aukes, P., Newton, R. and Stattker, E. 2012. Geodynamic interpretation of the Cape and the Karoo basins, South Africa. Phanerozoic Passive Marigins, Cratonic Basins and Global Tectonics Maps. USA and UK: Elsevier, 869pp.

Toksöz, M., Cheng, C., and Timur, A. 1976. Velocities of seismic waves in porous rocks. *Geophysics*, 41(4), p.621–645.

Torsvik, T.H., Ashwal, L.D., Tucker, R.D. and Eide, E.A. 2001. Neoproterozoic geochronology and palaeogeography of the Seychelles microcontinent: the India link. *Precambrian Research*, 110, p.47-59.

Torsvik, T.H., van der Voo, R., Preeden, U., Mac Niocaill, C., Steinberger, B., Doubrovine, P.V., van Hinsbergen, D.J.J., Domeier, M., Gaina, C., Tohver, E., Meert, J.G., McCausland, P.J.A., Cocks, L.R.M. 2012. *Phanerozoic polar wander, paleogeography and dynamics, Earth-Science Reviews*, 114, p.325-368.

Torsvik, T.H., Amundsen, H., Hartz, E.H., Corfu, F., Kusznir, N., Gaina, C., Doubrovine, P.V, Steinberger, B., Ashwal, L.D. and Jamtveit, B. 2013, A Precambrian microcontinent in the Indian Ocean, *Nature Geoscience*, 6, p.223-227.

Tucker, M. E. 2003. Mixed Clastic–Carbonate Cycles and Sequences: Quaternary of Egypt and Carboniferous of England. *Geologia Croatica*, 56(1), p.19–37.

Vail, P.R., Mitchum, R.M., Jr., Todd, R.G., Widmier, J.M., Thompson, S. Ill, Sangree, J.B., Bubb, J.N., and Hatlelid, W.G. 1977. Seismic stratigraphy and global changes of sea-level, in Payton, C.E., (Eds). *Seismic stratigraphy—Applications to hydrocarbon exploration: American Association of Petroleum Geologists Memoir*, 26, p.49-212.

Vail, P.R., Audemard, F., Bowman, S.A., Eisner, P.N., and Perez-Cruz, C. 1991. The stratigraphic signatures of tectonics, eustasy and sedimentology: an overview. In: Einsele, G., Ricken, W., and Seilacher, A., (Eds.). *Cycles and Events in Stratigraphy*. Berlin: Springer-Verlag, p.617-659.

Veevers, J.J., Cole, D.I., and Cohan, E.J. 1994. Southern Africa: Karoo Basin and Cape Fold Belt. In: Veevers, J.J., and Powell, C.McA. (eds), *Permian-Triassic Pangean Basins and fold belts along the Panthalassan margin of Gondwanaland*. Geological Society of America, Colorado, Memoir, 184, p.223-280.

Vincent, S.J., Macdonald, D.I.M. and Gutterige, P. 1998. Sequence Stratigraphy. In: Doyle, P. and Bennett, M. R., (Eds.). *Unlocking the Stratigraphical Record*, John Wiley and Sons, New York, 532pp.

Van Loon, A.J. 2000. The stolen sequence. *Earth-Science Reviews*, 52(1–3). p.237–244.

Walton, E.K. and Khanna. M. 1992. The Karoo Succession, Western Shelf, Seychelles. Paleoclimate and Geohistory Analyses in Seychelles Petroleum Exploration, in Plummer, P.S., (Ed.). *First Regional Indian Ocean Petroleum Seminar, Seychelles*, U.N. Dept. of Technical Cooperation for Development, p.245–259.

Walker, R.G. 1992, Facies, facies models and modern stratigraphic concepts. In: Walker, R.G. and James, N.P. (eds.), *b.*. Ontario: Geological Association of Canada, pp.1-14.

Walker, J.D., Geissman, J.W., Bowring, S.A. and Babcock, L.E. 2013. The Geological Society of America Geologic Time Scale. *Geological Society of America Bulletin,* 125 (3-4), p.259-272.

Wilson, M. E. J., Chambers, J. L. C., and Manning, C. 2012. Spatio-temporal evolution of a Tertiary carbonate platform margin and adjacent basinal deposits. *Sedimentary Geology*, 271–272, p.1–27.

Wolden, T. and Belle, E.R. 1992. Structural and Stratigraphic Evolution of the Seychelles Western and Southern Continental Shelf and its Implication on Mesozoic Source Rock Distribution. Im: Plummer, P.S., (Ed.), *First Indian Ocean Petroleum Seminar., Seychelles*, p.415–433.

Wopfner, H. and Kreuser, T. 1986. Evidence for Late Palaeozoic glaciation in southern Tanzania. *Palaeogeography, Palaeoclimatology, Palaeoecology*, 56, p.275–295.

Wyllie, M., Gardner, G., and Gregory, A. 1962. Studies of elastic wave attenuation in porous media. *Geophysics*, 27(5), p.569–589.

Yin, A. and Harrison, T.M. 2000. Geologic Evolution of the Himalayan-Tibetan Orogen. *Annual Review of Earth and Planetary Sciences*, 28, p.211-280.

Yubo, M., Shiguoa, W. Fuliangc, L., Dongdonga, D., Qilianga, S., Yintaoc, L., and Mingfengc, G. 2011. Seismic characteristics and development of the Xisha carbonate platforms, northern margin of the South China Sea. *Journal of Asian Earth Sciences*, 40, p.770–783.

Zachos, J., Pagani, M., Sloan, L., Thomas, E., and Billups K. 2001. Trends, Rhythms, and Aberrations in Global Climate 65 Ma to Present. *Science*, 292, p.686-693.

Appendixes

Appendix A: Detailed seismic interpretations

Relfection Profile TCO-106

Reflection profile TCO-106 below and the detailed interpretations are shown below, illustrating the various observed clinorform terminations identified (yellow boxes) and the interpretations used to identify the different events/horizons observed (solid red lines) according to literature (Figure A.6.2).

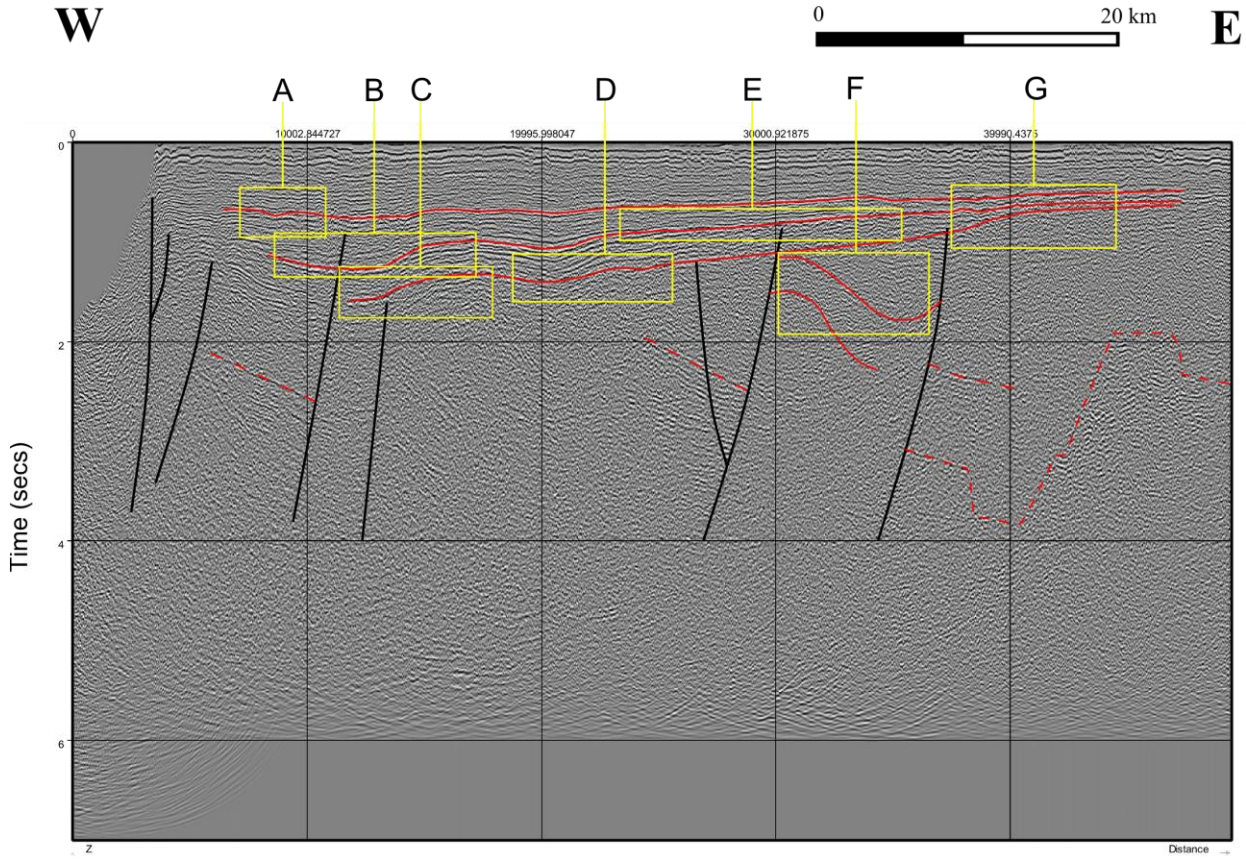

Figure A.6.2: Seismic profile TCO-106 indicating the positions of the clinorform terminations (A-G) used to identify the various horizons or boundary surfaces. The red lines represent identified sequence boundaries (unconformities) or seismic surfaces Faults are interpreted in black.

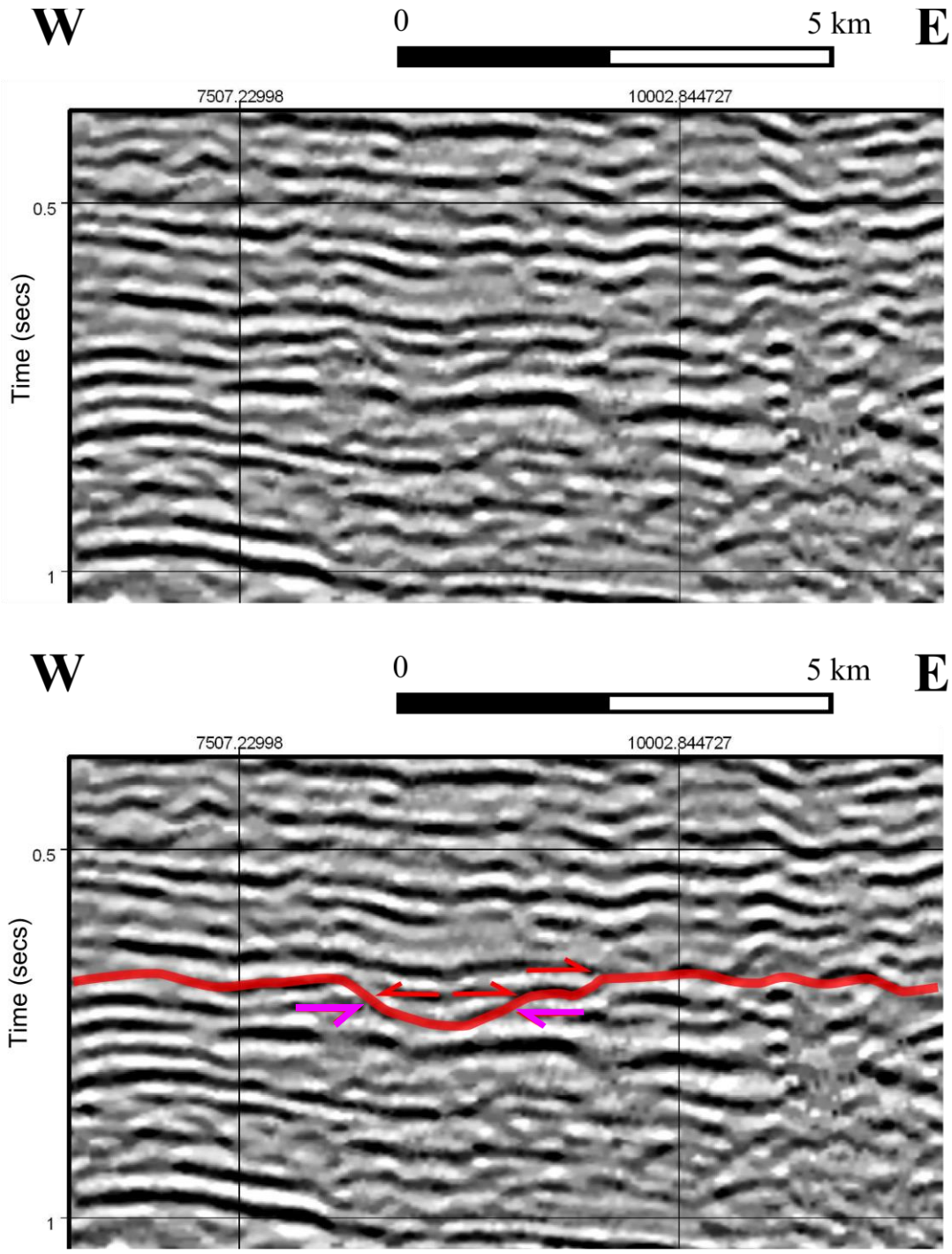

Figure A.6.3: A) Onlaps (red arrows) and toplaps (purple arrows) indicating bounding surface event interpreted by the red horizon and a possible mega channel (approximately 2 km wide) that may be part of an incision surface or unconformity.

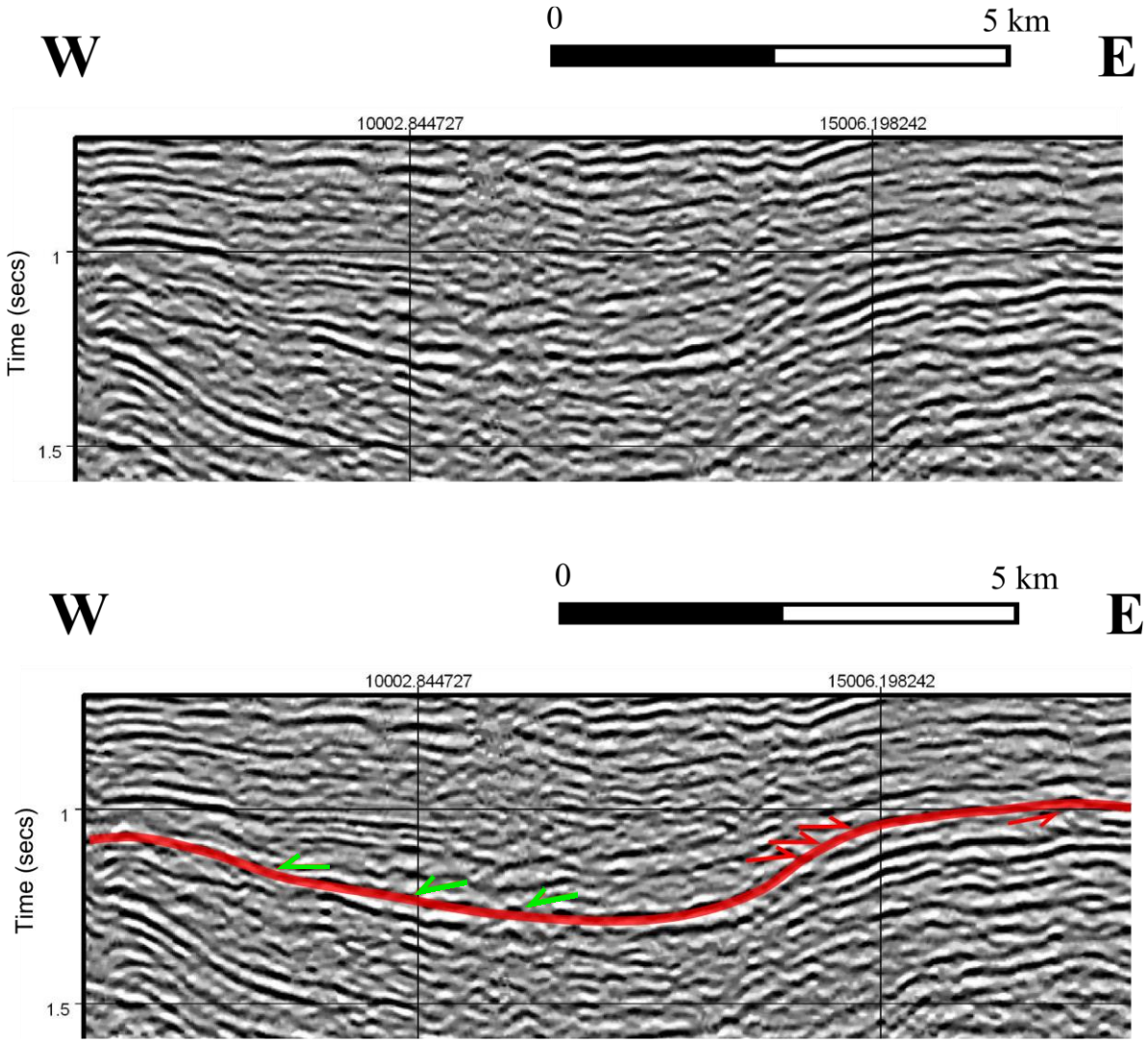

Figure A.6.4: B) Onlaps (red arrows) and downlaps (green arrows) indicating bounding surface event (red horizon) and sediment aggradation and progradation basinwards to the left , interpreted as a marine transgression.

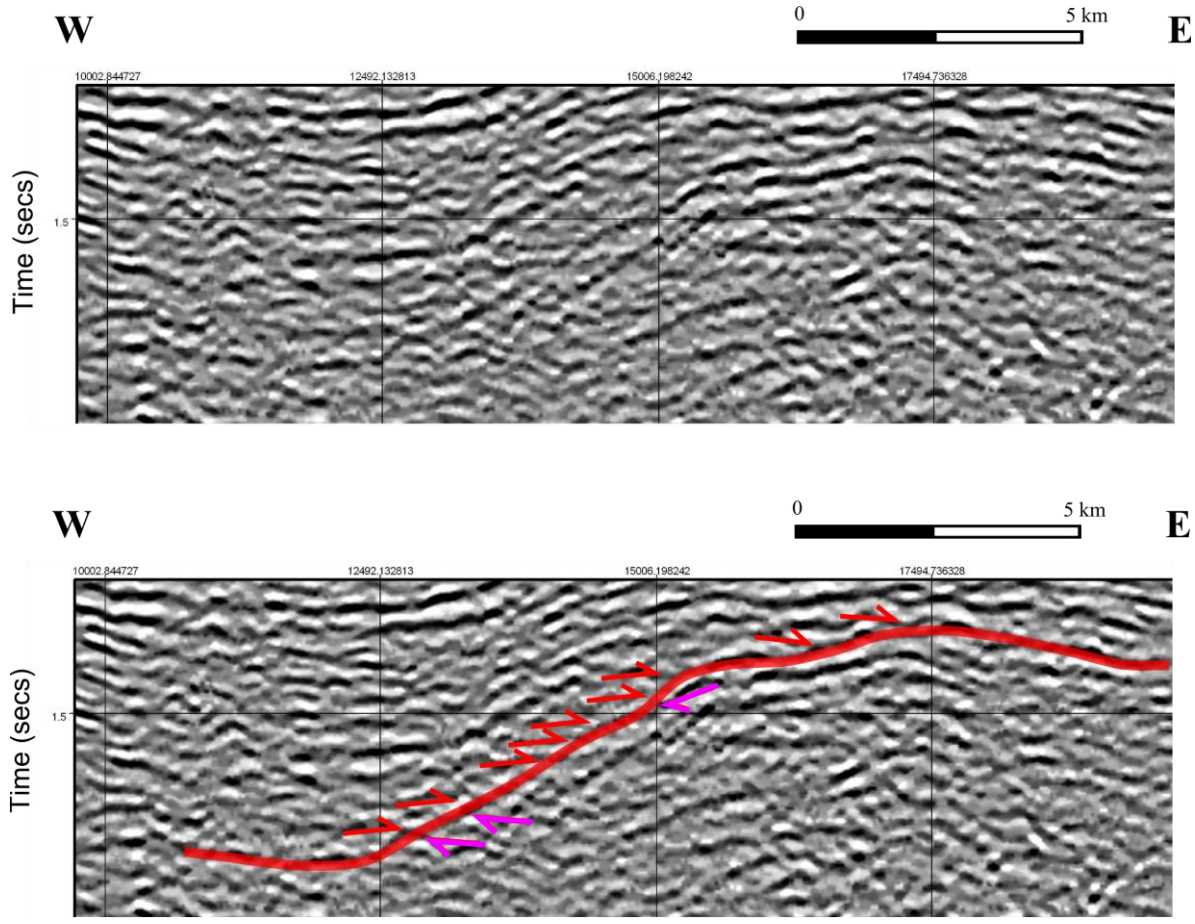

Figure A.6.5: C) Onlaps (red arrows) and toplaps (purple arrows) indicating a bounding surface event (red horizon) and sediment progradation basinwards to the left, interpreted as a marine transgression.

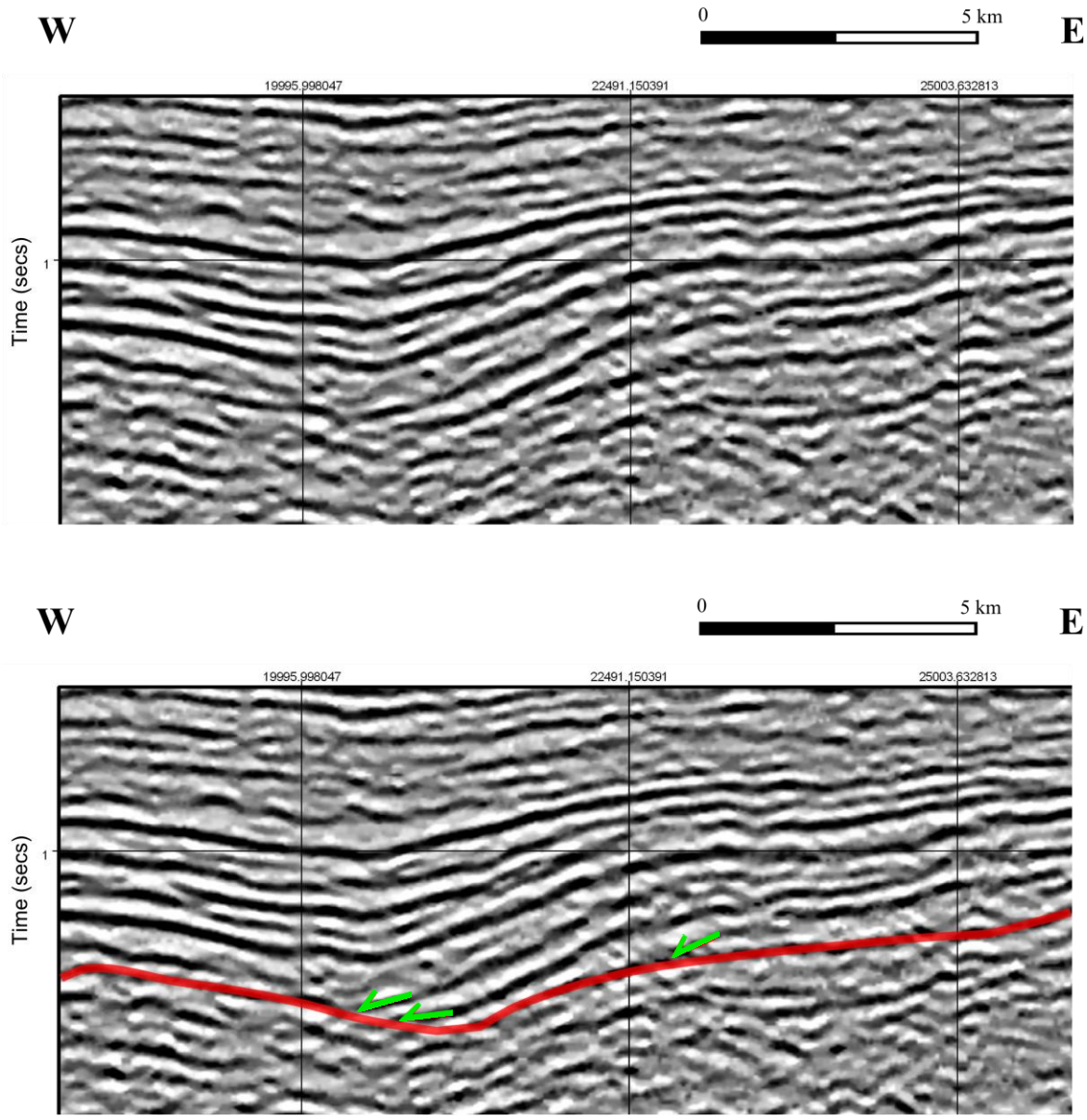

Figure A.6.6: D) Downlaps indicating bounding surface event (red horizon) and sediment aggradation, interpreted as a general transgression.

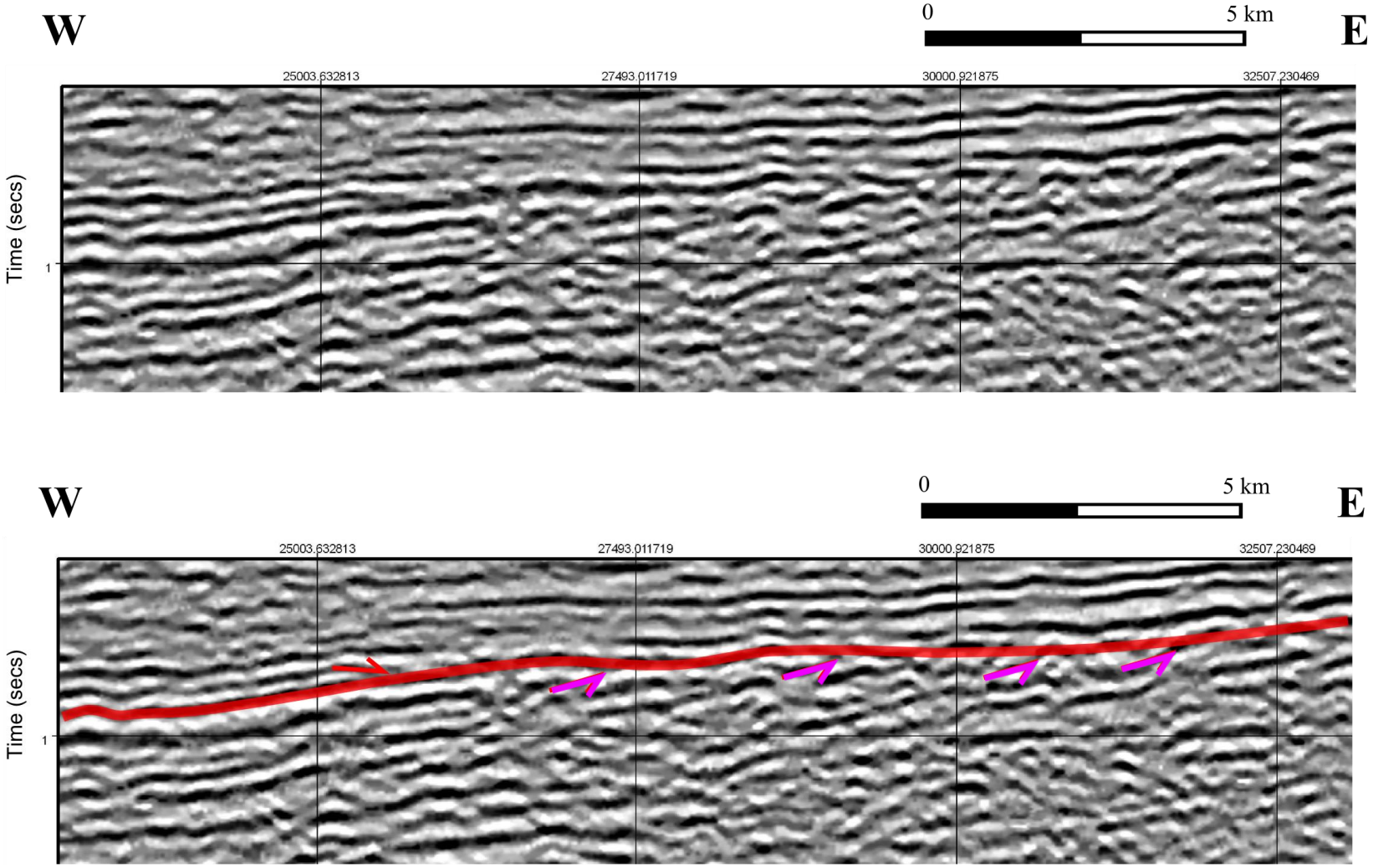

Figure A.6.7: E) Onlaps (red arrows) and toplaps (purple arrows) indicating a definite unconformity surface event(red horizon) and the toplaps are interpreted as sediment progradation due to transgression.

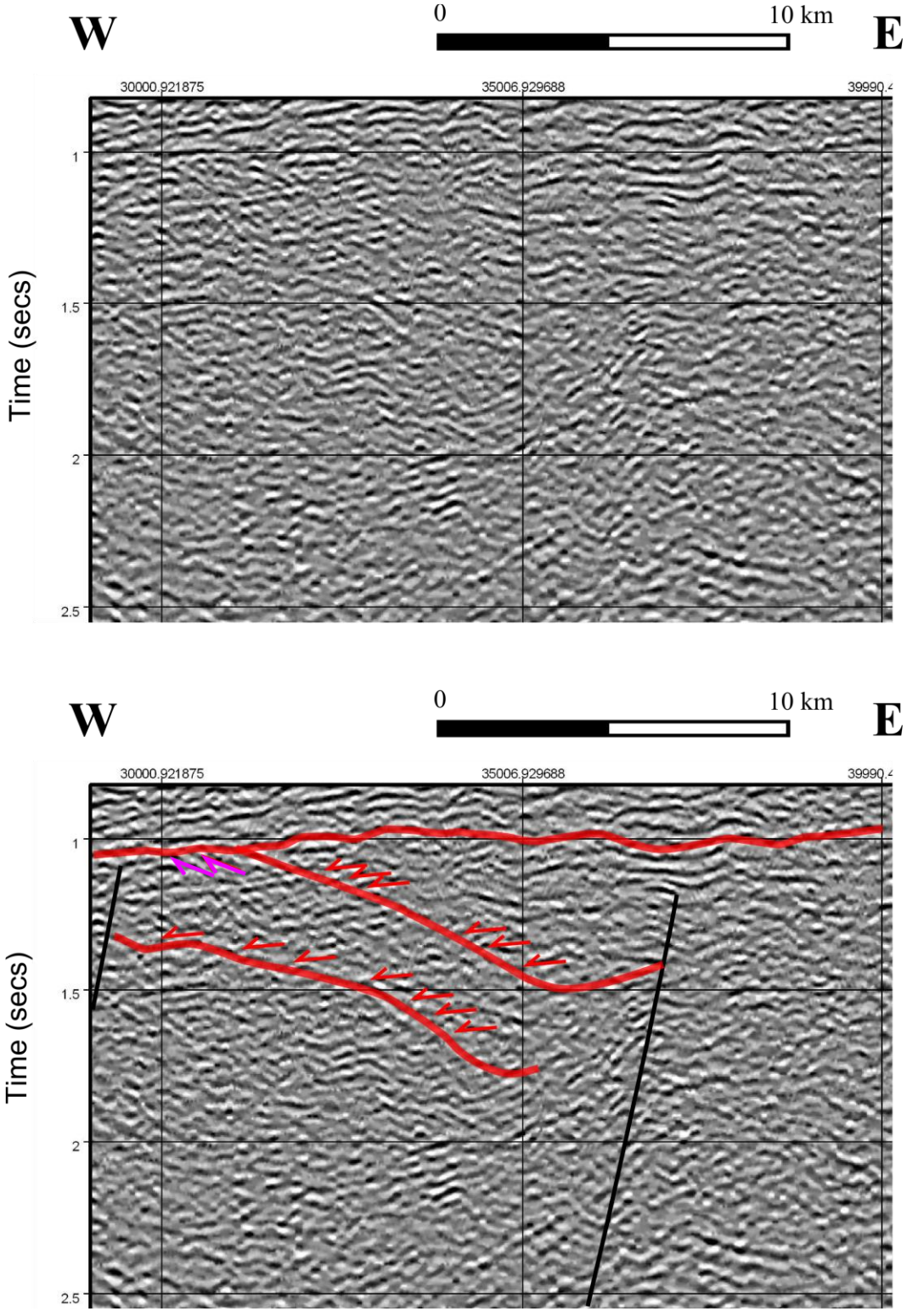

Figure A.6.8: F) Toplaps (purple arrows) indicating an unconformity surface event (top most red horizon) which is lying over dipping strata or horizons (lower two red horizons) indicated by the onlaps (red arrows). Notice the wedge shaped strata bounded by the faults (black lines).

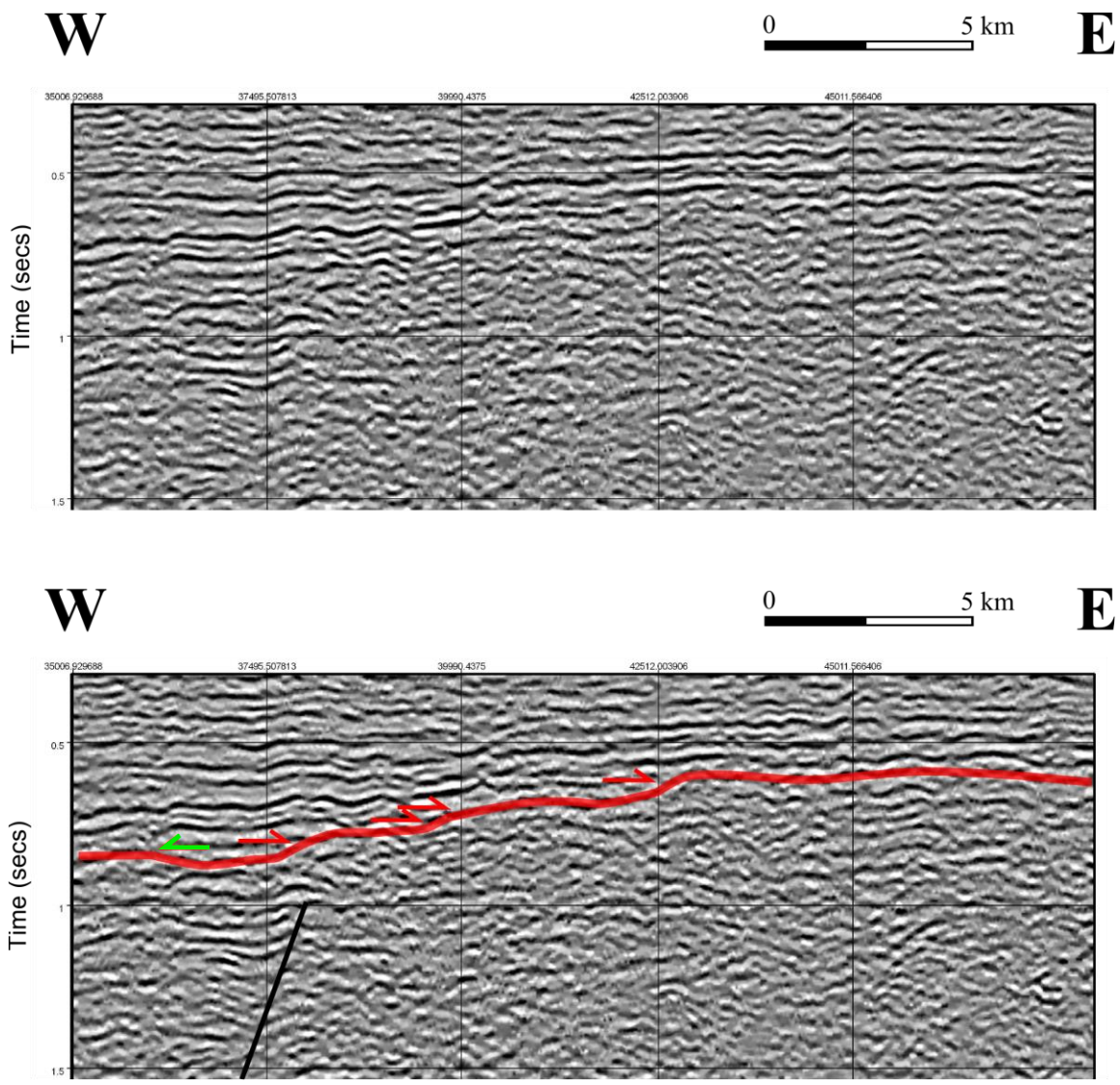

Figure A.6.9: G) Onlaps (red arrows) and downlap (green arrow) indicating a definite unconformity surface (red horizon) and sediment progradation basinwards (left to the west), interpreted as a marine transgression.

Reflection Profile TCO-106

Reflection profile TCO-106 below and the detailed interpretations are shown below, illustrating the various observed clinorform terminations identified (yellow boxes) and the interpretations used to identify the different events/horizons observed (solid red lines) according to literature (Figure 5.4).

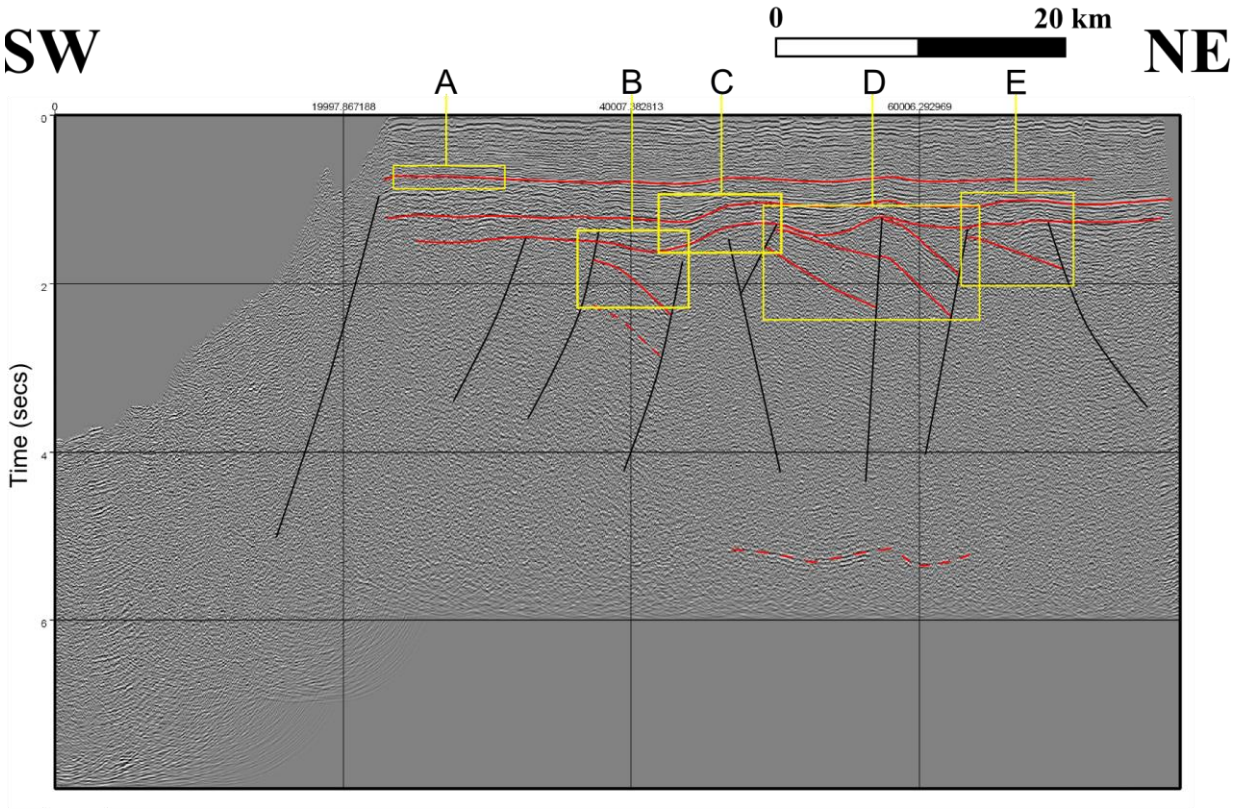

Figure A.6.10: Seismic profile TCO-115 indicating the positions of the clinorform terminations (A-E) used to identify the various horizons or boundary surfaces. The red lines represent identified sequence boundaries (unconformities) or seismic surfaces. Faults are interpreted in black.

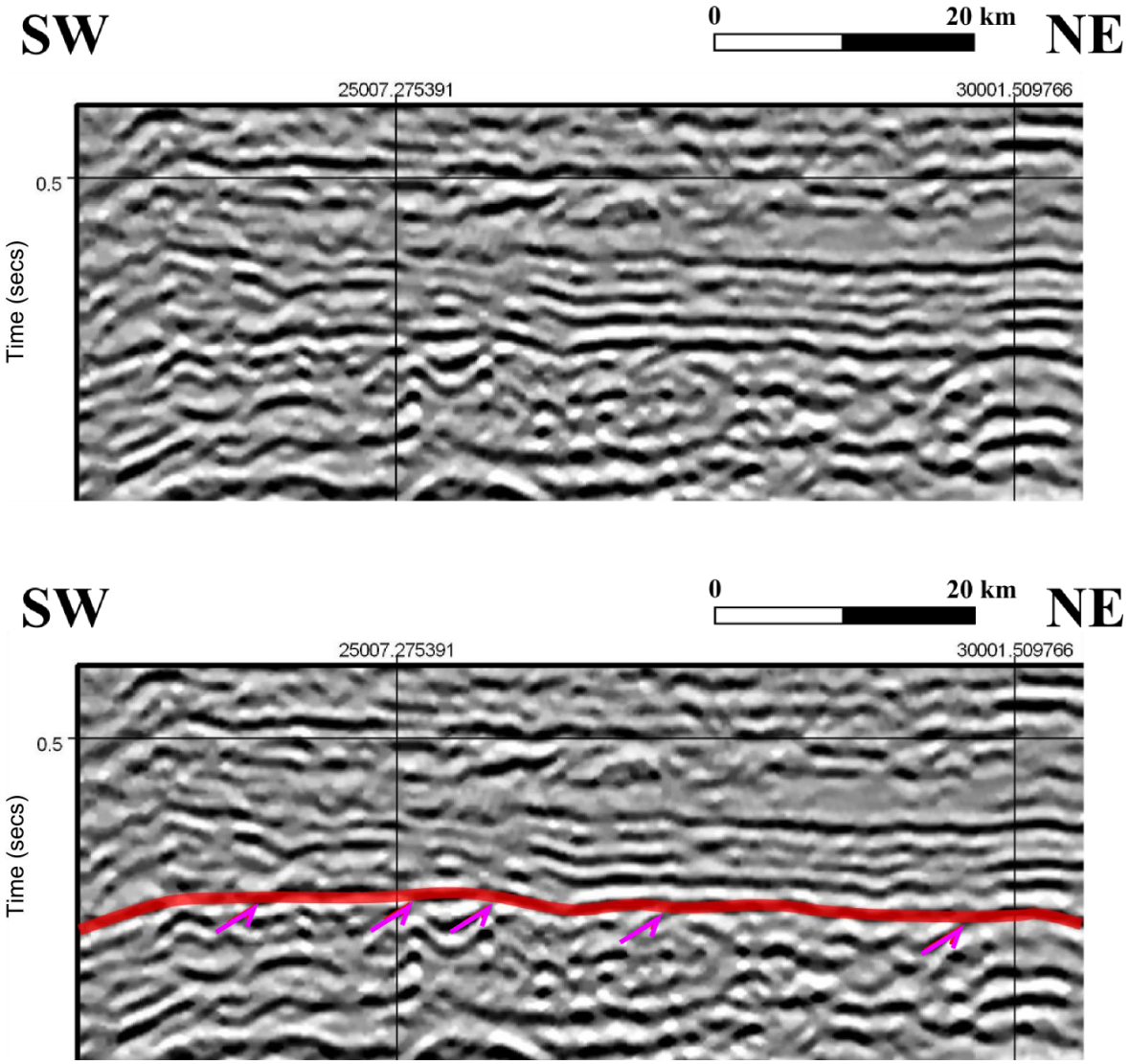

Figure A.6.11: A) Toplaps (purple arrows) indicating a definite unconformity (red horizon.

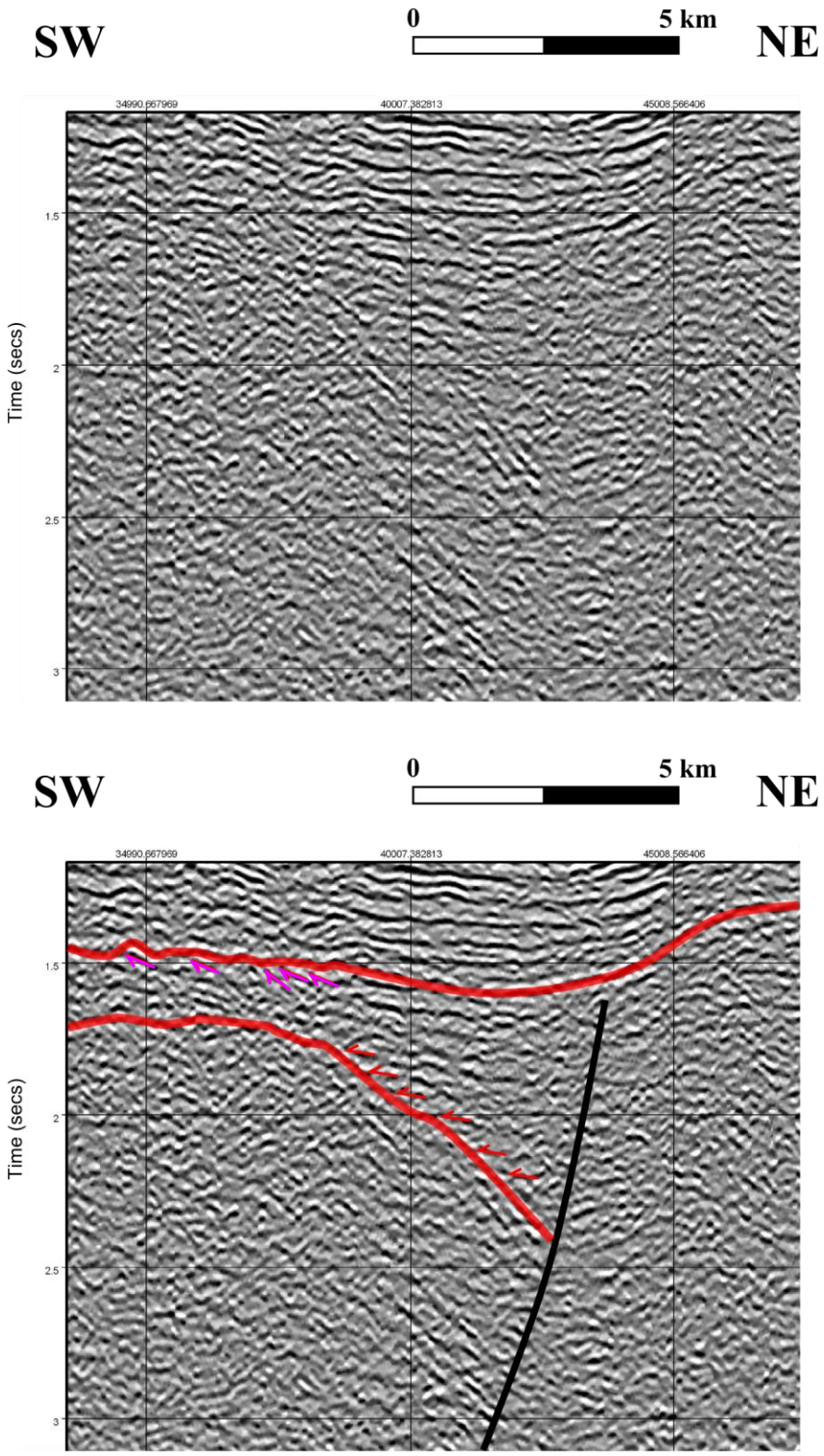

Figure A.6.12: B) Toplaps (purple arrows) indicating a definite unconformity (top-most red horizon) which is lying over dipping strata and horizon (bottom red horizon) indicated by the onlaps (red arrows). Notice the wedge shaped strata bounded by the fault (black line).

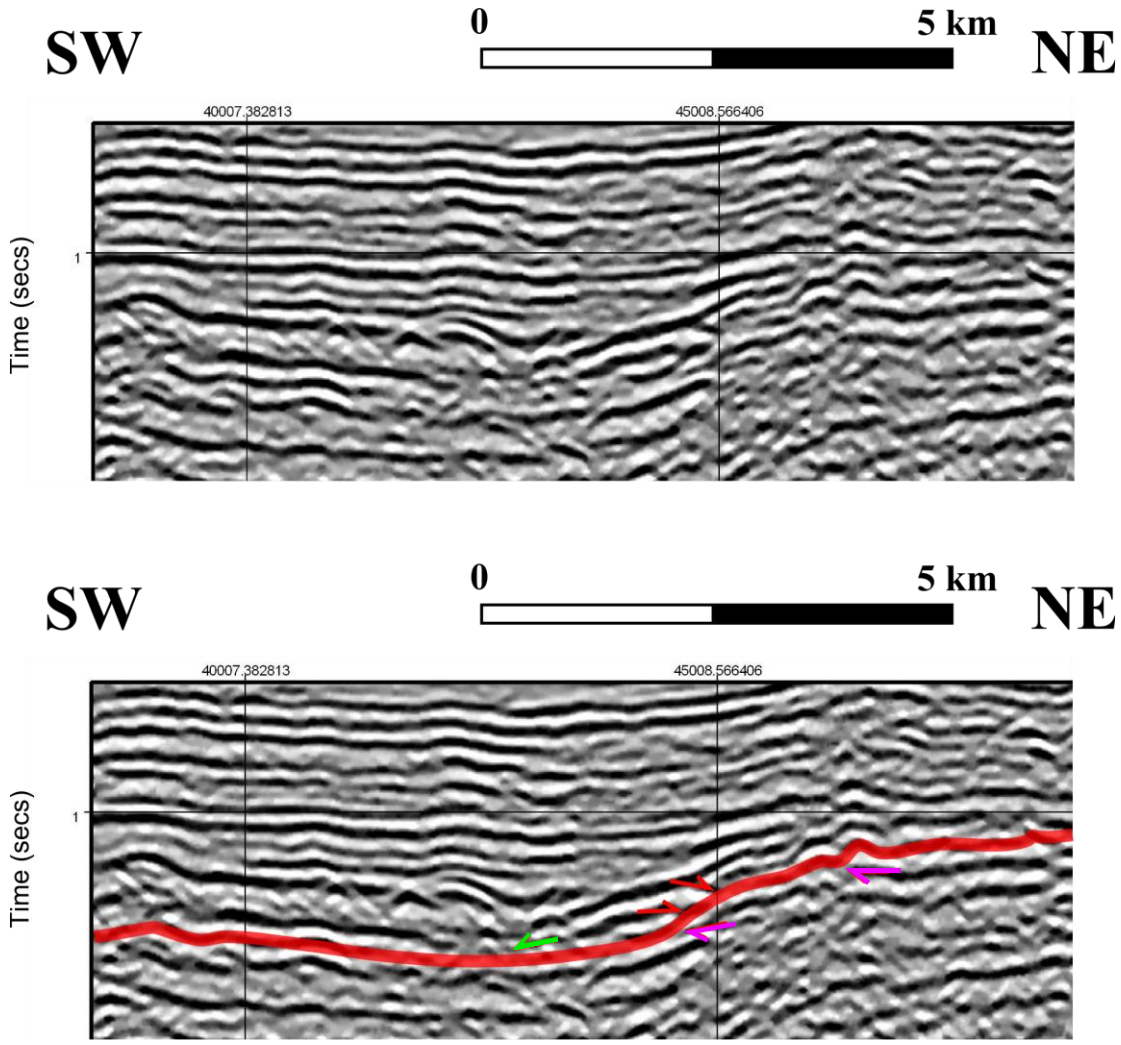

Figure A.6.13: C) Onlaps (red arrows), downlap (green arrow) and toplaps (purple arrows), indicating a bounding surface event (red horizon), interpreted as sediment aggradation and progradation basinwards to the left (south-west) most probably due to transgression.

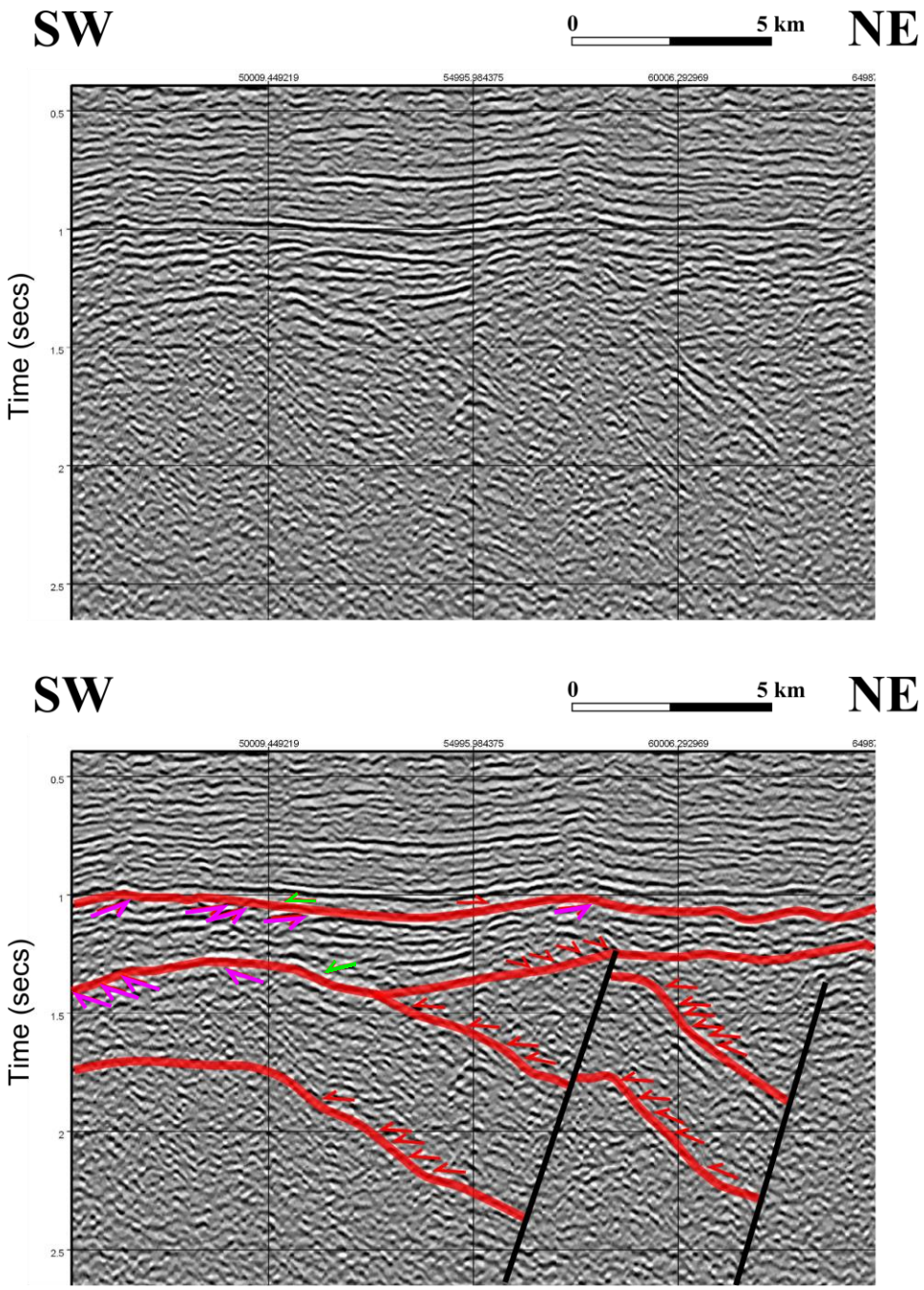

Figure A.6.14: D) Onlaps (red arrows), downlap (green arrow) and toplaps (purple arrows), indicating lateral accretion of unconformity surface event, (top-most red horizon), a second top bounding surface (second top red horizon) and is interpreted as aggradation and progradation of sediments which is lying over dipping strata or horizons indicated by the onlaps and the wedge shaped strata bounded by the north-east dipping boundary surfaces bounded by fault (black lines).

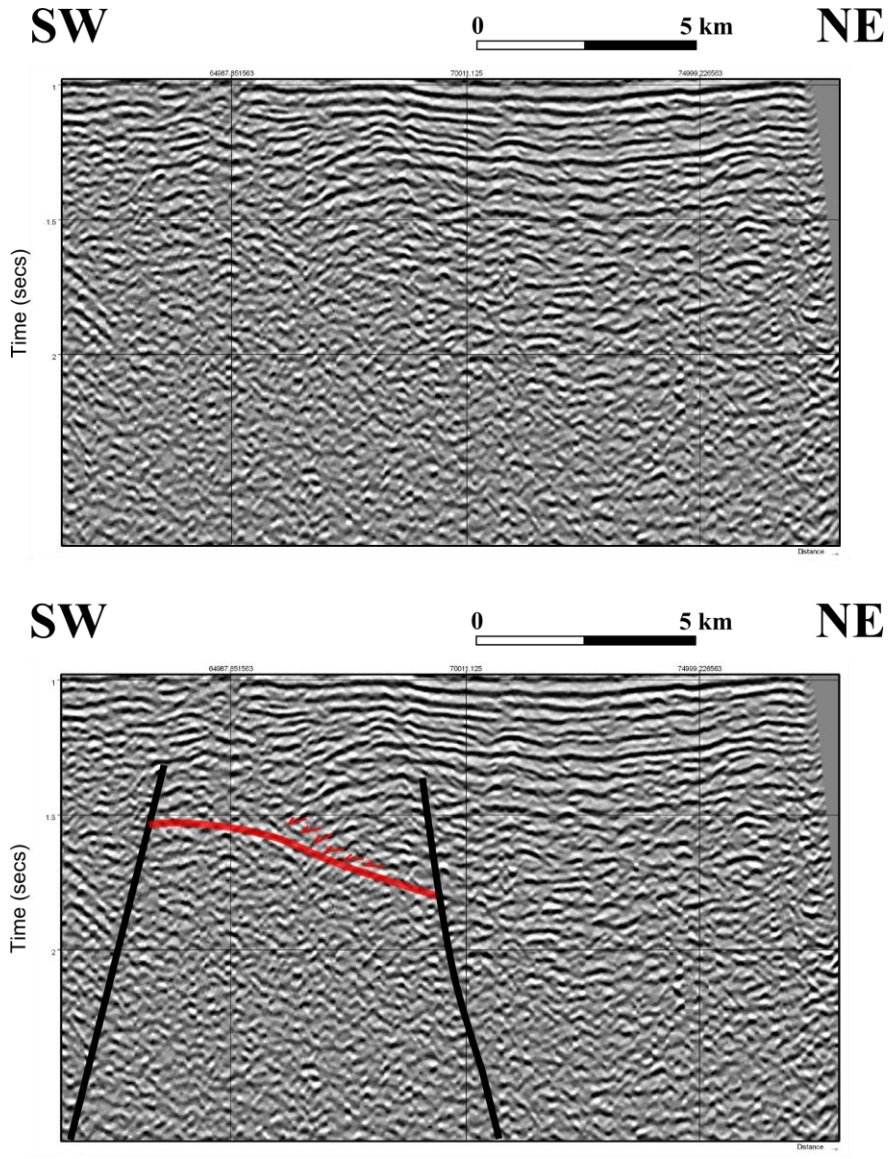

Figure A.6.15: E) Bounding surface (red) event indicated by the onlaps (red arrows). Notice the wedge shaped strata bounded by the faults (black lines).

Appendix B: Biostratigraphy

Table A.1: Species distributions of the fossil content from Owen Bank – A1

Owen Bank - 1				
Fossils	**depth (m)**			
	from	**to**	**from**	**to**
Benthic foraminifera				
Amphistegina SMc.	60.96	217.02	423.67	624.84
Sorites	60.96	217.02	423.67	624.84
Marginopora	60.96	217.02	423.67	624.84
Peneroplis	60.96	217.012	423.67	624.84
Homotrema rubra	60.96	217.02		
Gypsina plana	60.96	217.02		
Acervulina inhaerens	60.96	217.02		
Numulites spp.	624.84	789.43		
Discorbis spp.	789.43	1264.90		
Rotalia spp.	789.43	1264.90		
Fasciolites spp.	789.43	1264.90		
Glomalveolina spp.	789.43	1264.90		
Textularids	789.43	1264.90		
Omphalocuclus macroporus	1789.18	1798.30		
Siderolites spp.	1789.18	1798.30		
Lenticulina spp.	2282.96	2740.15		
Haplophragmoides spp.	2282.96	2740.15		
Saracenaria provoslavlevi	2801.11	3166.88		
Palynomorphs				
Dinocysts				
Areoligera spp.	2109.22	2282.95		
Dinogymnium spp.	2380.49			
KleithriaSMchaeridium	2282.95	2286		
Muderongia staurota	2313.43	2316.48		
Systemat the tophora spp.	2496.31	2499.36		
Kleithriasphaeridium fasciatum	2496.31	2499.36		
Chlamydophorella sp.	2496.31	2499.36		
Oliogosphaeridium spp.	2557.27	2560.32		
Batioladinium radiculu	2740.15	2773.68		
Oligosphaeridium porosum	2740.15	2773.68		
Dichadogonyaulax pannae	2801.11	2804.16		
Oligosphaeridium diluculum	2801.11	2804.16		
Komewuia glabra	2831.59	2834.64		
EpiploSMchaera areolata	2831.59	2834.64		
Belodinium sp.	2831.59	2834.64		
Ctenidodinium chondrum	2913.89	2926.08		
Nannocerat the topsis pellucida	2953.51	2956.56		
Palaeoperidinium paeminosum	3044.95	3084.58		

Gonyaulacysta jurassica	3044.95	3084.58		
Adnatosphaeridium filamentosum	3014.47	3048.00		
Scriniodinium galeritum	3093.72	3096.77		
S. crystallinum	3093.72	3108.96		
S. luridum	3105.91	3108.96		
Ctenidodinium ornatum	3105.91	3108.96		
Pareodinia sp.	3105.91	3108.96		
Sentusidinium spp	3136.39	3139.44		
Gonyaulacysta dangeardii	3136.39	3139.44		
Dichadogonyulax sp.	3288.79	3291.84		
Wanaea acollaris	3319.27	3322.32		
Ctenidodinium combazii	3380.23	3383.28		
Cymatiosphaera spp.	3974.59	4094.99		
Pareodinia spp.	3974.59	4094.99		
Pollen/microspores				
Ariadnaesporites sp.	2252.47			
Classopollis classoides	2496.31	2499.36		
Cicatricosisporites spp.	2496.31	2499.36		
Deltoidospora spp.	2496.31	2499.36		
Contignisporites fornicatus	2496.31	2773.68		
Ophiobolus spp.	2557.27	2560.32		
Bisaccates	2740.15	2773.68		
Classopollis classoides	3471.67	3657.60		
Callialasporites spp.	3471.67	3657.60		
Exesipollenites tumulus	3563.11	3566.16		
Callialasporites group	3867.91	3992.88		
Dichdogonyaulam adelos	3928.87	3931.92		
Ostracods	789.43	1264.92	2282.95	2740.15
Acanthomorphs acritarchs	3974.59	4094.99		

Table A.2: SMcecies distributions of the fossil content from Reith Bank –1

Reith Bank - 1				
Fossils	**depth (m)**			
	from	**to**	**from**	**to**
Benthic foraminifera				
Miogypsina	426.72	635.20		
Miogypsinoides	426.72	635.20		
Halkyardia bikiniensis	759.56	761.39		
Nummulites bayhariensis	820.83	987.55		
N.subdiscorbinus	820.83	987.55		
N. globulus	1231.39	1299.06		
Fasciolites	820.83	987.55		
Orbitolites complanatus	820.83	987.55		
Cibicides lobatulus patalaensis	1316.13			
Distichoplax biserialis	1317.35			
Rotalid foraminifera	1317.35	1447.50		
Lockhartia hunti	1324.36	1346.61		
Rotalia cf. trochidiformis	1447.80	1621.54		
Operculinoides bermudezi	1453.90	1456.95		
Glomalveolina primaeva	1484.38	1487.42		
Laffitteina spp.	1447.80	1621.54		
Glomalveolina primaeva	1447.80	1621.54		
Operculina spp.	1447.80	1621.54		
Elphidiella africana	1621.54	1630.68		
Thalmannita spp.	1621.54	1630.68		
Palaeohystrichophora infusorioides	1766.62			
Trocholina spp.	1845.87			
Planktonic foraminifera				
Globotrunacana coronata	1630.68	1633.73		
G. concavata	1616.96	1642.87		
G. carinata	1766.62			
Praeglobotruncana wilsoni	1639.82	1642.87		
Hedbergella spp.	1764.79	1770.89		
Globigerinelloides spp.	1764.79	1770.89		
Hedbergella planispira	1766.62			
Palynomorphs				
Dinocysts				
Areoligera spp.	1317.35	1447.50		
Spiniferites spp.	1317.35	1447.50	1616.964	
Hemicystodinium sp.	1317.35	1447.50		
Adnatosphaeridium multispinosum	1488.34			
Wetzeliella spp.	1536.80	1630.68		
W. homomorpha	1536.80	1630.68		
Palaeocystodinium	1581.91	1584.96		

Cannosphaeropsis utinensis	1581.91	1584.96		
Palaeohystrichophora infusorioides	1616.96		1766.62	1810.51
SMcinidinium echinoideum	1616.96	1766.62		
Xenascus ceratioides	1766.62	1810.51		
Pareodinia cerat the tophora	1766.62	1810.51		
Gonyaulacysta jurassica	1766.62	1810.51		
Dichadogonyaulax pannea	1766.62	1810.51		
Wanea acollaris	1831.54			
Dichadogonyaulax	1831.54			
Stauromatos	1831.54			
Pareodinia	1831.54			
P. Cerat the tophora	1831.54			
Pollen/microSMcores				
Syncolporites triangularis	1578.86	1581.91		
Verrucosisporites sp.	1581.91	1584.96		
Circumpolles meyeriana	1642.87	1645.92	1766.62	2834.64
Classopollis spp.	1764.79			
C. soinosus	1764.79			
Callialasporites turbatus	1766.62	1810.51	1875.13	2834.64
Classopollis spp.	1831.54			
Callialasporites dampieri	1831.54		1875.13	2834.64
Deltoidospora spp.	1831.54			
Vallasporites ignacii	3319.27	3328.42		
Duplicisporites verrucosus	3319.27	3328.42		
Aulisporites astigmosus	3319.27	3328.42		
Labiipollis granulatus	3319.27	3328.42		
Aratisporites spp.	3319.27	3328.42		
Parvispinosus	3319.27	3328.42		
Guthoerlisporites cancellosus	3319.27	3328.42		
Ovalipollis ovalis	3319.27	3898.39		
Weylandites spp.	3550.92	3553.97		
Raistrickia spp.	3638.70	3953.26		
Acanthotriletes spp.	3638.70	3953.26		
Apiculatisporis spp.	3638.70	3953.26		
Ostracod				
Bairdia sp.	1316.13			

Table A.3: SMcecies distributions of the fossil content from Seagull Shoals – 1

Seagull Shoals - 1	**depth (m)**			
Fossils	**from**	**to**	**from**	**to**
Benthic foraminifera				
Discorinopsis kerfornei	651.05	684.89		
Praerhapydionina sp.	684.89	748.28		
Fasciolites	1165.86			
Opertorbitolites	1165.86			
Cibicides lobatulus patalaensis	1235.66	1335.02		
Rotalia trochidiformis	1235.66	1335.02	1371.6	1438.66
Pararotalia nammalensis	1235.66	1335.02		
Sakesaria dukhani	1371.60	1438.66		
Lockhartia conditi	1371.60	1438.66		
Elphidiella africaensis	1371.60	1438.66		
Thalmannita glaessneri	1371.60	1438.66		
Laffitteina spp	1371.60	1438.66		
Glomalveolina sp.	1527.048	1530.10		
Stensioina pommerana	2008.63	2081.78		
Planktonic foraminifera				
Globotruncana spp.	2008.63	2011.68		
G. duwi	2017.78	2020.82		
G. ventricosa	2017.78	2081.78		
G. stuarti	2020.82	2081.78		
Palynomorphs				
Dinocysts				
Homotryblium pallidum	556.87			
Wetzeliela hyperacantha	1235.66	1323.44		
Adnatosphaeridium multiSMcinosum	1600.20	1603.25		
Dinogymnium sp.	2008.63	2081.78		
Cannosphaeropsis utinensis	2008.63	2081.78		
Callialasporites turbatus	2026.92			
Lanternosphaeridium axiale	2051.30	2054.35		
Adnatosphaeridium aemulum	2337.82	2340.86		
Hystrichosphaeridium recurvatum	2383.54	2386.58		
Pollen/microspores				
Proxapertites operculatus	1235.66	1323.44		
Circumpolles meyeriana	2081.78	2741.68		
Classopollis spp.	2081.78	2741.68		
Callialasporites spp.	2081.78	2741.68		
Ischyosporites and Klukisporites genera	2081.78	2741.68		
Protohaploxypinus	2270.76	2273.81		
Saturna enigmaticus	2319.53	2322.58		
Cicatricosporites sp.	2337.82	2505.46		
Gastropods, echinoderms and dasyclad	2209.80	2212.85		

Appendix C: Well stratigraphy

Table A.4: Stratigraphic facies association, facies description and depositional environment interpretation of Owen Bank – A1

Facies Association	Facies		Interpreted thickness from Gamma log (m)	Description
Open marine: Shelf carbonates (OB-C)	1	Argillaceous cavernous limestone with occasional intercalation of unconsolidated calcareous sandstone	320	White creamy, vuggy, micritic, vuggy and cavernous, occasionally intercalated with unconsolidated very fine grain carbonate sands, contains shell fragments and foraminifera
	2	Intercalated bioclastic pelloidal limestone laminated with fine calcareous siltstone	328	White-creamy, vuggy, porcelaneous, laminated by dark grey siltstone with evidence of vegetation fragments and shell fragments, occasional sparry calcite and dolomitic and pelloidal especially at base, abundant foraminifera, coral fragments and bioclastic aggregates
	3	Fossilliferous limestone laminated with unconsolidated sandstone	156	White creamy, vuggy, chalky, micritic, vuggy limestone intercalated with fine to coarse poorly sorted unconsolidated sandstone. Evidence of abundant foraminifera especially foraminifera, echinoid and shell fragments
	4	Fossilliferous limestone intercalated with calcareous siltstone	19	White creamy, vuggy, micritic, vuggy limestone, intercalated with light-dark grey siltstone with abundant rotalid foraminfera and miliolids
	5	Oolitic-pelloidal arenaceous limestone	99	White-creamy, oolitic-pelloidal, occasional sand grains
	6	Cavernous dolomite	20	Pink-grey-brown, mottled, cavernous (approx. 15m thick)
Open marine mixed carbonate and siliciclastics (OB-SC)	1	Pebbly calcareous claystone intercalated volcanic ash	432	White-grey, chalky, occasionally dolomitic, occasional pebbles of siltstones, decreasing amounts of foraminifera with depth, evidence of organic debris at base with traces of with white-grey volcanic ash??
Volcanics (OB-CV)	1	Basalt intercalated with claystone and tuff	594	Dark grey basalt, partially altered to clay, evidence of vesicles, magnetic (mottled with magnetite), very fine crystalline. Intercallted with light-dark grey claystone/soapstone and tuffs. Few beds of intrusive medium grained grey andesite (dykes?)
Restricted marginal marine mixed carbonate and	1	Calcareous silty claystone intercalated with fine tuff, limestone and siltstone films	117	Grey, calcareous, pyritic, silty, occasionally dolomitic and foraminifera, intercalated with fine grey tuff, white-light grey limestone and siltstone films

siliciclastics (OB-SC)	2	Chalky limestone intercalated with claystone	94	White, chalky, intercalated with fine films of calcareous claystone
Continent siliciclastics (OB-S)	1	Glauconitic bioturbated claystone intercalated fine chalky limestone	290	Medium-dark grey, intercalated occasionally with very fine chalky limestones and very fine sand grains, traces of pyrite, glauconite, plant remains and foraminifera
	2	Bioturbated siltstone, intercalated fine chalky limestone	842	Medium – dark grey siltstone, very argillaceous, abundant bioturbation, intercalated with alternating fine films of light grey limestones and dolomites and medium-coarse grained salmon – purple medium sorted rounded sandstone, with traces of pyrite, glauconite foraminifera. A distinct layer of intrusive andesite occurs in the middle of this section. Salmon – purple medium sorted rounded sandstone with basal rounded quarzitic pebbles, with traces of pyrite, and glauconite
	3	Gonglomeratic calcareous sandstone	23	Salmon – purple medium sorted rounded sandstone with basal rounded quarzitic pebbles, with traces of pyrite, and glauconite
	4	Oolitic, glauconitic-calcareous siltstone	203	Medium – dark grey-brown, traces of dolomite and siderite. Evidence of ooliths, foraminifera and pyrite, occasionally grades into dark grey calcareous claystone. Intercalated with fine grey claystone, white-grey limestone and dark carbonaceous mats
	5	Intercalations of carbonaceous, oolitic, calcareous claystone and sandstone	196	Dark-medium grey, micaceous, pyritic, oolitic, occasionally grades into fine siltstones, traces dark carbonaceous material interbedded by Light grey, fine to medium grain, angular to sub-angular, well sorted, occasionally grades to medium grey siltstone. Oolitic and evidence of foraminifera and carbonaceous material
	6	Oolitic limestone	14	White-grey, sparry-micritic, densely oolitic, occasionally argillaceous
	7	Slightly calcareous claystone	26	Medium grey, slightly calcareous, slightly oolitic, occasional foraminifera,
	8	Siltstone with bivalve shell	42	Light grey to medium brown, occasionally grades into sandstone, fragments of bivalve shell and foraminifera
	9	Bioturbated Claystone	28	Medium – dark grey, occasionally silty, bioturbated, traces of pyrite
	10	Carbonaceous – pyritic, argillaceous siltstone with bivalve	17	Light grey to medium brown, occasionally grades into sandstone, fragments of bivalve shells, traces of pyrite and carbonaceous mat
	11	Bioturbated foraminiferous claystone with brachiopod and plant debris	77	Medium – dark grey, occasionally silty, bioturbated, fragments of foraminifera and brachiopod, carbonaceous mat, evidence of pyrite and plant remains
	12	Intercalations of Carbonaceous pyritic siltstone and claystones	316	Light grey to medium brown, occasionally grades into sandstone, traces of pyrite and carbonaceous materials, evidence of plant remains with a distinct layer of thyolite in between with evidence of brachiopod and pelicpod at base

		with plant remains		

Table A.5: Stratigraphic facies association, facies description and depositional environment interpretation of Reith bank - 1

Facies Association	Facies		Interpreted thickness from Gamma log	Description
Open marine: Shelf carbonates (RB-C)	1	Foraminiferous bioturbated vuggy clayey limestone, intercalated with unconsolidated sandstone	838	White, chalky, soft, flakey, occasionally micritic, vuggy at the top and less vuggy with depth, occasionally intercalated with white-light brown-orange unconsolidated fine to medium sands, abundant foraminifera, occasionally carbonaceous and some degree of bioturbation
Open marine mixed carbonate and siliciclastics (RB-SC)	1	Calcareous, foraminiferous siltstone	110	White-light grey, calcareous, occasional fine quartz grains, abundant foraminifera
	2	Calcareous claystone laminated with lignite	101	White, chalky, soft, non vuggy, occasional fine clear quartz grains, intercalated with carbonaceous mat and brown dull lignite, abundant foraminifera
	3	Dolomitic limestone	57	
	4	Calcareous, dolomitic sandstone	11	White, Medium to fine grained, poorly sorted, traces dolomitic, poorly consolidated
	5	Dolomitic claystone laminated with carbonaceous material and lignite	120	White-light grey, dull lustre and traces of carbonaceous mat. Occasionally intercalated with brown lignite and traces of angular calcite crystals with foraminifera
	6	Fining upwards, glauconitic calcareous sandstone	27	Clear-white, angular to sub-rounded, well sorted, fining upwards, calcitic cement, glauconitic and limestone fragments
	7	Oolitic calcareous claystone with organic debris	72	Medium – dark grey, occasional quartz grains, traces of dark organic debris, evidence of ooliths
	8	Oolitic-pelloidal limestone intercalated with calcareous claystone	157	Light grey, crystalline, densely oolitic and pelloidal, intercalated by films of calcareous claystone, occasional fragments of pumice. Argillaceous at base
Volcanics (RB-V)	1	Intercalations of volcanic ash calcareous claystone	21	Intercalations of alternating red-brown pyritic non calcareous claystone and white-light grey weathered volcanic (ash?)
	2	Dacitic volcanic, intercalated with claystone	110	White-light grey, hard, angular fragments, generally crystalline (Dacite), traces of devitrified glass (volcanics), intercalated with medium to dark grey claystone, slightly calcareous and speckled with dark unidentified mineral
Mixed volcanics, with marine clastics and carbonates (RB-SCV)	1	Sandy Limestone intercalated with volcanic ash	20	Medium –dark grey, occasionally white, arenaceous; containing angular to sub-angular clear quartz grains, traces of black organic matter and calcite crystals. Occasional intercalations of light grey – white volcanics (ash)
	2	Carbonaceous-pyritic, calcareous sandstone	32	Grey, coarse grained, calcareous, angular to sub-angular, well sorted. Traces of pyrite, Fe-stains and carbonaceous specks. Occasional

				intercalations of light grey – white volcanics (ash)
Restricted marginal marine mixed carbonate and siliciclastics (RB-SCV)	1	Oolitic – pelloidal, clayey limestone intercalated with calcareous claystone	42	Dark grey, crystalline, densely oolitic, occasional quartz grains and quartz pebbles at base (limestone). Intercalated with dark grey, carbonaceous claystone
Continental siliciclastics (RB-S)	1	Claystone intercalated with volcanics	10	Red-brown claystone, occasionally grades to siltstone, intercalated with white to grey altered ashy volcanics (volcanic ash).
	2	Intercalations of claystone and sandstone with volcanic ash and traces of organic matter	247	Red-brown claystone, occasionally grades to siltstone, intercalated with white-clear, well sorted, fine grained sandstone. Fine laminations of white to grey altered ashy volcanics (volcanic ash) and traces of organic matter
	3	Intercalations of siltstone, claystone and sandstones with traces of organic matter	232	Red-brown Siltstone, occasionally green, speckled with black organic matter, occasionally intercalated with medium-dark grey claystone, speckled with black organic matter and white, fine to coarse grained, poorly sorted, fining upwards sandstone. Generally laminated with ashy volcanics and traces of devitrified glass
	4	Sandstone intercalated with volcanics and clay lenses	18	Clear-white, fine –coarse, intercalated with grey-white volcanics and contains clay lenses
	5	Arenaceous siltstone intercalated with volcanics	95	Intercalations of red arenaceous siltstones and clear-white, poorly sorted sandstone laminated with grey volvanics (ash) and traces of organic matter
	6	Flaser bedded siltstone and sandstones	128	White-light grey siltstones interbedded with white clear, fine-medium, sub-angular sandstones, with clay lenses
	7	Waxy claystone, with organic matter	9	Red-brown, waxy, intercalated with black organic matter
	8	Sandstone with organic matter	45	Clear-white, poorly sorted, traces of dark organic matter
	9	Arenaceous siltstone with slump structures	38	Red, arenaceous, also evidence of slump structures, and coarsening upwards
	10	Sandstone, laminated with organic films	31	Clear-white, fine –coarse grained, angular to sub-angular, poorly sorted, occasionally laminated with organic matter
	11	Waxy siltstone, intercalated with volcanics	226	Red-brown, occasionally maroon and speckled with fine quartz grains and sometimes waxy with organic debris, intercalated with white grey volcanics
	12	Arenaceous siltstone intercalated with volcanics	140	Red-brown, occasionally maroon intercalated with fine poorly consolidated iron stained sandstones, and further laminated with white grey volcanics ash
	13	Glauconitic flakey claystone	31	Flakey red-purple claystone, highly altered and traces of glauconite, and contains traces of grey volcanics throughout

	14	Planar cross bedded conglomeratic sandstone	18	Light grey-dark red-brown, silty, fine-coarse grained, finning upwards, planar cross bedded (approximately 1 cm), with basal conglomerate of quartzitic pebbles (8-15cm in size), laminated with 2-3 cm thick claystone
	15	Intercalations of parallel laminated claystones with flame structures and convolute bedding at base, with fining upwards and conglomeratic sandstone and planar cross beddings	655	Dark red-purple, with flame structures about 15cm high (convolute bedding), occasionally silty and speckled with dark mineral (chlorite) intercalated with clear-white, angular to sub-angular, poorly sorted, medium- coarse grained sandstones, with evidence of preserved organic matter and traces of volcanics. There are also interbed dark red-brown to dark maroon, fine-coarse grained, fining upwards conglomeratic pebbles of siltstone and quartz (approximately 15 cm) and small scale planar cross beds (approximately 1 cm)

Table A.6: Stratigraphic facies association, facies description and depositional environment interpretation of Seagull Shoals - 1

Facies Association	Facies		Interpreted thickness from Gamma log	Description
Open marine: Shelf carbonates (SS-C)	1	Vuggy, cavernous and foraminiferous clayey limestone	171	White-light grey, clayey, micritic, abundant foraminifera, vuggy and cavernous
	2	Vuggy, cavernous and foraminiferous limestone	103	Creamy-white, abundant foraminifera, vuggy and cavernous
	3	Foraminiferous calcareous claystone	23	White-light grey, abundant foraminifera
	4	Dolomitic foraminiferous limestone	147	Creamy-white-light grey limestone, traces of sucrosic dolomite at the top, generally abundant foraminifera, vuggy and cavernous
	5	Arenaceous foraminiferous limestone	357	Creamy-white, abundant foraminifera, vuggy and cavernous, becoming more massive at base, occasionally sandy (clear, fine grained, sub-angular)
Open marine mixed carbonate and siliciclastics (SS-SC)	1	Sucrosic-dolomitic limestone	232	Tanned, sucrosic, translucent, intercalated with creamy-white limestone
	2	Dolomitic calcareous claystone	137	Medium-dark grey, micritic claystone, intercalated with tanned dolomite films
	3	Calcareous Sandstone	25	Clear-opaque, fine-medium grained, well sorted
	4	Limestone intercalated with claystone	32	White-light grey, appears to be detrital in origin, intercalated with white claystone
	5	Calcareous glauconitic, speckled claystone	127	Medium-dark grey, speckled with fine-medium quartz grains and traces of glauconite
	7	Foraminiferous clayey limestone	45	Off-white-yellow-orange, abundant foraminifera Micritic
	8	Silty carbonaceous calcareous claystone	20	Dark, occasionally silty and traces of dark organic/carbonaceous material

	10	Calcareous arenaceous claystone intercalated with Bioclastic pyritic limestone, sandstone and volcanics	76	Red-grey-black-white, traces of organic, occasional clear quartz grains dark organic material and pyrite. Intercalated with white-creamy limestone occasionally yellow-orange, bulky, evidence of some bioclastics, traces of pyrite, occasionally argillaceous an porcellaneous in some parts and clear, fine-coarse, sub-rounded, well sorted, poorly consolidated sandstone and white grey volcanics. Occasionally silty in some parts. Traces of crystalline basalt, slightly weathered
Volcanics (SS-V)	1	Intercalations of altered amygdaloidal basaltic lava, volcanics ash, calcareous pyritic claystone and thin limestones	313	Dark green-grey, crystalline basaltic lava with amygdales filled with quartz and evidence of green alteration (chlorite?), intercalated with red-brown claystone, occasionally silty, speckled with white and green minerals (chlorite), (moderately calcareous) and white-buff limestone
Restricted marginal to open marine mixed carbonate and siliciclastics (SS-SCV)	1	Pyritic limestone intercalated with volcanics	30	White-yellow, crystalline, sucrosic, traces of pyrite and intercalated with volcanics
	2	Iron stained, calcareous, arenaceous claystone	27	Varv-white, iron stains, non-calcareous, with some occasional loose fine-coarse sandstones
	3	Pyritic limestone intercalated with arenaceous calcareous claystone	110	White-light grey, chalky, pyritic, intercalated with calcareous claystone and fine-medium angular sands
	4	Slightly oolitic pyritic argillaceous Limestone	15	White-yellow, chalky, pyritic, intercalated with volcanics, slightly oolitic
	5	Oolitic Calcareous Sandstone	12	Clear-light grey, fine-coarse grained, calcareous, slightly oolitic, poorly consolidated, traces of volcanics
	6	Oolitic limestone	27	White-light grey, oolitic, chalky and traces of pyrite
	7	Oolitic calcareous Sandstone	42	Clear-opaque, fine-medium grained, poorly consolidated, oolitic, traces of pyrite
	8	Oolitic calcareous claystone with traces of organic matter	33	Medium-dark grey, densely oolitic with traces of dark organic matter
Continental siliciclastics (SS-S)	1	Iron stained sandstone	48	Purple to orange, medium-coarse grain, pyritic, slightly oolitic sandstone, evidence of iron stains and well sorted. At base which appears to grade into light-dark grey, iron stained claystone, becoming silty in some parts and occasional sand grains
	2	Carbonaceous claystone	28	Medium-dark grey, specks of organic/carbonaceous matter

	3	Pyritic sandstone with calcareous cement	56	Clear, fine-medium grain, poorly consolidated, traces of pyrite, calcareous cement
	4	Speckled argillaceous siltstone with carbonaceous material	38	Red-brown, occasionally green to yellow speckled with chlorite and grades to claystone in parts with traces of organic/carbonaceous matter
	5	Intercalations of calcareous sandstone and Silty carbonaceous claystone, with basal conglomerate	47	Clear-opaque, fine-coarse, poorly sorted, angular to sub-angular calcareous sandstone, and varved-red-brown-light-dark grey-black claystone, silty in some parts, and contains traces of black coaly/carbonaceous/organic material (coal?), also waxy and pyritic. Also displays conglomerate at base of quartzitic pebbles (approx.. 15 cm in size)
	6	Oolitic, pyritic siltstone	13	Brown, pyritic, appears to be slightly oolitic, grades to red-brown silty claystone mottled with white and green mineral at base
	8	Speckled claystone	75	Red-brown-medium grey, speckled with white and green mineral
	9	Conglomeratic sandstone	10	Clear, fine-coarse, sub-angular to sub-rounded, poorly sorted, calcareous, contains conglomeratic fragments of volcanics at base
	10	Speckled, silty oolitic pyritic claystone	13	Red-brown-grey-green, speckled white chlorite, slightly oolitic and traces of pyrite
	11	Pyritic siltstone	37	Brown, slightly oolitic, grades to silty claystone in some parts, pyritic
	12	Speckled claystone	17	Red-brown, occasionally speckled with dark green mineral, and grades to silty claystone in some parts
	13	Poorly sorted sandstone	4	White, fine-coarse, poorly sorted
	14	Basalt	16	Dark green, crystalline, speckled with calcite crystals
	15	Intercalations of pyritic claystone and carbonaceous sandstone with basal conglomerate	46	Red-brown claystone with traces of pyrite intercalated with white, fine grain, iron stained sandstone with calcitic cement, and carbonaceous in some parts

Appendix D: Facies analysis

Table A.7: Facies classification and description of Owen Bank – A1

Facies	Thickness (m)	Description	Depositional process and comments
Carbonate			
Argillaceous cavernous limestone	320	White creamy, vuggy, micritic, cavernous limestone, intercalated with unconsolidated very fine grain carbonate sands and consists of abundant shell fragments and benthic foraminifera.	Low energy, carbonate production, dissolution (karstification)
Fossiliferous limestone laminated with fine grey siltstone	20- 328	White-creamy, vuggy and porcelaneous limestone, less cavernous than the previous. Laminated by fine dark grey siltstone with vegetal and shell fragments, occasional sparry calcite crystals and dolomitic in some parts. There is evidence of pelloids especially at base of this facies, and abundant benthic foraminifera, but also consists of coral fragments and bioturbation in some parts.	Low energy, carbonate production (cyclic)
Fossilliferous limestone laminated with unconsolidated sandstone	156	White creamy, vuggy, chalky, micritic limestone intercalated with fine to coarse poorly sorted unconsolidated calcareous sandstone. Abundant benthic foraminifera, shell and echinoid remains in some parts.	Low energy, carbonate production
Oolitic-pelloidal argillaceous limestone	99	White-creamy, oolitic-pelloidal micritic limestone, which occasionally contains sand grains.	High energy, shallow, carbonate production
Oolitic limestone	14	White-grey, sparry-micritic, densely oolitic limestone, occasionally argillaceous in some parts.	High energy, shallow, carbonate production
Cavernous dolomitic limestone	20	Pink-grey-brown, mottled, cavernous dolomite.	?
Volcanic			
Basalt intercalated with claystone/volcanic ash and tuff	594	Dark grey very fine crystalline basalt partially altered to clay. There is evidence of `vesicles and magnetite. Intercalated with light-dark grey claystone/soapstone, tuffs, and few beds of intrusive medium grained grey andesite.	Volcanic / flood basalts eruption (extrusive, igneous)
Siliciclastic (sandstone and mudstone)			
Calcareous sandstone	5 -30	Clear-white well sorted, poorly consolidated and fine-coarse grained sandstone, dolomitic in some parts.	Initial high energy to moderate energy and reducing environment
Glauconitic- calcareous sandstone with basal conglomerate	23	Salmon – purple, medium round grained, well sorted sandstone. The base is composed of a basal conglomeratic layer, made from rounded quartzitic	Initial high energy to moderate energy and reducing environment, proximal

		pebbles (approx.. 10-15 cm). Generally consists of traces of pyrite, and glauconite.	
Pebbly calcareous claystone	432	White-grey chalky claystone, which is occasionally dolomitic. Occasionally contains pebbles of siltstones and decreasing amounts of foraminifera with depth. Organic debris at base and possible traces of white-grey volcanic ash.	Low energy, followed by possible slumping (talus)
Calcareous silty claystone intercalated with fine tuff, limestone and siltstone films	117	Grey calcareous claystone, commonly pyritic, silty, and occasionally dolomitic and contains benthic foraminiferal fragments. Intercalated with fine grey tuff, white-light grey limestone and siltstone films (less than 10 cm thick).	Low to moderate energy, with carbonate production, reducing environment
Glauconitic bioturbated claystone intercalated fine chalky limestone	290	Medium-dark grey claystone, which is intercalated with very fine chalky limestones and very fine sand grains. It also contains traces of pyrite, glauconite, plan, benthic foraminiferal remains, and bioturbation.	Low energy, bioturbation, proximal and carbonate production
Bioturbated siltstone, intercalated fine chalky limestone	842	Medium – dark grey siltstone, with abundant bioturbation. Intercalated with alternating fine films of light grey limestones and dolomites and medium-coarse grained salmon – purple medium sorted rounded sand grains. Also contains pyrite, glauconite and foraminiferal remains.	Low energy, bioturbation, with carbonate production, reducing environment
Oolitic, glauconitic-calcareous siltstone	203	Medium – dark grey-brown siltstone, occasionally grades into dark grey calcareous claystone. Traces of dolomite, siderite, ooliths, foraminiferal fragments, pyrite and glauconite. Intercalated with fine grey claystone, white-grey limestone and dark carbonaceous material.	Low to moderate energy, proximal, reducing environment
Intercalations of carbonaceous, oolitic, calcareous claystone and calcareous sandstone	196	Dark-medium grey, micaceous, pyritic, oolitic claystone, occasionally grades into fine siltstones. Traces of dark carbonaceous material and also contains interbeds of light grey, fine to medium grain, angular to sub-angular, well sorted sandstone, occasionally grades to medium grey siltstone. There is evidence of ooliths, foraminiferal fragments and carbonaceous material.	Low to high energy alternations, in a shallow organic rich environment with episodic anoxic conditions
Siltstone with bivalve shell	42	Light grey - medium brown siltstone, occasionally grades into sandstone and further contains fragments of bivalve shell and foraminiferal fragments.	Low to moderate energy, possibly shallow-sheltered
Bioturbated claystone	28	Medium – dark grey claystone, occasionally silty in some parts, evidence of bioturbation and traces of pyrite.	Low energy, reducing environment
Carbonaceous – pyritic, argillaceous siltstone with bivalve	17	Light grey to medium brown siltstone, occasionally grades into sandstone. Evidence of bivalve shells fragments, traces of pyrite and carbonaceous material.	Low to moderate energy, organic rich, anoxic
Bioturbated foraminiferous claystone with brachiopod and plant debris	77	Medium – dark grey claystone, occasionally silty. There is evidence of bioturbation, foraminiferal and brachiopod fragments, carbonaceous material, pyrite and preserved plant remains.	Low energy, organic rich

Intercalations of Carbonaceous pyritic siltstone and claystones with plant remains	316	Light grey to medium brown siltstone, occasionally grades into sandstone. Traces of pyrite and carbonaceous materials throughout this facies and there is also evidence of plant remains. At the base of this facies there is also evidence of brachiopod and pelicpod remains.	Low to high energy alternations, organic rich, reducing environment

Table A.8: Facies classification and description of Reith Bank – 1

Facies	Thickness (m)	Description and comments	Depositional process and comments
Carbonate			
Foraminiferous bioturbated vuggy clayey limestone, intercalated with unconsolidated sandstone	838	White, chalky, soft, flakey limestone, occasionally micritic, becomes less vuggy with depth, and occasionally intercalated with white-light brown-orange unconsolidated fine to medium sand grains. Contains abundant benthic foraminifera, occasionally carbonaceous and some degree of bioturbation.	Low (-intermediate) energy, carbonate production
Dolomitic limestone	57	White-off white, chalky limestone with traces of dolomite, occasionally interbedded with white to clear medium grained subangular-subrounded sand grains.	Low energy, carbonate production
Oolitic – pelloidal, clayey limestone intercalated with calcareous claystone	157	Light grey, crystalline limestone, densely oolitic and pelloidal. Intercalated by films of calcareous claystone, occasional traces of pumice and seems to be argillaceous at base.	High energy, shallow, carbonate production
Volcanic			
Intercalations of volcanic ash calcareous claystone	21	Intercalations of red-brown, pyritic, claystone and white-light grey weathered volcanic ash which often grades into each other.	Volcanic eruption (explosive)
Dacitic intrusive body, intercalated with claystone	110	White-light grey, generally crystalline dacite, with traces of devitrified glass, and is further intercalated with medium to dark grey calcareous claystone.	Volcanic eruption (Igneous outpour)
Siliciclastic (sandstone and mudstone)			
Calcareous, dolomitic sandstone	11	White, medium to fine grained, poorly sorted and poorly consolidated sandstone, with traces of dolomite.	High energy
Fining upwards, conglomeratic calcareous sandstone	27	Clear-white, angular to sub-rounded, well sorted, fining upwards sandstone, with calcitic cement and traces glauconite.	Initial high energy to moderate energy
Carbonaceous-pyritic, calcareous sandstone	32	Grey, coarse grained, calcareous, angular to sub-angular, well sorted sandstone, with traces of pyrite, iron stains and carbonaceous specks. Intercalations of light grey – white volcanics ash.	High energy and reducing environment, organic rich
Flaser bedded sandstone intercalated with volcanics	128	Clear-white, fine –coarse grained fining upwards sandstone, intercalated with grey-white volcanic ash and also contains clay lenses (flasers).	Alternating high and low energy
Sandstone with organic matter	20 -50	Clear-white, poorly sorted sandstone, with traces of dark organic matter.	High energy, organic rich
Intercalations of flaser bedded siltstone and sandstones	128	White-light grey siltstones interbedded with white-clear, fine-medium, sub-angular sandstones, with clay lenses (flasers) throughout.	Alternating high and low energy

Calcareous, foraminiferous siltstone	110	White-light grey, calcareous siltstone, with occasional fine quartz grains and contains abundant foraminiferal fragments.	Low to moderate energy
Calcareous claystone laminated with lignite	101	White, chalky claystone, with occasional fine clear quartz grains, laminated with carbonaceous material and brown dull lignite, and also contains abundant foraminiferal fragments.	Low to moderate energy, organic rich
Dolomitic claystone laminated with carbonaceous material and lignite	120	White-light grey claystone, contains traces of carbonaceous material and intercalated with brown lignite and traces of foraminifera.	Low energy, organic rich
Oolitic calcareous claystone with organic debris	72	Medium – dark grey claystone, with occasional quartz grains, traces of dark organic debris and ooliths.	Low energy, organic rich
Arenaceous siltstone intercalated with sandstone and volcanic ash	95	Intercalations of red arenaceous siltstones and clear-white, poorly sorted sandstone, laminated with grey volcanics ash and traces of organic matter.	Low to moderate energy, humid, oxidizing environment
Waxy claystone, with organic matter	226	Red-brown, waxy claystone, which is intercalated with fine black organic matter.	Low energy, oxidizing environment
Arenaceous siltstone with slump structures	140	Red, arenaceous siltstone, evidence of slump structures, and displays coarsening upwards texture	Low to moderate energy, oxidizing environment, deep
Waxy siltstone, intercalated with volcanics	226	Red-brown, occasionally maroon siltstone and speckled with fine quartz grains, occasionally waxy with organic debris, and intercalated with white grey volcanic ash.	Low to moderate energy, oxidizing environment, deep, organic rich
Glauconitic flakey claystone	31	Flakey red-purple claystone, which is highly altered and contains traces of glauconite and traces of grey volcanics.	Low energy, alternating reducing and oxidizing environment
Planar cross bedded conglomeratic sandstone	18	Light grey-dark red-brown, silty, fine-coarse grained sandstone, fining upwards and contains planar cross beds (approximately 1 cm), with basal conglomerate of quartzitic pebbles (8-15cm in size), laminated with 2-3 cm thick claystone	High energy environment, unidirectional flow, with breaks of low energy
Intercalations of claystone and sandstone with volcanic ash and traces of organic matter	316	Red-brown claystone, occasionally grades to siltstone, intercalated with white-clear, well sorted, fine grained sandstone. Generally fine laminations of white to grey altered volcanic ash and traces of organic matter.	Alternating low to high energy environment, oxidation
Intercalations of siltstone, claystone and sandstones with traces of organic matter	232	Red-brown occasionally green siltstone, intercalated with medium-dark grey claystone and white, fine to coarse grained, poorly sorted, fining upwards sandstone.	Alternating low to high energy environment, with alternating oxic and anoxic environment
Intercalations of claystones and sandstones with flame structures and convolute beddings bedding, with	655	Dark red-purple claystone, with flame structures about 15cm high (convolute bedding), occasionally silty and is speckled with dark mineral (chlorite), and clear-white angular to sub-angular, poorly sorted, medium- coarse grained sandstones. Traces of preserved organic matter and volcanic ash. At the base is dark red-brown to	Alternating low to high energy environment, with alternating oxic and anoxic environment

basal fining upwards conglomeratic sandstone		dark maroon, fine-coarse grained, fining upwards conglomeratic pebbles of siltstone and quartz (approximately 15 cm).	

Table A.9: Facies classification and description of Seagull Shoals – 1

Facies	Thickness (m)	Description and comments	Depositional process and comments
Carbonates			
Vuggy, cavernous and foraminiferous clayey limestone	171	White-light grey, vuggy and cavernous, clayey-micritic limestone, abundant benthic foraminifera.	Low energy, carbonate production
Vuggy, cavernous and foraminiferous limestone	103	Creamy-white, vuggy and cavernous limestone, with abundant benthic foraminifera.	High energy, shallow, carbonate production
Dolomitic foraminiferous limestone	147	Creamy-white-light grey, vuggy and cavernous limestone, contains traces of sucrosic dolomite at the top, abundant benthic foraminifera.	Low energy, carbonate production
Arenaceous foraminiferous limestone	357	Creamy-white limestone, with abundant benthic foraminifera and occasionally sandy. Becomes less vuggy and cavernous and increasingly massive with depth.	High energy, shallow, carbonate production
Sucrosic-dolomitic limestone	232	Tanned, sucrosic-dolomitic limestone.	Low energy, carbonate production
Foraminiferous clayey limestone	45	Off-white-yellow-orange micritic limestone, abundant benthic foraminifera.	Low energy, carbonate production
Oolitic limestone	27	White-light grey, oolitic, chalky limestone, contains traces of pyrite and abundant foraminiferal fragments.	High energy, shallow, carbonate production
Volcanic			
Intercalations of altered amygdaloidal basaltic lava, volcanics ash, calcareous pyritic claystone and thin limestones	313	Dark green-grey, crystalline basaltic lava with amygdales filled with quartz and evidence of green alteration (chlorite?), intercalated with red-brown silty speckled calcareous claystone and white-buff limestone.	Volcanic / flood basalt eruption (Igneous extrusive)
Siliciclastic (sandstone and mudstone)			
Calcareous Sandstone	10-30	Clear-opaque, fine-medium grained, well sorted calcareous sandstone.	High energy
Oolitic Calcareous Sandstone	10-50	Clear-light grey, calcareous fine-coarse grained sandstone, slightly oolitic, poorly consolidated and contains traces of volcanic ash.	High to moderate energy, proximal
Iron stained sandstone	48	Purple to orange, medium-coarse grained, well sorted sandstone, pyritic, slightly oolitic, and displays iron stains. The base grades into light-dark grey, iron stained claystone, which is occasionally silty in some parts.	Alternating low to high energy environment, with alternating oxic and anoxic environment
Conglomeratic sandstone	10	Clear, sub-angular to sub-rounded, fine-coarse grained, poorly sorted, calcareous sandstone, gradually becomes conglomeratic at base.	Initial high energy to moderate energy and reducing environment

Foraminiferous calcareous claystone	23	White-light grey calcareous claystone, with abundant benthic foraminiferal fragments.	Low energy
Dolomitic calcareous claystone	137	Medium-dark grey, micritic claystone, intercalated with tanned dolomite films.	Low energy
Calcareous glauconitic, speckled claystone	127	Medium-dark grey speckled claystone, and contains fine-medium quartz grains and traces of glauconite.	Generally low energy with episodic high energy intervals, proximal
Silty carbonaceous calcareous claystone	20	Dark speckled claystone, occasionally silty and contains traces of dark organic/carbonaceous material.	Generally low energy with episodic moderate energy intervals, organic rich
Calcareous arenaceous claystone intercalated with bioclastic pyritic limestone, sandstone and volcanics	76	Red-grey-black-white arenaceous claystone, contains traces of organic matter and pyrite. Fine interbeds of white-creamy limestone, occasionally yellow-orange, and also contains traces of pyrite, argillaceous and porcellaneous in some parts. There is also occasional clear, fine-coarse, sub-rounded, well sorted, poorly consolidated sandstone and white grey volcanic ash. There are also traces of crystalline basalt, which is slightly weathered.	Alternating low to moderate energy, reducing environment
Iron stained, oolitic calcareous sandstone	27	Purple to orange, medium-coarse grained well sorted, pyritic, slightly oolitic sandstone, with iron stains. The base grades into light-dark grey, iron stained claystone, which is silty in some parts with occasional sand grains.	Initial low to high energy, shallow, reducing environment
Oolitic calcareous claystone with traces of organic matter	33	Medium-dark grey, densely oolitic claystone, traces of dark organic matter.	Low energy, anoxic, organic rich
Carbonaceous claystone	28	Medium-dark grey claystone, with specks of dark organic/carbonaceous material.	Low energy, anoxic, organic rich
Speckled argillaceous siltstone with carbonaceous material	38	Red-brown siltstone, occasionally green to yellow and speckled with chlorite and grades to claystone in some parts with traces of organic/carbonaceous material.	Low energy, organic rich
Intercalations of calcareous sandstone and silty carbonaceous claystone, with basal conglomerate	47	Intercalations of clear-opaque, angular to sub-angular, fine-coarse grained, poorly sorted calcareous sandstone, and varved-red-brown-light-dark grey-black silty-waxy claystone. Contains traces of black coaly/carbonaceous/organic material (coal?), and traces of pyrite. The base of this facies seems to grade into a layer of conglomerate quartzitic pebbles (approx. 15 cm in size).	Alternating low to high energy, and alternating reducing and oxidizing environment
Oolitic, pyritic siltstone	10 - 30	Brown, pyritic siltstone, slightly oolitic, occasionally grades to red-brown silty claystone with traces of glauconite.	High energy, shallow, anoxic near shore environment
Speckled claystone	75	Red-brown-medium grey claystone, which is speckled with white and green mineral.	Low energy
Speckled, silty oolitic pyritic claystone	13	Alternating red-brown and grey-green claystone, speckled with chlorite, slightly oolitic and contains traces of pyrite.	Low energy, episodic anoxic environment

Intercalations of pyritic claystone and carbonaceous sandstone	46	Intercalations of red-brown claystone with traces of pyrite and fine grained, white iron stained sandstone with calcitic cement, and contains carbonaceous material in some parts	Alternating low to high energy environment, with alternating oxic and anoxic environment

Appendix E: Sequence description

Table A.10: Summary description of the regional sequences identified across SMc identified through seismics, bio-stratigraphy and well-logs

Sequence	Description
7: Middle Triassic	This sequence is only penetrated at its top by Reith Bank – 1 and is bounded at the top by SB7 which is only identified from the bio-stratigraphy and the well-logs. This sequence is composed of mainly thick carbonaceous continental claystones with siltstone interbeds. These sediments are probably of fluvial – lacustrine origin.
6: Middle – Upper Triassic	This sequence is also only penetrated by Reith Bank – 1 and is bounded at the top by SB6 and base by SB7 which is only identified from the bio-stratigraphy and well-logs. This sequence is composed of mainly fluvial intercalation of sandstones, claystones and siltstones which display fining upward trends. These have formed from the migrating point bar deposits of the river channel.
5: Lower – Middle Jurassic	This sequence is penetrated by all three wells of the study site but only Reith Bank – 1 penetrated through its base. It is bounded at the top by SB5 and base by SB6. This has been identified via bio-stratigraphy and well-logs for Owen Bank – A1 and seismics for Reith Bank – 1 and Seagull Shoals - 1. This sequence is composed of mainly intercalations of sandstones and claystones from the Reith Bank – 1 which represent fluvial point bar migration. As for the section penetrated by Owen Bank – A1 and Seagull Shoals – 1, it is observed that the sequence displays a transition from base to top from fluvial to a marine incursion, probably deltaic. The top of this sequence (SB3) probably defines the end of the rifting phase and the start of the drifting phase between East and West Gondwana.
4: Middle Jurassic – Lower Cretaceous	This sequence is bounded at the top by SB3 and base by SB5 which is identified from the bio-stratigraphy, well-logs and seismics. This sequence is composed of a predominantly transgressive sequence, upwards fining from basal intercalation of sandstone, into thick calcareous siltstones and finally into thick calcareous claystones rich in organic matter. The very base of this sequence is marked by a distinct marker of oolitic facies (limestones and calcareous claystone). This sequence displays characteristics of shallow restricted marginal marine origin. A possible sequence boundary (SB4) is identified through the biostratigraphy only and is only seen through Owen Bank – A1. This boundary is absent in the other two wells probably due to erosion, because the rotated fault blocks seem structurally higher. This may also explain why Sequence 4 is much thinner in Reith Bank – 1 and Seagull Shoals - 1.
3: Upper Cretaceous	This sequence is bounded at the top by SB2 and base by SB3 which is identified from the bio-stratigraphy, well-logs and seismics. This sequence is composed mainly of volcanic: basaltic lava from Owen Bank – A1 and Seagull Shoals – 1 and dacitic lava from Reith Bank – 1. These volcanics originate from the eventual break-up of Seychelles from India (*ca.* 66 Ma). At the base of these volcanics are upward fining shelf carbonates (massive limestones, calcareous sandstone into claystones) which possibly represents a carbonate platform installation during the drifting phase that was followed by deeper marine conditions. This is supported by the planktonic foraminifera observed only at the base of this sequence seen through the Seagull Shoals – 1. This may also represent the drift phase after the continental break up of Madagascar from the Seychelles/India (*ca.* 84 Ma). In general, sigmoidal prograding clinoforms and oblique prograding clinoforms are observed in this sequence from the seismic reflection profile which denotes progradation.

2: Paleocene Middle Eocene	This sequence is bounded at the top by SB1 and base by SB2 which is identified from the bio-stratigraphy, well-logs and seismics. This sequence is composed of predominantly calcareous claystone intercalated by calcareous sansdstone, limestone and volcanic ash. These successions change to thicker limestones at the top where it is more dolomitic. An upward coarsening trend is observed in this sequence, and is further supported by the planktonic foraminifera observed only at the base of this sequence; seen through the Reith Bank – A1. This possibly indicates a drop in the MSL, or these sediments where deposited on the shelf slope.
1: Middle Eocene – Pleistocene	This sequence is the uppermost sequence and is bounded at the base by SB1 which is identified from the bio-stratigraphy, well-logs and seismics. It is composed of open marine carbonate sediments which is technically a continuation of the previous sequence into a sustainable carbonate platform.

Appendix F: Composite Stratigraphic sections

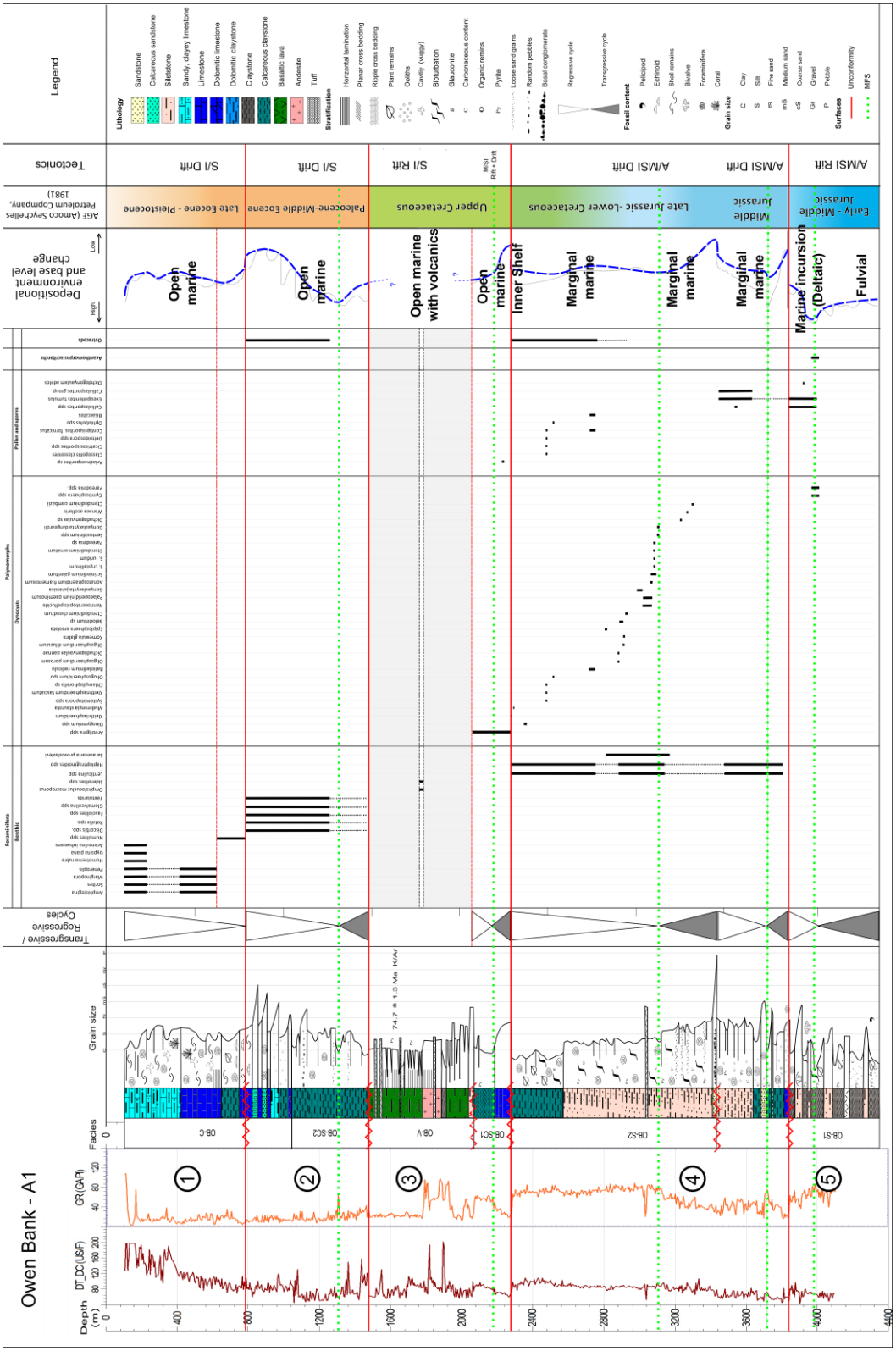

Figure A.6.16: Composite stratigraphic section of Owen Bank – A1, which includes the lithological log, the T-R cycles, bio-stratigraphy, base level curve with the depositional environment, tectonic events and the relative ages of sequences.

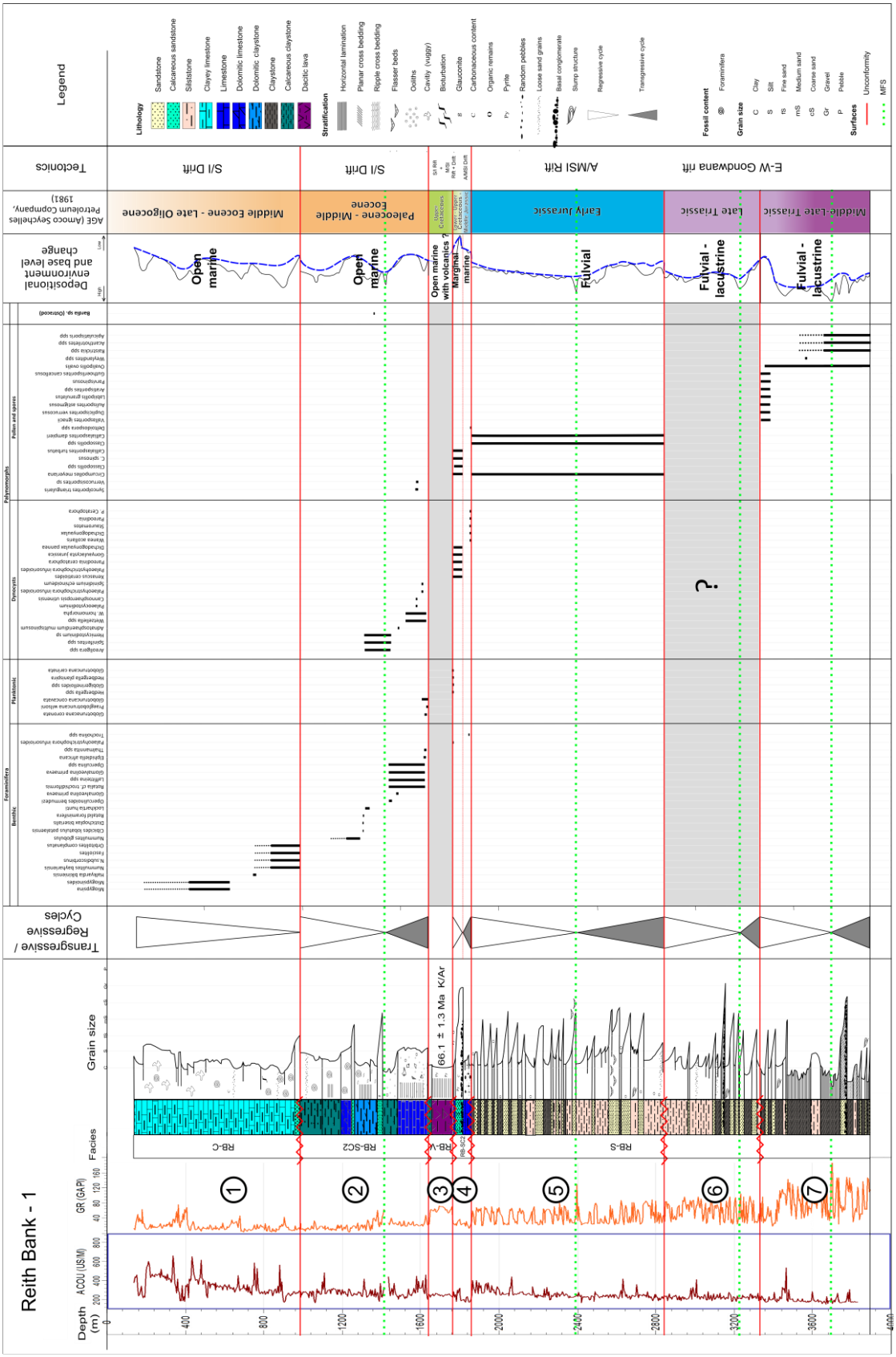

Figure A.6.17: Composite stratigraphic section of Reith Bank – 1, which includes the lithological log, the T-R cycles, bio-stratigraphy, base level curve with the depositional environment, tectonic events and the relative ages of sequences.

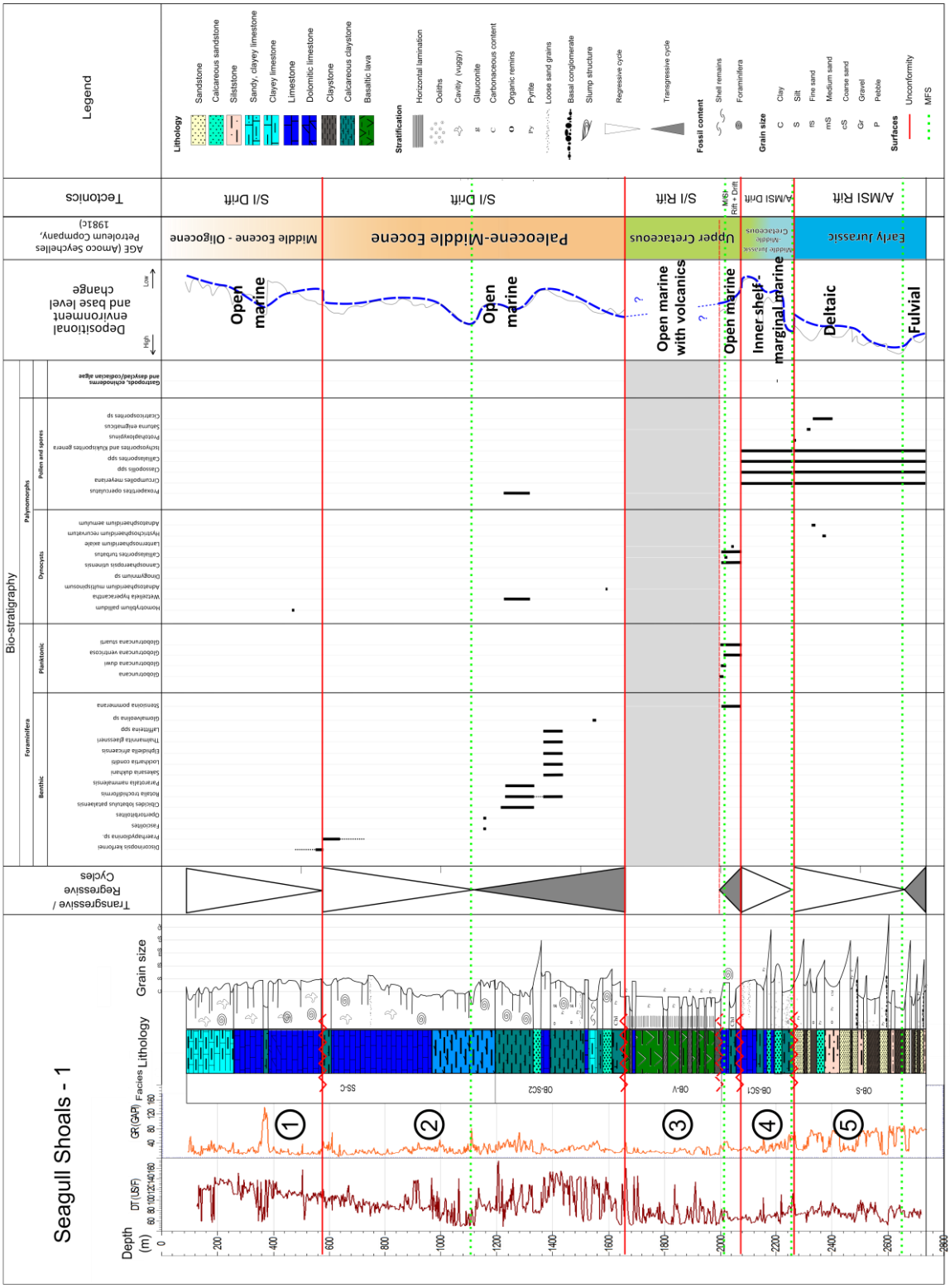

Figure. A.6.18: Composite stratigraphic section of Seagull Shoals – 1, which includes the lithological log, the T-R cycles, bio-stratigraphy, base level curve with the depositional environment, tectonic events and the relative ages of sequences.